Microvascular endothelial dilator function: role of COX and the effects of ecdysteroids

Asmaa Raees

A thesis submitted to the University College of London for the research degree of Doctor of Philosophy

2020

Division of Medicine
University College of London (UCL)

Declaration

I, Asmaa Raees, confirm that all the work presented is my own. Where information has been derived from other sources, I confirm that this has been indicated in the thesis.

Signature:

Date:

Abstract

Cyclooxygenase (COX), which can be expressed as COX-1 or COX-2 in endothelial cells has the unique ability to regulate microvascular tone through balanced production of dilator/constrictor prostanoids. This study investigated the roles of these isoforms in microvascular endothelial dilator function and how these are affected by supplement-derived ecdysteroids.

Acetylcholine or 20-hydroxyecdysone relaxation were recorded in Skeletal muscle (SKM) and mesenteric (ME) arteries from healthy sheep and omental (OM) and subcutaneous (SC) fat arteries from obese humans by wire myography in the absence and presence of inhibitors of nitric oxide synthase, cyclooxygenase (COX) isoforms 1 and 2 and endothelium-derived hyperpolarizing factors. Gene and protein expression analysis were also carried out to fully characterize the roles of COX in these arteries.

Non-selective COX inhibition attenuated acetylcholine relaxation in SKM arteries but enhanced it in ME arteries. Selective inhibition of COX-1 in both SKM and ME arteries also attenuated acetylcholine relaxation. In contrast, selective inhibition of COX-2 enhanced acetylcholine relaxation in ME arteries and had no effect in SKM arteries. In OM arteries from obese patients, selective inhibition of COX-1 but not COX-2 significantly improved acetylcholine relaxation. The OM arteries also displayed enhanced responsiveness to thromboxane A2 mimetic (U46619) compared with SC arteries. 20-hydroxyecdysone caused relaxation which was attenuated by NOS inhibition compared with COX inhibition in SKM and ME arteries.

COX roles in microvascular endothelial dilator function are isoform-specific and dependent on type and health of the vasculature. In healthy arteries, COX-1 promotes but COX-2 opposes vasodilation. In human obesity, COX-1 opposes while COX plays no part in OM endothelial dilator function. Although 20-hydroxyecdysone alters COX expression, its vasodilatory effect is more eNOS-dependent than COX-dependent.

Impact Statement

The findings of this thesis provide further insight into the pathways that drive COX enzyme direction in controlling vascular tone. The evidence presented in this thesis lends further support to the idea that effect of micro-environmental influence in different vascular beds governing many cellular responses including vascular tone. 20-HE, an ecdysteriod used in sport supplements has endothelium-dependent vasodilatory effects though increasing NO and not through COX products.

Together these findings could aid in better understanding of endothelial dependent relaxation mechanisms and its regulation in health and disease. Thus, this could aid in development of therapies targeted against pathways which promote endothelial dysfunction at an early stage of the disease. The findings of this study may also point to the vasodilatory effect of using 20-HE in sport supplements and potential risks around it.

Acknowledgement

Publications and conferences

Publication

- **Raees A**, Backhamis A, Mohamed-Ali V, Bashah M, Al-Jaber M, Abraham D, Clapp, Lucie H.; Orie, Nelson N. Altered cyclooxygenase-1 and enhanced thromboxane receptor activities underlie attenuated endothelial dilatory capacity of omental arteries in obesity. Life Sci. 2019 15 December 2019;239:117039.

- Orie N, Bakhamis A, **Raees A**, Bashah M, Alsayrafi M, Mohamed-Ali V. Reduced EDH but not NO per se is responsible for attenuated microvascular endothelium-dependent relaxation to Ach in morbid obesity. Acta Physiologica. 2015;215:14-.

Manuscript under review

- **Raees A**, Orie NN, Samsam W, Bakhamis AA, AlJaber MA, Banu S, Jaganjac M, Latiff AA, Abraham D, Alsayrafi M, Mohamed-Ali V. Vasocrine effects of supplement derived ecdysteroids.

Conference proceedings

- **Raees A**, Abraham D, Clapp L, Orie Nelson N. Double-edged vasomotor regulation of healthy resistance arteries by COX: Role of isoforms. Europhysiology 2018, London, UK, 2018, Proc Physiol Soc 41, PCB346.

- **Raees A**, Abraham D, Al-Jaber M, Mohamed Ali V, Al-Sayrafi M, Orie N. Understanding the mechanism and contribution of eNOS and COX to skeletal muscle arterial dilatation. 12th International Symposium on Resistance Arteries (ISRA 2017) Manchester, UK, September 3-6, 2017: Abstracts. J Vasc Res. 2017;54(suppl 2):1-64.

- **Raees, A**, Bakhamis, A, Bashah, MM, Alsayrafi, M, Mohamed-Ali, V, & Orie, NN. Microvascular Dysfunction in Morbid Obesity: Role of Enhanced Thromboxane A2 Sensitivity. ARC16, 2016, Doha, Qatar, Qatar Foundation Annual Research Conference Proceedings, 2016(1), Mar2016, HBPP2421, DOI:10.5339/qfarc.2016.hbpp2421.

ABBREVIATIONS

µg/ml: Microgram per milliliter

µg: Microgram

µl: Microliter

µm: Micrometer

µM: Micromolar

20-HE: 20-hydroxyecdysone

AA: Arachidonic acid

AC: Adenylyl cyclase

ACh: Acetylcholine

ACTA2: Actin alpha 2

ACTG2: Actin gamma 2

ADMA: Asymmetric dimethylarginine

ADP: Adenosine diphosphate

Akt: Protein kinase B also known as PKB

ANXA1: Annexin A1

ApoE: Apolipoprotein E

ATP: Adenosine triphosphate

ATPase: Adenosine triphosphatase

BH_4: (6R-)5,6,7,8-tetrahydrobiopterin

BK: Bradykinin

BMI: Body Mass Index

Ca^{2+}: Calcium ion

$CaCl_2$: Calcium Chloride

CaM: Calmodulin

cAMP: Cyclic adenosine monophosphate

CASP3: Caspase

CCL21: Chemokine (C-C motif) ligand

cDNA: Complementary DNA

cGMP: Cyclic guanosine monophosphate

cm: Centimeter

cm^2: Centimeter square

CNP: C-type natriuretic peptide

CO_2: Carbon dioxide

COX or PTGS: Cyclooxygenase or prostaglandin-endoperoxide synthase

COX-1 or PTGS1: Cyclooxygenase-1 or prostaglandin-endoperoxide synthase1

COX-2 or PTGS2: Cyclooxygenase-2 or prostaglandin-endoperoxide synthase2

CREB: cAMP response element-binding protein

CRP: C reactive protein

Ct: Cycle threshold

DAG: Diacyl-glycerol

DAPK3: Death-associated protein kinase 3

DDX5: DEAD (Asp-Glu-Ala-Asp) box helicase 5

DNA: Deoxyribonucleic acid

DNAJA1: DnaJ (Hsp40) homolog, subfamily A, member 1

DopEcR: Dopamine ecdysone receptor

DP: Prostaglandin D2 receptor 1

DUSP10: Dual specificity phosphatase 10

E2: Estradiol-17β

EC_{50}: Half maximal effective concentration

ECM: Extracellular matrix

EcR: Ecdysone Receptor

ED: Effective dose

EDCF: Endothelium-derived constricting factor

EDH: Endothelium-dependent hyperpolarization

EDHF: Endothelium-derived hyperpolarizing factor

EETs: Epoxyeicosatrienoic acids

EGR1: Early growth response 1

E_{max}: Maximum excitability effect

ENAP-1: eNOS-associated protein-1

eNOS or NOS3: Endothelial nitric oxide synthase

EP1: Prostaglandin E2 receptor 1

EP2: Prostaglandin E2 receptor 2

EP4: Prostaglandin E2 receptor 4

ER3: Prostaglandin E2 receptor 3

ERK: Extracellular signal-regulated kinase

ERα: Estrogen receptor α

ERβ: Estrogen receptor β

ET-1: Endothelin-1

ETA: Endothelin receptor A

ETB: Endothelin receptor B

FAD: Flavin adenine dinucleotide

FDR: False discovery rate

FFA: Free fatty acids

FMN: Flavin mononucleotide

FOS: FBJ murine osteosarcoma viral oncogene

FOSL1: FOS-like antigen 1

g: Gram

GAPDH: Glyceraldehyde 3-phosphate dehydrogenase

GC: Guanylyl cyclase

GPCR: G protein-coupled receptor

GPER or GPR30: G-protein coupled estrogen receptor

GTP: Guanosine triphosphate

GTPase: Nucleotide guanosine triphosphate hydrolase enzyme

GUCY1A3: Guanylate cyclase 1, soluble, alpha 3

G-αi: Inhibitory G protein

h or hr: Hour, unit of time

H2AFZ: H2A histone family, member Z

H_2O_2: Hydrogen peroxide

H_2S: Hydrogen sulfide

HCAEC: Human Coronary Artery Endothelial Cells

h-COX-1 and h-COX-2: Human COX-1 and human COX-2

HDL: High-density lipoproteins

HOMA-IR: Homeostatic model assessment-insulin resistance

Hsp90: Heat shock protein 90

HSPB1: Heat shock 27kDa protein 1

HUVEC: Human umbilical vein endothelial cell

IC_{50}: Half maximal inhibitory concentration

ID: Internal diameter

IGF-1: Insulin-like growth factor 1

IKCa: Intermediate conductance calcium-activated potassium channel

IL15: Interleukin 15

ILK: Integrin-linked kinase

I_{max}: Maximum inhibitory effect

IP: Prostaglandin I2 receptor

IP3: Inositol-1,4,5-trisphosphate

IPA: Ingenuity pathway analysis

JNK: c-Jun N-terminal kinases

JUNB: JUNB proto-oncogene

K^+: Potassium ion

KCa: Calcium-activated channels

KCl: Potassium Chloride

KDa: kilodalton

$Kg.m^{-2}$: Kilogram per square meter

Kg: Kilogram

KH_2PO_3: Potassium Dihydrogen Phosphite

KPa: Kilopascal

LDL: Low-density lipoproteins

L-NAME: Nω-Nitro-L-arginine methyl ester

LPS: Lipopolysaccharides

M: Molar

m^2: Square meter

M3: Muscarinic acetylcholine receptor

MAP: Mean arterial pressure

MAPK: Mitogen-activated protein kinases

ME: Mesenteric

mg/dL: Milligram per deciliter

$MgCl_2$: Magnesium Chloride

Min: Minutes

mIU/L: Milli-international unit per liter

ml: Milliliter

MLC: Myosin light chain

MLC20: Myosin light chain 20 kDa

MLCK: Myosin light chain kinase

mm: Millimeter

mM: Millimolar

mmHg: Millimeters of Mercury

mmol/L: Millimole per liter

mN: Millinewton

MPP: Methyl-piperidinopyrazole

mRNA: Messenger RNA

MYL9: Light chain 9, regulatory

MYPT1: Myosin Phosphatase Target Subunit 1

NA: Noradrenaline

Na^+: Sodium ion

NaCl: Sodium chloride

NADPH: Nicotinamide adenine dinucleotide phosphate

NaH_2PO_3: Sodium Dihydrogen Phosphite

$NaHCO_3$: Sodium Bicarbonate

NFkB: Nuclear factor kappa B

NFKBIB: NF-kappa-B inhibitor beta

NF-κB: Nuclear factor kappa-light-chain-enhancer of activated B cells

ng: Nanogram

nm: Nanometer

NO: Nitric oxide

NPSS: Normal physiological salt solution

NR2F2: Nuclear receptor subfamily 2, group F, member 2

NSAIDs: Nonsteroidal anti-inflammatory drugs

O_2: Oxygen molecule

^{o}C: Degree Celsius

OM: Omental

OTC: Over the counter

Ov-COX-1 and Ov-COX-2: Ovine COX-1 and ovine COX-2

p38MAPK: p38 mitogen-activated protein kinases

PAEC: Pulmonary artery endothelial cells

PBS: phosphate-buffered saline

PCA: Principal component analysis

PDE4 :phosphodiesterase 4

PG: Prostaglandin

PGD_2: Prostaglandin D_2

PGE_2: Prostaglandin E_2

$PGF_{2\alpha}$: Prostaglandin $F_{2\alpha}$

PGG_2: Prostaglandin G_2

PGH_2: Endoperoxide precursor prostaglandin H_2

PGI_2: Prostaglandin I_2

pH: Potential of hydrogen

PI3K: Phosphatidylinositol 3-kinase

PIP2: Phospho inositol diphosphate

PKA: Protein kinase A

PKC: Protein kinase C

PLA_2: Phospholipase A_2

PLC: Phospholipase C

PLCβ: Phospholipase Cβ

POX: Peroxidase

PPARs: Peroxisome proliferator-activated receptors

PRKG1: Protein kinase, cGMP-dependent, type I

q-PCR: Qualitative polymerase chain reaction

RAP2A: RAP2A, member of RAS oncogene family

RGS4: Regulator of G protein signaling 4

Rho: Termination of transcription factor

RhoA: Ras homolog family member A

RIPA: Radioimmunoprecipitation assay

RMA: Robust multiarray average

RNA: Ribonucleic acid

ROCCs: Receptor-operated Ca^{2+} channels

ROCs: Receptor-operated channels

ROS: Reactive oxygen species

rpm: Round per minute

s or sec: Second, unit of time

SARMs: Selective Androgen Receptor Modulators

SC: subcutaneous

SD: Standard deviation

SDS: Sodium dodecyl sulfate

SEM: Standard error of the mean

SERCA2: Sarco/endoplasmic reticulum Ca2+-ATPase

SHR: Spontaneously hypertensive rat

SKCa: Calcium-activated potassium channel

SKM: Skeletal muscle

SNAI2: Snail family zinc finger 1

SNP: Sodium nitroprusside

SOCCs: Store-operated Ca^{2+} channels

SOD: Superoxide dismutase

T. Cholesterol: Total cholesterol

TEK: TEK tyrosine kinase, endothelial

TG: Triglyceride

TNF: Tumor necrosis factor

TNF-α: Tumor necrosis factor-α,

TP or TBXA2R: TXA_2/PGH_2 endoperoxide receptor

TXA_2: Thromboxane A_2

TXB_2: Thromboxane B_2

U/mL: Units Per Milliliter

V: Volt

VDCCs: Voltage-dependent Ca^{2+} channels

VEGF: Vascular endothelial growth factors

VSMCs: Vascular smooth muscle cells

ZIPK: Zipper interacting protein kinase

ΔΔCT: Comparative cycle threshold

TABLE OF CONTENTS

LIST OF TABLES

LIST OF FIGURES

CHAPTER 1: Introduction and literature review

1.1 Vascular architecture

Blood vessels are dynamic tubes of diverse sizes and structure that are joined together to form a functional network delivering nutrients to metabolically active tissues and removing waste products (1). There is a hierarchical network of three main types of blood vessels; arteries, veins and capillaries characterized by location, size, function, and structural composition (2). The arterial or venous wall is composed of three layers of tissues namely: the tunica intima (also known as the endothelium), the tunica media (also known as vascular smooth muscle) and the tunica externa (also known as adventitia) (Figure 1). The intima or endothelium is a single layer of cells which continues as capillaries in tissues where it allows for exchange of materials between the blood and tissues. In addition to vascular smooth muscle cells (VSMCs), the tunica media also contains collagen fibers, elastin and other components of the extracellular matrix (ECM) (1). VSMCs provide structural support, strength and elasticity, and control blood pressure and blood flow through highly regulated contractile mechanisms. In comparison to similar-sized arteries, veins have a thinner media. Tunica externa or adventitia consists of fibroblasts, loose connective tissue, fat cells and perivascular nerves. The adventitia serves as a dynamic compartment for cell trafficking, growth and repair of blood vessels and communication with VSMCs and endothelial cells (3). The adventitia anchors the vessel and provides passage for small nerves, lymphatic vessels, and smaller blood vessels that supply the tissues of the larger vessel. Moreover, it contains resident populations of macrophages, T-cells, B-cells, mast cells, and dendritic cells that carry out important surveillance and innate immune functions in response to foreign antigens (4-6).

Arterial network is organized in a hierarchical order. Arteries are typically divided into three types; conducting arteries arising directly from the heart and their main branches, whose walls have a high degree of elasticity; distributing arteries that transport blood to specific organ systems, with a high muscular component in their walls; the small and muscular resistance arteries or

arterioles (7). Resistance arteries includes both small arteries and arteriole that enter an organ to distribute blood into capillary beds and they make up the greater part (%80) of the vascular network and are major determinants of peripheral vascular resistance and pressure (8).

These blood vessels vary significantly in diameter depending on species, vascular bed or location, and state of contraction. For example, in conscious rat resistance mesenteric arteries size is 100 to 300 μm (9).
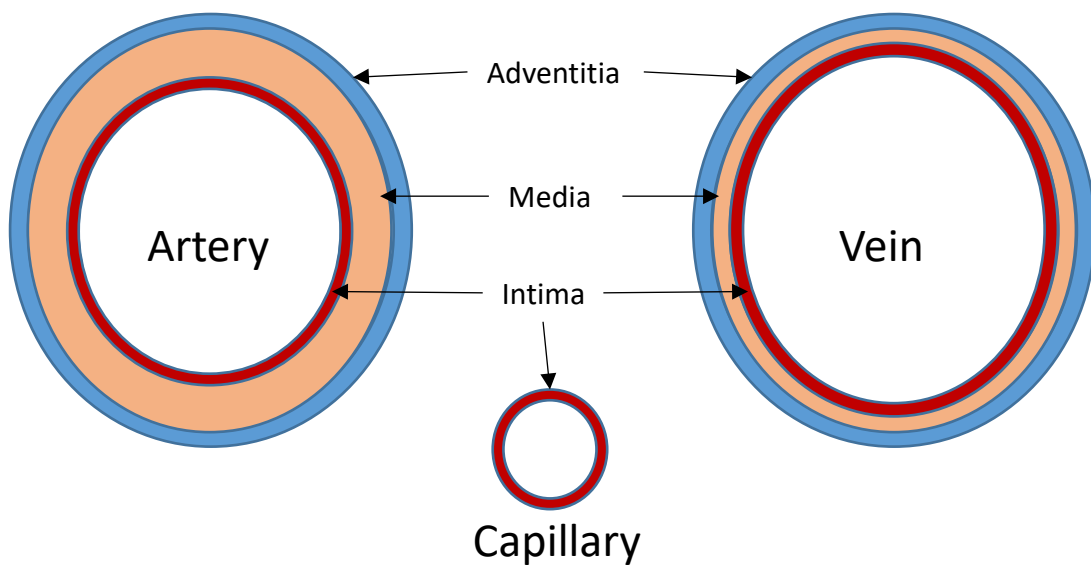
Figure 1: Cross-sectional diagram of an artery, vein and capillary.
The walls of the artery and vein are made up of tunica intima, tunica media, and tunica adventitia. The artery has a thicker tunica media and relatively narrow lumen compared with the vein which has thinner media but larger lumen. Capillaries are made of only the tunica intima (endothelium), with no other layers.

1.1.1   Microvasculature

Small vessels of diameter 300 μm or less make up the greater part of the vascular network and are major determinants of peripheral vascular resistance and pressure. The endothelial cells cover a large surface estimated to be 3000 m^2 and form a diffuse tissue of about 720 g in an adult person (10). Most of

these cells (over 600 g) and the surface exposed to blood are represented by capillary endothelial cells. As capillaries, they allow for exchange of nutrients and hormones facilitated by the relatively large surface area for a relatively small volume of blood (up to 5000 cm^2/ml) (10). Consequently, endothelial cells from micro vessels usually make a much larger contribution to circulating factors that reflect endothelial functions than those from large vessels (11).

1.2 Endothelial function

The endothelium plays important roles in both blood and vascular homeostasis. The cells secrete chemokines which regulate vascular tone as well as repel blood cells and platelets from attaching to the wall under normal conditions (12). In the lung, they are involved in the conversion and catabolism of vasoactive agents such as the transformation of angiotensin I to angiotensin II (13). Endothelial cells control the recruitment of leukocytes in areas where these inflammatory cells are needed. Furthermore, they are involved in wound healing by promoting angiogenesis, smooth muscle cell proliferation, and the formation of new blood vessels from existing ones - processes essential for proper tissue repair (11). In these conditions, inflammatory mediators can induce the transcription of new genes for new proteins that could alter the functions of these cells (14, 15).

Although a healthy endothelium performs all the above functions, the importance of the endothelium was first recognized by its effect on vascular tone. Vascular tone is established by state of contraction of blood vessel relative to its maximally dilated state. Arteriolar tone is a major determinant of peripheral vascular resistance and blood pressure. All arteries and veins show some degree of smooth muscle contraction that affects the tone of the vessel. Though, vascular tone varies among different organs (16).

1.2.1 Regulation of vascular tone

Vascular tone is primarily regulated by the sympathetic nervous system via the tonic release of noradrenaline (NA) on the vascular smooth muscle. NA binds to α-adrenergic receptors on the vascular smooth muscle membrane to induce proportionate degree of vasoconstriction (17). In addition to sympathetic control, vascular tone is influenced by circulating humoral factors, which work through pharmaco-mechanical coupling to promote contraction or relaxation (17). There is also the inherent ability of the vascular smooth muscle to contract in response to stretch or local increase in transmural pressure and to dilate in response to pressure reduction that is independent of neuronal or humoral influences (18). This inherent independent ability of the vascular smooth muscle to regulate its tone is referred to as the myogenic mechanism (18) and can be observed both in isolated, pressurized blood vessels (19-21) and in vivo (22-24). The myogenic mechanism is especially significant in the kidneys, where the glomerular filtration rate (the rate of blood filtration by the nephron) is particularly sensitive to changes in blood pressure and hence flow. However, with the assistance of the myogenic mechanism, the glomerular filtration rate remains very insensitive to changes in in blood pressure and hence flow (25).

1.2.1.1 Signaling for vascular smooth muscle contraction

Regardless of the stimulus for contraction, the contractile force of arterial smooth muscle is regulated by the intracellular concentration of calcium ion (Ca^{2+}) (26). An increase in intracellular free Ca^{2+} concentration induces activation of Ca^{2+}/CaM-dependent myosin light chain kinase (MLCK), which phosphorylate 20 kDa regulatory myosin light chain (MLC20). The phosphorylation of MLC20 by Ca^{2+}/calmodulin leads to actin-myosin interaction and force development (27). The increase in intracellular Ca^{2+} could come from release from intracellular stores, particularly the sarcoplasmic reticulum, and/or influx from extracellular space, depending on the stimulus (28). The membrane channels involved in Ca^{2+} entry from extracellular space include, voltage-dependent (VDCCs), receptor-operated (ROCCs) and store-operated (SOCCs) Ca^{2+} channels (29). On the other hand, Ca^{2+} is extruded from vascular smooth

muscle cells by a plasma membrane adenosine triphosphatase (ATPase) and Na^+/Ca^{2+} exchanger (29). Thus the duration of contraction is determined by the balance between Ca^{2+} mobilization and its removal (30) from the vascular smooth muscle cells.

Vasoconstrictors such as noradrenaline, angiotensin II and endothelin bind to their respective G-protein coupled receptors which are linked to phospholipase C (PLC) activity to cause contraction. This enzyme is specific for the membrane lipid phosphatidylinositol 4,5-bisphosphate which catalyzes the formation of two potent second messengers: inositol trisphosphate (IP3) and diacylglycerol (DAG). The binding of IP3 to its receptors on the sarcoplasmic reticulum results in the release of Ca^{2+} into the cytosol. DAG, along with Ca^{2+}, activates protein kinase C (PKC), which phosphorylates specific target proteins. In many cases, PKC has contraction-promoting effects such as phosphorylation of L-type Ca^{2+} channels or MLC20 which regulate cross-bridge cycling (31).

A decrease in intracellular level of Ca^{2+} induces the dissociation of the Ca^{2+}-CaM-MLCK complex, resulting in dephosphorylation of the MLC20 by MLCP and thus smooth muscle relaxation. Thus, the phosphorylation level of MLC20 is determined by the opposing activities of MLCK and MLCP and both enzymes' activities are well-regulated in smooth muscle (32). MLCP removes the high-energy phosphate from the light chain of myosin to promote smooth muscle relaxation. On the other hand, inhibition of MLCP activity allows MLC20 to remain phosphorylated, thereby promoting contraction through a process of Ca^{2+} sensitization (33).

Ca^{2+} sensitization maintains contraction even after intracellular Ca^{2+} returns to basal levels via two ways; MLC20 phosphorylation by Ca^{2+}-independent kinases and regulated inhibition of MLCP. An important step in maintaining contraction via MLCP inhibition involves activation of the small G protein Ras homolog family member A (RhoA) and its downstream target Rho kinase. Rho kinase, a serine/threonine kinase, phosphorylates the myosin-binding subunit of MLCP, inhibiting its activity and thus promoting the phosphorylated state of

MLC20 (34). For this reason, pharmacological inhibitors of Rho kinase cause relaxation of arterial smooth muscle and lowering of blood pressure (35).

RhoA Activation can also lead to diacylglycerol formation and activation of Ca^{2+}-dependent and -independent PKC isozymes. Rho kinase and PKC act concurrently and cooperatively to inhibit MLCP activity and sustain contraction. Other kinases such as Zipper interacting protein kinase (ZIPK) and Integrin-linked kinase (ILK) can also inhibit MLCP and mediate MLC20 phosphorylation (32).

1.2.1.2 Signaling for vascular smooth muscle relaxation

Vascular smooth muscle relaxation is initiated by MLC20 dephosphorylation, which can be due to MLCK inactivation and/or removal of MLCP inhibition, both of which require a decrease in intracellular Ca^{2+} concentration. Most stimuli that cause relaxation decrease Ca^{2+} by stimulating the production of cyclic adenosine monophosphate (cAMP) or cyclic guanosine monophosphate (cGMP) which inhibit mechanisms of calcium release and entry and promote extrusion and sequestration. Thus cAMP-activated protein kinase A (PKA) and cGMP-activated protein kinase G (PKG) are key components of the mechanism of relaxation in vascular smooth muscle (32). They target different components of the contractile signaling pathways to attenuate MLCK activity and/or augment MLCP activity, which eventually results in dephosphorylation of MLC20 and relaxation (32).

PKA and PKG indirectly target MLCK inactivation by primarily decreasing $[Ca^{2+}]i$. Both PKA and PKG can inhibit Ca^{2+} mobilization by inhibiting IP3 formation and arachidonic acid formation in muscle. Inhibition of IP3 formation in muscle involves phosphorylation of regulator of G protein signaling 4 (RGS4), leading to more rapid degradation of Gαq-GTP and inhibition of PLC-β1 activity. PKG-mediated phosphorylation of sarco/endoplasmic reticulum Ca^{2+}-ATPase (SERCA2), and sarcoplasmic reticulum IP3 receptors accelerates Ca^{2+}

reuptake into the stores and inhibits IP3-induced Ca^{2+} release, respectively. In addition, both kinases inhibit the activity of membrane Ca^{2+} channels and stimulate the activity of membrane K^+ channels, leading to hyperpolarization of the plasma membrane and interruption of Ca^{2+} influx into the cell (32).

PKG and PKA augment MLCP activity by different ways; first, they phosphorylate the activated form of RhoA (Rho-GTP) at Ser188 leading to its inactivation and translocation back to the cytosol (36). Second, both enzymes can phosphorylate Myosin Phosphatase Target Subunit 1 (MYPT1) at Ser695, preventing the inhibitory regulation of Rho kinase-mediated phosphorylation of MYPT1 at Thr696 (37). Finally, both kinases can phosphorylate (at Ser13) and enhance the activity of telokin, a smooth muscle-specific endogenous activator of MLCP (38).

1.3 Endothelium-dependent vasodilation

Endothelial cells release vascular relaxing substances to control the tone of the underlying smooth muscle. Nitric oxide, prostacyclin, and endothelium-derived hyperpolarizing factors are the three major endothelium-derived relaxing factors.

1.3.1 Role of eNOS

Endothelial nitric oxide synthase (eNOS) catalyzes the formation of perhaps the most recognized endothelium-derived vasodilator, nitric oxide (NO) using L-arginine and molecular oxygen as substrates. The enzyme consists of two monomers and two calmodulins (CaMs), that are relatively tightly-bound to cofactors which include reduced nicotinamide-adenine-dinucleotide phosphate (NADPH), flavin adenine dinucleotide (FAD), flavin mononucleotide (FMN), and (6R-)5,6,7,8-tetrahydrobiopterin (BH_4) and iron protoporphyrin IX (haem) (39). Cellular and tissue specific localization and expression of the eNOS can be regulated by CaM/Ca^{2+}, caveolin-1 and -3, Heat shock protein 90 (Hsp90),

eNOS-associated protein-1 (ENAP-1), and by covalent modifications; myristoylation, palmitoylation, and phosphorylation (39).

NO is a soluble gas with a half-life of ~6–30 s. It is therefore continuously synthesized from the amino acid L-arginine in endothelial cells in a calcium-calmodulin-dependent manner (40) and requiring a multitude of cofactors as illustrated in (Figure 2).
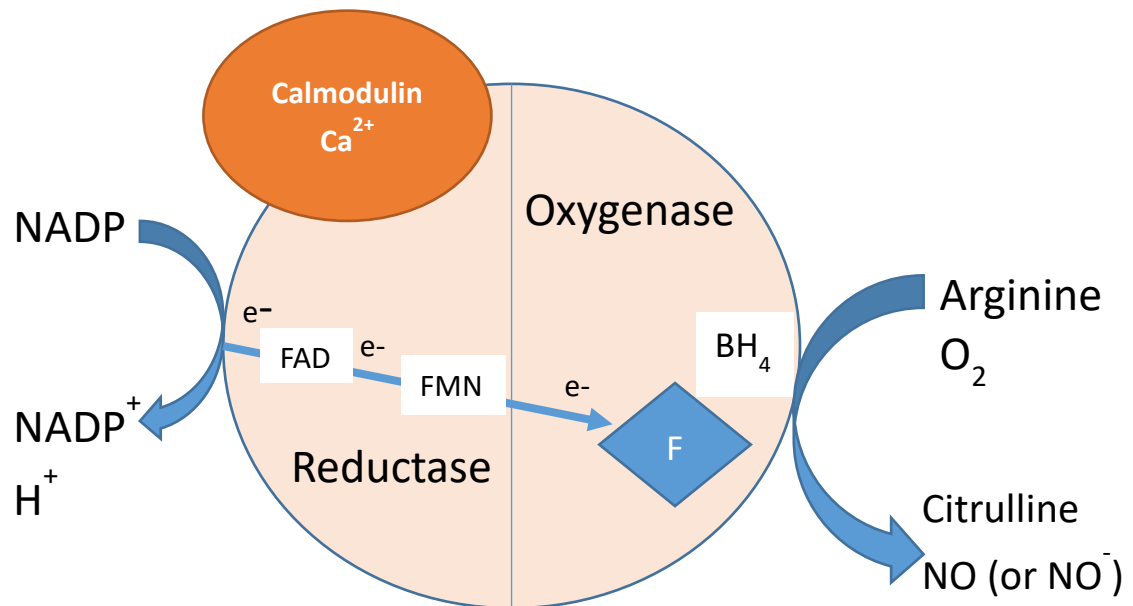
Figure 2: NOS functional dimer.

Electrons (e−) are donated by NADPH to the reductase domain of the enzyme and proceed via FAD and FMN redox carriers to the oxygenase domain in the presence of bound Ca^{2+}/CaM. In the oxygenase domain, the electrons interact with the haem iron and BH4 at the active site to catalyze the reaction of oxygen with L-arginine, generating citrulline and NO as products. In some circumstances, NO^- may be a product instead of NO. Adapted from (39).

1.3.1.1 Mechanism of NO - induced vasodilation

Nitric oxide, released from the endothelium as a gas or attached to other molecules, stimulates soluble guanylyl cyclase, producing increased concentrations of cyclic guanosine monophosphate (cGMP) (Figure 3). Depending on the direction of nitric oxide release and the site of cGMP

activation, differing biological effects can be observed. For example, increased cGMP in vascular smooth muscle cells underlying the endothelium activates GMP-dependent kinase that among other effects activate the large-conductance Ca^{2+}-activated potassium (K^+) channels leading to K^+ efflux, hyperpolarization and closure of Ca^{2+} channels. These leads to decreased intracellular calcium and relaxation (41). Nitric oxide governs basal systemic, coronary, and pulmonary vascular tone by increased cGMP in smooth muscle, inhibition of synthesis and receptor binding of a potent constrictor peptide, endothelin-1 (42), and by inhibition of the release of noradrenaline (NA) from sympathetic nerve terminals (43, 44).

Following the original work of Furchgott and Zawadzki (45), a variety of agonists (e.g., acetylcholine (ACh), histamine, thrombin, serotonin, adenosine diphosphate (ADP), bradykinin, substance P, and isoproterenol) are now known to increase the synthesis and release of nitric oxide from the endothelium, although many of these same agonists (e.g., ACh, serotonin, and histamine) constrict vascular smooth muscle in the absence of endothelium (43). Vasoactive substances produced within the endothelium, such as bradykinin, may also stimulate nitric oxide release by autocrine and paracrine effects on endothelial B2 kinin receptors (46). However, the principal physiologic stimulus for nitric oxide synthesis and release from the endothelium is likely the shear stress of blood flowing over the surface of the vessel by a non-receptor-dependent mechanism (47, 48), probably involving activation of Phosphatidylinositol 3-kinase and protein kinase B (PI3K-Akt) pathway which phosphorylates eNOS.
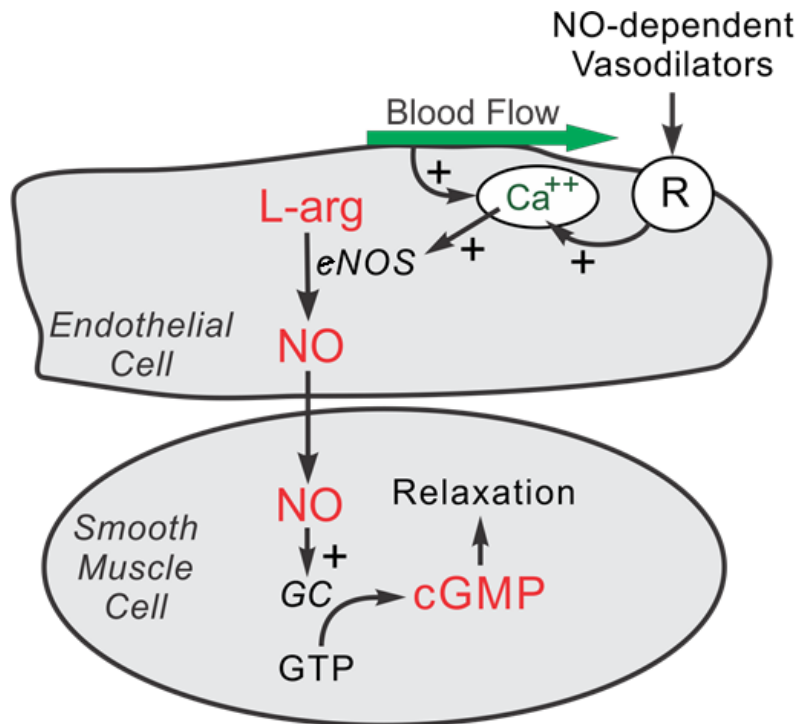
Figure 3: Mechanism of NO-induced vasodilation.

In endothelial cell, NO-dependent vasodilators activate their receptors (R, e.g. muscarinic ACh receptor (M3)) causing increase in intracellular calcium that activate eNOS to convert L-arginine into Nitric Oxide. Then, Nitric oxide diffuses into the smooth muscle cell where it activates guanylyl cyclase (GC) to increase cyclic GMP and cause relaxation. eNOS activity is also increased by blood flow that activates PI_3 kinase which causes activation of protein kinase B (Akt) which then phosphorylates eNOS to increase its activity (49).

1.3.2 Role of COX

Cyclooxygenase (COX) also called prostaglandin-endoperoxide synthase (PTGS), is an endogenous lipid compound enzyme that catalyzes the first committed step in the conversion of arachidonic acid into prostaglandins (50). There are two isoforms of the enzyme, COX-1 and COX-2 with COX-1 being constitutively and more widely expressed in every cell of the body (50). Both COXs are homodimers of 70 kDa subunits and consist of three structural domains as it presented in (Figure 4): a short N-terminal epidermal growth

31

factor domain, a membrane binding domain, and a large, globular C-terminal catalytic domain (51). Ovine COX-1 was one of the first membrane protein to be crystallized and to have its structure solved (52). Each subunit contained a cyclooxygenase and a peroxidase active site, with inhibitor bound only to the cyclooxygenase active site. Although it has been assumed that both subunits are active simultaneously, recent work suggests that substrate or inhibitor binding in the cyclooxygenase active site at one subunit precludes binding of another molecule at the other subunit (51, 53).
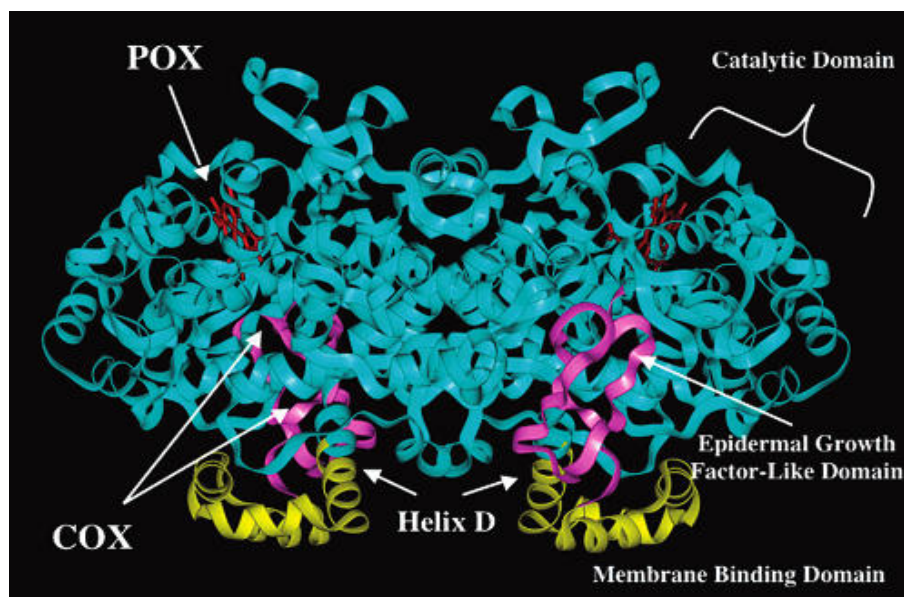
Figure 4: Ribbon diagram of COX molecules.

The diagram shows catalytic domain where COX enzymes catalyzes the arachidonic acid to produce prostaglandin G2 (PGG_2), which then diffuses to the peroxidase (POX) and undergo reduction reaction to form endoperoxide precursor prostaglandin H2 (PGH_2) (51).

The two COXs are encoded by two different genes; COX-1 and COX-2 genes respectively, prefixed with species symbol for example, h-COX-1 and h-COX-2 genes for human (54) and Ov-COX-1 and Ov-COX-2 for ovine (55). Mature, processed COX-1 contains 576 amino acids; the mature form of COX-2 contains 587 amino acids (50). There is a 60%–65% sequence identity between

COX-1 and 2 from the same species and 85%–90% identity among individual isoforms from different species (50). The homology between human and ovine COX is 90% (51). The major sequence differences between COX isoforms occur in the membrane binding domains which is the site of substrate binding and nonsteroidal anti-inflammatory drugs (NSAIDs) action (50).

The activity and expression of these enzymes are regulated differentially, and they can function independently within the same cell type (56). Table 1 summaries other differences between COX isoforms. Moreover, an enzymatically active splice variant of COX-1, termed COX-3, is expressed in the heart and cerebral cortex, but the regulation of its transcription appears like that of COX-1 (57). However, COX-3 is unlikely to have prostaglandin (PG)-producing activity in human tissues because the difference in COX-3 sequence resulting in a completely different protein without the possibility of COX activity (58). Indeed, rat COX-3 has been fully expressed and demonstrated to have no COX activity (58).

Table 1: Comparative presentation of COX-1 and COX-2 properties (59).

Properties	COX-1	COX-2
Gene size	22 kb	8.3 kb
Exons	11	10
Chromosome	9q32-q33.3	1q25.2-q25.3
mRNA	2.8 kb	4.1 kb
mRNA regulation	Constitutive	Inducible, although may be constitutive in some tissues
Inducers		LPS, phorbol esters and cytokines such as interleukin 1β, IFN-γ and tumor necrosis factor alpha (TNF)
Molecular weight	70 kD	70-72 kD
Localization	Endoplasmic reticulum	Nuclear membrane
Cofactors	1 mol of heme	1 mol of heme
Glycosylation	-N, 3 sites	-N, 3 or 4 sites
Substrate specificity	AA, γ-linolenic acid	AA, γ-linolenic acid, α-linolenic acid
Eicosapentaenoic acid Activity	23 mmol of AA/mg/ml	12 mmol of AA/mg/ml

Since COX-1 is ubiquitously and constitutively expressed, disruption to it leads to decreased constitutive prostaglandin synthesis. This has been demonstrated in COX-1 deficient mice with no effect on inducible synthesis of PGs (60-62). The mice showed reduced hypertensive response to angiotensin II and, in isolated aortic rings, a complete inhibition of endothelium-dependent contractions (63). COX-1 deletion prevents atherosclerotic lesion formation in apolipoprotein E (ApoE) null mice (57, 64).

COX-2 is normally undetectable in most tissues (65) except when induced at sites of inflammation. However, constitutive expression has been reported including in endothelial cells where its expression is also up-regulated by shear stress (66). In addition, COX-2 is found to be constitutive in multiple discrete regions of the body, including the brain, gut, and kidney suggesting that it may play a homeostatic role under certain physiological conditions (66-69). Other organs, such as the heart, show negligible expression (70). The phenotype associated with COX-2 deletion is more severe. In one study 30 to 40% of the pups from COX-2 knockout mice died within 48 h from a patent ductus arteriosus (71). Furthermore, the surviving animals had a shorter life span than the wild-type mice. Constitutive PG synthesis remained normal in these COX-2 null mice while inducible PG decreased (72). Although platelet aggregation was normal since mature platelets only express COX-1, they were nonetheless more susceptible to thrombosis (61, 62, 73). They showed an enhanced pressor effect in response to angiotensin II and no or minor inhibition of endothelium dependent contractions. In mice with a specific deletion of COX-2 in the cardiomyocytes, heart failure and fibrosis are observed (74).

1.3.2.1 Biosynthesis of Prostanoids

COX-1 and COX-2 are bi-functional enzymes that carry out two sequential reactions of (1) di-oxygenation of Arachidonic acid to prostaglandin G_2 (PGG$_2$) and (2) the reduction of PGG$_2$ to endoperoxide precursor prostaglandin H_2 (PGH$_2$). Arachidonic acid oxygenation occurs in the cyclooxygenase active site,

and PGG$_2$ reduction occurs in the peroxidase active site. PGH$_2$ diffuses from the COX proteins and is transformed by different tissue-specific isomerases to prostaglandins (PGE$_2$, PGD$_2$, PGF$_{2\alpha}$, and PGI$_2$) and TXA$_2$ (Figure 5).
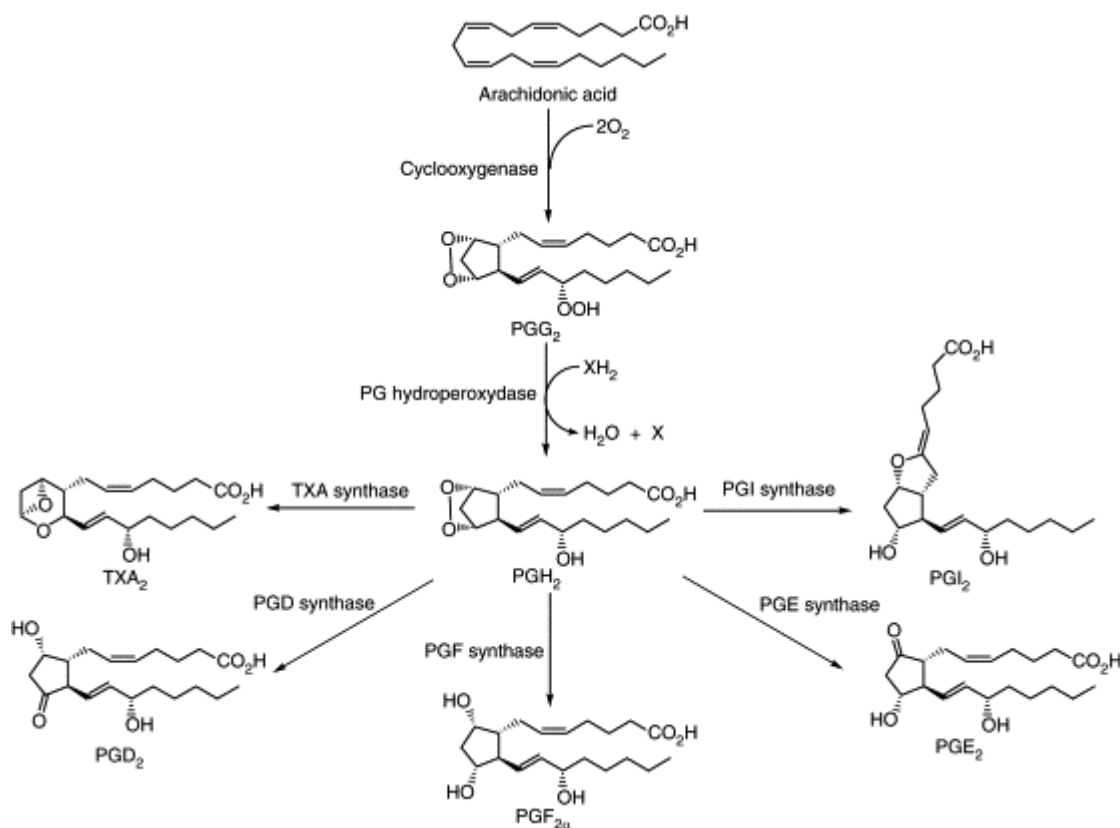
Figure 5: Generation of prostanoids.

Prostanoids, such as prostaglandin E$_2$ (PGE$_2$) and prostaglandin F$_{2\alpha}$ (PGF$_{2\alpha}$), are generated from arachidonic acid via the cyclooxygenase-prostaglandin G/H synthase pathway (75).

1.3.2.2 Mechanisms of the vasoactive actions of prostanoids

The actual prostanoid profile synthesized by a cell type is determined by the presence of different downstream PG and TXA synthases and isomerases (76). The effects of prostanoids then depend on the expression pattern and localization of specific receptors and the subsequent signaling pathways activation (77). In the vascular system, when the receptors are localized on the smooth muscle, the activation of prostaglandin receptors IP, EP2, EP4, or DP

receptors by prostanoids induces vasodilation, while the activation of TP, EP1, EP3, or FP receptors is responsible for vasoconstrictions (Table 2) (78). Most vascular smooth muscle express TP and IP receptors that are involved in the control of vascular tone (79).

Table 2: Types and subtypes of prostanoid receptors.

Main characteristics and cell signaling pathways associated to each receptor.

Prostanoid Receptor	Activating prostanoids (80)	Classification	G protein linkage (81)	Pathways (81)
IP	PGI2>>PGD2=PGE2=PGF2α>TXA2	Relaxant	Gs alpha	stimulates AC & PKA; cAMP ↑ (IP3 ↑)
TXA₂	TXA=PGH2>>PGD2=PGE2=PGF2α=PGI2	contractile	Gq alpha	stimulates PLC & IP3↑; ↑ Ca2+ (cAMP ↓ ↑)
EP1	PGE2>PGF2α=PGI2>PGD2=TXA2	contractile	Gq alpha	stimulates PLC, IP3↑, PKC, ERK, p38 Mpk, and CREB; Ca2+ ↑
EP2	PGE2>PGF2α=PGI2>PGD2=TXA2	Relaxant	Gs alpha	stimulates AC, raises cAMP ↑, stimulates beta catenin and Glycogen synthase kinase 3
EP3	PGE2>PGF2α,PGI2>PGD2=TXA2	Inhibitory	Gi	inhibits AC, decreases cAMP, stimulates PLC & IP3, raises Ca2+
EP4	PGE2>PGF2α=PGI2>PGD2=TXA2	Relaxant	Gs alpha	stimulates AC, PKA, PI3K, AKT, ERK, p38MAPK, & CREB; raises cAMP ↑
FP	PGF2α>PGD2>PGE2>PGI2=TXA2	contractile	Gq alpha	stimulates PLC, IP3 ↑, & PKC; raises Ca2+
DP1	PGD2>>PGE2>PGF2α>PGI2=TXA2	Relaxant	Gs alpha	activates AC, increases cAMP, raises Ca2+ ↑
DP2	PGD2>>PGF2α=PGE2>PGI2=TXA2	Inhibitory	Gi alpha	inhibits AC to depress cAMP ↓ levels

1.3.2.3 Mechanism of PGI$_2$-induced vasodilation

PGI$_2$ (or prostacyclin) is considered the main arachidonic acid metabolite synthesized by vascular endothelium (82) and major regulator of vascular tone under normal physiological conditions. It is synthesized and released in response to flow/shear stress (83) and a range of agonists, notably, molecules involved in the coagulation process (e.g. BK and thrombin) or secreted by aggregating platelets (e.g. adenosine triphosphate (ATP) and adenosine diphosphate (ADP)). Its synthesis is triggered by increased intracellular Ca^{2+} concentrations in endothelial cells, which initiates Ca^{2+}-sensitive hydrolysis of arachidonic acid from membrane phospholipids by phospholipase A$_2$ (PLA$_2$). In addition to elevated Ca^{2+}, PGI$_2$ synthesis requires the phosphorylation and activation of the 42/44 kDa extracellular-signal regulated protein kinase (ERK), which in turn phosphorylates phospholipase A$_2$ and enhances its sensitivity to Ca^{2+} (83).

PGI$_2$ induces vasodilation by activating prostanoid IP, EP2 or EP4 receptors on the vascular smooth muscle (84) (Figure 6). These PGI$_2$ receptors belong to G protein-coupled receptors (GPCRs) and are coupled to the GTP-binding protein G$_s$, which mediate increases in cyclic adenosine monophosphate (cAMP) (85-88) and SMC relaxation. PGI$_2$/IP activation of protein kinase A (PKA) could impair ERK signaling, and thus interfere with TXA$_2$ signaling (89). PGI$_2$ may act via cAMP-independent pathways to control various cellular processes (87, 90), including vasorelaxation (91). PGI$_2$ can directly activate K$^+$ channels located on the vascular smooth muscle membrane (91), which lead to hyperpolarization and relaxation. Intracrine PGI$_2$ binding to perinuclear peroxisome proliferator-activated receptors (PPARs) causes translocation of PPAR to the nucleus and the formation of heterodimers with retinoic acid receptors, which in turn bind to peroxisome proliferator response element and lead to genomic effects (92). Besides, PPAR β/δ signal non-genomic and acute response in prostacyclin-induced vasodilation by acting on calcium-activated potassium channels (KCa) in pulmonary arteries (93).
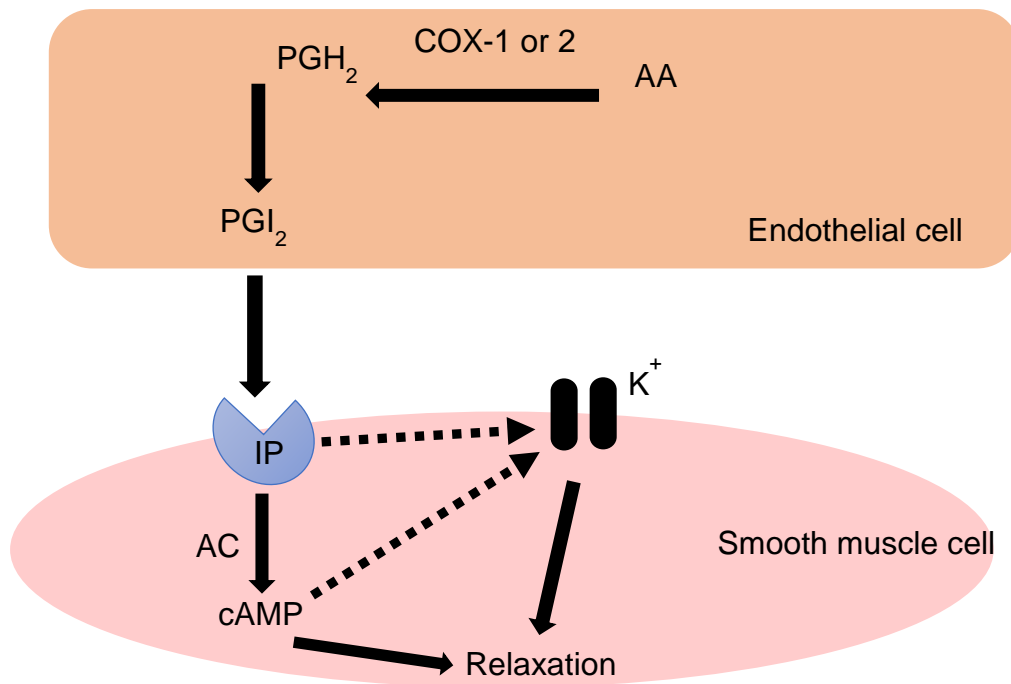
Figure 6: Mechanism of prostacyclin-induced vasodilation.

PGI_2 produced in endothelial cell activates prostacyclin IP receptors on the smooth muscle cell membrane. The IP-receptor is coupled to stimulatory Gs-protein which activates adenylyl cyclase (AC) leading to increased formation of cAMP and relaxation of smooth muscle cell. Alternatively, IP receptor activation could lead directly to opening of K^+ channels to cause relaxation. Adapted from (91).

1.3.3 Role of Endothelium-dependent hyperpolarization

Endothelium-dependent hyperpolarization (EDH) represents the predominant mechanism of endothelium-dependent vasodilation in small arteries (94). As vessel size decreases with decreasing role for NO along the vascular tree, the role of EDH increases (95, 96). This mechanism involves the release from the endothelium of yet-to-be identified factor(s) generally referred to as endothelium-derived hyperpolarizing factor(s) [EDHF(s)], which open K^+ channels on the VSMCs leading to vasodilation. EDHF release from the endothelial cell occurs following the opening of endothelial small conductance calcium-activated potassium channel (SKCa) and intermediate conductance

calcium-activated potassium channel (IKCa) (97). However, the identity of this factor(s) remains uncertain. The candidate factors so far proposed include, hydrogen peroxide (H_2O_2; (98)), hydrogen sulfide (H_2S; (99)), metabolites of arachidonic acid such as epoxyeicosatrienoic acids (EETs; (100)), potassium ions (K^+; (101)), and C-type natriuretic peptide (CNP; (102)) and vary according to vasculature. There have also been suggestions that EDH may involve an electrical coupling through myoendothelial junctions (103). Thus, EDHF varies according to vasculature and should be characterized for each vessel.

1.4   Endothelium-dependent vasoconstriction

The endothelium not only mediates relaxation but is a source of contracting factors, which can also impact the tone of the underlying smooth muscle, although normally much less than it produces vasodilators. ET-1 and TXA_2 are considered the major endothelium-derived contracting factors (EDCFs) (104). Nevertheless, other mediators also could contribute to constriction particularly in pathological conditions such as Angiotensin II, cytokines, superoxide anions, platelet-derived factors and coagulation products (104).

1.4.1   Role of contractile prostanoids

TXA_2 is the main contractile prostanoid produced from the PGH_2 endoperoxide precursor in the endothelium. It has a short half-life of 30 seconds due to its spontaneous hydrolysis to the stable metabolite thromboxane B_2 (TXB_2) (105). TXA_2 causes vasoconstriction by binding to the TP receptor to activate phospholipase Cβ (PLCβ) via Gq. The activated receptor then signals PLCβ to start the hydrolysis of phospho inositol diphosphate (PIP2) to diacyl-glycerol (DAG) and inositol-1,4,5-trisphosphate (IP3) that increase intracellular Ca^{2+}. TXA_2 synthesis and release is activated by stretch and several humoral factors including ACh, angiotensin I and II, ADP and ATP (106, 107).

The endoperoxide precursor intermediate PGH_2 can also act as an EDCF (108-110). Although its vasoconstrictor effect is limited by its very short half-life, PGH_2 can bind and activate TP receptors on vascular smooth muscle (109, 111-113) similar to TXA_2.

1.4.2   Role of other endothelium-derived vasoconstrictors

Endothelin-1 or ET-1 is one of three endothelins encoded by three separate genes and processed to the amino acid sequences designated as ET-1, ET-2 and ET-3 (114). ET-1 is believed to act as a feedback control system to NO in the regulation of vascular tone (115) and has a plasma half-life of approximately one minute (114, 116). ET-1 actions are mediated by two subtypes of receptors, the ET-A and ET-B receptors. ET-1 causes vasoconstriction by binding and activating ET-A receptor, which is coupled to Ca^{2+} mobilizing mechanisms within vascular smooth muscle cells to cause vasoconstriction (117-119). On the other hand, activation of ET-B receptors may cause either vasodilation by releasing NO and PGI_2, or vasoconstriction dependent upon different pathophysiological conditions. ET-A receptors are predominately present in human microvasculature (smooth muscle and endothelium), unlike ET-B (120, 121).

Reactive oxygen species (ROS) are oxygen-derived free radicals, which includes the superoxide and hydroxyl species. ROS are key mediators of ischemia–reperfusion injury that inactivate endothelial NO release and stimulate vascular smooth muscle contraction (122). In physiological conditions, oxygen-derived free radicals are continuously scavenged by endogenous antioxidant systems, including superoxide dismutase (SOD), glutathione peroxidase, and catalase; however, imbalance between pro-oxidants and antioxidants, and both excess production of ROS and deficiency in cellular antioxidant defenses, result in endogenous oxidative stress (123). Excessive ROS induces mitochondrial membrane pore transmission and

impairs the membrane integrity, leading to the release of cytochrome c, activation of caspase, and apoptosis (124).

1.5 Comparison between skeletal muscle and mesenteric arterioles

Arterioles are the primary resistance vessels that enter an organ to distribute blood flow into capillary beds. Arterioles are considered part of the resistance vasculature that provides more than 80% of the resistance to blood flow in the body. Consequently, they are vital to the regulation of hemodynamics, contributing to the control of blood pressure and the regional distribution of blood (8). Both skeletal muscle and mesenteric arterioles are regulated sympathetically by nerves and autoregulated locally by both myogenic and metabolic mechanisms (125, 126). These blood vessels vary significantly in diameter depending on species, vascular bed, and state of contraction (8). Skeletal and mesenteric arterioles are widely used in vascular studies hence it's important to be aware that those arterioles could vary in their response to vasodilator and constrictor mediators as part of their unique physiology.

In rat mesenteric arterioles, the primary dilation is NO (127), whereas in rat gracilis muscle arterioles (128) both NO and dilator prostaglandins are involved. Interestingly increases in flow elicit primarily the release of prostaglandins in skeletal muscle cremasteric arterioles (129, 130). Moreover, in both arterioles EDH- type mechanisms also contribute in dilation as high extracellular $[K^+]$ and/or blockade of K^+ channels attenuated relaxation (131, 132). Both arterioles contract in response to ET-1 by ETB receptor (133-135) and to H_2O_2 in a concentration-dependent biphasic effect (136, 137). In general, increase in vascular oxidant stress appears to contribute to alteration to the arteriolar constrictor reactivity to thromboxane and other constrictors (138).

1.6 Endothelium dysfunction

Abnormal endothelial physiology precedes cardiovascular diseases, peripheral vascular disease, stroke, chronic kidney failure, cancer, aging, and infectious diseases. It is the hallmark of vascular complications of obesity, hypertension and diabetes. Endothelial dysfunction is commonly described as a state of reduced or absence of endothelium-dependent relaxation due to reduction or absence of NO (139) such as in diabetes (140) and aging (141). However, this description is limited because endothelial dysfunction could also result from EDHF deficiency (142) or increases in EDCF (143, 144). EDHF is impaired in pathological conditions such as aging (145), hypertension (146), obesity (142) and diabetes (147). In response to a damage, the endothelial cells produce cell adhesion molecules that induce leukocytes and platelets to adhere to the surface of the wall and initiate their defensive actions(148).

Experimentally, acetylcholine, which is commonly used to test endothelial function, produces a well-defined dilator response on application. Thus, when the endothelium is damaged as in many vascular diseases, responses to acetylcholine are blunted as NO and other mediators produced in the endothelium in response to ACh are compromised whereas the response to the endothelium-independent sodium nitroprusside remains unaltered (149).

1.6.1 In obesity

Obesity is a global epidemic and Qatar has one of the highest rates of both childhood and adult obesity in the world (150) which correlate with increased incidence of type 2 diabetes and cardiovascular disease. In obesity, the endothelium is negatively impacted by dysregulated secretions from the expanding adipose tissues. The increased circulating levels of pro-inflammatory cytokines such as tumor necrosis factor-alpha and interleukin-6 adversely affect the cardiovascular system causing endothelial dysfunction by increased oxidative stress and vascular hypertrophy (151, 152). The impact is

particularly pathogenic in central or abdominal obesity marked by increased visceral adipose tissue (dispersed around the omental (OM), intestines and peri-renal areas,(153)) which is more metabolically active by secreting more proinflammatory cytokines (154, 155) than peripheral adipose tissue such as subcutaneous tissue (SC) (156, 157). Both chronic inflammation and insulin resistance in these circumstances are strongly associated with impaired vasodilatory responses (156, 157), endothelial dysfunction and the initiation and progression of atherosclerosis (158). However, the key molecular determinants of the severity of the impact of the adipose tissue micro-environment on the local blood vessels are still not well understood especially for a relatively young obese population such as in Qatar.

Recently, the malfunction of the cyclooxygenase (COX) enzyme in the endothelium was identified as a potential molecular determinant of omental endothelial dysfunction in obesity (159). Under physiological conditions, COX produce dilator and constrictor prostanoid with a balance tilted toward vasodilators (63, 82). Thus, COX reversibly shift the balance in favor of constrictor prostanoids in pathological conditions (160, 161). That increase in constrictor prostanoid activity is conceivably a potential risk factor for endothelial dysfunction.

As noted previously, COX enzyme is expressed in endothelial cells in two isoforms. COX-1 is expressed constitutively (162) while COX-2 is in large part inducible by share stress (162, 163) and inflammatory stimuli (164). Thus, the expression and activity of these isoforms are differentially regulated, and they can function independently within the same cell (56, 82). Obesity has been associated with increased COX-1 expression in adipose tissues linked with increase contracting prostanoid (165, 166). We recently showed that increased COX-1 and enhanced TXA_2 receptor activity could account for the reduction in endothelial dilatory capacity of these arteries compared with subcutaneous arteries in obesity (142). However, COX-2 expression in renal interlobar arteries (167) and adipocytes (168) might underlie alteration in the balance of prostanoids produced in those tissues. Thus, both COX-1 and COX-2 derived

prostanoids can alter the balance in prostanoid activity (82), which could alter endothelial function.

1.6.2 In other diseases

Endothelial dysfunction is considered an early stage of vasculopathy in the two most prevalent diseases; diabetes and hypertension. In type 2 diabetes, excess liberation of free fatty acids (FFA), hyperglycemia, insulin resistance and hyperinsulinemia impact negatively on endothelial function. The result is a weakening of endothelium-mediated vasomotor function, increasing endothelial apoptosis, activation of monocyte adhesion, increasing atherogenic response and suppressing barrier function (139). In type 1 diabetes glucotoxicity adversely affects endothelial function by multiple signaling pathways. For instance, it impairs endothelial response to insulin and accelerates atherosclerosis (169). It could also lead to excessive FFA which could induce endothelial oxidative stress, apoptosis and inflammatory response, and inhibits insulin signaling (169). Altered vascular PG metabolism plays a key role in diabetes-related changes in local vaso-regulatory mechanisms. It was found that in mesenteric arteries of type 1 diabetic dogs, exogenous arachidonic acid elicited TXA_2–mediated constriction, whereas in control animals, it caused prostacyclin (PGI_2)-dependent dilation (170). Under these conditions, EDHF-mediated responses can be up-regulated not only to compensate for the reduced bioavailability of NO but also probably to counteract the production or action of endothelium-derived contracting factors (171). Oxidative stress and inflammation are predicted to be among the first alterations which may trigger other downstream mediators in diabetes associated with endothelial dysfunction (172).

Hypertensive patients also commonly suffer endothelial dysfunction (173-175) as a result of increased NO breakdown (176), although decreased synthesis caused by increased asymmetric dimethylarginine (ADMA) cannot be ruled out (177). The increased breakdown of NO in these circumstances is often a consequence of increased oxidative stress. The increased superoxide ion reacts with NO to destroy it and produce peroxynitrite (178). Interestingly,

NAD(P)H oxidase, xanthine oxidase and COX have all been described as sources of ROS in endothelial cells in hypertension. In parallel with this alteration, an increased production of EDCFs, including endothelin (via ETA) and angiotensin II contribute to the condition of endothelial dysfunction of these patients (179). The mechanisms that regulate the balance between endothelium-derived relaxing and contracting factors and the processes transforming the endothelium from a protective organ to a source of vasoconstrictors, such as COX-derived EDCFs remain to be determined.

1.7 Ecdysteroids

Ecdysteroids are polyhydroxylated ketosteroids with long carbon side chains produced primarily in insects and plants (180). They can also be found in fungi and marine sponges (180). Over 517 different ecdysteroids have been identified so far (181, 182). 20-hydroxyecdysone (20-HE) is the major insect molting hormone, a 27-carbon molecule derived from sterol with a long sterol alkyl side chain on C-17, but some insect species contain its C28 or C29 homologs, makisterone C and makisterone A, respectively. as shown in (Figure 7).

Ecdysteroids differ markedly from vertebrate steroid hormones in their polarity (polyhydroxylated), bulk (C27–C29) and shape (A/B-cis-ring junction) (180). In addition, Ecdysteroids lack the ketone group in the C3 position and they have a long carbon chain at C17, making them much bulkier than androgens. This reduces the likelihood that ecdysteroids would fit in the ligand binding pockets of the nuclear receptors designed for androgens (183).
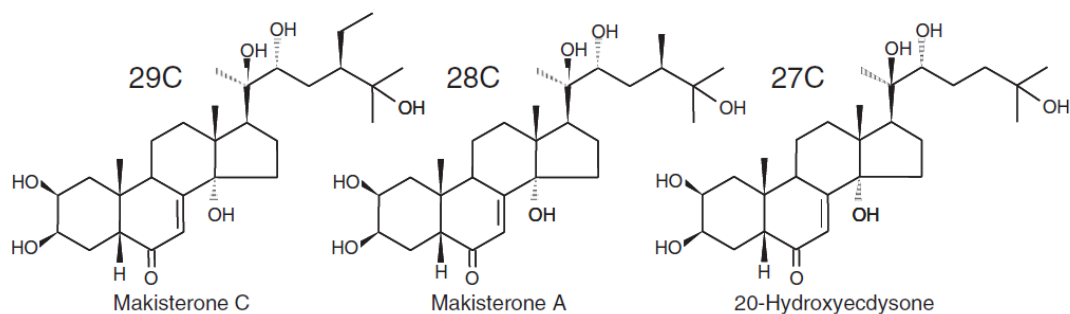
Figure 7: Structures of the main insect ecdysteroids.
(184).

1.7.1 Why are they of interest in sport supplement?

The characteristic pharmacological results of ecdysteroid treatment have led to the appearance of numerous ecdysteroid containing health-improvement products, food supplements and tonics (185) that is available commercially as over the counter (OTC) drugs. Over 140 different preparations containing ecdysteroids for oral use can be found on the market (185).

Ecdysteroids are considered adaptogenic and such preparations containing ecdysteroids are widely marketed to healthy peoples, body-builders and athletes as dietary supplements that can increase strength and muscle mass during resistance training, reduce fatigue and stress as well as ease recovery. The ecdysteroid-containing preparations are used with the aim of increasing physical power and endurance (186) in professional sports and building up the muscle fibers (187) (lean muscle), reduce fat (188) of body-builders, together with the consumption of protein. These products are made from various plant species, the most important of which are Leuzea, certain Pfaffia, Cyanothis, Ajuga and Polypodium species (185). They appear to be a deserved substitute for popular, but forbidden preparations such as the anabolic-androgenic products: Nerobol®, Durobolan® or Proviron®, used in speed and power sports (189) and selective Androgen Receptor Modulators (SARMs) or Insulin-like growth factor 1 (IGF-1) (187). The administration of anabolic-androgens is subject to severe limitation in both chemotherapeutic practice and the sports world, where these drugs are classified as prohibited stimulants.

Ecdysteroids have been used by athletes in Russia and some Asian countries since 1980. Ecdysteroids appear to be harmless to humans, even in high doses (5 mg/kg body weight per day of 20-HE, the most commonly consumed ecdysteroid, is generally recommended) and are not prohibited (190). The non-androgenic nature of these compounds makes their potential use in treating post-damage muscle regeneration and enhancing athletic performance (183, 191, 192).

1.7.2 Anabolic effects

Anabolic activities of increasing muscle size and strength is the most highlighted effect. The anabolic effects of ecdysteroids been reported in animals with increases in muscle fibers reported in rat (193-195) and mice (196-198) and growth and endurance in a wide variety of animals; sheep, pigs, and quail (194, 199-202) . These are consistent with these compounds having the ability to increase protein synthesis in skeletal muscle (187) and to reduce fat (188), both of which would enhance total work during training (186). The increase in protein synthesis appears to be related to increased messenger RNA (mRNA) translation efficiency and not to increased mRNA synthesis (199, 203). 20-hydroxyecdysone (the most commonly consumed ecdysteroid) attenuated tenotomy-induced muscle atrophy in predominantly slow-twitch muscle in rat (204). Thus, 20-hydroxyecdysone may have the potential to promote muscle recovery from disuse muscle atrophy (204) or regeneration of damaged muscle (192).

The most interesting aspects of ecdysteroids anabolic activity is that it seems to lack the androgenic side effects common among anabolic compounds. Although the anabolic effects of ecdysteroids are without androgenic side effects (183, 191), their potency have been compared with those of anabolic androgenic steroids, SARMs or IGF-1 in rats (187). However, this could not be demonstrated in resistance-trained human males who took the compound (205), thereby casting doubts on their effectiveness in human performance (192).

Many reports tried to explain ecdysteroids possible mode of action on the muscle. Although they are also steroids, ecdysteroids are structurally very different from androgens and androgen analogues. This reduces the likelihood that ecdysteroids would fit in the ligand binding pockets of the nuclear receptors designed for androgens. One suggestion is that their anabolic effects involve the activation of estrogen receptors (193). It has also been suggested that they stimulate protein synthesis by increasing polyribosomal activity (206) and translocation processes instead of the induction of new RNA synthesis. They may also increase mRNA translation efficiency (199, 203). Recent report showed that 20-HE attenuated tenotomy-induced muscle atrophy in predominantly slow-twitch muscle, partially mediated by ubiquitin proteasome pathway in rat skeletal muscle (204). These show that ecdysteroids are not likely to act as the classical steroids, via cytoplasmic receptor and regulation of gene transcriptional activity (207). These findings led to the hypothesis that ecdysteroids possibly bind to membrane bound receptors and they are likely to influence signal transduction pathways. A 20-HE GPCR on the cell membrane that would lead to activation of PI3K/Akt have been proposed, although there is yet no evidence for it (180, 208).

Vitamin D receptor has been proposed for the actions of ecdysteroids. This hypothesis was proposed based of their closely related chemical structures. Ecdysteroids exert some similar effects in vertebrates to those of the hormone 1,25-dihydroxyvitamin D3 which is produced in the kidney from 25-hydroxyvitamin D3. However, only one attempt is known to have been made to support this hypothesis, where docking of the 6-enol form of 20-HE to the vitamin D receptor resulted in a gold score value acceptable for the indication of a strong ligand-protein interaction (209). If this holds true, then ecdysteroids could benefits vascular system and muscle function in the same way that vitamin D status is well-described in clinical studies (210).

1.7.3 Vascular effects

In a recent report, ecdysteroids were shown to activate estrogen receptor β (ERβ) in-silico docking experiments (187) with 50% effective dose (ED$_{50}$) of 13 nM at human ERβ (193). Estrogen receptors are nuclear, and membrane bound receptors and generates biological responses via both genomic and rapid, nongenomic mechanisms. Since these receptors are expressed in endothelial cells and estrogen is a vasodilator (211, 212), ecdysteroids acting via these receptors would potentially cause vasodilation, which will increase blood flow and muscle performance. Moreover, 20-HE reported to increase the pool of free arachidonic acid and the synthesis of leukotrienes and prostaglandins (185) which might contribute to vasodilation. A 20-HE GPCR on the cell membrane had been proposed, which could signal vasodilation via the activation of PI3K/Akt/eNOS pathway (180, 213-216) besides PKC/MAPK (216) and ERK/MAPK (217) signaling cascades in some in vitro systems. In other reports, the antiatherosclerotic (218), antiarrhythmic (219, 220), antioxidative, antihypertensive (191) and anti-inflammatory (221) effects of phytoecdysteroids had been demonstrated. 20-HE have been also reported to counteract tumor necrosis factor (TNFα)-induced damage in human umbilical vein endothelial cells (222).

1.7.4 Other biological effects

Because of their steroidal structure and anabolic action, ecdysteroids have often been suspected of possessing the hormonal effects of vertebrate steroids (estrogens, androgens and corticoids). The estrogenic effect was assayed in female rats in the case of 20-HE but neither estrogenic nor antiestrogenic effects were observed (223). It also does not appear to have androgenic effect as already stated (224).

The glucocorticoid effect of ecdysteroids have been investigated with two different results. Minglei et al. (225, 226) identified compound-protein interaction of mineralocorticoid receptor with ecdysone. Moreover, ecdysone

was capable of both inducing and activating mineralocorticoids receptors, as evidenced by mineralocorticoids receptors nuclear accumulation in glomerular cells both in vitro and in vivo following ecdysone treatment. However, in vitro radioligand binding assays using estrogen, glucocorticoid and androgen receptor selective-radioligands failed to show effective ecdysteroid binding to the vertebrate steroid receptors (207).

Apart from protein synthesis (227), ecdysteroids reportedly affect lipid (218, 228-230) and carbohydrate metabolisms (231, 232) in mammals. They may also have hepatoprotective (233), nephroprotective (234), immune-protective (235, 236), antioxidant (237), anti-obesity and anti-diabetic (215, 230) properties. Ecdysteroid showed favorable effect on the subcutaneous thickness of the fat layer (238) as well as reducing abdominal fat depots of ovariectomized rats (239). In addition, ecdysteriods might promote skin regeneration (240).

1.8 Hypothesis and Aims

This study tested two main hypotheses:

1. The ability of COX to produce both vasodilators and vasoconstrictors puts it in a unique position to determine endothelial function and dysfunction. **Thus, the first hypothesis tested is that "the role of COX in altering endothelial function in small arteries is isoform specific".** To test this hypothesis, the following aims were developed and investigated:

    1.1 Determination of the specific roles of each of the two isoforms of the enzyme (COX-1 or COX-2) in the endothelial dilatory capacities of small arteries with varying degrees of endothelial functions.

    1.2 Determination of the role of thromboxane A2 prostanoid receptor (TP) activities in altering the endothelial dilatory capacities of small arteries with varying degrees of endothelial functions.

    1.3 Determination of the roles of nitric oxide and endothelium-derived hyperpolarization factors and their interaction with COX in small arteries with varying degrees of endothelial functions.

2. COX activity can be upregulated by reactive oxygen species (ROS) (167). In turn, ecdysteroids can both inhibit ROS formation and activate estrogen receptors (241). Therefore, the second **hypothesis is that "ecdysteroids have vasodilatory properties which are endothelium-dependent and involves changes in COX activity.** To test this, the following aims were developed and investigated:

    2.1 Characterization of the direct vasodilatory effect of 20-HE, the most common supplement-derived ecdysteroid.

    2.2 Determination of the roles COX and eNOS in the vasodilatory effect of 20-HE.

    2.3 Determination of the effect of 20-HE on COX isoform and eNOS gene and protein expression.

    2.4 Determination of the role of estrogen receptors in the observed effects of 20-HE.

Multiple experimental approaches were employed to address all the aims, including functional recording of vascular reactivity (wire myography), gene (q-PCR, microarray) and protein expression (Western blot) analysis. It is hoped that the vascular test model developed during this study would have application in the future for assessment of the vascular effects of substances that might affect blood flow and sports performance.

CHAPTER 2: Material and methodology

2.1 Samples collection

2.1.1 Human arteries

Arteries were dissected from within omental (OM) and subcutaneous (SC) adipose tissue samples obtained from consented obese patients who were undergoing laparoscopic bariatric surgery for weight loss at Hamad general hospitals and Al Emadi in Doha, Qatar. (Figure 8) is a representative picture of an adipose tissue sample and the arteries and veins within it.

The study was approved by the institutional (Anti-Doping Lab Qatar [SCH-ADL-070] and Hamad medical corporation Qatar [SCHJOINT-111]) and national (Shafallah Medical Genetic Centre [2011-013]) ethics committees and conducted in accordance with institutional guidelines. All participants provided written consents. Patients with serious illness were excluded such as coronary artery disease, malignancy and any other inflammatory conditions. Physical measurements of height and weight as well as blood pressure were taken at pre-surgery clinic visits. Body mass index (BMI) was calculated as the weight (kg) divided by the square of the height (m^2).

Two adipose tissue samples were obtained during surgery from the abdominal subcutaneous and intra-abdominal omental depots and immediately transported in serum-free medium (Cellgro) to the lab (Figure 8). Isolated arteries embedded in the tissues were then isolated and were either freshly assessed for reactivity by wire myography or stored at -80ºC until analyzed for mRNA and protein expression.
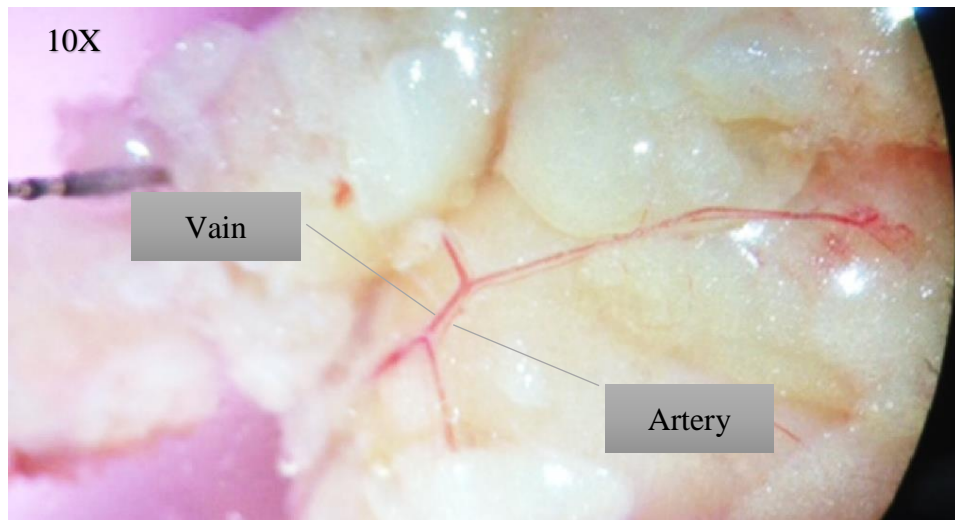
Figure 8: Sample of human adipose tissue with arteries and veins within it.

Under dissecting microscope x10, the arteries and veins can be seen running parallel to each other within the adipose tissue. Segments of arteries were taken and mounted, and the diameters were determined automatically as described in section 2.2.1.3 Normalization.

2.1.2 Ovine arteries

Arteries were isolated from within skeletal muscle (SKM, abdominal external oblique) and mesenteric (ME) tissue samples obtained from male sheep, which were euthanized at a government-controlled slaughter house in Doha. Pictures of representative samples are shown in Figure 9. Since the sheep were farmed and slaughtered for food in a government-controlled abattoir, no ethics approval was required.

Samples were quickly transported to the lab in normal physiological salt solution (NPSS). The NPSS contained (in mM) 112 sodium chloride, 5 potassium chloride, 1.8 calcium chloride, 1 magnesium chloride, 25 sodium hydrogen carbonate, 0.5 potassium dihydrogen phosphate, 0.5 sodium dihydrogen phosphate, and 10 glucose (bubbled with 95% O_2/5% CO_2 to pH 7.4). Arteries were then isolated from within the tissues. Some of the arteries were assessed

for reactivity by wire myography and the remainder were either treated with 1 µM 20-HE for 1 hour and snap frozen or were stored untreated at -80ºC until analyzed for mRNA and protein expressions.
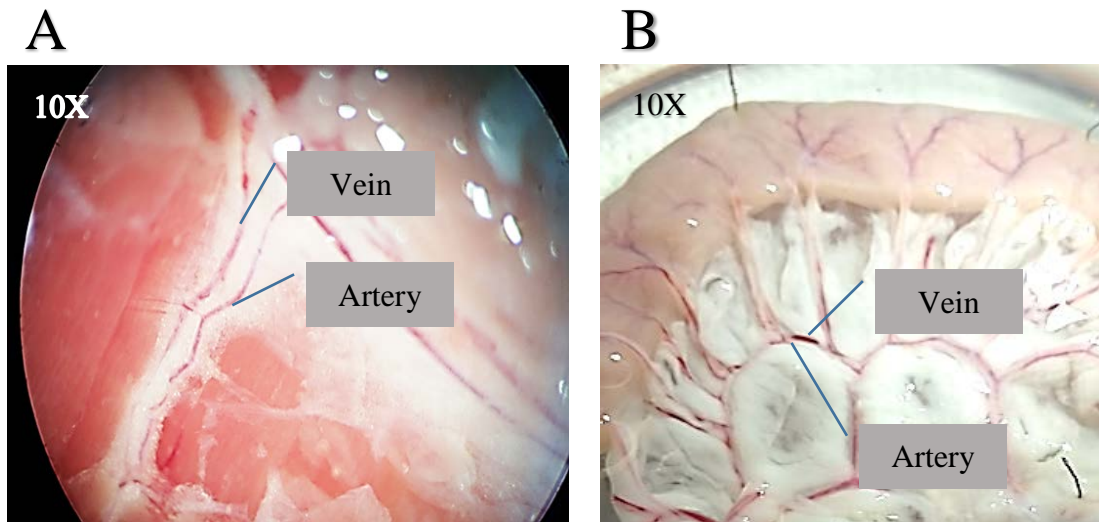
Figure 9: Ovine tissue samples.

Samples of ovine (A) SKM and (B) ME tissue with arteries and veins within them. Under dissecting microscope 10X, the arteries and veins can be seen running parallel to each other within the tissues. Segments of arteries were taken and mounted, and the diameters were determined automatically as described in section 2.2.1.3 normalization.

2.1.3 Human coronary artery endothelial cells (HCAEC)

Human Coronary Artery Endothelial Cells (HCAEC) were purchased from Lonza (CC-2585, Walkersville, USA) and maintained in Microvascular Endothelial Cell Growth Medium-2 (EGM®-2MV BulletKit®, CC-3202, Lonza, Walkersville, USA) supplemented with human hepatocytes media singleQuots (HCM, CC-4182, Lonza, Walkersville, USA), in accordance with the manufacturer's protocol. All cells were maintained at 37ºC in a humidified atmosphere with 5% CO_2. After the cells reach 70-85% confluency, cells were transferred to multiwell cell culture plates ready for experimenting.

2.2 Measurement of vascular reactivity

2.2.1 Artery preparation

2.2.1.1 Dissection

Under a dissecting microscope, arteries were isolated from within the tissues described above. They were carefully cleaned of surrounding tissues and cut into segments (~2 mm long).

2.2.1.2 Mounting

Segments of the arteries were mounted on a pair of wires (40 μm thick) in an auto dual wire myograph system (model 510A, Danish Myo Technology, DMT, Aarhus, Denmark) covered in NPSS. The mounting steps are as represented in Figure 10. In brief, a wire with length of ~2.2 cm was 1st attached to the jaws of the myograph and clamped. Using forceps, the vessel was held close to the proximal end, and pulled over the wire. A second wire was then inserted and aligned in parallel with the 1st within the vessel. The ends of the wires were then screwed onto the left and right nuts on the mounting jaws.

When necessary, further cleaning was carefully carried out at this stage to remove any surrounding connective tissues before the segment was tensioned to normalize it for experiments.
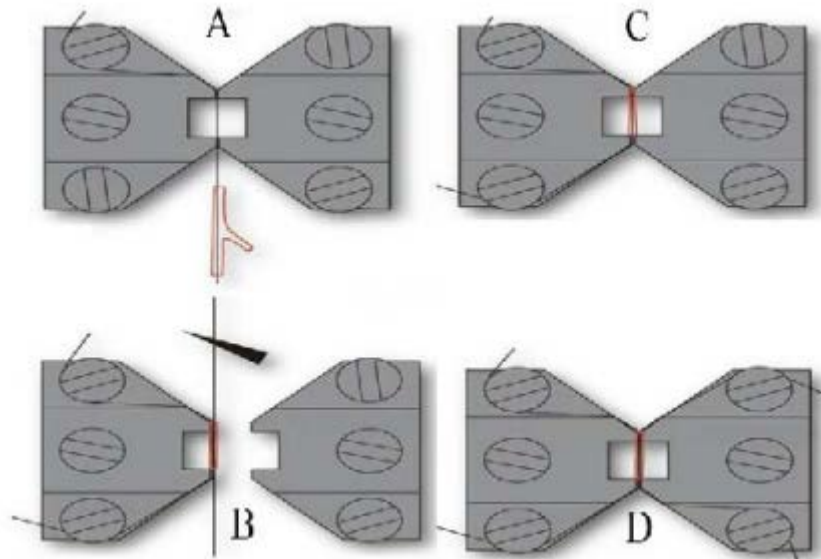
Figure 10: Mounting of a vessel segment on the wire myograph.

A-D represent the main steps during the mounting of an arterial segment on the wire myograph as described in the text (DMT User Manual).

2.2.1.3   Normalization

The segments were pre-tensioned automatically under a transmural pressure that was equivalent to 100 mmHg (13.3 kPa) and were continuously aerated with 95% O_2 and 5% CO_2 at 37°C. The internal diameter (ID) of each artery mounted segments was determined automatically as described in manufacture manual (DMT User Manual) and as previously described (91).

2.2.1.4   Equilibrium

After normalization, an equilibration period of at least 1 hour was allowed before experiments were conducted. During this period, the vessel was stimulated with 90 mM potassium chloride (KCl) to assess vessel viability and with noradrenaline (10 µM for human arteries, 10-100 µM for ovine arteries) to optimize contractile responses. The segment was considered viable if tension

57

of at least 1 mN was recorded in response to 90 mM KCl. Segments that failed this test were replaced.

Dose response to ACh was recorded in most vessel segments as a measure of endothelial function. In few cases where such responses were not recorded, single response to 10 μM ACh was recorded to determine endothelial integrity.

2.2.2 Experimental protocol

2.2.2.1 Assessment of vasodilation

To assess vasodilation, vessels were first contracted with noradrenaline (1-10 μM, equivalent to E_{max75} for each segment). When tone was stable, cumulative concentration-relaxation curves were generated for acetylcholine (ACh, classical endothelium-dependent dilator, 10^{-10}-$10^{-4.5}$ M), bradykinin (BK, potent endothelium-dependent dilator, 10^{-11}-10^{-6} M), sodium nitroprusside (SNP, endothelium-independent dilator, 10^{-10}-$10^{-4.5}$ M), 20-hydroxyecdysone (20-HE, ecdysteroid, 10^{-10}-$10^{-5.5}$ M) or β-estradiol (estrogen receptor agonist, 10^{-9}-$10^{-5.5}$ M). Each drug was applied in a cumulative manner starting from the smallest dose to the highest and allowing for the effect of each dose to be established before the next was applied. Where possible, more than one curve was obtained for same segment separated by 30-60 min washout period. Percentage relaxation was calculated as change in tone caused by each dose, divided by the initial tone due to noradrenaline, then multiplied by 100.

2.2.2.2 Role of eNOS, COX, EDH and ER in vasodilation responses

To assess the roles of eNOS, COX, EDH and ER in the vasodilation recorded in this study, experiments were conducted in the presence of respective antagonist. Concentrations of various agents used were chosen based on previous reports as referenced in each case below.

58

The contributions of COX were determined by pretreatment with 10 µM indomethacin (non-selective COX inhibitor) (141), 1 µM FR122047 (selective COX-1 inhibitor) (242) or 4 µM celecoxib (selective COX-2 inhibitor) (243). The contribution of endothelial NOS was assessed by pretreatment with 100 µM Nω-Nitro-L-arginine methyl ester (L-NAME) (244), while the role of endothelium-dependent hyperpolarization (EDH), were determined in the presence of 30 mM KCl (245, 246).

The involvement of ERα and β in 20-HE-induced relaxation were assessed in the presence of 1 uM ICI.182.780 (unspecific ER antagonist) (211, 247), 1 µM PHTPP (selective ER-β antagonist) (247, 248), or 0.5 µM methyl-piperidinopyrazole (MPP) (selective ERα antagonist) (249, 250).

2.2.2.3   Assessment of vasoconstriction

Vasoconstriction was assessed by constructing cumulative concentration-contraction curves for noradrenaline (10^{-9} - $10^{-5.5}$ M) and the thromboxane analogue U46619 (10^{-9} - 10^{-6} M). Where possible, more than one dose–response curve was obtained in the same preparation separated by a washout period of 30–60 min.

2.3   Gene expression studies

2.3.1   RNA extraction

Isolated arteries (~0.5g) were crushed in liquid nitrogen using a mortar and pestle and RNA solubilized using 0.8 ml TRIzol™ reagent (Ambion, USA). On a vortex, Trizol were mixed by 10 cycles of 5 seconds each and separated by 5 seconds on ice then liquid transferred to new cold tube. Afterward chloroform (1/10 of recorded volume) was added followed by 15 seconds of mixing on a vortex and incubation for 5 minutes on ice. This was followed by centrifugation

for 15 minutes at 14,000 rpm in 4°C. Aqueous phase was then collected in separate cold tube and equal volume of isopropanol was added to cause phase separation. Samples were left at -20 °C for 1.5 hours, then centrifuged for 15 minutes at 14,000 rpm at 4°C. Isopropanol was then removed very carefully. The resulting pellet was washed several times with 75% ethanol followed by drying period on ice with lid opened tube until ethanol evaporation. Finally, the pellet was re-suspended in 45 µl of RNase free water and left at room temperature for 10 min. The yield and purity of RNA extracted were checked using NanoDrop spectrophotometer (NanoDrop 2000, Thermo Fisher, USA). The concentration of RNA was measured at 260 nm and purity from contamination determined by the ratios between 260 nm and 280 nm (260/280) and between 260 nm and 230 nm (260/230). 260/280 and 260/230 ratios within [1.8-2] were accepted purity for RNA. RNA was normalized based on concentration (200 ng). RNA samples were stored at -80°C until used for microarray or q-PCR.

2.3.2   Microarray gene expression

Total RNA was used to synthesize complementary RNA (cRNA) probes for hybridization to Affymetrix GeneChip™ Ovine Gene 1.1 ST 24-Array Plate high-density transcriptome profiling microarrays (including 508,538 probe sets corresponding to about 22,047 genes with probes/gene ratio 23) (Affymetrix, USA) allowing Gene-level expression profiling of well-annotated genes (Gene Expression Analysis Technical Manual, Figure 11). In brief, equal quantities of high-quality total RNA was reverse transcribed into single-stranded cDNA using an oligo(dT)24 primer containing a T7 polymerase promoter binding site. The cDNA was then used as a template to synthesize cRNA by in vitro reverse transcription, with incorporation of biotinylated nucleotides (GeneChip® WT PLUS Reagent Kit). Labeled ss-cDNAs were fragmented and hybridized to oligonucleotide microarray (Affymetrix GeneChip™ Ovine Gene 1.1 ST 24-Array Plate). Hybridized arrays were washed, then stained with streptavidin–phycoerythrin, rewashed, treated with biotinylated antistreptavidin–

phycoerythrin antibodies and re- stained with streptavidin–phycoerythrin, according to the manufacturer's protocols for affymetrix GeneTitan system. The stained arrays were finally scanned in the same system (Affymetrix, USA). the CEL files generated from the scanning were analyzed through Affymetrix Expression Console Software (TAC, version 4).
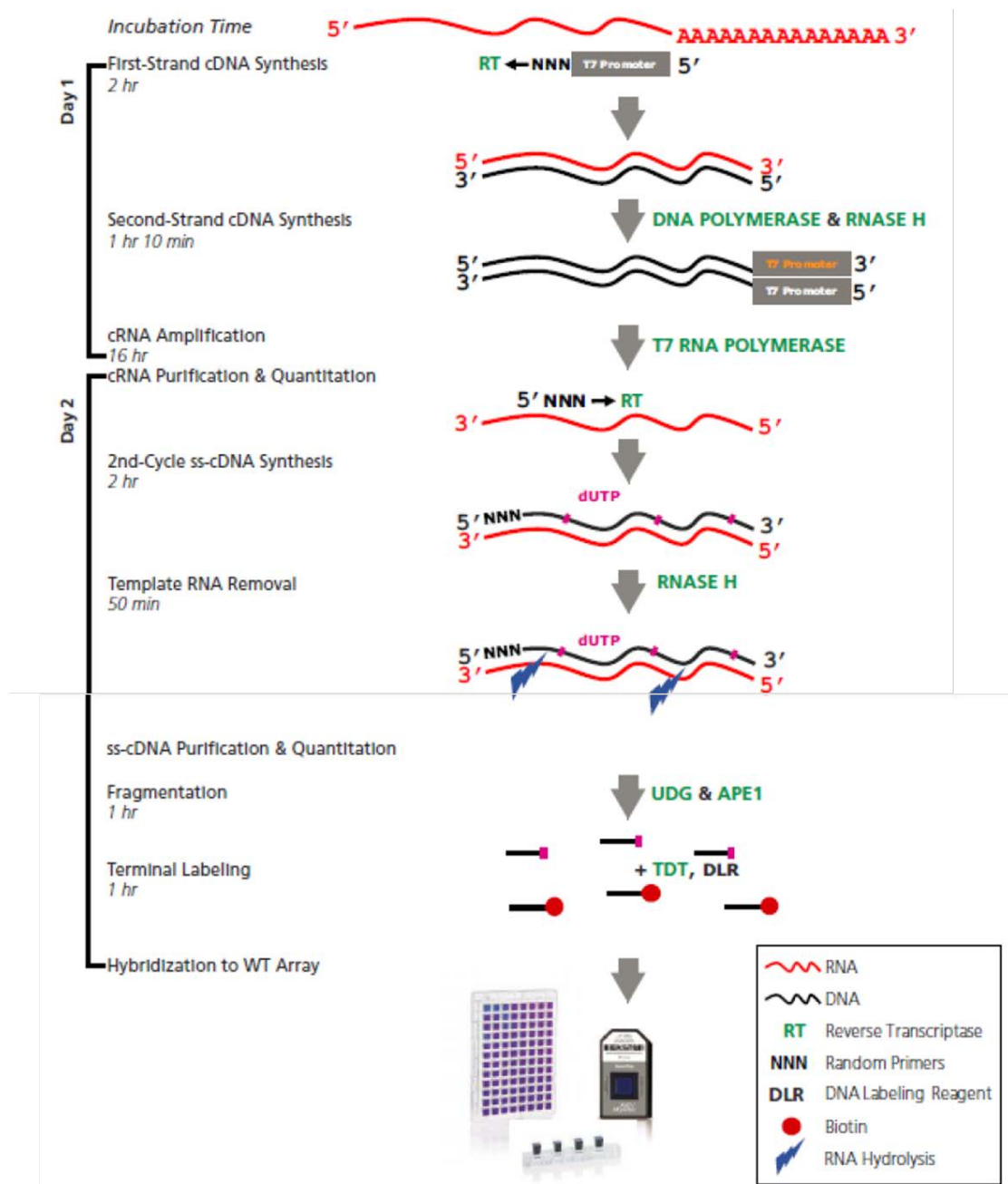
Figure 11: Whole Transcript (WT) PLUS Amplification and Labeling process.

(WT PLUS reagent kit manual).

2.3.3 cDNA synthesis

RNA was converted into cDNA prior to q-PCR by the following procedure. For the first strand of cDNA synthesis, 100-200 ng of total RNA was added into reverse transcription reaction mixture (High-Capacity cDNA Reverse Transcription Kit, Applied Biosystems™, USA) according to manufacturer's instructions. Reverse transcription was carried out by incubating samples for 10 min at 25°C; 120 min at 37°C; 5 min at 4°C on PCR machine (Applied Biosystems™, USA). cDNA samples were stored at -20°C until used.

2.3.4   Quantitative PCR (q-PCR)

Quantitative analysis of target mRNA expression was performed with Quantitative Polymerase Chain Reaction q-PCR using the comparative cycle threshold ($\Delta\Delta$CT) curve method. For this, total RNA was analyzed using commercial primers. Target gene transcription was measured by RT^2 SYBR green qPCR (Qiagen, Germany) according to manufacturer's instructions. Primer of housekeeping gene were used for normalization. 100 µM of each primer was reconstituted and diluted in 1:40. Reaction was carried out in duplicate in 96-well plate using 20 µl total volume per well. Each well contained mixture of SYBER green solution, primer, cDNA and nuclease-free water. Reaction was carried out on ViiA7 real-time PCR system (Applied Biosystems™, USA). Initial denaturation (95°C, 15 min), followed by (95°C, 15 Sec; 55 °C, 30 Sec and 70°C, 30 Sec) for 40 PCR cycles, after that melting curve stage (95°C, 15 Sec; 60 °C, 1 Sec and 95°C, 15 Sec). The cycle threshold (Ct) results were at (0.02), target threshold was set at (0.2), Ct value was used to quantify the gene expression between the cycles 4 to 25 with CT having inverse relationship with gene expression. Data were therefore expressed as ratio of housekeeping gene to target gene. Results are grouped as tissue type or control compared to each treated group with 1 µM 20-hydroxyecdysone.

2.4 Protein expression studies

2.4.1 Protein extraction

Frozen isolated arteries or HCAEC were crushed into powder and solubilized in radioimmunoprecipitation assay (RIPA) lysis buffer with protease inhibitors (50 mM Tris-HCl, pH 8.0, 1% NP-40, 0.5% sodium deoxycholate, 0.1% SDS, 150 mM NaCl, 2 mM phenylmethylsulfonyl fluoride, 0.2 U/ml aprotinin) (Sigma, Germany). After lysis for 50 min on ice, the mixture was centrifuged at 12,000 × g at 4°C for 5 min. The protein concentration of the supernatant was determined by BCA protein assay (Pierce™ BCA™ Protein Assay, 23225, Thermo Scientific™, USA). In brief, standard curve was built by using diluted bovine serum albumin (concentration: 0.125, 0.25, 0.5, 0.75, 1, 1.5 and 2 µg/ml). Working reagent was prepared by mixing 50 parts of BCA Reagent A with 1 part of BCA Reagent B (50:1, Reagent A:B). Then, 10 µl standards and samples were loaded into 96-well plate followed by 200 µl of working reagent. The plate was incubated at 37°C for at least 30 min. Change in color was observed from light to darker blue or purple. Plate was cooled to room temperature and absorbance was measured at 562 nm. The results were calculated by plotting the standard concentration and absorbance to derive the equation $Y=mX+C$, where X= protein concentration, Y is the absorbance, m is the slope and C is intersection.

2.4.2 Western blot

Protein samples were mixed with sodium dodecyl sulfate (SDS) loading buffer (1:1) before denaturation in boiling water bath for 10 min. Afterwards, calculated volume of 50 µg of protein of samples and 7 µl protein ladder (Amersham ECL Rainbow Molecular Weight Markers, GE Healthcare, USA) were loaded into 12 % sodium dodecyl sulfate-polyacrylamide gel for electrophoresis (mini-protean tgx precast gels, 456-1045, BioRad, USA). Gel was run at 150 V for 45 min in a running buffer (1X Tris-glycine: 25 mM Tris base, 190 mM glycine and 0.1% SDS, pH around 8.3) until the bromophenol blue dye front has reached the bottom.

The resolved proteins were transferred in a "sandwich "to nitrocellulose membranes on ice (125 V, 2 hour) in transfer buffer (48 mM Tris, 39 mM glycine, 0.04% SDS, 20% methanol) The transfer "sandwich" was assembled by three sponges, first filter paper, gel, nitrocellulose membrane, second filter paper and the other three sponges. The electrophoretic gel transfer was carried out in the transfer blotting module (XCell II Blot Module, Invitrogen, UK) and the membranes blocked in 20 ml blocking solution (5% skimmed milk in phosphate-buffered saline (PBS) with 0.1% Tween 20) for 1 hour at room temperature. The membranes were then incubated with primary antibody diluted in blocking solution (3% skimmed milk in PBS) at 4°C overnight. After washing (x3 of 15 min) with PBS containing 0.1% Tween-20, the membranes were incubated with appropriate horseradish peroxidase-conjugated secondary antibody for 45 min at room temperature. Thereafter, the membrane was washed (x3 of 15 min) with PBS containing 0.1% Tween-20 and developed with chemiluminescence detection kit (Pierce™ ECL Western Blotting Substrate; 32209; Thermo Fisher, USA) for imaging. Images were acquired by ImageQuant LAS 4000 (28955810, GE Healthcare, USA) and analyzed with GASepo software (WADA (251)). The relative content of proteins was expressed as target protein to GAPDH ratio.

2.5   Statistical analysis

2.5.1   Vascular reactivity

Vascular reactivity data were recorded using powerLab acquisition system and Lab Chart software (DMT, Denmark). In response to each drug dose, vessel tension was recorded. Change in contractile tension was expressed relative to vessel ID, while relaxation was expressed as % change relative to the initial tension due to noradrenaline.

Data were analyzed using GraphPad Prism software version 6.00 for Windows (GraphPad Inc. La Jolla, Ca. USA). Normality of distributions was tested with the Kolmogorov-Smirnov test. Data are shown as mean ± standard error of mean (SEM) or Standard deviation (SD), and for non-normally distributed data as median (interquartile range). Agonist concentration-response curves were constructed on log scale and data fitted using the sigmoidal fitting routine in Prism. The concentration of agonist causing 50% of maximum response is expressed as the log EC_{50} and used as a measure of sensitivity to the agonist. Significant effects were determined using Student's paired and unpaired t-test or two-way ANOVA as appropriate. Significance was defined as $p < 0.05$ and n = number of samples or experiments.

2.5.2 Microarray gene expression

Differential gene expression and clustering row data were analyzed using TAC 4.0 as computational tools (Applied Biosystems, Foster City, CA, U.S.A.) which use a robust multiarray average (RMA) algorithm (252) for background correction and normalization of fluorescent hybridization array signals, both at internal (intra-microarrays) and comparative (inter-microarrays) levels. RMA was selected over others available, MAS5 (Affymetrix 2001) and PLIER, (a model-based algorithm, Affymetrix 2003) because it was deemed to provide the best precision in signal detection to achieve adequate multiple-chip normalization (253), especially in cases of low-level gene expression (252, 254) by producing efficient quantile normalization of the distribution of probe intensities from each array in the context of a complete set of arrays.

RMA was applied to the data set of 24 microarray hybridizations including replication corresponding to each of the different treatment under study. After quantitation of expression level of each probe set in all microarrays analyzed, the false discovery rate (FDR) algorithm (255, 256) was used to identify probe sets displaying significant differential expression when comparing the

experimental to the control group. This algorithm performs multiple hypothesis testing to correct for multiple comparisons.

Normalized data were analyzed, an unpaired t-test was applied to identify differentially expressed transcript genes between sample pairs and probes with corrected FDR P-values < 0.05 were declared significant. The filtered gene list was functionally annotated with the use of reports from databases. Hierarchical cluster analysis with signal intensity of differentially expressed genes and the distance metric used between objects is the euclidean distance. Distances between clusters of objects are computed using the complete linkage method (maximum distance between a pair of objects in the two clusters). Results are displayed in principal component analysis (PCA), table, volcano plot, heat map and dendrogram.

2.5.3 IPA

Ingenuity pathway analysis (IPA, http://www.ingenuity.com, Ingenuity Systems, USA) was used to inter-connect differential expressed genes in a context specific manner within signaling and metabolic pathways, molecular networks and biological processes that are most significantly perturbed. A cut off value of 2 (fold change) was set as a threshold for up- and down-regulation. IPA-Core analysis integrates experimental data with its knowledge base containing a repository of molecular interactions and functional annotations extracted from selected, manually curated, literature sources and databases. IPA version 8.6 (content version 3002) has been used with following filter settings: (data sources = Additional interactions OR Ingenuity Expert Findings OR MicroRNA-mRNA interactions OR Protein-protein interactions).

The significance of the association between the data set and the canonical pathways identified was measured by Fisher's exact test (p<0.01). This was followed by Benjamini-Hochberg multiple testing correction to calculate a p-value determining the probability that the association between the genes in the

data set and the canonical pathway can be accounted for by chance only. The generated networks were ranked by a score based on the inverse log of a p-value generated using the same Fisher's exact test as above. This considers the number of genes that participated in a given network relative to the total number of genes in the global molecular network stored in the Ingenuity pathway knowledge base. A score of three indicates that there is a 1/1,000 chance that the focus genes are in a network due to random chance. Therefore, scores of three or higher have a 99.9% confidence level of not being generated by random chance alone.

2.5.4   q-PCR

Data analyses were performed using the comparative CT Method (ΔΔCT Method) with housekeeping gene to which changes in mRNA levels were normalized against.

$$2^{\Delta\Delta CT} = (2^{-\Delta CT \ of \ group})/(2^{-\Delta CT \ of \ control})$$

The average Ct values and standard deviations for the housekeeping gene and the gene being tested were calculated. Then the differences between tested experimental group and housekeeping experimental was delta Ct value (ΔCt) values. Double delta Ct (ΔΔCt) value were calculated by the difference between groups ΔCt. The value of 2^-ΔΔCt were calculated to get the expression fold change. Results are expressed in ratio of housekeeping gene to target gene. Significance was defined as $p<0.05$ and n = number of samples or experiments.

2.5.5   Western blot

Analysis was quantified in triplicates. Image quantification analysis was performed using the GASepo software (WADA (251)). Statistical analysis was performed using Graphpad Prism software (GraphPad, USA) and values are given as mean ± standard deviation (SD). For comparison between the groups, the Student's t-test or Mann Whitney U test was used as appropriate. Results

are expressed in ratio of target gene to GAPDH. Significance was defined as p<0.05 and n = number of samples or experiments.

CHAPTER 3: Double-edged regulation of vascular tone by COX in healthy resistance arteries-role of isoforms

3.1 Introduction

COX is the rate limiting enzyme in the production of prostanoids including PGI_2 (vasodilator) and TXA_2 (vasoconstrictor). It converts arachidonic acid to unstable endoperoxide intermediates PGG_2 and PGH_2 (257). PGH_2 can either function as an active molecule or is metabolized by the action of specific isomerases or synthases into prostaglandins, PGD_2, PGE_2, $PGF\alpha_2$, PGI_2, or TXA_2 (257).

PGI_2 acts mainly through activation of the G-protein coupled prostacyclin (IP) receptor. PGI_2/IP receptor interaction stimulates increases in cAMP and protein kinase A, resulting in decreased intracellular calcium ion ($[Ca^{2+}]i$), and could also cause inhibition of Rho kinase, leading to vascular smooth muscle relaxation (89). TXA_2 acts through specific G-protein coupled TP receptor. Activation of TP receptor leads to phospholipase C activation, release of inositol triphosphate (IP3), and an increase in $[Ca^{2+}]i$, thus triggering the smooth muscle contraction (258). Therefore, the PGI_2/TXA_2 balance is critical in the regulation of vascular tone, specifically because most vascular smooth muscle expresses TP and IP receptors (79).

COX-1 is the constitutive isoform of the COX enzyme and is highly expressed in the endothelium, monocytes, platelets, renal collecting tubules, and seminal vesicles (50). On the other hand, COX-2 is the inducible form which is expressed mainly in response to inflammatory stimuli such as bacterial lipopolysaccharides (LPS), growth factors, cytokines, and phorbol esters (259-261). Under these conditions, COX-2 expression is notably increased in monocytes, macrophages, neutrophils, and endothelial cells (262-264). Thus, COX-2 is undetectable in most tissues in the absence of stimulation.

In recent times, both COX-1 and COX-2 have been shown to catalyze the synthesis of prostaglandins under physiological conditions in both animals and humans. McAdam et.al (265) identified COX-2 as a major source of systemic prostacyclin biosynthesis in healthy humans, while Baber et.al (266) reported that TXA_2 produced by both COX-1 and COX-2 is a major prostanoid formed in healthy rat lung. In addition, Caughey et.al. (82) observed that untreated HUVEC expressed only COX-1 and that predominant COX-1 product was TXA_2. However, in the vasculature, the involvement of these isoforms in determining the balance between relaxant (PGI_2, PGE_2) and contractile TXA_2 prostanoids is not well understood (267-269). Thus, the aim of this chapter is to determine the roles of COX-1 and COX-2 in the double-edged effects of this enzyme in resistance arteries under healthy conditions.

Aims

1.1 Determination of the activities of the different COX isoforms in arteries with normal endothelial functions.

1.2 Determination of the responsiveness to contractile prostanoids of arteries with normal endothelial functions.

3.2 Methods

3.2.1 Vessel preparation

Arteries were isolated from samples of abdominal SKM and ME collected from healthy male sheep, which were slaughtered for meat at a local slaughterhouse. The arteries were cleaned of surrounding tissues and either tested for reactivity or ground in liquid nitrogen for gene and protein expression analysis.

3.2.2 Vascular reactivity studies

Vascular reactivity was investigated using the method described in detail in chapter 2 section 2. The normalized internal diameter for arteries used in this chapter were 286±18 µm for SKM arteries and 334±15 µm for ME arteries.

3.2.2.1 Endothelium-dependent relaxation

Endothelium-dependent relaxation was assessed by constructing concentration-relaxation curves for ACh (the classical endothelium-dependent dilator). Arteries were first precontracted with 10 µM NA to build a stable tone. Thereafter, ACh (10^{-9} - $10^{-4.5}$ mM) was added cumulatively starting with the least concentration, and changes in tone recorded. A representative tracing is shown in (Figure 12) in SKM arteries. Data were recorded with a PowerLab/LabChart data acquisition system (ADinstrment/Myotech, Denmark) as described previously in chapter 2 section 2.
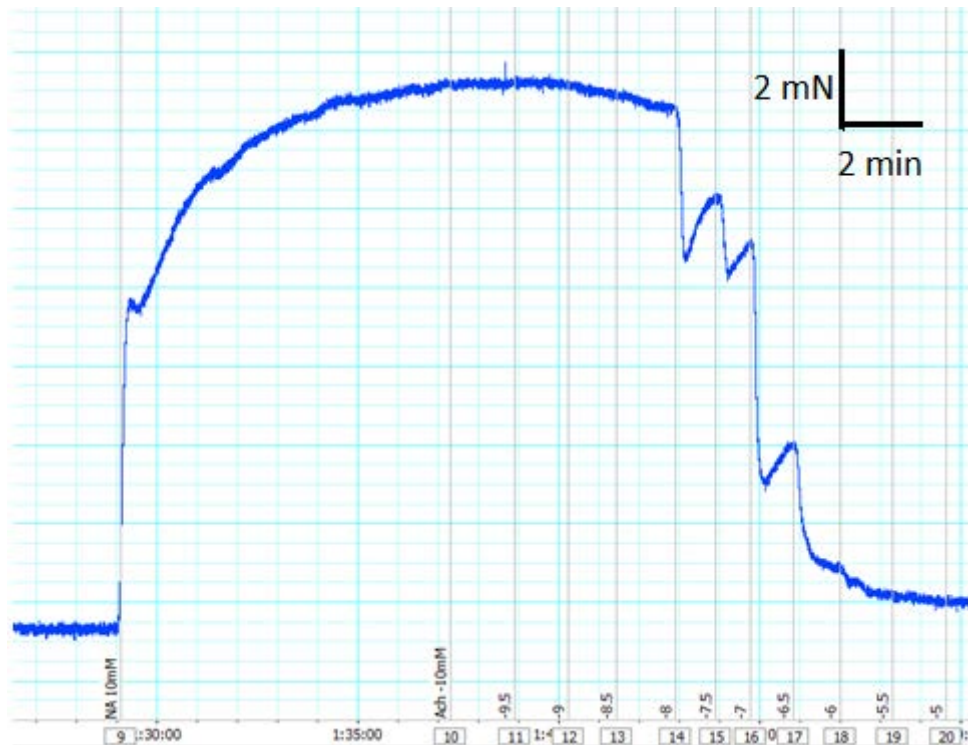
Figure 12: Representative tracing showing the general protocol of relaxation response to ACh in SKM arteries.

The vessel tone decreased with increasing doses of ACh (10^{-9} - $10^{-4.5}$ mM). Image was acquired using LabChart software. Lowest point of each response was taken and % relaxation calculated relative to initial tone by NA.

3.2.2.2 Role of eNOS, COX and EDH in Endothelium-dependent relaxation

Endothelial nitric oxide synthase, cyclooxygenase enzyme, and endothelium-dependent hyperpolarization are the three main mediators of endothelium-dependent relaxation. To determine their contributions to ACh relaxation of SKM and ME arteries, curves were generated in the presence of 100 µM L-NAME, 10 µM indomethacin or 30 mM KCl, respectively. L-NAME and indomethacin were added at least 30 minutes before ACh curves were generated. KCl was added just prior the addition of NA.

To determine the roles of specific COX isoforms, FR122047 (1 μM) and celebcoxib (4 μM) were used to specifically block COX-1 and COX-2 respectively and were added at least 30 minutes before ACh curves were generated.

To test whether basal TP receptor activity had any influence on the ACh response, curves were constructed in the presence of ICI 185.282 (0.1 μM), which was added for 30 min prior to recording ACh relaxation.

3.2.2.3 Endothelium-independent relaxation

Endothelium-independent relaxation was assessed by constructing concentration-relaxation curves for sodium nitroprusside (SNP, a direct NO donor). Artery segments were first precontracted with 10 μM NA to build a stable tone. Thereafter, SNP (10^{-10} - $10^{-3.5}$ mM) was added cumulatively starting with the least concertation and changes in tone were recorded.

3.2.2.4 Vasoconstrictor responses

Vasoconstriction was assessed by constructing cumulative concentration-response curves for NA (10^{-8} - $10^{-3.5}$ M) and U46619 (thromboxane A2 analogue, 10^{-9} - 10^{-5} M) on the same segment with a washout period of at least 30 minutes between the two curves. With this protocol, there was no apparent time-dependent change in the response to any of the vasoconstrictors. This protocol allowed for comparison between TXA_2 receptor-mediated vs. noradrenergic receptor-mediated contractile responsiveness of the same segment. (Figure 13) is a representative tracing of NA contractions in ME arteries.
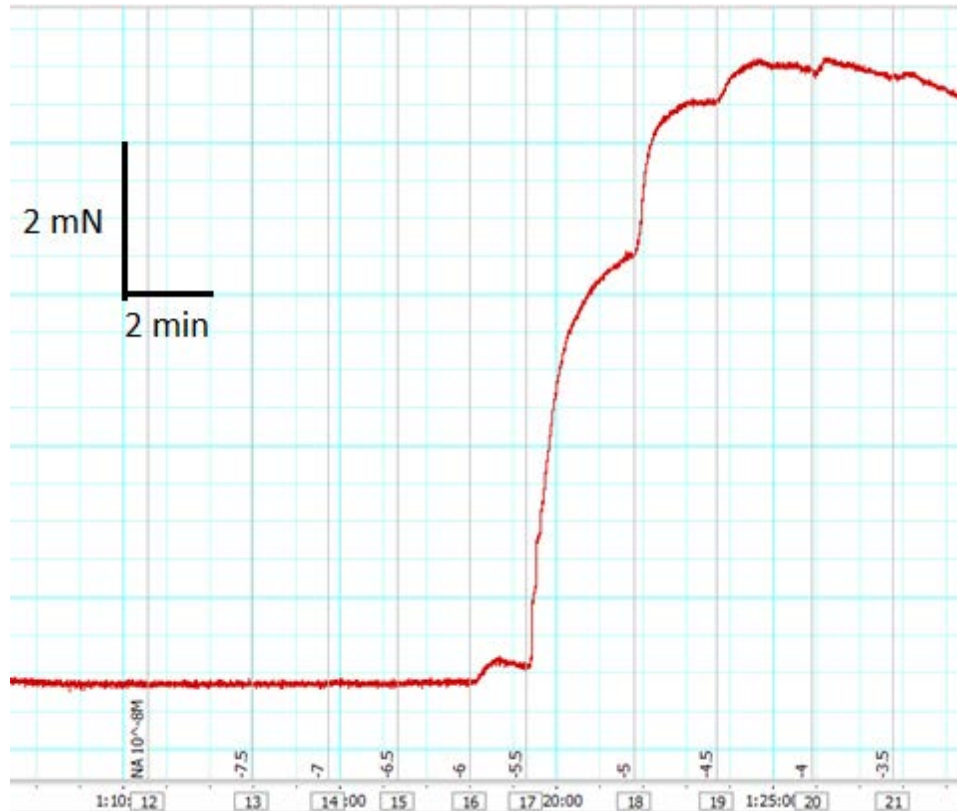
Figure 13: Representative tracing showing the general protocol of contractile response to NA.

The vessel tone increased with increasing doses of NA (10^{-9} - $10^{-4.5}$ mM). Image was acquired using LabChart software. The maximum points were taken as responses to the doses for NA.

3.2.3 Gene expression studies

3.2.3.1   Microarray gene expression analysis

SKM and ME isolated arteries were ground in liquid nitrogen and RNA extracted using Trizol following manufacturer's instructions (Invitrogen, Carlsbed, CA, USA). Total RNA was then used to synthesize cRNA (GeneChip® WT PLUS Reagent Kit) probe for hybridization to GeneChip™ Ovine Gene 1.1 ST 24-Array Plate high-density transcriptome profiling microarrays obtained from (Affymetrix, USA). This microarray was used to analyze regulated gene expression in SKM and ME arteries. An experimental approach using six microarray per group (n=6) was applied. Analysis of differential gene

expression was performed by comparison of gene expression patterns using TAC software (Affymetrix, USA) which normalizes array signals using RMA algorithm. Details described in chapter 2 section 3. Results are presented in PCA, table, volcano plot, heat map and dendrogram.

3.2.3.2   q-PCR analysis

SKM and ME arteries were ground in liquid nitrogen and RNA extracted using Trizol following manufacturer's instructions (Invitrogen, Carlsbed, CA, USA). cDNA was synthesized from 200 ng total RNA using Reverse Transcription Reagent Kit (Applied Biosystems, New Jersey, USA). The mRNA expressions of target genes were determined by q-PCR performed on ViiA7 (Applied Biosystems™, USA). Target gene primers COX-1, COX-2 and eNOS were obtained from Integrated DNA Technologies (IDT, USA). 100 µM of each primer was diluted (1:40) (Table 3) and reactions were carried out in duplicate in 96-well plate using 20 µl total volume per well. Each well contained mixture of SYBER green solution, primer, cDNA and nuclease-free water. Data were normalized to GAPDH as house-keeping gene and expressed as ratio (GAPDH/ target gene). Details described in chapter 2 section 3.

Table 3 :Ovine primer sequences for q-PCR.

Gene Primer Name	Forward primer sequence (5'-3')	Size (bp)	Reverse primer sequence (5'-3')	Size (bp)
β-actin	5'-ATGCCTCCTGCACCACCA-3'	18	5'-GCATTTGCGGTGGACGAT-3'	18
GAPDH	5'-GTTCCACGGCACAGTCAAGG-3'	20	5'-ACTCAGCACCAGCATCACCC-3'	20
COX-1	5'-ATGAGTACCGCAAGAGGTTTGG-3'	22	5'-ACGTGGAAGGAGACATAGG-3'	19
COX-2	5'-CAGAGCTCTTCCTCCTGTGC-3'	20	5'-CAAAAGGCGACGGTTATGC-3'	19
eNOS	5'-GGCAGACCCCACCTTCTTGG-3'	20	5'-CCACACTCTTCAAGTTGCCCAT-3'	22

3.2.4 Protein expression studies

To determine the expression levels of COX-1, COX-2 and eNOS proteins in SKM and ME isolated arteries, western blot analysis was conducted using specific primary antibodies for COX-1 (polyclonal antibody, dilution factor 1:200, 160103, Cayman Chemical, USA), COX-2 (polyclonal antibody, dilution factor 1:200, 160106, Cayman Chemical, USA), eNOS (polyclonal Antibody, dilution factor 1:1000, PA1-037, Invitrogen, USA) and GAPDH control antibody (polyclonal antibody, dilution factor 1:2500, ab9485, abcam, UK). As a secondary antibody, anti-rabbit IgG (polyclonal antibody, dilution factor 1:30,000, A0545-1ML, Sigma, USA) and anti-mouse immunoglobulin/HRP (polyclonal antibody, dilution factor 1:2000, P0161, DAKO, USA) were used as appropriate. Detailed procedures are described in chapter 2 section 4.

3.3   Results

3.3.1 Vascular reactivity studies

3.3.1.1   Endothelium-dependent relaxation of ME and SKM arteries

To assess the functional state of the endothelium in SKM and ME arteries, ACh-induced endothelium-dependent relaxation was recorded in segments of both arteries. ACh caused concentration-dependent relaxation of both SKM and ME arteries (Figure 14) with an I_{max} of 88.9±1.7 % and 86.2±4.1 % respectively. The log IC_{50} values for relaxation of the two arteries were -7.6±0.1 M and -6.9±0.2 M for SKM and ME arteries respectively, representing significantly greater sensitivity of the SKM compared with ME arteries to ACh ($p < 0.0001$, 2way-ANOVA, n=24).
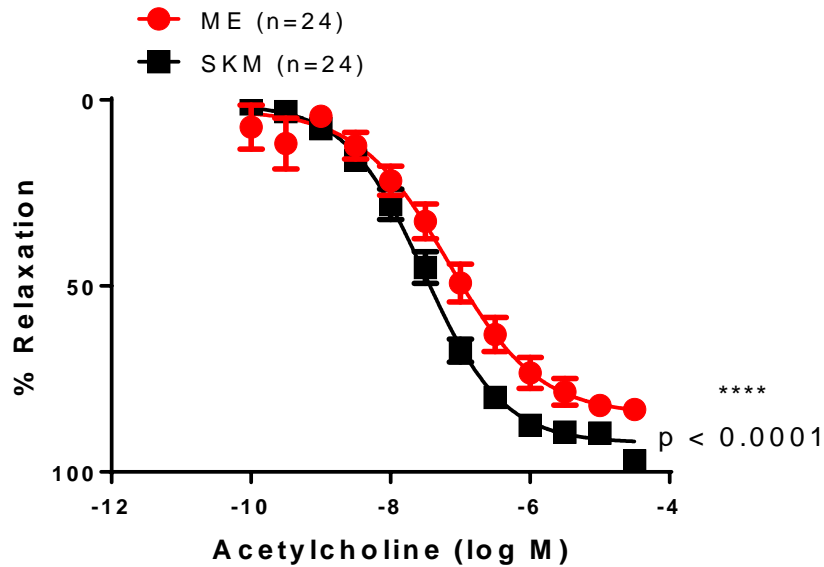
Figure 14: Endothelium-dependent ACh relaxation curves for ME and SKM arteries.

ACh relaxation was greater in SKM compared with ME arteries with the curve for ME arteries shifted to the right of the curve for SKM arteries (****$p < 0.0001$, 2way-ANOVA, n=24). Data are expressed as % relaxation (mean ± SEM) of the initial tone induced by noradrenaline and were fitted with GraphPad Prism software.

3.3.1.2 Roles of COX in the endothelium-dependent relaxation of SKM and ME arteries

To assess the roles of COX in the endothelium-dependent relaxation of SKM and ME arteries, ACh response was recorded in the absence and presence of indomethacin (general COX enzyme inhibitor, 10 μM). Indomethacin did not alter ACh relaxation in SKM arteries (Figure 15, A) except in arteries previously treated with L-NAME (eNOS inhibitor, 100 μM), which curves were shifted to the right (Figure 15, B, $p<0.01$, 2way-ANOVA, n=8). In contrast, indomethacin did enhance relaxation in ME arteries (Figure 16, A, $p<0.01$, 2way-ANOVA, n=7), regardless of whether the segment was previously treated with L-NAME or not (Figure 16, B, $p < 0.01$, 2way-ANOVA, n=7).
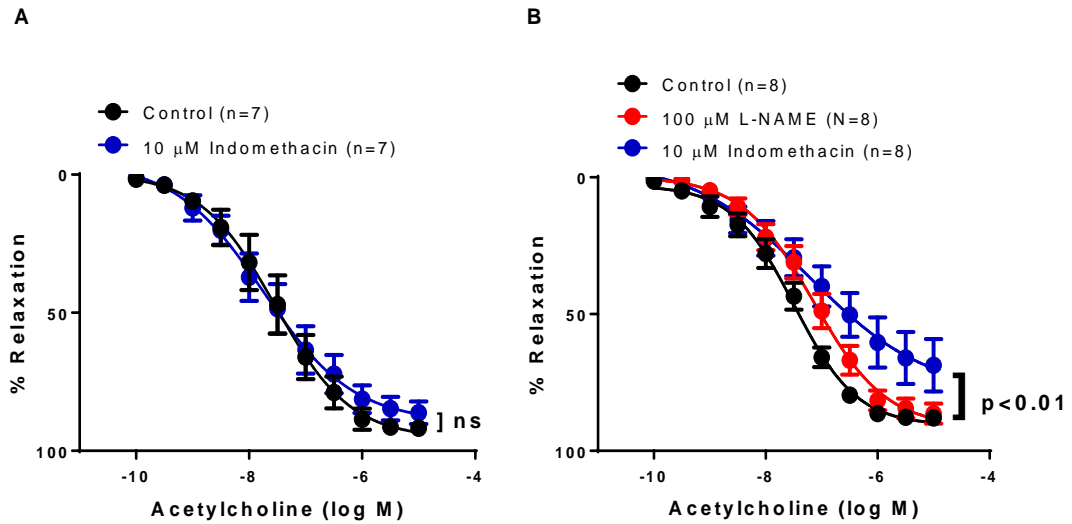
Figure 15: Effect of COX inhibition on ACh relaxation in SKM arteries.

(A) The effect of 10 µM indomethacin on ACh relaxation in SKM arteries. Indomethacin had no apparent effect on ACh-induced relaxation of these arteries (n=7). (B) The effect of 10 µM indomethacin on ACh relaxation in SKM arteries previously treated with 100 µM L-NAME. Under these conditions, 10 µM indomethacin caused a significant rightward shift in the ACh curve ($p < 0.01$, 2way-ANOVA, n=8). Data are expressed as % relaxation (mean ± SEM) of the initial tone induced by noradrenaline and were fitted with GraphPad Prism software.
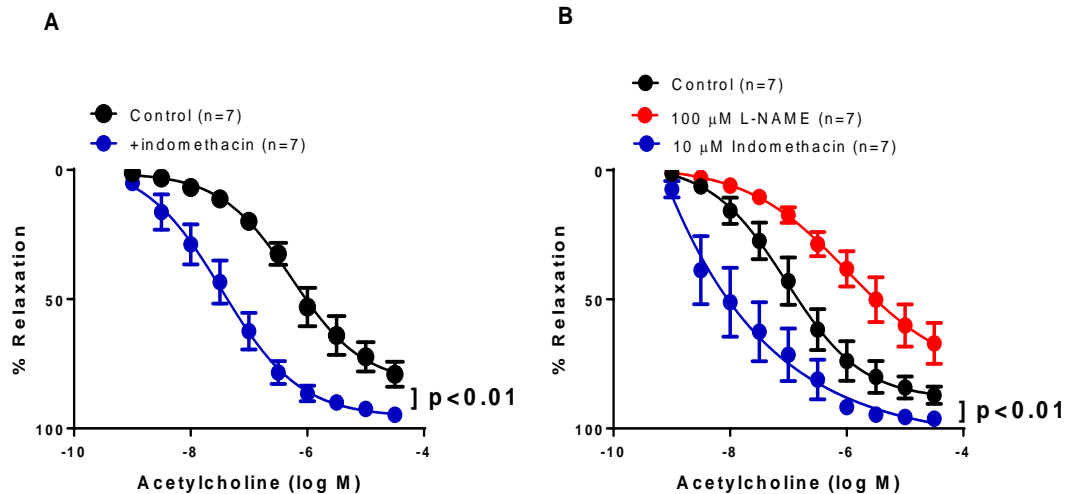
Figure 16: Effect of COX inhibition on ACh relaxation in ME arteries.
(A) The effect of 10 µM indomethacin on ACh relaxation in ME arteries. Indomethacin caused leftward shift of the ACh curve ($p < 0.01$, 2way-ANOVA, n=7). (B) The effect of 10 µM indomethacin on ACh-induced relaxation in ME arteries previously treated with 100 µM L-NAME. ACh curve was shifted to the left by indomethacin ($p < 0.01$, 2-way ANOVA, n=7). Data are expressed as % relaxation (mean ± SEM) of the initial tone induced by noradrenaline and were fitted with GraphPad Prism software.

3.3.1.3 Role of COX isoforms in the relaxation of SKM and ME arteries

To determine whether the differential effects of COX in SKM and ME arteries were isoform-specific:

Role of COX-1 in the relaxation of SKM and ME arteries

To measure the role of COX-1 in the relaxation of these arteries, ACh curves were constructed in the presence of FR122047 (selective COX-1 inhibitor, 1 µM). FR122047 caused a rightward shift of the ACh curve in SKM arteries

(Figure 17, A, $p < 0.05$, 2-way ANOVA, n=5) but did not affect the curve in ME arteries (Figure 17, B, 2-way ANOVA, n=8).
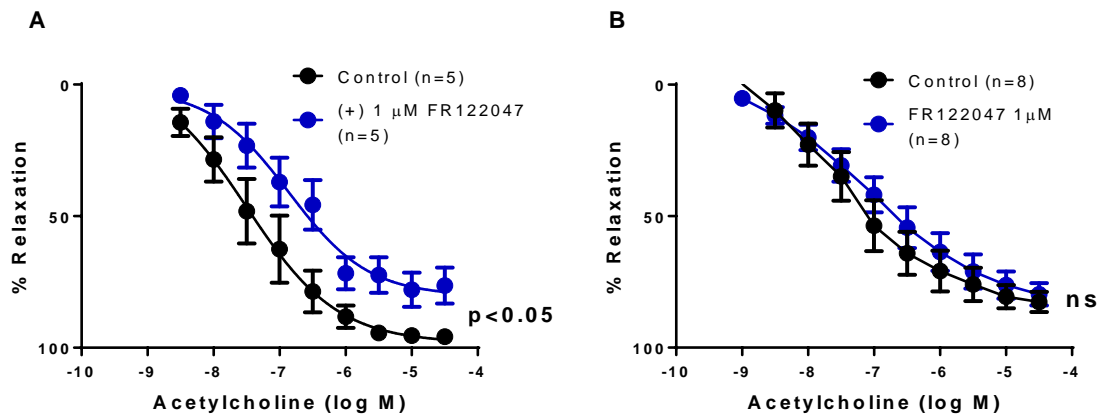
Figure 17: Effect of selective COX-1 inhibition on ACh relaxation in SKM and ME arteries.

(A) 1 µM FR122047 caused a rightward shift of the ACh curve for SKM arteries ($p < 0.05$, 2way ANOVA, n=5), with I_{max} values decreased from 98.24±6.7 to 80.94± 6.9 %. (B) 1 µM FR122047 had no significant effect on the ACh curve for ME arteries (n=8). Data are expressed as % relaxation (mean ± SEM) of the initial tone induced by noradrenaline and were fitted with GraphPad Prism software.

Role of COX-2 in the relaxation of SKM and ME arteries

In the presence of celecoxib (selective COX-2 inhibitor, 4 µM), ACh relaxation was unaffected in SKM (Figure 18, A, n=5) but was shifted to the left in ME arteries (Figure 18, B, P<0.01, 2way ANOVA, n=5), representing an enhancement in ACh relaxation in ME arteries.
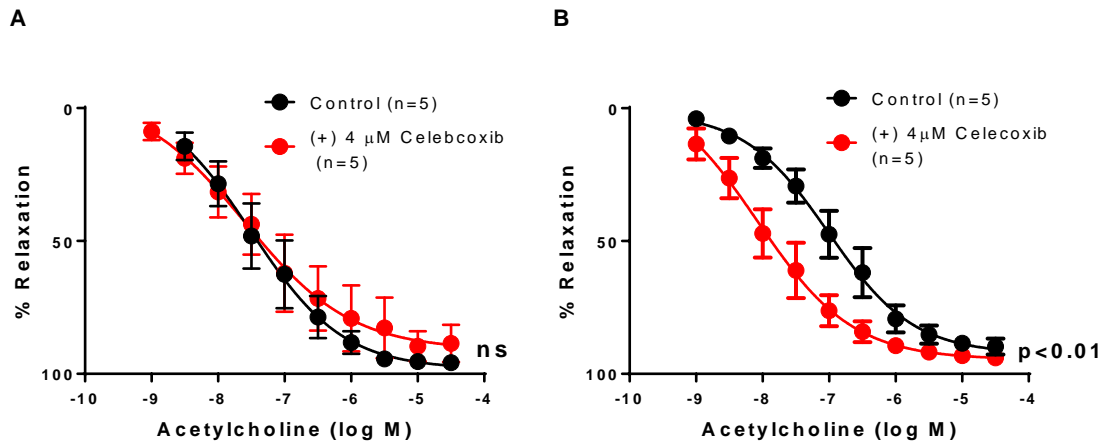
Figure 18: Effect of selective COX-2 inhibition on ACh relaxation in SKM and ME arteries.

(A) Selective inhibition of COX-2 using 4µM Celebcoxib had no significant effect on the ACh curve in SKM arteries (n=5). (B) 4µM Celebcoxib caused a leftward shift of the ACh curve in ME arteries (P<0.01, 2way ANOVA, n=5), with Imax values increased from 92.45±4.9 to 94.62±4.3. Data are expressed as % relaxation (mean ± SEM) of the initial tone induced by noradrenaline and were fitted with GraphPad Prism software.

3.3.1.4 Role of eNOS in the relaxation of SKM and ME arteries

To assess the roles of eNOS in ACh-induced relaxation in these arteries, ACh curves were constructed in the absence and presence of L-NAME (NOS inhibitor, 100 µM). L-NAME caused a rightward shift of the ACh curve in SKM arteries (Figure 19, A, p<0.05, 2way ANOVA, n=8), which was exaggerated in segment previously treated with 10 µM indomethacin (Figure 19, B, p<0.01, 2way ANOVA, n=7). Similarly, L-NAME caused a rightward shift of the ACh curve for ME arteries (Figure 20, A, p<0.05, 2way ANOVA, n=5), but this was not exaggerated in segments previously treated with indomethacin (Figure 20, B, p<0.05, 2way ANOVA, n=7).
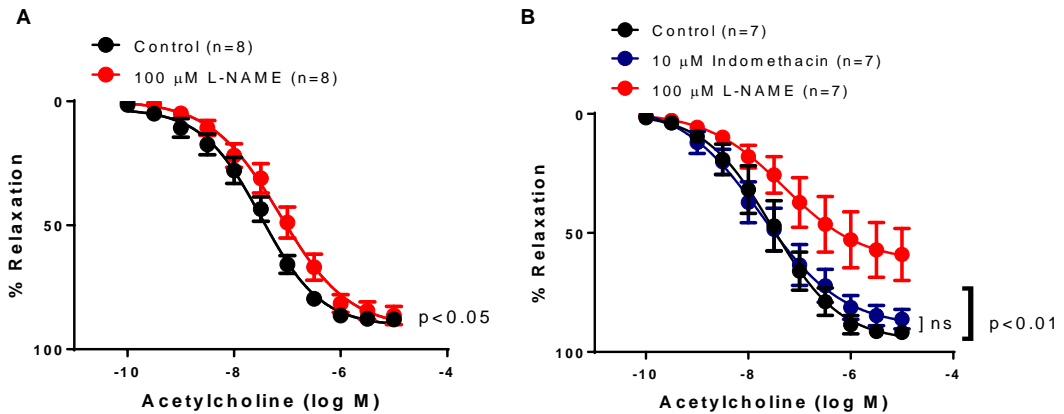
Figure 19: Effect of eNOS inhibition on ACh relaxation in SKM arteries.

(A) The effect of 100 µM L-NAME on ACh relaxation in SKM arteries. L-NAME caused rightward shift on ACh-induced relaxation of these arteries (P<0.05, 2way ANOVA, n=8). (B) Effect of 100 µM L-NAME treatment on ACh relaxation in SKM arteries previously treated with 10 µM indomethacin. Under these conditions, 100 µM L-NAME caused a much greater right-ward shift in the ACh curve (P<0.01, 2way ANOVA, n=7). Data are expressed as % relaxation (mean ± SEM) of the initial tone induced by noradrenaline and were fitted with GraphPad Prism software.
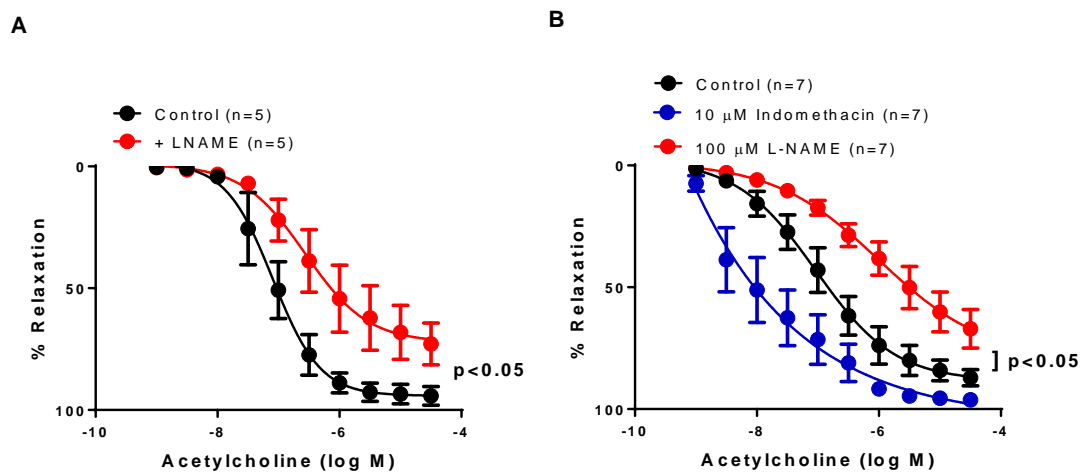
Figure 20: Effect of eNOS inhibition on ACh relaxation of ME arteries.

(A) 100 µM L-NAME caused comparable rightward shifts of the ACh curves in untreated segments (p<0.05, 2way ANOVA, n=5). (B) In segments previously treated with 10 µM indomethacin (B, p<0.05, 2way ANOVA, n=7). Data are expressed as % relaxation (mean ± SEM) of the initial tone induced by noradrenaline and were fitted with GraphPad Prism software.

3.3.1.5 Agonist dependence of the redundancy between COX and eNOS in SKM arteries

Following the observation of a functional relationship between COX and eNOS in ACh relaxation of SKM arteries whereby one vasodilator compensates when the formation of another vasodilator is impaired. Experiments were repeated with BK, another endothelium-dependent vasodilator, to determine whether this functional relationship was agonist-specific or not. Unlike ACh, the BK curve was independently shifted to the right by 10 µM indomethacin (Figure 21, $p < 0.05$, 2way ANOVA, n=9) and 100 µM L-NAME (Figure 21, $p < 0.01$, 2way ANOVA, n=9).
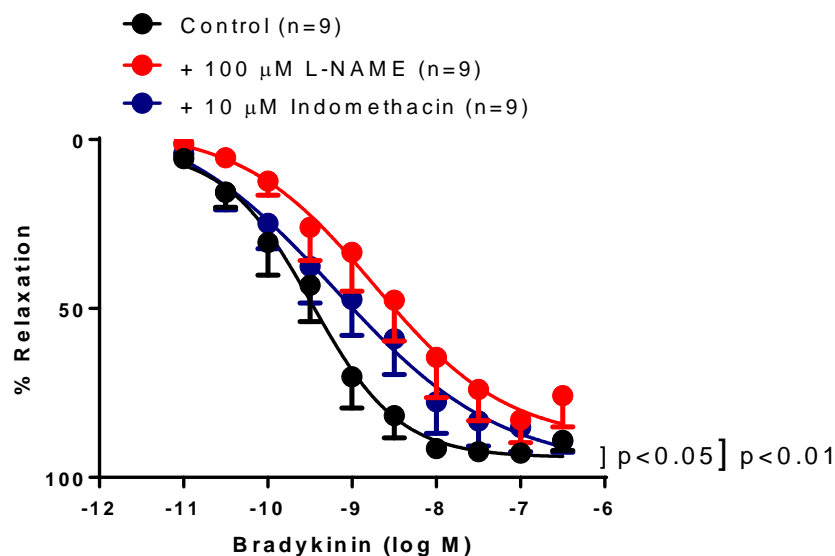
Figure 21: Effect of COX or eNOS inhibition on BK relaxation in SKM arteries.

COX or eNOS inhibition with 10 µM indomethacin or 100 µM L-NAME respectively, separately and independently caused rightward shifts of the BK relaxation curve, indicating independent inhibition of BK relaxation ($p < 0.05$ and $p < 0.01$ respectively, 2way ANOVA, n=9). The control curve was followed by treatment with L-NAME and then indomethacin. Data are expressed as % relaxation (mean ± SEM) of the initial tone induced by noradrenaline and were fitted with GraphPad Prism software.

3.3.1.6 Role of EDH in the endothelium dependent relaxation of SKM arteries

To record EDH contribution in ACh-induced relaxation of SKM arteries, ACh curves were generated in the presence of 30 mM KCl, just enough to block EDH (245, 246).

This treatment significantly attenuated the ACh-induced relaxation (Figure 22, A, $p<0.01$, 2way ANOVA, n=7). When this treatment was repeated in segment previously treated with a combination of 10 µM indomethacin and 100 µM L-NAME, ACh-induced relaxation was abolished (Figure 22, B, n=6).
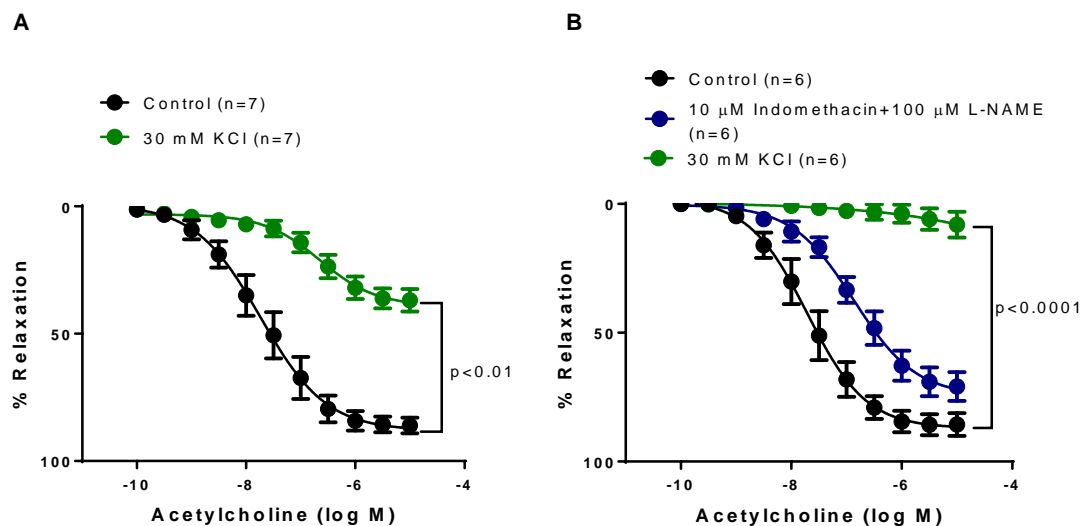
Figure 22: Effect of 30 mM KCl on ACh relaxation in SKM arteries.

(A) 30 mM KCl caused a significant rightward shift of the ACh curve in these arteries ($p < 0.01$, 2way ANOVA, n=7). (B) 30 mM KCl abolished ACh-induced relaxation in segments previously treated with a combination of 10 µM indomethacin and 100 µM L-NAME ($p < 0.001$, 2way ANOVA, n=6). Data are expressed as % relaxation (mean ± SEM) of the initial tone induced by noradrenaline and were fitted with GraphPad Prism software.

3.3.1.7 Role of basal Thromboxane A2 receptor activity in the relaxation of SKM and ME arteries

Following the observation that COX opposed relaxation in ME arteries, experiments were carried out to determine whether basal TP receptor activity interfered with ACh response. To measure this, ACh curves were generated in the presence of TP receptor antagonist ICI 185.282 (0.1 µM). While this treatment had no significant effect on the ACh curve for these arteries (Figure 23, A, n=9), it enhanced ACh-induced relaxation in ME arteries (Figure 23, B, p<0.01, 2way ANOVA, n=6).
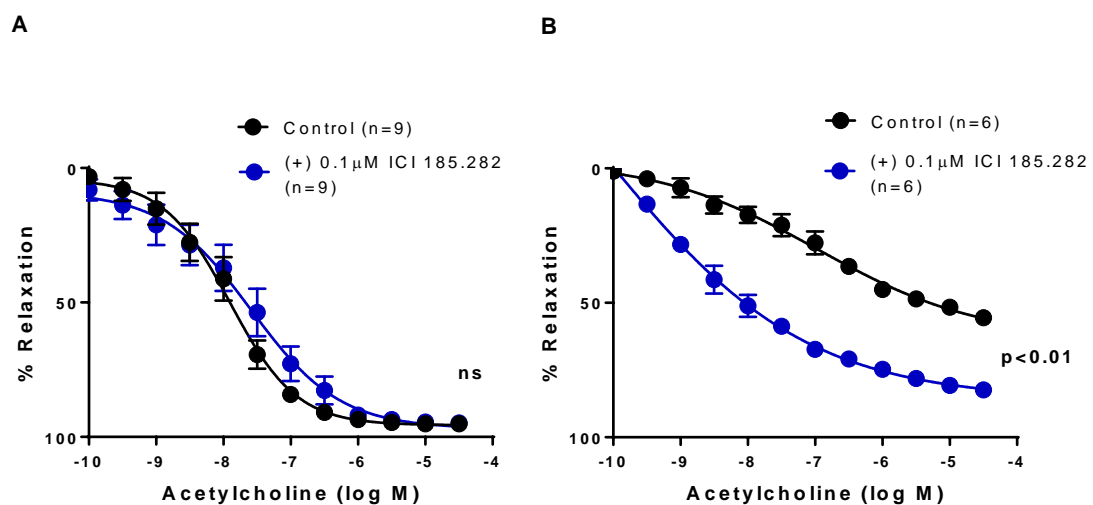
Figure 23: The effects basal TP receptor inhibition on ACh relaxation of SKM and ME arteries.

(A) ACh relaxation was recorded in the absence and then after exposure to TP receptor blocker ICI 185.282 (0.1 µM) on SKM arteries. This treatment had no significant effect on these arteries (2way ANOVA, n=9). (B) In contrast, 0.1 µM ICI 185.282 caused a significant leftward shift of the ACh curve for ME arteries, (p < 0.01, 2way ANOVA, n=6). Data are expressed as % relaxation (mean ± SEM) of the initial tone induced by noradrenaline and were fitted with GraphPad Prism software.

3.3.1.8 Thromboxane and noradrenergic receptor-mediated contractions in SKM and ME arteries

Following the observation that basal TP receptor activity influenced endothelium-dependent reactivity of ME arteries, experiments were carried out to determine whether activated TP receptor responses (agonist TP receptor-mediated contractions) were also different between SKM and ME arteries. To achieve this, cumulative concentration-contraction curves were generated for the TXA$_2$ analogue U46619 in both arteries. U46619 contractions were greater in ME compared with SKM arteries (Figure 24, A, p<0.01, n=8) with log EC$_{50}$ of -5.92±0.08 vs. -5.54±0.08 and E$_{max}$ of 0.0052± 0.003 vs. 0.0204±0.003 mN/μm respectively. NA contraction were greater in ME compared with SKM arteries with E$_{max}$ 0.06213±0.002 vs. 0.05930±0.002 and log EC$_{50}$ of -5.965±0.002 and -5.549±0.002 respectively (Figure 24, B, p<0.01, 2way ANOVA, n=12).
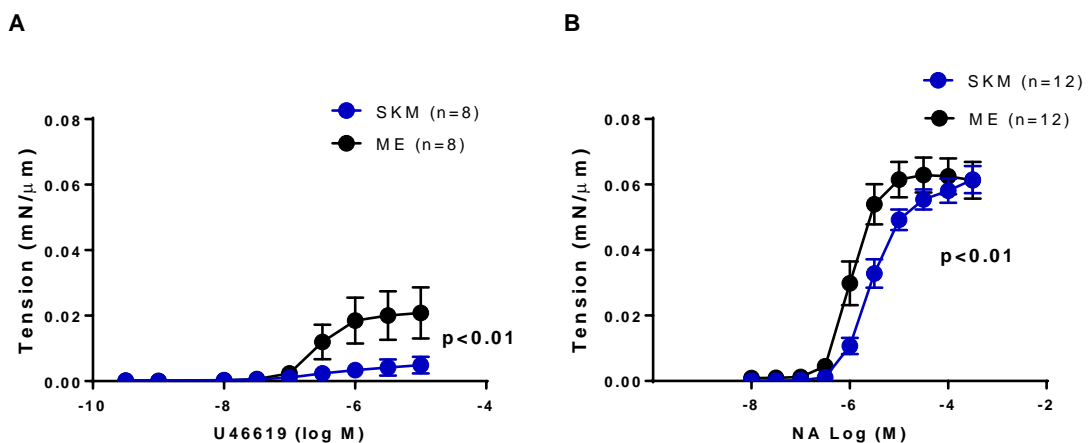
Figure 24: Concentration-contraction curves for U46619 and noradrenaline in SKM and ME arteries.

(A) U46619 contractions in SKM and ME arteries. U46619 contractions were significantly greater in ME compared with SKM arteries (p<0.01, 2way ANOVA, between the curves, n=8). (B) Noradrenaline contraction in SKM and ME arteries. Although maximum contractions to noradrenaline were comparable in both arteries, the curve for ME arteries was significantly shifted to the left of the curve for SKM arteries (p<0.01, 2way ANOVA, n=12). Data are expressed as tension/diameter (mN/μm, mean ± SEM). The curves were generated by fitting data with GraphPad Prism software.

3.3.1.9 PGI$_2$- and PGE$_2$-induced relaxation in SKM and ME arteries

Since COX opposition to relaxation in ME arteries could involve other prostanoids such as PGI$_2$ or PGE$_2$ acting on contractile receptors, experiments were conducted to determine the direct effects of these prostanoids on both SKM and ME arteries. Both PGI$_2$ and PGE$_2$ caused relaxation in both SKM and ME arteries (Figure 25).
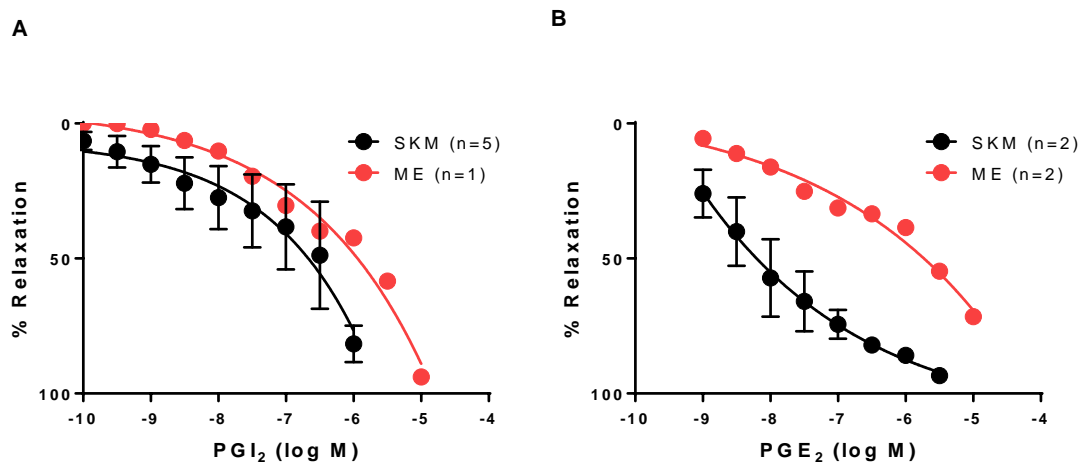
Figure 25: PGI$_2$ and PGE$_2$ relaxation in SKM and ME arteries.

(A) PGI$_2$ relaxation of SKM and ME arteries. (B) PGE$_2$ relaxation of SKM and ME arteries. Both prostanoids caused relaxation in both arteries. Data are expressed as % relaxation (mean ± SEM) of the initial tone induced by noradrenaline and were fitted with GraphPad Prism software.

3.3.1.10 Endothelium-independent relaxation of ME and SKM arteries

The ability of SKM or ME arteries to relax independently of the endothelium was assessed by their relaxation to SNP (NO donor and endothelium-independent dilator). SNP caused significantly greater relaxation in ME arteries compared with SKM arteries (Figure 26, p<0.01, 2-way ANOVA, n=5).
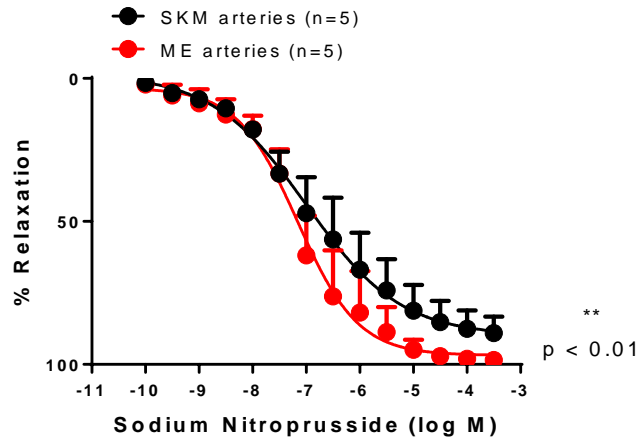
Figure 26: Endothelium-independent SNP relaxation curves for ME and SKM arteries.

SNP relaxation was greater in ME compared with SKM arteries with the curve for SKM arteries shifted to the right of the curve for ME arteries (**$p < 0.01$, 2way ANOVA, n=5). Data are expressed as % relaxation (mean ± SEM) of the initial tone induced by noradrenaline and were fitted with GraphPad Prism software.

3.3.2 Gene expression studies

3.3.2.1 Microarray expression analysis in SKM and ME arteries

Microarray analysis revealed a total of 1019 genes (4.6%) out of 22141, which were differentially expressed (Adjusted P-value FDR P-value <0.05). 717 genes were up-regulated in SKM and 302 up-regulated in ME arteries (Figure 27).
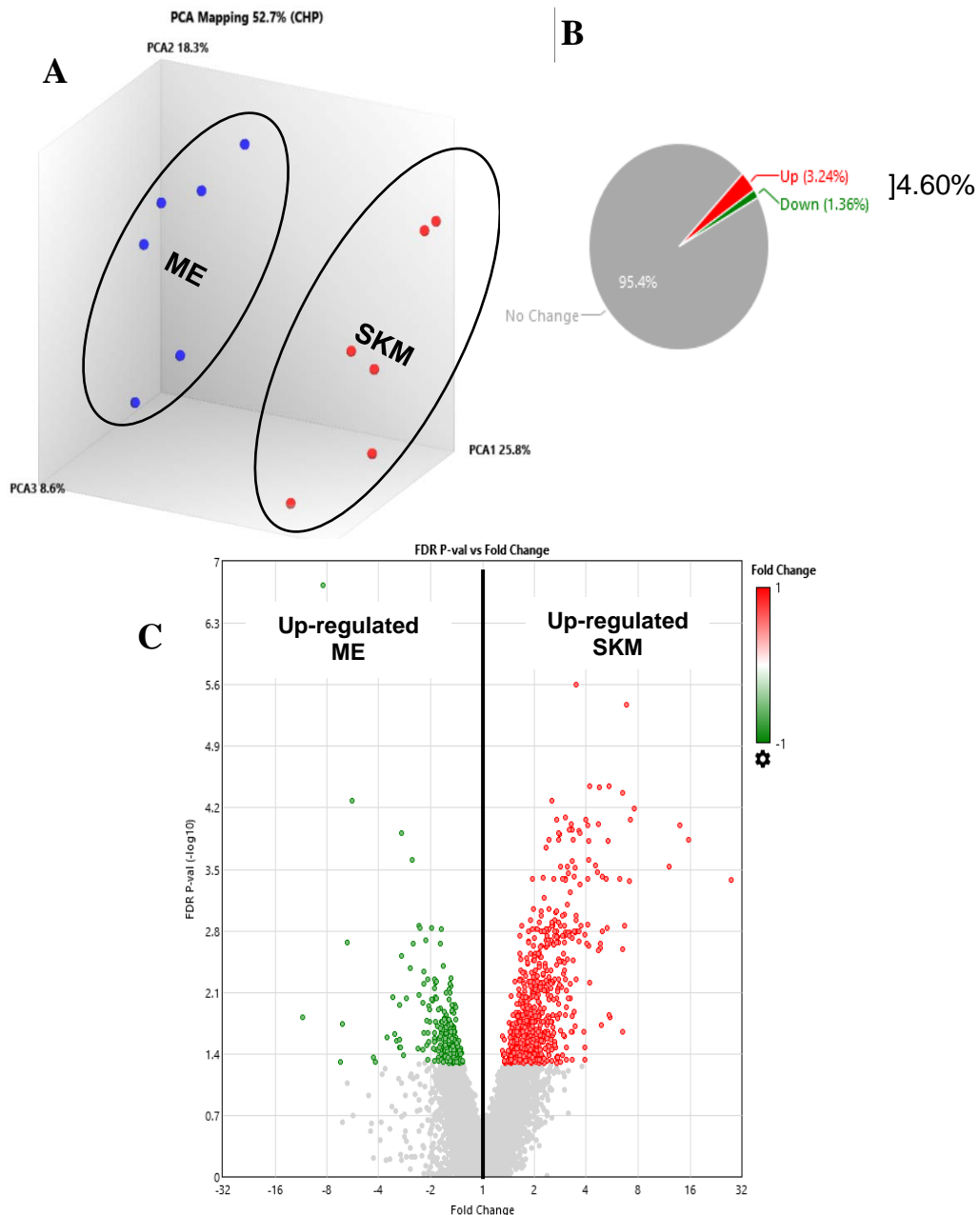
Figure 27: Differentially expressed genes between SKM and ME arteries (FDR P value < 0.05; RMA).

(A) PCA 2-dimensional (Dim.) scatter plots representing the gene expression patterns of the different samples (SKM and ME arteries). Each dot represents a sample. Samples were divided into 2 distinct groups based on their gene expression profiles. (B) Pie chart showing the percentages of differentially expressed genes. (C) Volcano plot of gene expression fold changes vs. FDR P-value. The 717 genes upregulated in SKM are indicated in red, and the 302 genes upregulated in ME are indicated in green. Genes that were not different are indicated in gray.

Expression of genes encoding smooth muscle contractile proteins in SKM and ME arteries

Transcripts of genes that encode components of the muscle contractile machinery or that positively regulate muscle contraction, such as light chain 9, regulatory (MYL9), actin gamma 2 (ACTG2), actin alpha 2 (ACTA2) and chemokine (C-C motif) ligand 21 (CCL21) were significantly down regulated in SKM compared with ME arteries. While genes that promote muscle relaxation such as guanylate cyclase 1, soluble, alpha 3 (GUCY1A3) and protein kinase, cGMP-dependent, type I (PRKG1) were upregulated in SKM arteries (Figure 28, Table 4).
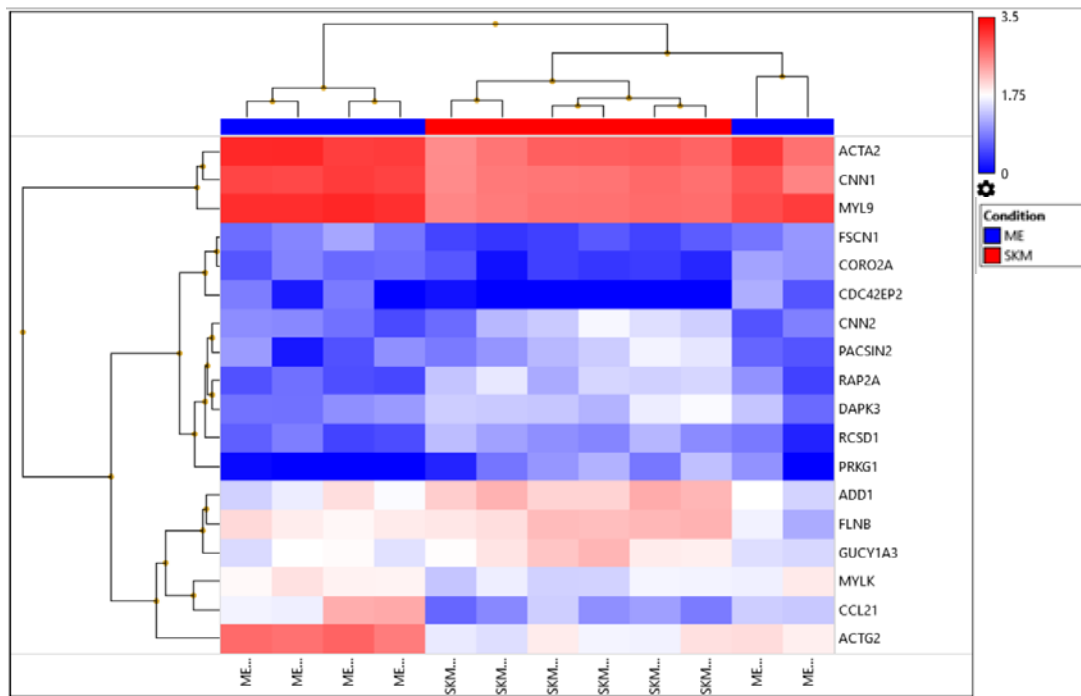
Figure 28: Supervised hierarchical clustering expression of genes encoding smooth muscle contractile proteins in SKM and ME arteries. Each column represents one biological sample.

The molecular signatures of SKM and ME arteries were visualized by hierarchical clustering based on the differentially expressed transcripts. Genes are arranged in rows and the 12 arteries samples are arranged in columns. All 6 SKM samples were clustered in 1 branch and all ME samples in another branch. In each artery group, the tree represents the relationship among samples and the branch length reflects the degree of similarity between samples according to their gene expression profile. Genes that were upregulated are indicated in red and genes that were downregulated are indicated in blue.

Table 4: List of differentially expressed genes encoding smooth muscle contractile proteins in SKM and ME arteries.

The genes are classified according to molecular functions. 9 Up-regulated genes in SKM that encode proteins that negatively regulate contraction, while 9 up-regulated genes in ME that encode protein that function as positive regulators of contraction (FDR-P value < 0.05).

Gene Symbol	Fold change	Regulation	GO biological process term	p-value	FDR-p-value
RAP2A	2.43	Up-regulated in SKM	Negative regulation of Actin / JNK	2.56E-06	0.0009
ADD1	2.58	Up-regulated in SKM	Negative regulation of Actin/ calmodulin	1.50E-05	0.0023
PRKG1	2.23	Up-regulated in SKM	Positive regulation of Muscle relaxation/ cGMP	0.0019	0.046
FLNB	2.07	Up-regulated in SKM	Negative regulation of Actin	0.0014	0.0399
CNN2	1.93	Up-regulated in SKM	Negative regulation of myosin/Actin/ calmodulin	0.001	0.0323
GUCY1A3	1.87	Up-regulated in SKM	Positive regulation of Muscle relaxation/ cGMP/NO	0.0007	0.0271
PACSIN2	1.87	Up-regulated in SKM	Negative regulation of Actin	0.0018	0.045
DAPK3	1.75	Up-regulated in SKM	Negative regulation of Muscle contraction/myosin/Actin/ ATP	0.0007	0.0257
RCSD1	1.49	Up-regulated in SKM	Negative regulation of Actin	0.0011	0.0346
ACTG2	-11.08	Up-regulated in ME	Positive regulation of Muscle contraction/ ATP	0.0003	0.0153
MYL9	-5.72	Up-regulated in ME	Positive regulation of myosin	2.12E-08	5.2E-05
ACTA2	-3.15	Up-regulated in ME	Positive regulation of Muscle contraction/ ATP	0.0008	0.0282
CNN1	-3.03	Up-regulated in ME	Positive regulation of myosin/Actin/ calmodulin	0.001	0.0333
CCL21	-2.36	Up-regulated in ME	Positive regulation of Actin/JNK/ERK/NFKB	0.0011	0.0346
CDC42EP2	-1.76	Up-regulated in ME	Positive regulation of Actin	0.0012	0.0354
MYLK	-1.6	Up-regulated in ME	Positive regulation of myosin/Actin/ calmodulin	0.001	0.0333
CORO2A	-1.42	Up-regulated in ME	Positive regulation of Actin	0.0018	0.0449
FSCN1	-1.36	Up-regulated in ME	Positive regulation of Actin	0.0018	0.0449

Expression of genes encoding proteins involved in eNOS pathway regulation in SKM and ME arteries

Although eNOS or NOS3 gene expression was not significantly different between SKM and ME arteries, genes that encode components of NO signaling such as guanylate cyclase 1, soluble alpha 3 (GUCY1A3) was upregulated in SKM compared to ME arteries (Figure 29, Table 5). An important antioxidant enzyme superoxide dismutase 1 (SOD1) that protects the cell from reactive oxygen species (ROS) toxicity was also upregulated in SKM arteries. In contrast, several genes that positively regulate oxidative stress such as early growth response 1 (EGR1); promoter in response to hypoxia, are upregulated in ME arteries (Figure 29, Table 5).

 Furthermore, heat shock 27kDa protein 1 (HSPB1) were upregulated in ME arteries which inhibit cyclic nucleotide (270, 271). Several genes that encode regulator gene of JUK/JUN that reducing its action promote relaxation found to be upregulated in SKM arteries such as DnaJ (Hsp40) homolog, subfamily A, member 1 (DNAJA1), RAP2A, member of RAS oncogene family (RAP2A), and dual specificity phosphatase 10 (DUSP10). In contrast, genes that enhance JUNK/JUN where upregulated in ME arteries such as JUNB proto-oncogene (JUNB), chemokine (C-C motif) ligand 21 (CCL21) (Figure 29, Table 5).
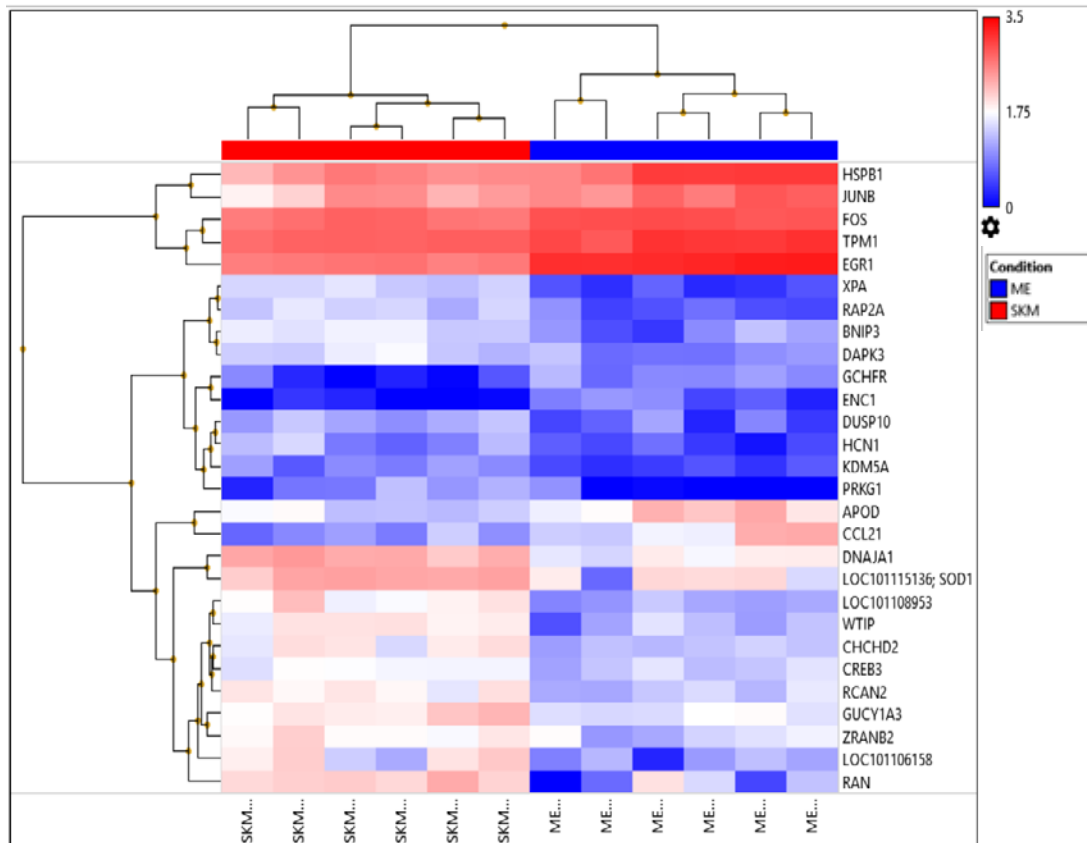
Figure 29: Supervised hierarchical clustering of genes encoding proteins involved in eNOS pathway regulation in SKM and ME arteries. Each column represents one biological sample.

The molecular signatures of SKM and ME arteries were visualized by hierarchical clustering based on the differentially expressed transcripts. Genes are arranged in rows and the 12 arterial samples are arranged in columns. All 6 SKM samples are clustered in 1 branch and all ME samples in another branch. In each artery group, the tree represents the relationship among samples and the branch length reflects the degree of similarity between samples according to their gene expression profile. Genes that were upregulated are indicated in red and genes that were downregulated are indicated in blue.

Table 5: List of differentially expressed genes encoding proteins involved in eNOS pathway regulation in SKM and ME arteries.

The genes are classified according to molecular functions. 19 Up-regulated genes in SKM that encode proteins with positive regulatory function in the eNOS pathway, while 9 up-regulated genes in ME that encode proteins that function as negative regulators of the eNOS pathway. (FDR-P value < 0.05).

Gene symbol	Fold change	Regulation	GO biological process term	p-value	FDR-p-value
RAN	4.17	Up-regulated in SKM	Positive regulation of NOS/cGMP	6.15E-05	0.0061
DNAJA1	3.12	Up-regulated in SKM	Negative regulation of JNK/JUN	5.20E-07	0.0003
LOC101106158	2.83	Up-regulated in SKM	Negative regulation of ROS	0.0005	0.0216
WTIP	2.71	Up-regulated in SKM	Negative regulation of HIF1A	9.52E-06	0.0018
LOC101108953	2.55	Up-regulated in SKM	Positive regulation of cAMP	4.71E-06	0.0013
XPA	2.54	Up-regulated in SKM	Negative regulation of ROS	1.95E-08	5.22E-05
CHCHD2	2.48	Up-regulated in SKM	Negative regulation of ROS	8.24E-05	0.0072
RAP2A	2.43	Up-regulated in SKM	Negative regulation of JUN cascade	2.56E-06	0.0009
LOC101115136; SOD1	2.38	Up-regulated in SKM	Negative regulation of ROS	0.0003	0.0149
RCAN2	2.24	Up-regulated in SKM	Negative regulation of ROS	4.37E-05	0.0049
PRKG1	2.23	Up-regulated in SKM	Positive regulation of NOS/cGMP	0.0019	0.046
BNIP3	2.06	Up-regulated in SKM	Negative regulation of ROS	0.0001	0.0091
GUCY1A3	1.87	Up-regulated in SKM	Positive regulation of NOS/cGMP	0.0007	0.0271
DAPK3	1.75	Up-regulated in SKM	Positive regulation of cAMP	0.0007	0.0257
DUSP10	1.66	Up-regulated in SKM	Negative regulation of JNK/JUN	0.0018	0.044
HCN1	1.64	Up-regulated in SKM	Positive regulation of cAMP	0.002	0.0464
ZRANB2	1.58	Up-regulated in SKM	Positive regulation of NOS/cGMP	0.002	0.0471
CREB3	1.56	Up-regulated in SKM	Positive regulation of cAMP	0.0016	0.0421
KDM5A	1.47	Up-regulated in SKM	Negative regulation of ROS	0.0011	0.0347
EGR1	-8.42	Up-regulated in ME	Negative regulation of cAMP, Positive regulation of ROS	8.31E-12	1.84E-07
HSPB1	-6.51	Up-regulated in ME	Response to oxidative stress	0.0004	0.0184
APOD	-3.04	Up-regulated in ME	Positive regulation of ROS	0.0007	0.0274

JUNB	-2.99	Up-regulated in ME	Positive regulation of cAMP, JNK/JUN	0.001	0.0333
TPM1	-2.94	Up-regulated in ME	Positive regulation of ROS	2.21E-05	0.003
CCL21	-2.36	Up-regulated in ME	Positive regulation of JNK/JUN	0.0011	0.0346
FOS	-2.14	Up-regulated in ME	Positive regulation of ROS	1.18E-05	0.002
GCHFR	-1.64	Up-regulated in ME	Negative regulation of NOS/cGMP	0.0012	0.0362
ENC1	-1.56	Up-regulated in ME	Positive regulation of ROS	0.0017	0.0434

Expression of genes encoding proteins involved in COX pathway regulation in SKM and ME arteries

Both COX isoforms; PTGS1 and PTGS2 genes were not significantly changed between SKM and ME arteries. In addition, thromboxane A2 receptor (TBXA2R) or any gene in prostanoid synthesis pathway were also not significantly changed.

COX-1 is constitutively expressed in most cells, thus regarded as a housekeeping molecule. On the other hand, the expression of COX-2 is induced by several signals including pro-inflammatory and growth-promoting stimuli. All signals were converge on the activation of mitogen-activated protein kinases (MAPK) that regulate cyclooxygenease-2 mRNA levels both at the transcriptional and post-transcriptional level (272).

Genes that encode proteins regulating nuclear factor kappa B (NFkB), growth factors and inflammatory response such as heat shock 27kDa protein 1 (HSPB1), NF-kappa-B inhibitor beta (NFKBIB), early growth response 1 (EGR1), FBJ murine osteosarcoma viral oncogene homolog (FOS), chemokine (C-C motif) ligand 21(CCL21) and interleukin 15 (IL15) were upregulated in ME compared with SKM arteries (Figure 30, Table 6).
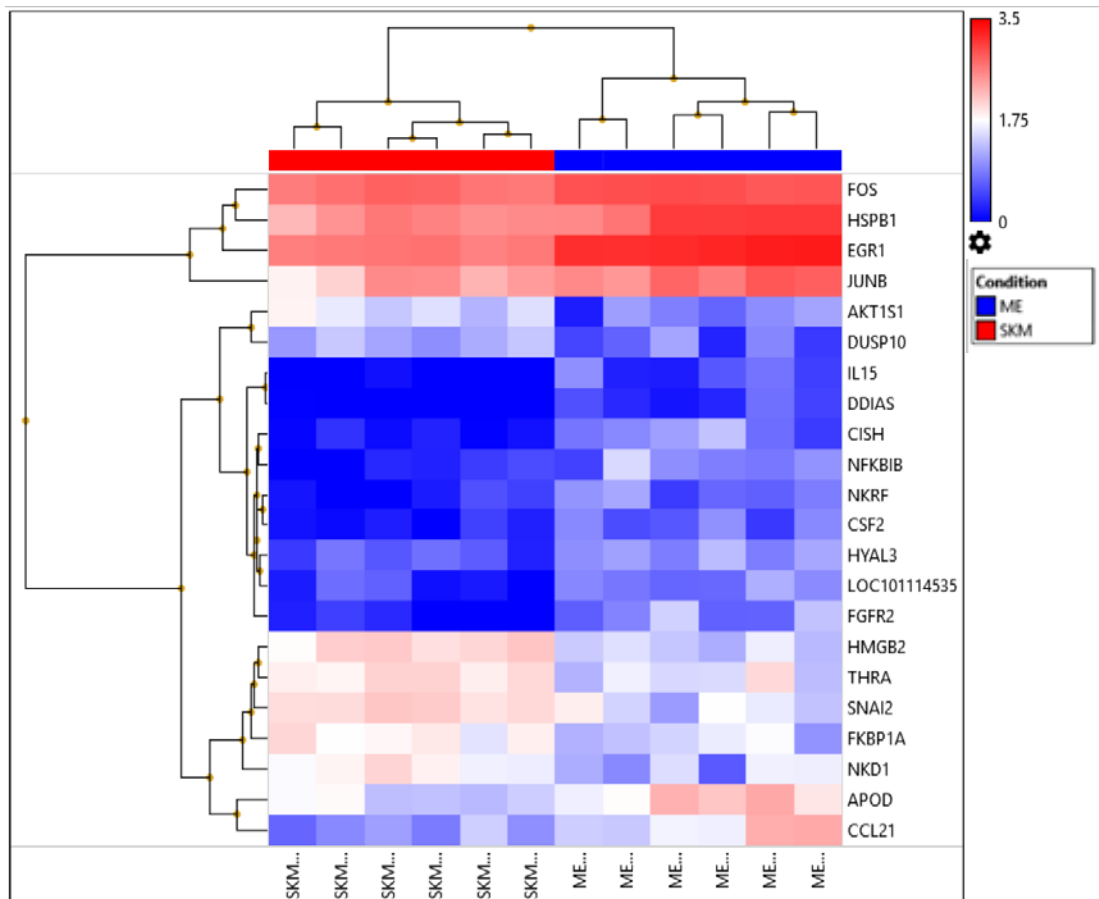
Figure 30: Supervised hierarchical clustering expression of genes encoding proteins involved in COX-2 pathway regulation in SKM and ME arteries. Each column represents one biological sample.

The molecular signatures of SKM and ME arteries were visualized by hierarchical clustering based on the differentially expressed transcripts. Genes are arranged in rows and the 12 arteries samples are arranged in columns. All 6 SKM samples were clustered in 1 branch and all ME arteries samples in another branch. In each artery group, the tree represents the relationship among samples and the branch length reflects the degree of similarity between samples according to their gene expression profile. Genes that were upregulated are indicated in red and genes that were downregulated are indicated in blue.

Table 6: List of differentially expressed genes encoding proteins involved in COX-2 pathway regulation in SKM and ME arteries.

The genes are classified according to molecular functions. 7 Up-regulated genes in SKM that encode proteins with negative regulatory effects on COX-2, while 15 up-regulated genes in ME that encode proteins that function as positive regulators of COX-2. (FDR-P value < 0.05).

Gene Symbol	Fold change	Regulation	GO biological process term	p-value	FDR-p-value
HMGB2	2.93	Up-regulated in SKM	Positive regulation of endothelial cell proliferation; inflammatory response to antigenic stimulus; response to lipopolysaccharide; positive regulation of interferon-beta production; defense response to Gram-negative bacterium; defense response to Gram-positive bacterium; positive chemotaxis	0.00000976	0.0004
SNAI2	2.16	Up-regulated in SKM	Negative regulation of canonical TOR signaling pathway	6.47E-05	0.0062
THRA	2.13	Up-regulated in SKM	Hormone-mediated signaling pathway; intracellular receptor signaling pathway; steroid hormone mediated signaling pathway; negative regulation of receptor biosynthetic process; regulation of lipid metabolic process; negative regulation of toll-like receptor 4 signaling pathway; response to leptin; cellular response to lipopolysaccharide; positive regulation of cholesterol homeostasis	0.0013	0.0384
AKT1S1	1.97	Up-regulated in SKM	Negative regulation of canonical Wnt signaling pathway, phosphatidylinositol-mediated signaling	0.0001	0.0087
FKBP1A	1.9	Up-regulated in SKM	Negative regulation of growth factor (TGF)-β receptor I signaling. It binds to the TGF-β receptor I and inhibits receptor-mediated signaling.	0.0012	0.0357
NKD1	1.86	Up-regulated in SKM	Negative regulation of Wnt signaling pathway; positive regulation of non-canonical Wnt signaling pathway via JNK cascade; positive regulation of Wnt signaling pathway	0.0021	0.0473
DUSP10	1.66	Up-regulated in SKM	Inactivation of MAPK activity; protein dephosphorylation; response to lipopolysaccharide; negative regulation of stress-activated MAPK cascade; peptidyl-tyrosine dephosphorylation; negative regulation of JUN kinase activity; negative regulation of JNK cascade	0.0018	0.044
EGR1	-8.42	Up-regulated in ME	IL-1 pathway, hypoxia, cAMP response, negative regulation of canonical Wnt signaling pathway	8.31E-12	1.84E-07

HSPB1	-6.51	Up-regulated in ME	Positive regulation of interleukin-1 beta production; positive regulation of endothelial cell chemotaxis by VEGF-activated vascular endothelial growth factor receptor signaling pathway; positive regulation of tumor necrosis factor biosynthetic process; negative regulation of apoptotic process; regulation of I-kappaB kinase/NF-kappaB signaling; regulation of mRNA stability	0.0004	0.0184
APOD	-3.04	Up-regulated in ME	response to reactive oxygen species; negative regulation of cytokine production involved in inflammatory response	0.0007	0.0274
JUNB	-2.99	Up-regulated in ME	Response to lipopolysaccharide; response to cytokine; regulation of cell proliferation; response to cAMP; AP-1	0.001	0.0333
CCL21	-2.36	Up-regulated in ME	G-protein coupled receptor signaling pathway; positive regulation of actin filament polymerization; response to prostaglandin E; positive regulation of I-kappaB kinase/NF-kappaB signaling; positive regulation of phosphatidylinositol 3-kinase activity; positive regulation of protein kinase activity; positive regulation of JNK cascade; positive regulation of ERK1 and ERK2 cascade; inflammatory response; cellular response to interferon-gamma; cellular response to interleukin-1; cellular response to tumor necrosis factor	0.0011	0.0346
FOS	-2.14	Up-regulated in ME	MyD88; GFR; LPS; cytokines; TLR; MAPK; ERK	1.18E-05	0.002
CISH	-1.71	Up-regulated in ME	Protein kinase C-activating G-protein coupled receptor signaling pathway; cytokine-mediated signaling pathway	0.0003	0.017
NFKBIB	-1.63	Up-regulated in ME	Response to lipopolysaccharide, Inhibits NF-kappa-B by complexing with and trapping it in the cytoplasm.	0.001	0.0334
LOC101114535	-1.6	Up-regulated in ME	Positive regulation of tumor necrosis factor production; positive regulation of interleukin-1 beta secretion; positive regulation of inflammatory response	0.0021	0.0477
FGFR2	-1.54	Up-regulated in ME	Positive regulation of phospholipase activity; positive regulation of Wnt signaling pathway; positive regulation of MAPK cascade; positive regulation of ERK1 and ERK2 cascade	0.0004	0.0197
NKRF	-1.54	Up-regulated in ME	Negative regulation of transcription, DNA-templated	0.0017	0.0427
CSF2	-1.5	Up-regulated in ME	Positive regulation of interleukin-23 production; positive regulation of tyrosine phosphorylation of Stat5 protein; interferon-tau production	0.0017	0.0431

IL15	-1.48	Up-regulated in ME	Inflammatory response; positive regulation of interleukin-17 production; positive regulation of tyrosine phosphorylation of Stat3 protein	0.0015	0.041
HYAL3	-1.45	Up-regulated in ME	Inflammatory response; cellular response to interleukin-1; cellular response to tumor necrosis factor	0.0018	0.0439
DDIAS	-1.38	Up-regulated in ME	cellular response to DNA damage stimulus; cellular response to cytokine stimulus; cellular response to hydroperoxide	0.0015	0.0414

3.3.2.2 Expression of COX-1/2 and eNOS mRNA determined by q-PCR in SKM and ME arteries

COX-1 expression was significantly higher in SKM compared with ME arteries (Figure 31, A, $p < 0.05$, t-test, n=8). There was no difference in COX-2 expression between the SKM and ME arteries (Figure 31, B, n=8). There was also no significant difference in eNOS gene expression, between the two arteries (Figure 31, C, n=8).
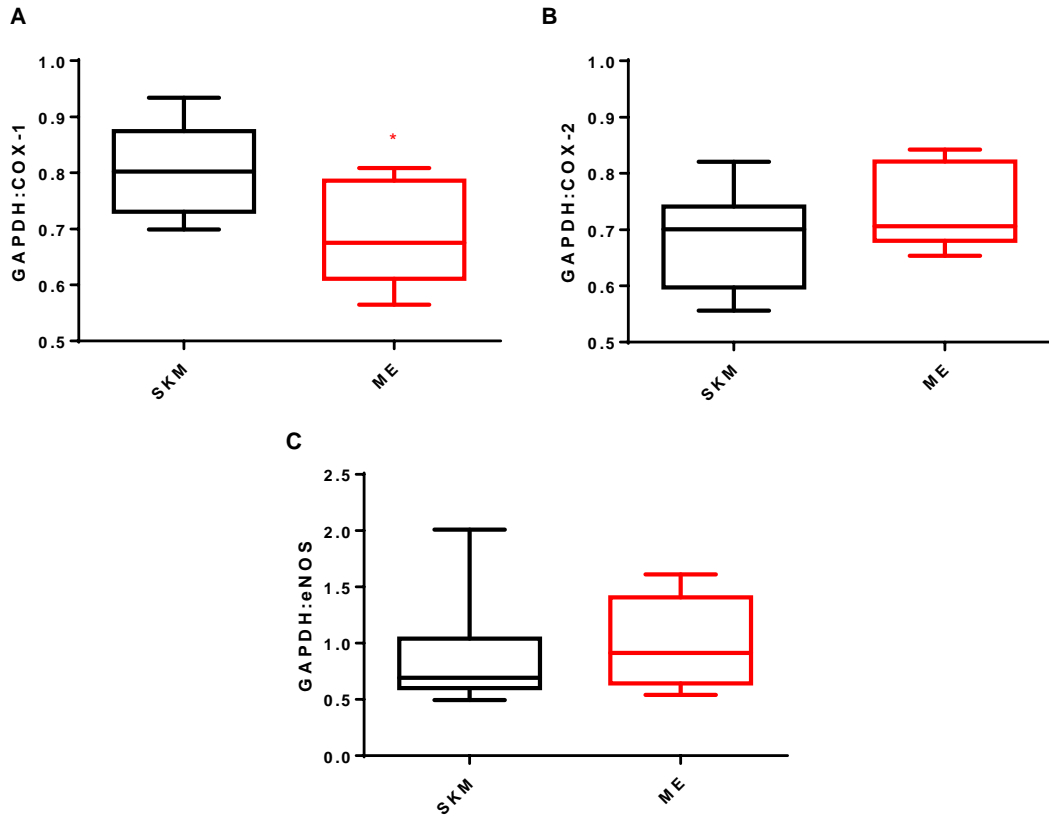
Figure 31: COX-1, COX-2 and eNOS mRNA expressions determined by single q-PCR in SKM and ME arteries.

(A) COX-1 was relatively more abundant in SKM compared with ME arteries, ($P<0.05$). (B) Comparable expressions of COX-2 in SKM and ME arteries. (C) Comparable expressions of eNOS mRNA in SKM and ME arteries. Data represented as ratio of GAPDH expression to target gene, n= 8, *p < 0.05, paired t-test was used.

3.3.3 Protein expressions of COX1/2 and eNOS in SKM and ME arteries

To determine whether the COX isoform and eNOS protein expressions were different in these arteries, western blot analyses were conducted. The expressions of COX-1 and COX-2 proteins in SKM arteries were comparable (Figure 32, D). In contrast, COX-1 was significantly more highly expressed compared with COX-2 in ME arteries (Figure 32, E, t-test, $p<0.05$). The ratios of COX-2 to COX-1 in these arteries were 25%±18% and 26%±7% in SKM and ME arteries respectively. When the 2 arteries were compared, both COX-1 (Figure 32, B) and COX-2 (Figure 32, C) proteins were comparable between the arteries. The expressions of eNOS proteins were also comparable between SKM and ME arteries (Figure 33).
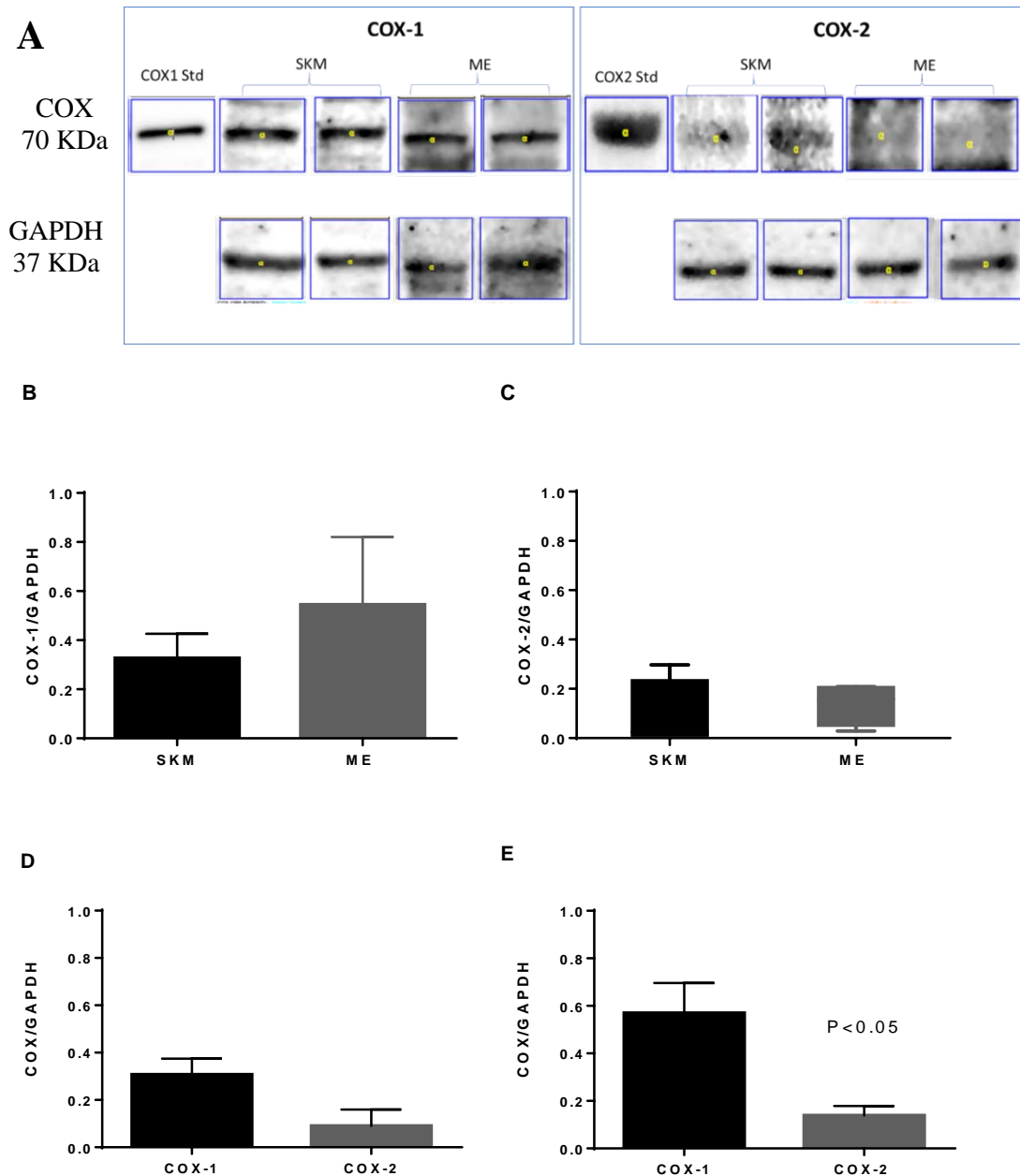
Figure 32: COX-1 and COX-2 protein expressions in SKM and ME arteries.
Total protein was analyzed for COX-1, COX-2, and GAPDH proteins by western blot. (A) Representative blots of SKM and ME arteries for COX-1/2 (70 KDa) and GAPDH (37 KDa). (B) Comparable expression of COX-1 in SKM and ME arteries. (C) Comparable expression of COX-2 in SKM and ME arteries. (D) Comparable expression of COX-1 and COX-2 in SKM arteries. (E) Expression of COX-1 were significantly higher than COX-2 in ME arteries. Data are reported as ratio of target protein to GAPDH of n=4, $p < 0.05$, paired t-test.
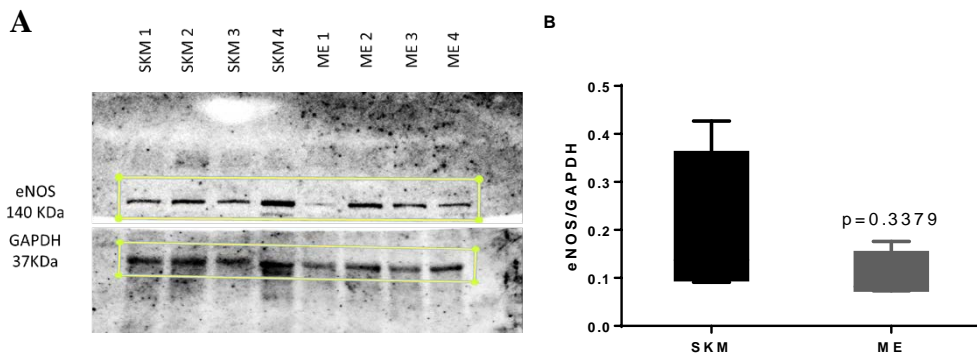
Figure 33: eNOS protein expression in SKM and ME arteries.

Total protein was analyzed for eNOS and GAPDH proteins by western blot. (A) Representative blots for eNOS (140 KDa) and GAPDH (37 KDa) proteins in SKM and ME arteries. (B) Expression of eNOS in SKM and ME arteries. Data are reported as mean ± SEM of target protein to GAPDH ratio of n=4, paired t-test.

3.4 Discussion

The results clearly show that COX can both decrease and increase vascular tone under healthy conditions. The data also demonstrates that these double-edged roles are isoform-specific in resistance arteries. While COX activity is favorable to endothelium-dependent relaxation in SKM arteries, it opposes it in ME arteries obtained from the same healthy animal. This is interesting because COX is often thought to oppose vasodilation only in disease such as hypertension, coronary artery disease, aging and respiratory distress syndrome (273-277). The data revealed COX-1 as the isoform that favored relaxation in SKM arteries while COX-2 did the opposite in ME arteries, making these roles isoform-specific in these resistance arteries.

There have been inconsistent reports about the role of COX isoforms in vascular functions. While COX-1 is thought mediate vasorelaxation in human forearm arteries (278) and mice arteries (279, 280), it appears to contract rat aorta or coronary arteries (244, 281). COX-2 was reported to mediate relaxation and produce relaxing prostaglandins in healthy human subjects (282), canine coronary arteries (283), abdominal aorta or gracilis muscle arterioles from eNOS-/- mice (284, 285), COX-1-/- mice (286) and mice aortic rings (287). In contrast, other reports showed contraction mediated by COX-2 in coronary arterioles from diabetic patients or mice small mesenteric artery and aorta as well as aortae of aged hamsters (288-290). Furthermore, reports showed that both COX-1 and COX-2 could synthesize TXA_2 in physiological conditions as it found in rat pulmonary artery (266), COX-1 or COX-2 knockout mice (291).

This study shows that COX-mediated opposition to relaxation in ME arteries appears at least in part, to involve both basal and activated TP receptor activities. Other studies also demonstrated TP receptor involvement in enhanced contractions in rat mesenteric resistance arteries (292), Spontaneously hypertensive rat (SHR) rat aorta (293), TP-receptor knockout mice (294) and type 2 diabetic Goto-Kakizaki rats (295). In addition, the data clearly showed that TXA_2 and not PGI_2 nor PGE_2 is the mediator of the

opposition to relaxation in these arteries, as, while the TXA_2 analogue, U46619 could cause contraction, both PGI_2 and PGE_2 caused relaxation in these arteries.

COX-1 protein expression was higher in both arteries compared with COX-2, consistent with both tissues being obtained from healthy donors (296). COX-2 protein expression was much less than COX-1 in both SKM and ME arteries as COX-2 is hardly detectable under physiological conditions (297). There was no difference in COX-2 expression between the SKM and ME arteries. Thus, the difference in activity of these isoforms in these arteries maybe related to post translational modifications.

The role of COX enzymes is controlled by their micro-environment, the level of substrate available, the expression of individual prostanoid synthase enzymes, and the expression and cellular targets of the prostanoid receptors which mediate their actions (298). The micro-environment of the arteries appears to favor the formation of dilator prostanoids by COX-1 in SKM arteries but constrictor prostaniods by COX-2 in ME arteries. Mesenteric arterial bed is a primary toxicity target organ (299) and more exposed to inflammation markers such as cytokines, tumor necrosis factor (TNF)-α, DAPK3 (300), C reactive protein (CRP) (301), and phosphodiesterase 4 (PDE4) well known to activate EDCF (299-301) that increases to abnormal limit in pathological conditions (298). When comparing gene expression based on vascular bed, a trend was the relative consistency of ME arteries of expressing pro-inflammatory and hypoxia mediated response than SKM arteries. The data showed genes involved in pro-inflammatory and hypoxic response such as 1 HSPB1, NFKBIB, EGR1, FOS, CCL21 and IL15 were higher in ME arteries. In contrast, SKM arteries expressed more of the genes involved in anti-inflammatory and antioxidant activity such as GUCY1A3, SOD1, SNAI2, AKT1S1 and FKBP1A. Furthermore, genes which encode for proteins involved in contraction machinery were upregulated in ME arteries. Taken together, these differences may have impacted the responses of these arteries. Other reports have also showed that transcript levels differed between SKM and ME arteries (302).

Several reports testing vascular function in human patients or disease models showed elevated level of ROS (303), vascular endothelial growth factors (VEGF) (304), cytokines (305) and LPS (306, 307) that promote COX-2 expression. In this study, genes that encode for protein regulating those mediators were found upregulated in ME arteries, and may have contributed to the isoform activity reported.

Endothelium-dependent relaxation in small arteries is mostly mediated by EDH. It accounts for almost all non-prostaglandin/non-NO (70%) relaxation of SKM arteries and together with COX and eNOS could completely account for endothelium-dependent relaxation of SKM arteries in this and other studies (145, 308-310), making all three dilator pathways major players in SKM vasodilation and by extension SKM circulation (311, 312). Interestingly, COX and eNOS displayed a functional relationship that meant one could compensate for the absence of the other in mediating the relaxation of these arteries - a state of functional redundancy (313), which has also been noted by others (284, 314, 315). In these respects, the ovine SKM arteries are like the human skeletal muscle vasculature (316) and therefore a good model to study. However, the functional redundancy observed in this study was agonist-dependent as it was observed with ACh but not with BK even though both agonists are known to activate both COX and eNOS as endothelium-dependent vasodilators (311, 317-320). The difference maybe related to involvement of distinct pathways by these agonists (318).

3.5 Limitation

The ovine SKM and ME tissue samples were obtained from the abattoir for human consumption with limited knowledge of the animal condition that could affect the uniformity of samples. However, this were overcome by collecting SKM and ME arteries from the same animal in some experiments.

3.6 Conclusion

In summary, the study demonstrates that COX's double-edged roles in the regulation of SKM and ME arteriolar tone are isoform-specific, with COX-1 activity dilatory but COX-2 activity constrictor in these arteries respectively. The micro-environment of the arteries may have influenced the COX isoform function. Endothelium-dependent relaxation in these arteries rely mainly on EDH than on eNOS and COX products.
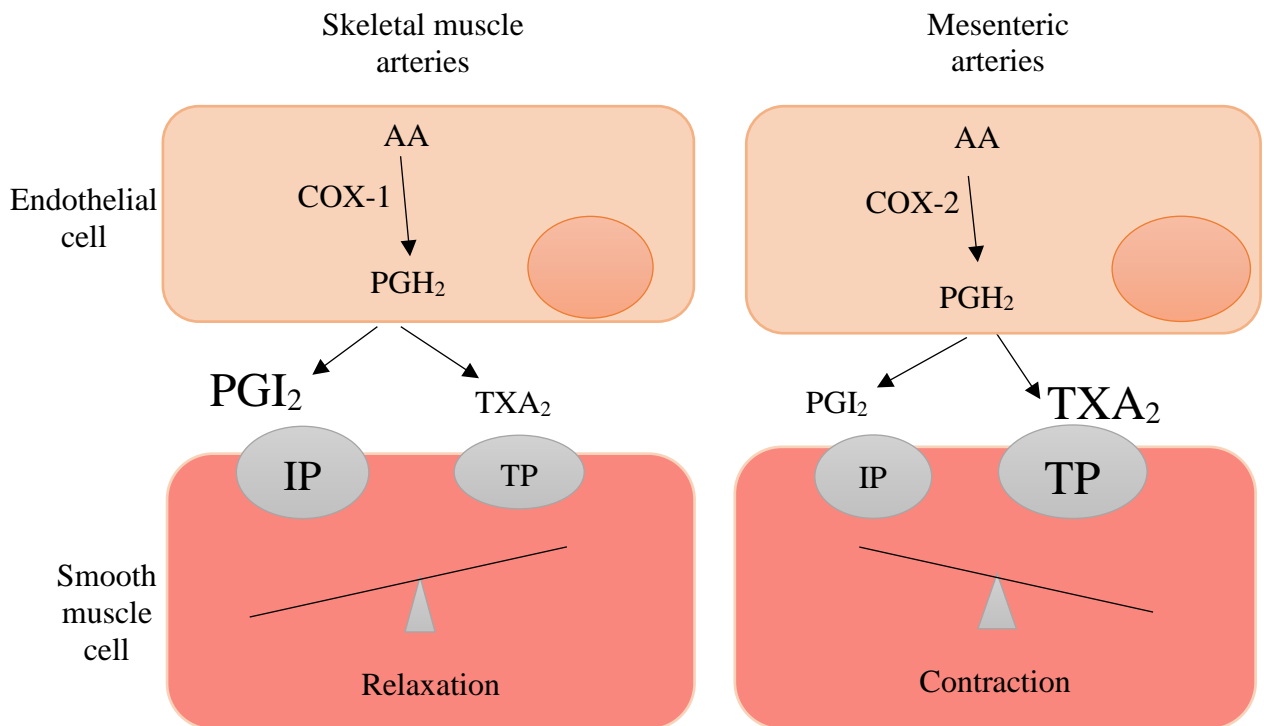
Figure 34: Illustration of proposed mechanism of regulation by COX enzyme isoforms in SKM and ME arteries.

COX-1 in endothelial cells of SKM arteries favor converting PGH_2 intermediate to PGI_2 which favor activation of IP receptor and cause relaxation of smooth muscle cells. In contrast, COX-2 in endothelial cells of ME arteries favors converting the intermediate PGH_2 to TXA_2 which favor activation of TP receptor and cause contraction of smooth muscle cells.

CHAPTER 4: COX role in differential endothelial dilatory capacities of human arteries in obesity

4.1 Introduction

Prostanoids play an important role in vascular homeostasis, often contributing to the maintenance of a fine balance between vasoconstriction and vasodilation. Much of this role is mediated through PGI_2, TXA_2 and to a lesser extent, PGE_2. Recently, the malfunction of COX in the endothelium was identified as a potential molecular determinant of the endothelial dilatory capacity of omental arteries in obesity (159). COX catalyze the first step in the conversion of arachidonic acid into prostanoids which includes prostacyclin (PGI_2, a vasodilator) and thromboxane A_2 (TXA_2, a vasoconstrictor) (50). Under physiological conditions, the endothelium in most arteries produce more dilator than constrictor prostanoids, a regulated balance essential for the maintenance of vascular homeostasis (57, 82). Thus, a reversal of this balance has often been associated with pathological consequences (57, 82), notably, in hypertension and diabetes where increased constrictor prostanoid activities have been linked to vascular dysfunctions (139, 173-175, 321). Since obesity is associated with both hypertension and diabetes, an increase in constrictor prostanoid activity is conceivably a potential risk factor for endothelial dysfunction (322).

Two isoforms of the enzyme (COX-1 and COX-2) are found in the vascular endothelium. COX-1 is expressed constitutively (323) while COX-2 is in large part induced by shear stress and inflammatory stimuli (66). Thus, the expression and activity of these isoforms are differentially regulated, and they can function independently within the same cell (56). For instance, mice with disruption to COX-1 activity lost constitutive but not inducible prostaglandin synthesis (61, 324, 325). COX-1 deficient mice also displayed reduced hypertensive response to angiotensin II and a complete inhibition of endothelium-dependent contractions (mediated by COX-1) in isolated aortic rings (244). On the other hand, inflammation upregulates COX-2 but not COX-1 expression in most tissues (57, 326, 327) and COX-2-derived prostanoids

have been suggested to induce abnormal vasoconstrictor responses or to account for the development of endothelium-derived vasoconstrictor activity in diabetic animal models (288, 289, 328). As a low-level inflammatory condition, obesity, has been associated with increased COX-2 expression in tissues such as renal interlobar arteries (167) and adipocytes (329, 330) which might underlie alteration in the balance in the prostanoids produced. Thus, both COX-1 and COX-2 derived prostanoids can alter the balance in prostanoid activity (82) and induce abnormal endothelium-dependent vasoconstriction response. This study tested the hypothesis that differences in COX and TXA_2 receptor (TP) activities are the drivers of the depot-specific differences in endothelial dilatory capacities of OM and SC arteries in obesity.

Aims

1.1 Determination of the activities of the different COX isoforms in arteries with abnormal endothelial functions.
1.2 Determination of the responsiveness to contractile prostanoids of arteries with abnormal endothelial functions.

4.2 Methods

4.2.1 Sample collection

Obese and young patients who were undergoing laparoscopic bariatric surgery for weight loss were recruited and adipose tissue samples were collected during surgery. The surgeries were performed at Al Emadi and Hamad general hospitals in Doha, Qatar. The study was approved by the institutional (Anti-Doping Lab Qatar [SCH-ADL-070] and Hamad medical corporation Qatar [SCHJOINT-111]) and national (Shafallah Medical Genetic Centre [2011-013]) ethics committees and conducted in accordance with institutional guidelines. All participants provided written consents. Patients with serious illness were excluded such as coronary artery disease, malignancy and any other inflammatory conditions. Physical measurements of height and weight as well

as blood pressure were taken at pre-surgery clinic visits. Body mass index (BMI) was calculated as the weight (kg) divided by the square of the height (m^2). Two adipose tissue samples were obtained during surgery from the abdominal subcutaneous (SC) and intra-abdominal omental (OM) depots and immediately transported in serum-free medium (Cellgro) to the lab. Arteries embedded in the tissues were then isolated and assessed either for reactivity by wire myography or stored at -80°C until analyzed for mRNA expression analysis.

4.2.2 Vascular reactivity studies

Vascular reactivity was investigated using the method described in detail in chapter 2 section 2. Normalized internal diameter for arteries used in this chapter were 217±16 µm for SC arteries and 213±24 µm for OM arteries.

4.2.2.1   Vasodilation

Following equilibration, segments were stimulated with noradrenaline (1-5 µM) to build initial tone. After tone stabilization, Vasodilation was assessed by constructing cumulative concentration-response curves for ACh (10^{-9} - $10^{-4.5}$ mM) starting with the lowest concentration and relaxation responses were recorded. The dose–response curves were obtained in the same preparation separated by a washout period of 30–60 min. With this protocol, there was no apparent time-dependent change in the response to any of the vasoconstrictors. Data were recorded with a PowerLab/LabChart data acquisition system (ADInstruments /Myotech, Denmark) as described previously in chapter 2 section 2.

4.2.2.2 Endothelium-dependent relaxation

Following equilibration, segments were stimulated with noradrenaline (1–5 µM) to build initial tone. When the tone was stable, acetylcholine (ACh, 10^{-9} - $10^{-4.5}$ M), the classical endothelium-dependent dilator was added cumulatively starting with the lowest concentration and relaxation responses were recorded.

4.2.2.3 Endothelium-independent vasorelaxation

To measure the ability of the segments to relax independently of the endothelium, ACh was replaced with sodium nitroprusside (SNP, direct NO donor, 10^{-9} - $10^{-4.5}$ M) and applied cumulatively to the same segments.

The generation of curves for both ACh and SNP on the same segments allowed for comparison between endothelium-dependent and –independent relaxation of same artery.

4.2.2.4 Roles of COX isoforms in the endothelium-dependent relaxation of SC and OM arteries

To determine COX isoform contributions to ACh relaxation of SC and OM arteries, curves were generated in the presence of 1 µM FR122047 (selective COX-1 inhibitor) and 4 µM celecoxib (selective COX-2 inhibitor). FR122047 and celecoxib were added at least 30 min before ACh curves were generated.

4.2.2.5 Vasoconstriction

Vasoconstriction was assessed by constructing cumulative concentration-response curves for NA (10^{-9} - $10^{-5.5}$M) and U46619 (thromboxane A_2 analogue, 10^{-9} - $10^{-5.5}$ M) on the same segment with a washout period of at least 30 minutes between the two curves. This protocol allowed for comparison

between thromboxane A_2 receptor-mediated vs. noradrenergic receptor-mediated contractile responsiveness of the same segment.

4.2.3 Gene expression studies

OM and SC isolated arteries were ground in liquid nitrogen and RNA extracted using Trizol following manufacturer's instructions (Invitrogen, Carlsbed, CA, USA). cDNA was synthesized from 200 ng total RNA using Reverse Transcription Reagent Kit (Applied Biosystems, New Jersey, USA). The mRNA expressions of COX-1/2 genes were determined by q-PCR performed on ViiA7 (Applied Biosystems™, USA) using primer sequences for COX1/2 (Forward: A15629/Reverse: A15630, ThermoFisher, USA) in (Table 7). Data were normalized to β-actin (PPH00073G, NM_001101, Qiagen, Germany) as house-keeping gene and expressed as β-actin to target gene. Details described in chapter 2 section 3.

Table 7: Human primer sequences for q-PCR.

Gene Primer Name	Forward primer sequence (5'-3')	Size (bp)	Reverse primer sequence (5'-3')	Size (bp)
COX-1	CATTTCTGGCAGAGACCTGTGG	22	CGCTTACTTCCTCTGCCCAGC	21
COX-2	ACACAACCCAAATTCCCAGGTTT	23	GCCTATGTGCTAGCCCACAAAGAA	24

4.3   Results

4.3.1 Patients Characteristics

OM and SC arteries from a total of 18 female patients were studied. The patients' characteristics are summarized in (Table 8). Notably, the patients were morbidly obese with body mass index (BMI > 40; obese BMI > 30), insulin-

resistant (HOMA index of insulin resistance >2) and hyper insulinemic (plasma insulin > 7.0 mIU/L). Otherwise, they had relatively normal lipid profile (Less than 200 mg/dL= 5.172 mmol/L) and relatively normal blood pressure.

Table 8: Characteristics of patients whose OM and SC arteries were studied.

Age (years)	35±2
BMI (Kg.m^{-2})	46.2±1.8
MAP (mmHg)	95±3
Glucose (mmol/L)	6.2±0.4
Insulin (mIU/L)	17.0±1.8
HOMA-IR	5.1±0.6
HDL (mmol/L)	1.27±0.09
LDL (mmol/L)	2.87±0.26
TG (mmol/L)	1.33±0.18
T. Cholesterol (mmol/L)	4.71±0.28

(Mean±SEM, n=18)

4.3.2 Vascular reactivity studies

4.3.2.1 Endothelium-dependent relaxation of OM and SC arteries

To determine the functional state of the endothelium in the OM and SC arteries, ACh relaxation was recorded in both arteries pre-constricted with 1 µM noradrenaline, which formed comparable initial tone in both arteries. ACh relaxation was significantly attenuated in OM compared with SC vessels (in the dose range [log M] $^{-7}$ to $^{-6}$), with the OM curve significantly shifted to the right of the SC curve (Figure 35, $p<0.01$, 2-way ANOVA, n=9). I$_{max}$ values for OM were lower than SC both arteries (51.06±7.3% vs. 72.22±3.4%). The OM arteries were significantly less sensitive to ACh compared with SC arteries (log IC$_{50}$ = -6.76±0.43 M vs. -7.08±0.1 M) for OM vs. SC arteries respectively.
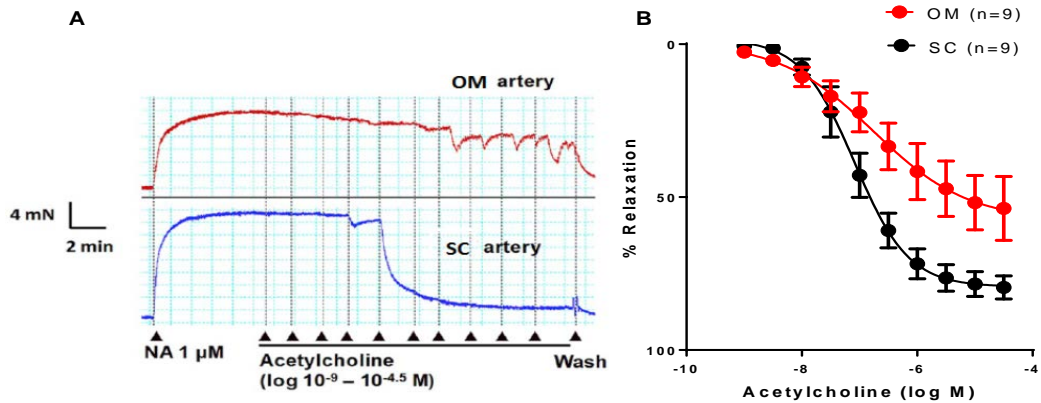
Figure 35: Endothelial-dependent ACh-induced relaxation of OM and SC adipose tissue arteries.

(A) Typical recording of ACh relaxation in OM and SC arteries from same patient. Lowest point of each response to ACh was taken and % relaxation calculated relative to initial tone by NA. (B) The relaxation of OM arteries was significantly attenuated compared with SC arteries with a significant difference between the curves ($p<0.01$, 2-way ANOVA, n=9). The OM arteries were significantly less sensitive to ACh compared with SC arteries (log IC_{50} = -6.54±0.28 M vs. -7.07±0.1 M for OM vs. SC arteries respectively, $p<0.01$). Data are expressed as % relaxation (Mean ± SEM) of the initial tone induced by noradrenaline and were fitted with GraphPad Prism software.

4.3.2.2 Endothelium-independent relaxation of OM and SC arteries

SNP is NO donor used for assessment of endothelial-independent relaxation Endothelial function. Compression were made between ACh relaxation (classical endothelium-dependent relaxation) and SNP recorded in OM and SC arteries. ACh relaxation was significantly attenuated compared to SNP in OM arteries (Figure 36, A, $p < 0.001$ between the curves, 2-way ANOVA, $n = 5$). Mean maximum relaxation to ACh was 66.02 ± 4.52 % while mean maximum relaxation to SNP was 93.61± 3.46 % in OM arteries. While in SC arteries the difference was much less between ACh and SNP relaxation (Figure 36, B) with 87.51 ± 3.46 % and 91.75 ± 13.9 respectively.

116
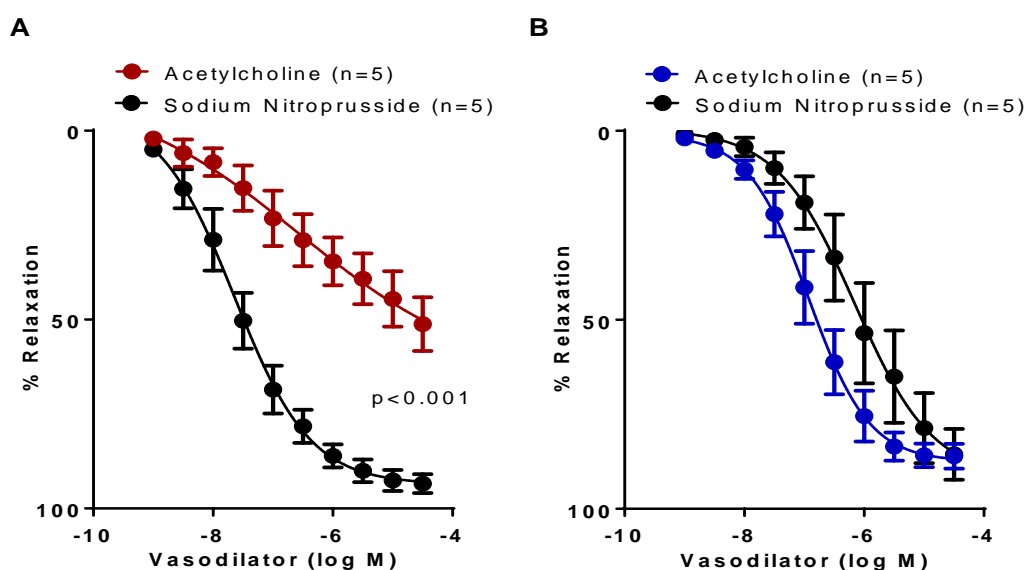
Figure 36: Concentration-relaxation curves for acetylcholine or sodium nitroprusside in OM and SC adipose tissue arteries.

(A) ACh curve was significantly shifted to the right of the curve for sodium nitroprusside (p<0.001, between the curves, 2-way ANOVA, n = 5) in the OM arteries. (B) SC arteries were slightly more responsive to ACh compared with sodium nitroprusside, although the curves were not statistically different from each other (n = 5). Data are expressed as % relaxation (mean ± SEM) of the initial tone induced by noradrenaline and were fitted with GraphPad Prism software.

4.3.2.3 Role of COX isoforms in the relaxation of OM and SC arteries

Following the result with indomethacin, which showed that COX opposed rather than contributed to endothelium-dependent relaxation of OM arteries (142), we investigated the roles of the COX-1 in this observation using selective inhibitors. Experiments were repeated in the presence of 1 µM FR122047, a selective COX-1 inhibitor (IC$_{50}$ 0.028 and 65 µM for COX-1 and COX-2 respectively). FR122047 (Figure 37, A, p<0.01, 2-way ANOVA, n=7) significantly enhanced ACh-induced relaxation of these arteries with significant leftward shift of the

ACh curve. The maximum relaxation I_{max} values increased from 38.2±7.3 % to 73.2±11.9 % in the presence of FR122047 (p<0.01). Investigation of the role of the COX-2 using 4 µM celecoxib, a selective COX-2 inhibitor (IC_{50} 15 and 0.04 µM for COX-1 and COX-2 respectively), showed no effect on relaxation curve (Figure 37, B).
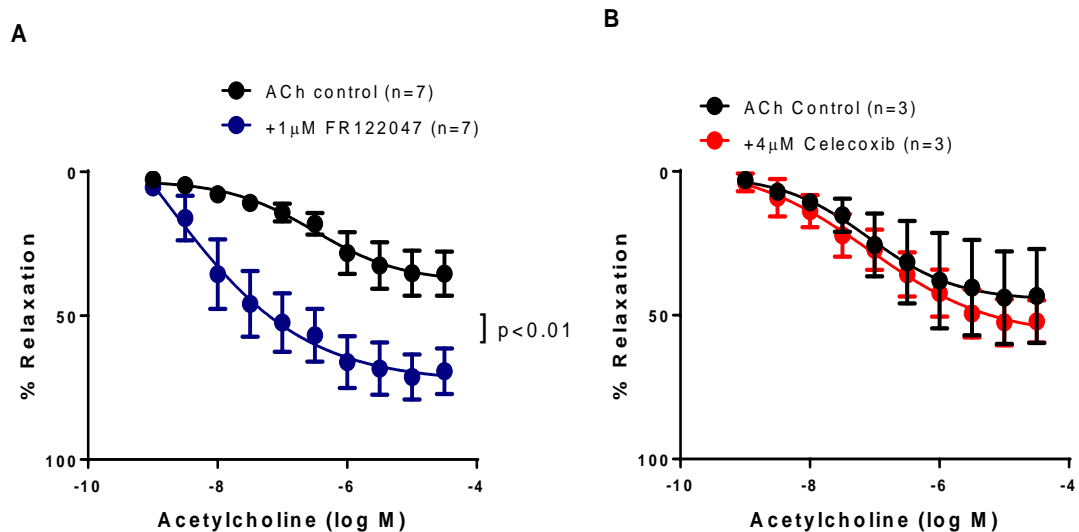
Figure 37: Effect of COX-1 and COX-2 inhibition on ACh-induced relaxation of OM arteries.

(A) 1 µM FR122047 caused a leftward shift of the ACh curve for OM arteries (p<0.01) with I_{max} values increased from 38.2±7.3 % to 73.2±11.9 %. (B) 4 µM celecoxib had no significant effect on the ACh curve for these arteries. Data are expressed as % relaxation (mean ± SEM) of the initial tone induced by noradrenaline and were fitted with GraphPad Prism software.

4.3.2.4 Thromboxane receptor vs. noradrenergic receptor-mediated contractions

COX opposition to endothelium-dependent relaxation is commonly driven by increased contractile prostanoid activity via TP receptor activation. For this reason, we compared the responsiveness of OM and SC arteries to U46619, a thromboxane A_2 (TXA_2) analogue and TXA_2 (TP) receptor agonist. We also

compared TP receptor- and noradrenergic receptor-mediated contractile responsiveness in same arteries. Both U46619 and noradrenaline caused contractions of both SC (Figure 38, A) and OM (Figure 38, B) arteries, with greater contractions generally recorded for U46619 compared with noradrenaline and the curves for U46619 shifted to the left compared with for noradrenaline. However, significant differences between the two curves were recorded only in OM arteries (Figure 38, B, $p < 0.01$, 2-Way ANOVA, n=12) and the log EC_{50} significantly more sensitive to U46619 compared with NA (log EC_{50}, -7.91 ± 0.10 vs. -6.67 ± 0.14 M respectively). When U46619 contractions for both arteries were compared, greater contractions were recorded in OM compared with SC arteries (Figure 39, B, $p < 0.01$, 2-Way ANOVA, n=4). NA contractions for both arteries were comparable (Figure 39, A).
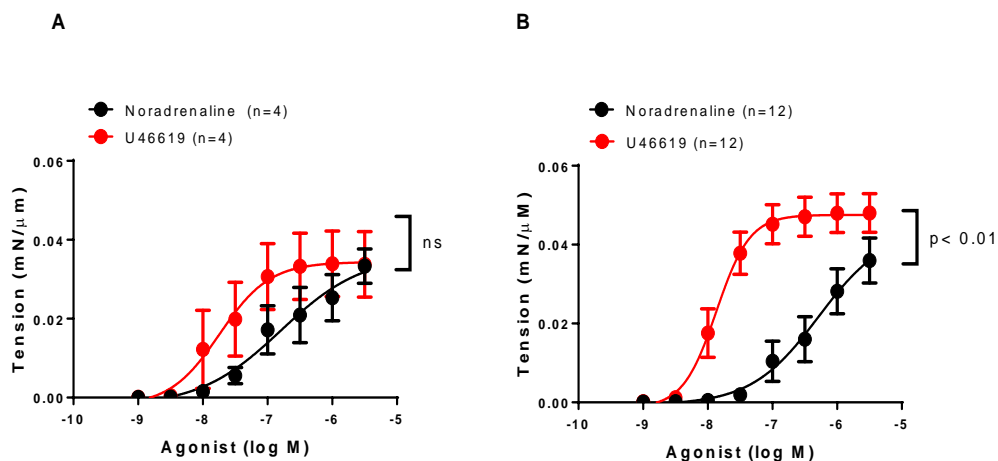
Figure 38: Concentration-contraction curves for U46619 and Noradrenaline in SC and OM adipose tissue arteries.

(A) Contractions to U46619 (TXA_2 analogue) in SC arteries were slightly shifted to the left of the contractions to NA but the differences were not significant (n=4). (B) Contractions to U46619 (TXA_2 analogue) in OM arteries were significantly greater than to NA ($p < 0.01$, 2-Way ANOVA, n=12). The OM arteries were also more sensitive to U46619 compared with NA. The curves were generated by fitting data with GraphPad Prism software.
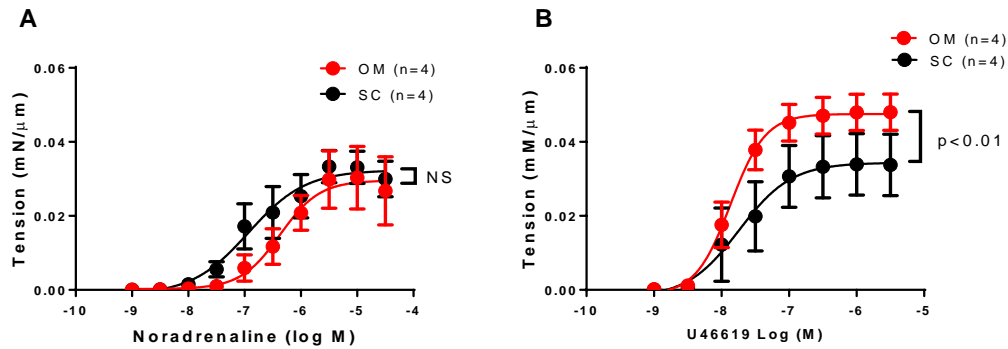
Figure 39: Concentration-contraction curves for Noradrenaline and U46619 in human OM and SC adipose tissues from the same individuals.
(A) Noradrenaline contractions were slightly greater in SC arteries compared with OM arteries, but the difference was not significant (n=4). (B) U46619 contractions were significantly greater in OM arteries compared with SC arteries (P<0.01 between the curves, 2-Way ANOVA, n=4). The curves were generated by fitting data with GraphPad Prism software.

4.3.3 COX isoforms gene expression in human OM and SC arteries

The relative expression of COX-1 and COX-2 genes in both OM and SC arteries from obese patients using q-PCR were studied. The results showed upregulation of COX-1 gene in both arteries compared with COX-2. However, significant upregulation of COX-1 was only seen in OM arteries (Figure 40, A, p<0.05, n=5). In contrast, COX-2 gene expression was relatively the same in both arteries (Figure 40, B, n=4).
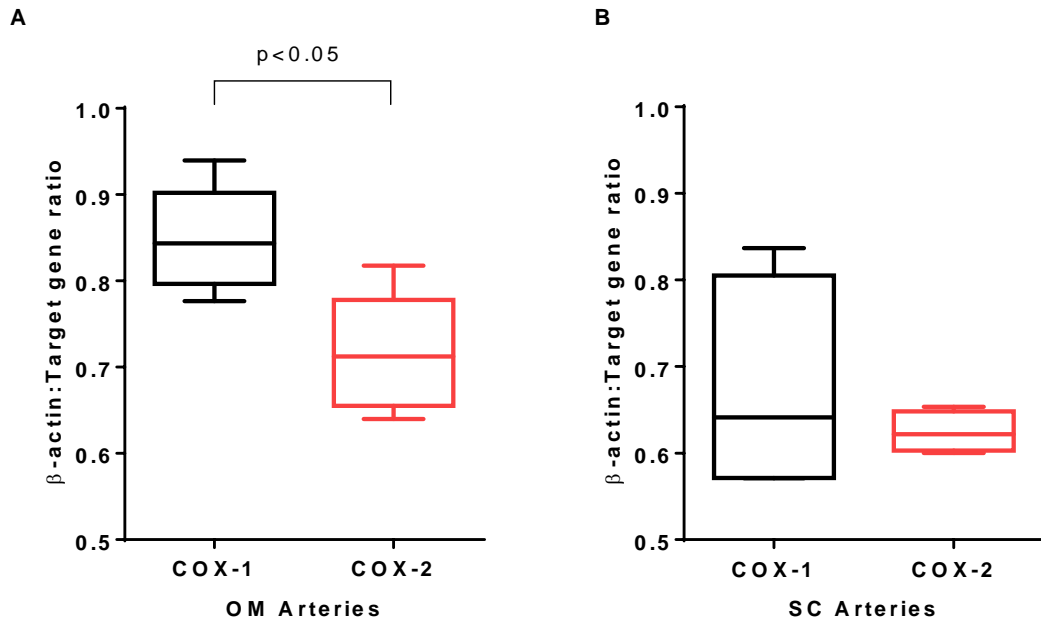
Figure 40: mRNA expression of COX-1 and COX-2 in OM and SC arteries.
(A) COX-1 expression was upregulated in OM compared with COX-2 ($p<0.05$, n=5). (B) COX-1 and COX-2 expression was relatively unchanged (n=4) in SC arteries. Data represented as ratio of β-actin to target gene expression. $p <$ 0.05, paired t-test was used.

4.4 Discussion

It is widely recognized that the microvascular circulation is a major target for obesity-related endothelial dysfunction (322). Although the mechanism of this abnormality is not well understood, it is often attributed to reduction in NO availability (322). In fact, the reduction in EDHF rather than NO per se accounts for decreased endothelial dilatory capacity of OM compared with SC arteries in morbid obesity (142, 331). In this study, we showed that decreased dilatory capacity of OM arteries is orchestrated by increased and altered COX-1 and thromboxane TP receptor activities which oppose endothelium-dependent relaxation of these arteries. The depot-specific difference in endothelial dilatory capacity between OM and SC arteries is in agreement with previous reports albeit for a different (North American) obese population (332) that also suggested that COX-1-derived vasoconstrictor prostanoids were partly responsible for this abnormality (159). The current study has gone further to demonstrate that the OM arteries which suffer reduced endothelial dilatory capacity, also display enhanced TP receptor activity, demonstrated by hyper contractile response to the TP receptor agonist U46619 compared with SC arteries. This provides the first direct evidence for the greater vulnerability of human OM arteries to exaggerated contractile prostanoid activity that has the potential to limit their endothelium-dependent dilatory capacity in obesity. This is also consistent with COX-1 being the primary isoform related to endothelium-dependent contractions (244, 333-335) and enhanced TP receptor-dependent vascular contractions being associated with metabolic diseases (336, 337). Moreover, COX-1/TXA$_2$ pathway has been shown to mediate vascular hypercontractility linked to endothelial dysfunction in obesity (337) and experimental model of hyperlipidemia (338). TP receptor is coupled to guanine nucleotide-binding protein G$_q$ in vascular smooth muscle (VSM) (339). Activation of the receptor stimulates membrane-bound G$_q$-dependent phospholipase C (PLC) β to hydrolyze Phosphatidylinositol 4,5-bisphosphate (PIP$_2$) to inositol triphosphate (IP$_3$) and diacyl glycerol (DAG) (340). IP3 activates the mobilization of intracellular Ca^{2+}, and DAG activates PKC, to initiate and promote vasoconstriction respectively.

The OM depot is more heavily implicated in metabolic syndrome compared with SC. Obese individuals with excess fat stored in visceral adipose depots generally suffer greater adverse metabolic consequences compared with similarly overweight subjects with excess fat stored predominantly in subcutaneous sites (341). COX-1 was upregulated in OM arteries While COX-2 gene was relatively the same in both arteries. This is consistent with OM being more extensively infiltrated with immune-inflammatory cells, such as macrophages and T-lymphocytes (155) and having the capacity to secrete more interlukin-6 (IL-6), (342) and tumor necrosis factor-alpha (TNF-α) (322, 343) which could modulate the deleterious impact of local fat on vasomotor function. TNF-α downregulates eNOS expression at the posttranscriptional level (322, 344) and IL-6 attenuates EDHF-mediated vasodilation (345) and can induce monocyte chemoattractant protein-1 (MCP-1) formation in the vascular smooth muscle via JAK (janus-activated kinase)/STAT (signal and transducers and activators of transcription) signaling pathway (346) to further disrupt vascular tone. Thus, as an important source of low-grade inflammation, visceral fat can directly contribute to the local development of endothelial dysfunction (322). The current study shows that altered endothelial COX-1 and vascular smooth muscle TP receptor activity leads to reduction in the endothelial dilatory capacities of local vessels.

4.5 Limitations

A potential limitation of this study is that only patients with morbid obesity undergoing bariatric surgery were sampled, which might limit its applicability to the wider obese population. However, this limitation is outweighed by the clinical feasibility of accessing both OM and SC simultaneously in same patients to ensure a more robust comparison between the two depots. To avoid the confounding effects of ethnicity, only patients of Arab origin were studied. Thus, the relevance of the specific mechanisms revealed by this study in other ethnic obese populations might require further studies in those populations.

4.6 Conclusion

Increased synthesis of vasoconstrictor prostanoids occur in human diseases and have been implicated in endothelial dysfunction associated with hypertension, diabetes and atherosclerosis. Unsurprisingly, circulating level of thromboxane A_2 is increased in obesity which is a risk factor for not only these diseases but also for endothelial dysfunction. The current study shows that the depot-specific reduction in endothelial dilatory capacities of omental arteries in morbid obesity is in large part due to altered/enhanced COX-1 and TP receptor activities resulting in reduction in endothelial function. This study therefore provides evidence for a direct link between enhanced endothelial COX-1, TP receptor activities and reduction in endothelial function in human obesity. Thus, it opens the possibility that selective thromboxane inhibition could be an effective means of preventing or ameliorating endothelial dysfunction in obesity.
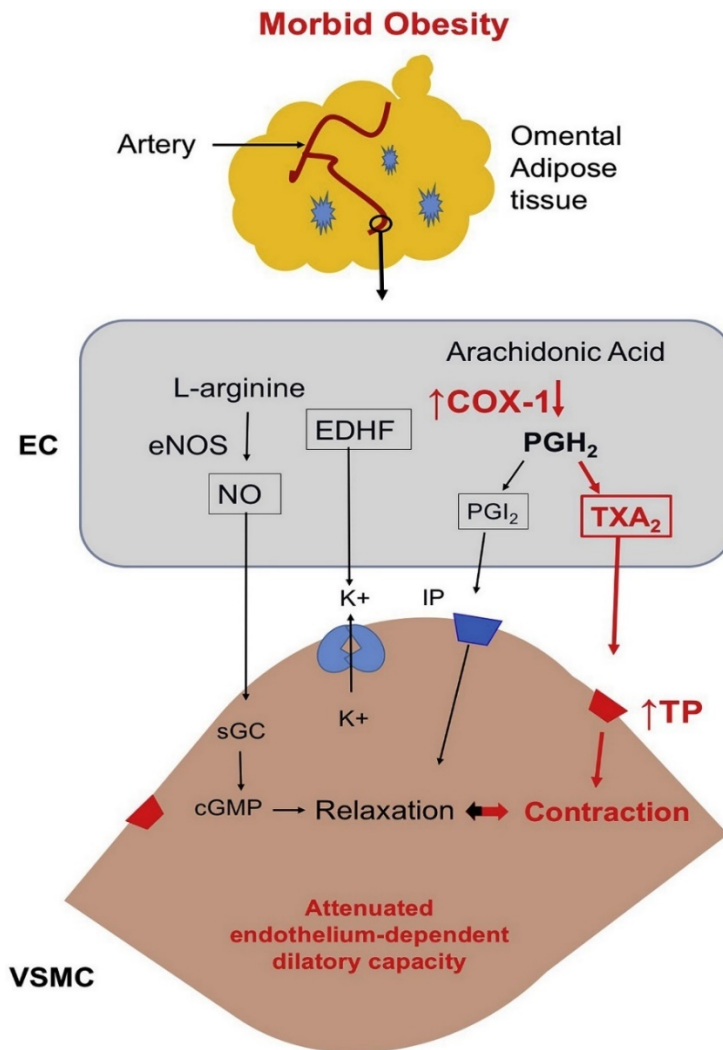
Figure 41: Illustration of proposed role of altered COX-1 and enhanced thromboxane A_2 TP receptor activities in mediating impaired omental endothelial dilatory capacity in morbid obesity.

As the omental adipose tissue expands beyond its homeostatic limit, its secretory and metabolic activities are dysregulated. Consequently, it becomes pathogenic and adversely impacts the local vasculature resulting in the upregulation of the pathway highlighted in red. This includes (1) enhanced but altered COX-1 activity in the endothelial cell (EC) which favor the production of more contractile prostanoids, TXA_2 and (2) enhanced thromboxane A_2 TP receptor activity in the underlying vascular smooth muscle cell (VSMC) which favors increased thromboxane A_2 TP receptor-mediated contractions. Both molecular changes lead to attenuated endothelium-dependent dilatory capacity.

CHAPTER 5: Effect of 20-HE, a supplement-derived ecdysteroid on vascular tone and COX expression in healthy resistance arteries

5.1 Introduction

Ecdysteroids are used by an increasing number of sports interested individuals as anabolic compounds that stimulates muscle growth (185). Such anabolic effects result in increased physical performance (347). In 2020, world antidoping agency (WADA) added 20-Hydroxyecdysone (20-HE) to the monitoring program for substances in sport under anabolic agent category (348). Although ecdysteroids like androgens produce anabolic effects in animals, they appear to have different pharmacological profiles. Notably, ecdysteroids do not have androgenic side effects associated with androgen analogues (194). This is probably because of structural differences, which prevent them from binding to and activating the nuclear androgen receptor (214). In a silico modeling system of compound-protein interaction, the mineralocorticoid receptor was identified as one of the top-ranking proteins with putative interactions with ecdysone (225), but the functional significance has not been confirmed.

There is a growing body of information that support the connection between ecdysteroids and estrogen (187, 193, 349-356). Estrogen acts through its classical receptors ERα and ERβ as well as the newly classified G protein-coupled estrogen receptor GPR30. Binding of estrogen to ERα activates phosphatidylinositol 3- kinase (PI3K), a protein kinase cascade that is coupled to eNOS activation. Beside NO, estrogen also increases PGI_2 production thorough COX regulation in vascular tissues (357) including, cultured ovine fetal pulmonary artery endothelial cells (PAEC) (358, 359), human umbilical vein endothelial cell (HUVEC) (360, 361), rat isolated mesenteric arteries (362) and mice isolated aortic rings (363). Both ERα and ERβ (211, 364, 365) appear to mediate this relationship between estrogen and COX activity in the regulation of vascular tone. Furthermore, selective estrogen receptor modulators (SERMs) rapid vascular effects are mediated through COX-pathways (366).

126

Interestingly though, these effects are not always related to changes in the abundance of COX-1 or COX-2 protein (359), but might relate to increased activity due to availability of substrates. For instance, 20-HE increases the pool of free arachidonic acid and the synthesis of leukotrienes and prostaglandins (185) which might contribute to vasodilation.

Since estrogen receptors are expressed in endothelial cells and estrogen is a vasodilator, which acts by stimulating NO release (367), ecdysteroids acting via these receptors would potentially cause vasodilation via PI3K/Akt/NOS pathway (352). Moreover, an interaction between ecdysterone and eNOS has been demonstrated (368). In another respect, these compounds can protect tissues against oxidative stress-induced injury by scavenging free radicals and modulating NF-κB and JNK pathways (241). Thus, they could potentially reverse ROS-induced upregulation in COX activity, which might adversely impact endothelial function (167).

Aims

This chapter investigates the effect of 20-HE, the most widely used ecdysteroid, on endothelial function (vascular tone) and the expression of COX.

5.2   Method

5.2.1   Vessel preparation

Arteries were isolated from samples of abdominal SKM and ME collected from healthy male sheep, which were slaughtered for meat at a local slaughterhouse. The arteries were cleaned of surrounding tissues and either tested for reactivity or ground in liquid nitrogen for gene and protein expression analysis.

5.2.2 Vascular reactivity studies

Vascular reactivity was investigated using the method described in detail in chapter 2 section 2. In addition, vessels were tested by ACh 10 uM single dose. Normalized internal diameter for arteries used in this chapter were 266±12 µm for SKM arteries and 327±16 µm for ME arteries.

5.2.2.1 Vasorelaxation by 20-HE and β-estradiol

Arteries were precontracted by 10 µM NA before vasodilation experiments. Vasodilation was assessed by constructing cumulative concentration-response curves for 20-HE (10^{-10} - $10^{-5/-5.5}$M) and β-estradiol (10^{-9} - $10^{-5.5}$M). The dose–response curves were obtained in the same preparation separated by a washout period of 30–60 min. With this protocol, there was no apparent time-dependent change in the response to any of the vasodilators. Data were recorded with a PowerLab/LabChart data acquisition system (ADinstrment/Myotech, Denmark) as described previously in chapter 2 section 2.
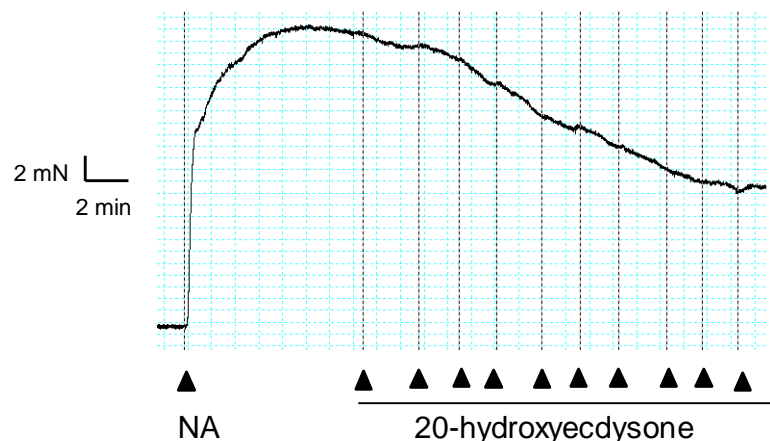
Figure 42: Representative tracing showing the general protocol for of relaxation response to 20-HE in SKM arteries.

Artery segments were pre-contracted with 10 µM NA and 20-HE doses added in a cumulative fashion once the contractions had plateaued. The vessel tone decreased with increasing doses of 20-HE (10^{-10} - $10^{-5.5}$ M). Lowest point of each response to 20-HE was taken and % relaxation calculated relative to initial tone by NA. Image was acquired using LabChart software.

5.2.2.2 Roles of eNOS and COX in 20-HE relaxation of SKM and ME arteries

Endothelial nitric oxide synthase and cyclooxygenase enzyme are mediators of endothelium-dependent relaxation. To determine their contributions to 20-HE relaxation of SKM and ME arteries, curves were generated in the presence of 100 µM L-NAME or 10 µM indomethacin respectively. L-NAME or indomethacin were added at least 30 minutes before 20-HE curves were generated.

5.2.2.3 Role of estrogen receptors in 20-HE and β-estradiol relaxation of SKM and ME arteries

To determine whether estrogen receptors played any part in 20-HE-induced relaxation, curves were generated in the presence of 1µM ICI 182.780 (ER antagonist), 0.5 µM MPP (ERα antagonist) and 1 µM PHTPP (ERβ antagonist). Parallel curves were generated for β-estradiol to measure the effectiveness of these antagonists. All inhibitors were added at least 30 minutes before 20-HE or β-estradiol curves were generated.

5.2.3 Tissue and cell culture

5.2.3.1 SKM and ME arteries

SKM and ME arteries were incubated in Dulbecco's Modified Eagle's Medium (DMEM, Sigma) supplemented with 100 U/ml penicillin (Sigma) and 100 µg/ml streptomycin (Sigma) for the control group while 1 µM 20-HE were added to the previously mentioned medium for 1 hr. The concentration of 20-HE chosen gave maximum vasodilation in SKM and ME arteries as demonstrated in (Figure 43) and used in other report (369). The arteries were treated for 1 hr to match the duration of recorded relaxation to 20-HE and to mimic non-genomic effect (369-371). Thereafter, they were removed and freeze-stored at -80ºC.

5.2.3.2 Human Coronary Artery Endothelial Cells (HCAEC)

Human Coronary Artery Endothelial Cells (HCAEC) were purchased from Lonza (CC-2585) and maintained in Microvascular Endothelial Cell Growth Medium-2 (EGM®-2MV BulletKit®, CC-3202, Lonza) supplemented with HCM singleQuots (CC-4182, Lonza) at 37ºC in a humidified atmosphere with 5% CO_2, according to manufacturer's protocol. The cells were tested at 70-85% confluency.

After the culture reached to 70-85% confluence, control cells were incubated with the maintenance media for 1 hour while 1 µM 20-HE were added to the maintenance media in 20-HE treated group for 1 hour also. After the incubation period, the cells were removed and freeze-stored at -80ºC.

5.2.4 Gene expression studies

5.2.4.1 Microarray gene expression analysis

SKM and ME arteries were ground in liquid nitrogen and RNA extracted using Trizol following manufacturer's instructions (Invitrogen, Carlsbed, CA, USA). Total RNA from experimental groups was then used to synthesize cRNA (GeneChip® WT PLUS Reagent Kit) probe for hybridization to GeneChip™ Ovine Gene 1.1 ST 24-Array Plate high-density transcriptome profiling microarrays obtained from (Affymetrix, USA). This microarray was used to analyze regulated gene expression in SKM and ME arteries. Comparison analysis was carried out on n=6 in duplication for non-treated control and n=11 for 20-HE treated SKM arteries. Comparison analysis was carried out on n=4 in duplication for non-treated control and n=4 for 20-HE treated ME arteries. Analysis of differential gene expression was performed by comparison of gene expression patterns using TAC software (Affymetrix, USA) which normalizes array signals using RMA algorithm. Details described in chapter 2 section 3. Results are presented in PCA, table, volcano plot, heat map and dendrogram.

Ingenuity Pathways Analysis (IPA, Ingenuity® Systems, www.ingenuity.com) were applied. For each pairwise comparison, (20-HE arteries vs. control), p-values < 0.05 from the limma analysis were selected for functional analysis.

5.2.4.2 q -PCR analysis

SKM, ME arteries and HCAEC were ground in liquid nitrogen and RNA extracted using Trizol following manufacturer's instructions (Invitrogen, Carlsbed, CA, USA). cDNA was synthesized from 200 ng total RNA using Reverse Transcription Reagent Kit (Applied Biosystems, New Jersey, USA). The mRNA expressions of COX-1/2 genes were determined by q-PCR performed on ViiA7 (Applied Biosystems™, USA). Target ovine gene primers COX-1 & 2, estrogen receptors ERα & ERβ and eNOS were obtained from Integrated DNA Technologies (IDT, USA). Target human gene primers ; COX-1, COX-2 and eNOS were obtained from (Invitrogen, USA) .100 µM of each primer was diluted (1:10) (Table 9, Table 10). Reaction was carried out in duplicate in 96-well plate using 20 µl total volume per well. Each well contained mixture of SYBER green solution, primer, cDNA and nuclease-free water. Data were normalized to GAPDH as house-keeping gene and expressed as ratio (GAPDH / target gene). Details described in chapter 2 section 3.

Table 9: Ovine primer sequences for q-PCR.

Gene Primer Name	Forward primer sequence (5'-3')	Size (bp)	Reverse primer sequence (5'-3')	Size (bp)
β-actin	5'-ATGCCTCCTGCACCACCA-3'	18	5'-GCATTTGCGGTGGACGAT-3'	18
GAPDH	5'-GTTCCACGGCACAGTCAAGG-3'	20	5'-ACTCAGCACCAGCATCACCC-3'	20
ERα	5'-ATCCCCACAC GCTCTGCCTTG-3'	21	5'-TGCCGGAACGGCTTTGGTGTGT-3'	22
ERβ	5'-ATGGATGTCA AAAACTCACC A-3'	21	5'-GTCTTTGGGGTCCGAGTCACT-3'	21

Gene Primer Name	Forward primer sequence (5'-3')	Size (bp)	Reverse primer sequence (5'-3')	Size (bp)
COX-1	5'-ATGAGTACCGCAAGAGGTTTGG-3'	22	5'-ACGTGGAAGGAGACATAGG-3'	19
COX-2	5'-CAGAGCTCTTCCTCCTGTGC-3'	20	5'-CAAAAGGCGACGGTTATGC-3'	19
eNOS	5'-GGCAGACCCCACCTTCTTGG-3'	20	5'-CCACACTCTTCAAGTTGCCCAT-3'	22

Table 10: Human primer sequences for q-PCR.

Gene Primer Name	Forward primer sequence (5'-3')	Size (bp)	Reverse primer sequence (5'-3')	Size (bp)
COX-1	5'-CATTTCTGGCAGAGACCTGTGG-3'	22	5'- CGCTTACTTCCTCTGCCCAGC -3'	21
COX-2	5'-ACACAACCCAAATTCCCAGGTTT-3'	23	5'- GCCTATGTGCTAGCCCACAAAGAA-3'	24
eNOS	5'-GCTTGTTCCTGTCCCATTGTGTATG-3'	25	5'- CGACTCTGATCCTGGTCTCCTTTC-3'	24

5.2.5 Protein expression studies

To determine the expression levels of COX-1, COX-2 ,eNOS, ERα and ERβ proteins in SKM and ME isolated arteries and HCAEC, western blot analysis was conducted using specific primary antibodies for COX-1 (polyclonal antibody, dilution factor 1:200, 160103, Cayman Chemical, USA), COX-2 (polyclonal antibody, dilution factor 1:200, 160106, Cayman Chemical, USA), eNOS (polyclonal Antibody, dilution factor 1:1000, PA1-037, Invitrogen, USA), estrogen receptor α antibody (polyclonal antibody, dilution factor 1:200, ab75635, abcam, UK), estrogen receptor β antibody (monoclonal antibody dilution factor 1:200, ab187291, abcam, UK) and GAPDH control antibody

(polyclonal antibody, dilution factor 1:2500, ab9485, abcam, UK). As a secondary antibody, anti-rabbit IgG (polyclonal antibody, dilution factor 1:30,000, A0545-1ML, Sigma, USA) and anti-mouse immunoglobulin/HRP (polyclonal antibody, dilution factor 1:2000, P0161, DAKO, USA) were used. Detailed procedure was described in chapter 2 section 4.

5.3 Results

5.3.1 20-HE and β-estradiol-induced relaxation of SKM and ME arteries

Both 20-hydroxyecdysone and β-estradiol caused dose-dependent relaxation of both SKM and ME arteries (Figure 43 and Figure 44). I_{max} values were 49.66±6.57 % and 62.28±19.35 % for SKM and ME arteries respectively. The log IC_{50} values for relaxation of both arteries were -8.30±0.95M and -8.7±0.77 M for SKM and ME arteries respectively (Figure 43). Curves for β-estradiol in both arteries were overlapped (Figure 44).
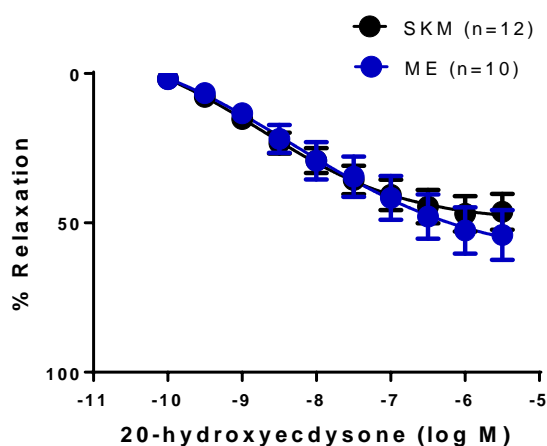
Figure 43: 20-HE relaxation curves for SKM and ME arteries.
20-HE caused relaxation in SKM (n=12) and ME arteries (n=10). There was no difference between the SKM and ME curves. Data are expressed as % relaxation (mean ± SEM) of the initial tone induced by noradrenaline and were fitted with GraphPad Prism software.
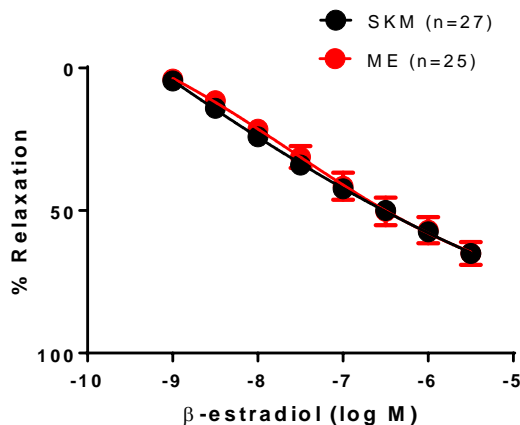
Figure 44: β-estradiol relaxation in SKM and ME arteries.

β-estradiol caused relaxation in SKM (n=27) and ME arteries (n=25). There was no difference between the SKM and ME curves. Data are expressed as % relaxation (mean ± SEM) of the initial tone induced by noradrenaline and were fitted with GraphPad Prism software.

5.3.2 Role of COX in 20-HE relaxation of SKM and ME arteries

To determine the role of COX in the relaxation induced by 20-HE, cumulative concentration-response curves were generated in both SKM and ME arteries for 20-HE in the absence and presence of 10 µM indomethacin. There was no effect of COX inhibition on 20-HE curve in SKM arteries (Figure 45, A, n=5) and ME arteries (Figure 45, B, n=3).
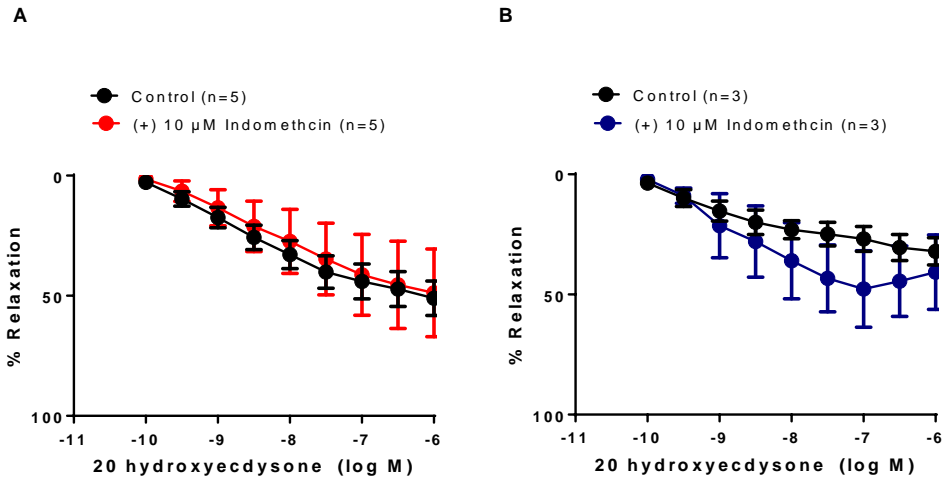
Figure 45: The effect of COX inhibition on 20-HE relaxation in SKM and ME arteries.

(A) The effect of 10 µM indomethacin on 20-HE relaxation in SKM arteries. There was no effect of COX inhibition on 20-HE relaxation in SKM arteries (n=5). (B) The effect of 10 µM indomethacin on 20-HE relaxation in ME arteries. There was no effect of COX inhibition on 20-HE relaxation in ME arteries (n=3). Data are expressed as % relaxation (mean ± SEM) of the initial tone induced by noradrenaline and were fitted with GraphPad Prism software.

5.3.3   Role of eNOS in 20-HE relaxation of SKM and ME arteries

To determine the role of eNOS in 20-HE relaxation, arteries were treated with 100 µM L-NAME for 30 min prior of 20-HE dose response treatment. Curves generated for 20-HE were significantly shifted to the right in the presence of L-NAME (100 µM) in both SKM (Figure 46, A, $P<0.01$, 2-Way ANOVA, n=7) and ME arteries (Figure 46, B, $P<0.05$, 2-Way ANOVA, n=6).

Role of eNOS were also investigated in β-estradiol-induced relaxation of these arteries. The arteries were treated with 100 µM L-NAME for at least 30 minutes prior to generating curve for estradiol. L-NAME caused significant rightward shift of the curves for both SKM (Figure 47, A, $P<0.01$, 2-Way ANOVA, n=4) and ME arteries (Figure 47, B, $P<0.05$, 2-Way ANOVA, n=5).

135
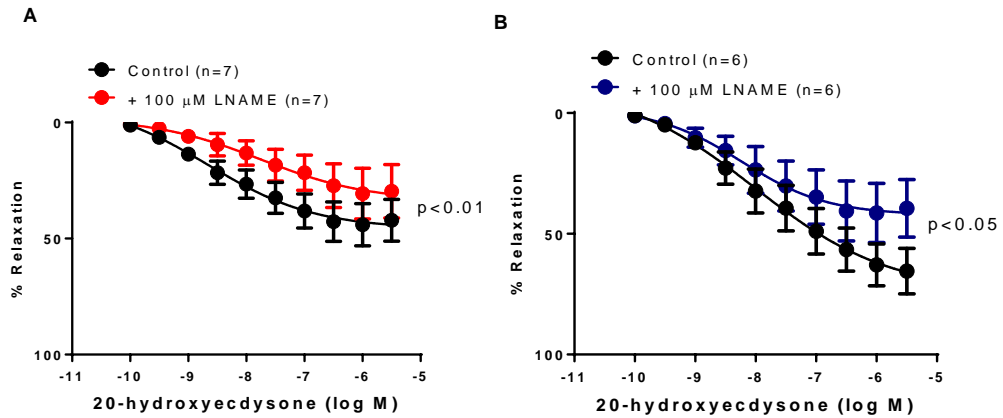
Figure 46: The effect of eNOS inhibition on 20-HE relaxation in SKM and ME arteries.

(A) The effect of 100 µM L-NAME on 20-HE relaxation in SKM arteries. 100 µM L-NAME caused significant rightward shift of the 20-HE relaxation in SKM (P<0.01, 2way-ANOVA, n=7). (B) The effect of 100 µM L-NAME on 20-HE relaxation in ME arteries. 100 µM L-NAME caused significant rightward shift of the 20-HE relaxation in ME arteries (P<0.05, 2way-ANOVA, n=6). Data are expressed as % relaxation (mean ± SEM) of the initial tone induced by noradrenaline and were fitted with GraphPad Prism software.
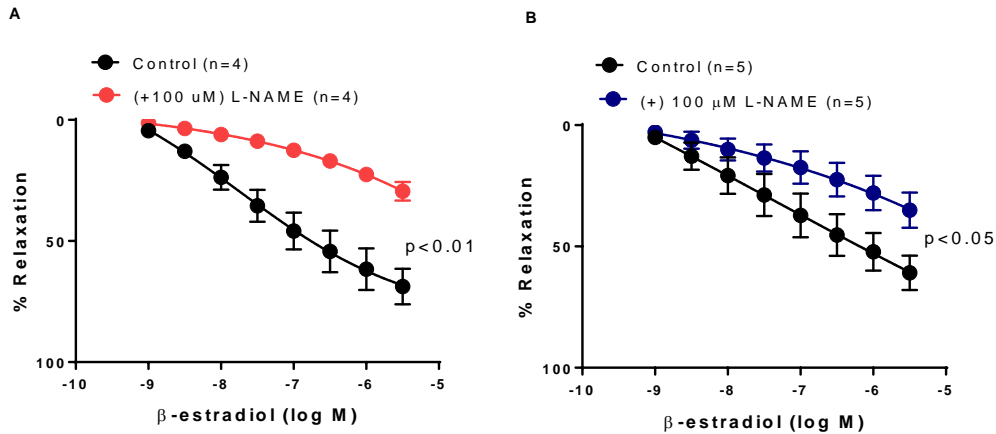
Figure 47: The effect of eNOS inhibition on β-estradiol relaxation in SKM and ME arteries.

(A) The effect of 100 μM L-NAME on estradiol relaxation in SKM arteries. 100 μM L-NAME caused significant rightward shift of the β-estradiol relaxation in SKM arteries (P<0.01, way-ANOVA, n=4). (B) The effect of 100 μM L-NAME on estradiol relaxation in ME arteries. 100 μM L-NAME caused significant rightward shift of the β-estradiol relaxation in ME arteries (P<0.05, way-ANOVA, n=5) arteries. Data are expressed as % relaxation (mean ± SEM) of the initial tone induced by noradrenaline and were fitted with GraphPad Prism software.

5.3.4 Role of estrogen receptors in 20-HE relaxation

Since 20-HE reported to activate estrogen receptors (187, 193), the roles of the two estrogen receptors ER-α and ER-β were investigated in 20-HE relaxation. In the presence of 1 μM ICI.182.780 a blocker of higher potency for ER-α than ER-β, the relaxation curve was not changed (Figure 48, A, n=3). Similarly, the presence of 1 μM PHTPP which selectively blocks ER-β did not alter 20-HE relaxation (Figure 48, B, n=4).

Relaxation to β-estradiol, the agonist for these receptors was also not altered by these receptor blockers. In the presences of 0.5 μM MPP (Figure 49, A, B, n=3-4), 1 μM PHTPP (Figure 50, A, B, n=4-5), 1 μM ICI.182.780 (Figure 51, A, B, n=4-5), the relaxation to β-estradiol was not altered.
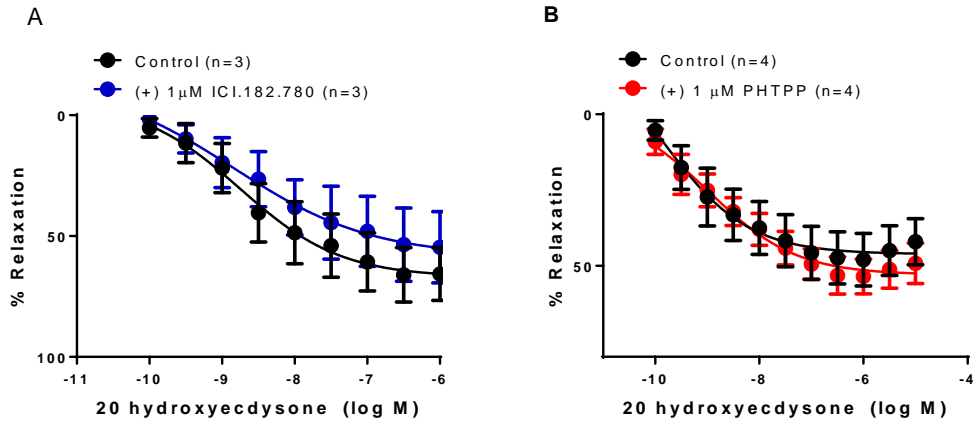
Figure 48: The effects of estrogen receptor blockade on 20-HE relaxation of SKM arteries.

(A) Effect of 1 µM ICI.182.780 on 20-HE relaxation in SKM arteries. 1µM ICI.182.780 had no effect on 20-HE relaxation of SKM arteries (n=3). (B) The effect of 1 µM PHTPP on 20-HE relaxation in SKM arteries. PHTPP had no effect on 20-HE relaxation of ME arteries (n=4). Data are expressed as % relaxation (mean ± SEM) of the initial tone induced by noradrenaline and were tested using 2-Way ANOVA and fitted with GraphPad Prism software.
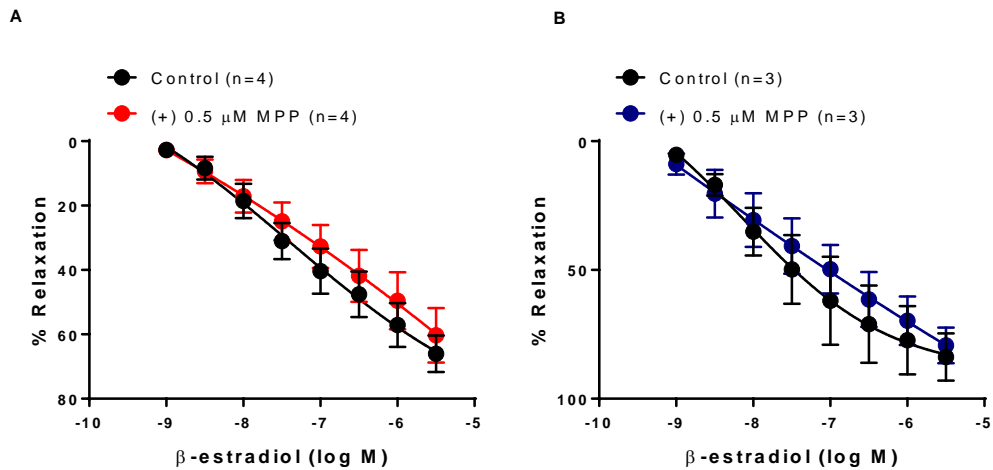
Figure 49: The effect of estrogen receptor α inhibition on β-estradiol relaxation in SKM and ME arteries.

0.5 µM MPP did not alter β-estradiol relaxation in (A) SKM arteries (n=4) and (B) ME arteries (n=3). Data are expressed as % relaxation (mean ± SEM) of the initial tone induced by noradrenaline and were tested using 2-Way ANOVA and fitted with GraphPad Prism software.
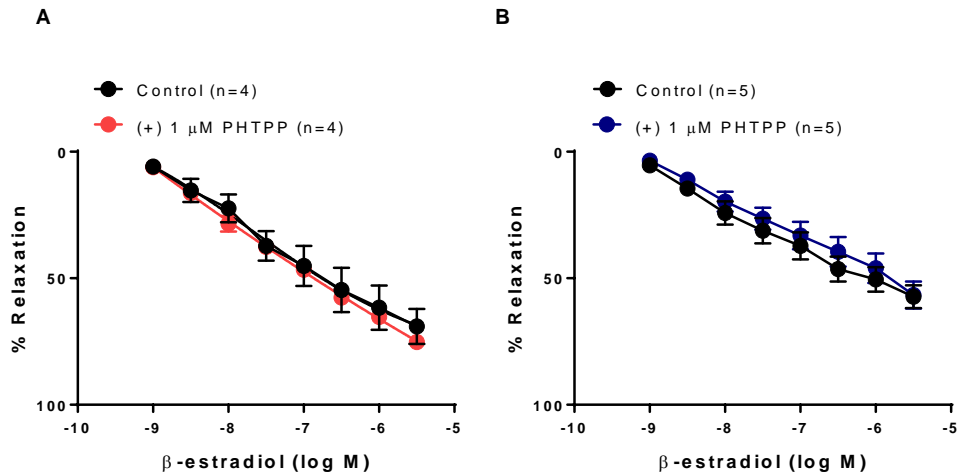
Figure 50: The effect of estrogen receptor β inhibition on β-estradiol - induced relaxation in ovine SKM and ME arteries.

1 μM PHTPP did not alter β-estradiol relaxation in (A) SKM arteries (n=4) and (B) ME arteries (n=5). Data are expressed as % relaxation (mean ± SEM) of the initial tone induced by noradrenaline and were tested using 2-Way ANOVA and fitted with GraphPad Prism software.
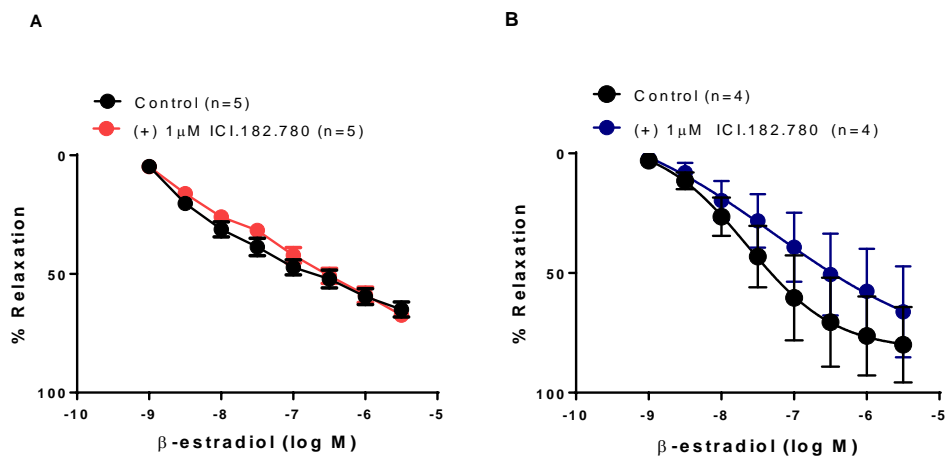
Figure 51: The effect of non-selective inhibition of estrogen receptor α\β on β-estradiol relaxation in SKM and ME arteries.

The general estrogen receptor α\β blocker, 1 μM ICI 182.680 had no significant effect on the β-estradiol relaxation in (A) SKM arteries (n=5) and (B) ME arteries (n=4). Data are expressed as % relaxation (mean ± SEM) of the initial tone induced by noradrenaline and were tested using 2-Way ANOVA and fitted with GraphPad Prism software.

5.3.5 Gene expression studies

5.3.5.1 Microarray gene expression analysis in arteries treated with 20-HE

In SKM arteries, microarray analysis revealed a total of 2560 genes (11.56%) whose expression were differentially expressed according to criteria chosen (adjusted P-value FDR P-value <0.05). 788 (69.22%) were up-regulated and 1772 (30.78%) were down-regulated genes in SKM 20-HE treated arteries (Figure 52).

In ME arteries, microarray analysis revealed a total of 7 genes (0.03%) whose expression were differentially expressed according to criteria chosen (adjusted P-value FDR P-value <0.05). 5 (71.43%) up-regulated and 2 (28.57%) genes were down-regulated in ME 20-HE treated arteries (Figure 53).

IPA organized genes into biological functions and tested whether each function is significantly over-represented in the selected list of genes; over-representation may indicate that a specific biological process was affected by the 20-HE treatment. In the categories of Cardiovascular Systems and Cardiovascular Diseases. There are no statistically significant entries found in these results for cardiovascular functions and diseases in both SKM and ME treated arteries with 20-HE. A list of the outcomes by IPA can be found in the appendix.
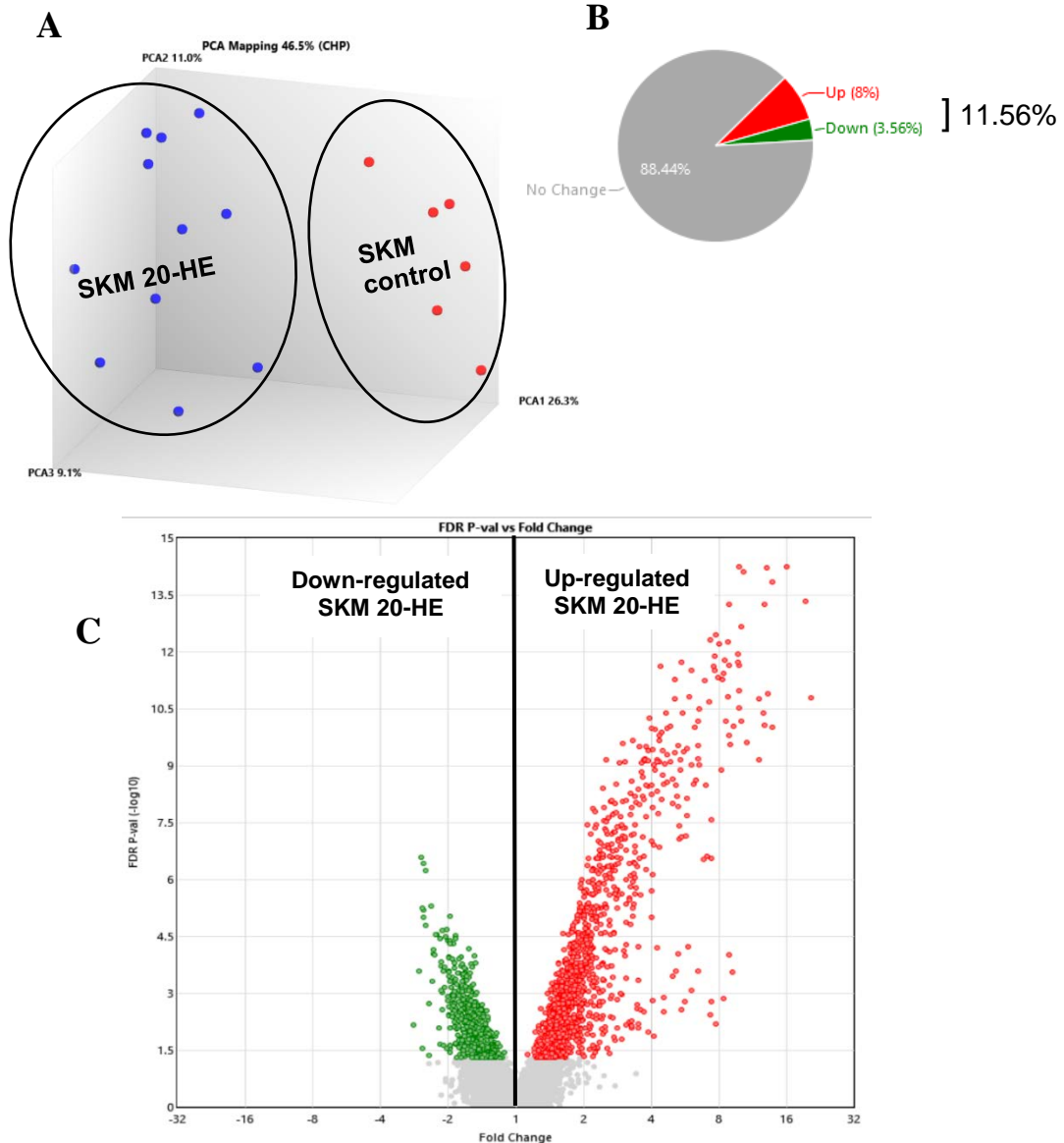
Figure 52: Differentially expressed genes between 20-HE treated SKM and non-treated (control) arteries (FDR P-value < 0.05; RMA).

(A) PCA 2-dimensional (Dim.) scatter plots representing the gene expression patterns of the different samples (SKM 20-HE and SKM control arteries). Each dot represents a sample. Samples were divided to 2 distinct groups based on their gene expression profiles. (B) Pie chart showing the percentages of differentially expressed genes. (C) Volcano plot of gene expression fold changes vs. FDR P-value. The 1772 genes up-regulated in SKM 20-HE arteries are indicated in red, and the 788 genes down-regulated genes in SKM 20-HE arteries are indicated in green. Genes that were not different are indicated in gray.
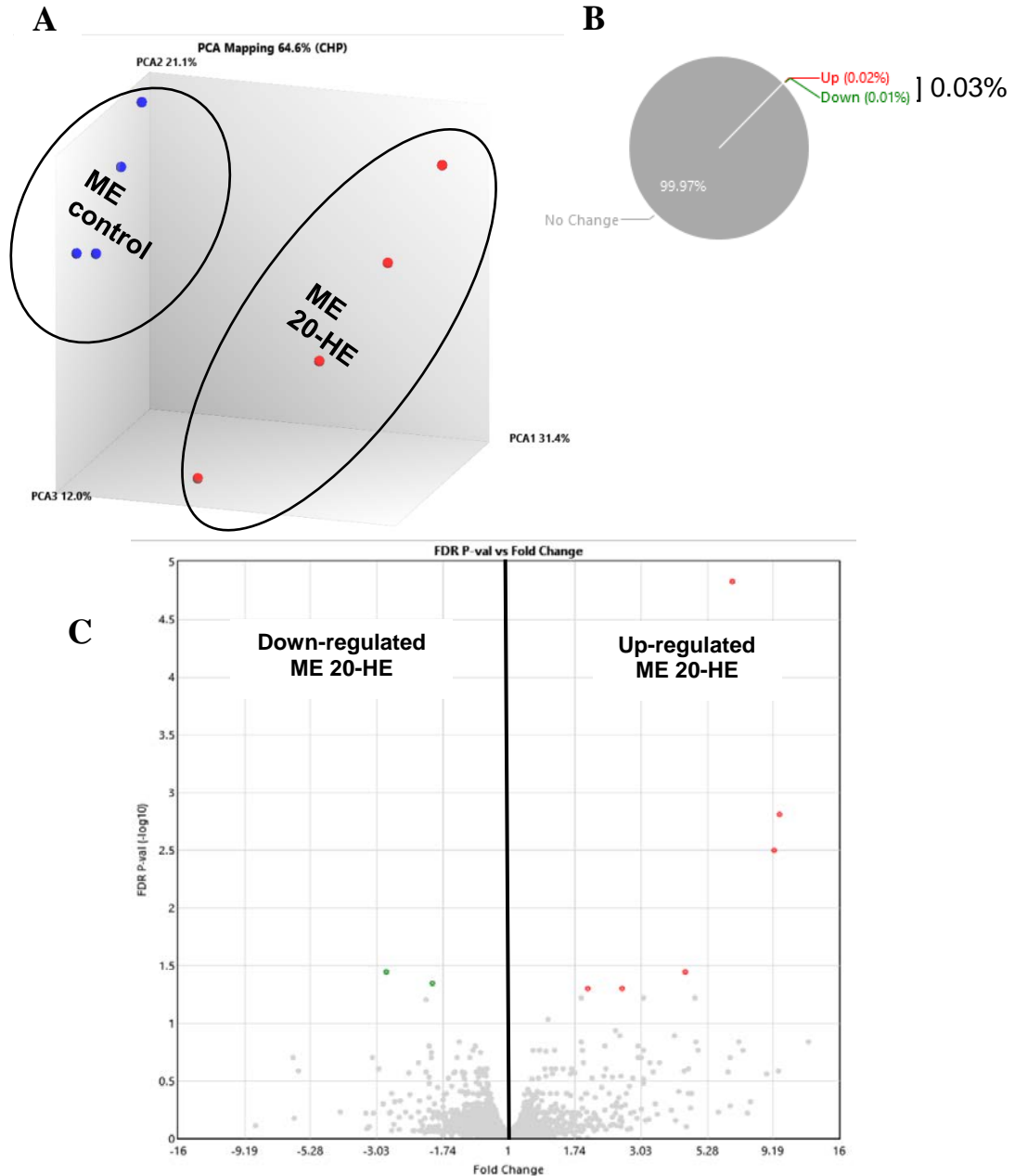
Figure 53: Differentially expressed genes between ME 20-HE and ME control arteries (FDR P-value < 0.05; RMA).

(A) PCA 2-dimensional (Dim.) scatter plots representing the gene expression patterns of the different samples (ME 20-HE and ME control arteries). Each dot represents a sample. Samples were divided into two distinct groups based on their gene expression profiles. (B) Pie chart showing the percentages of differentially expressed genes. (C) Volcano plot of gene expression fold changes vs. FDR-P-value. The 5 genes up-regulated in ME 20-HE arteries are indicated in red, and the 2 genes down-regulated in ME 20-HE arteries are indicated in green. Genes that were not different are indicated in gray.

142

Expression of genes encoding smooth muscle contractile proteins in SKM and ME arteries treated with 20-HE

From the transcripts of genes that encode muscle contractile machinery regulation mentioned in chapter 3, PRKG1 was down-regulated in 20-HE treated SKM arteries. Genes GUCY1A3, MYL9, ACTG2, ACTA2 were not changed (Figure 54). In ME arteries there was no difference in expression of any gene in this category.
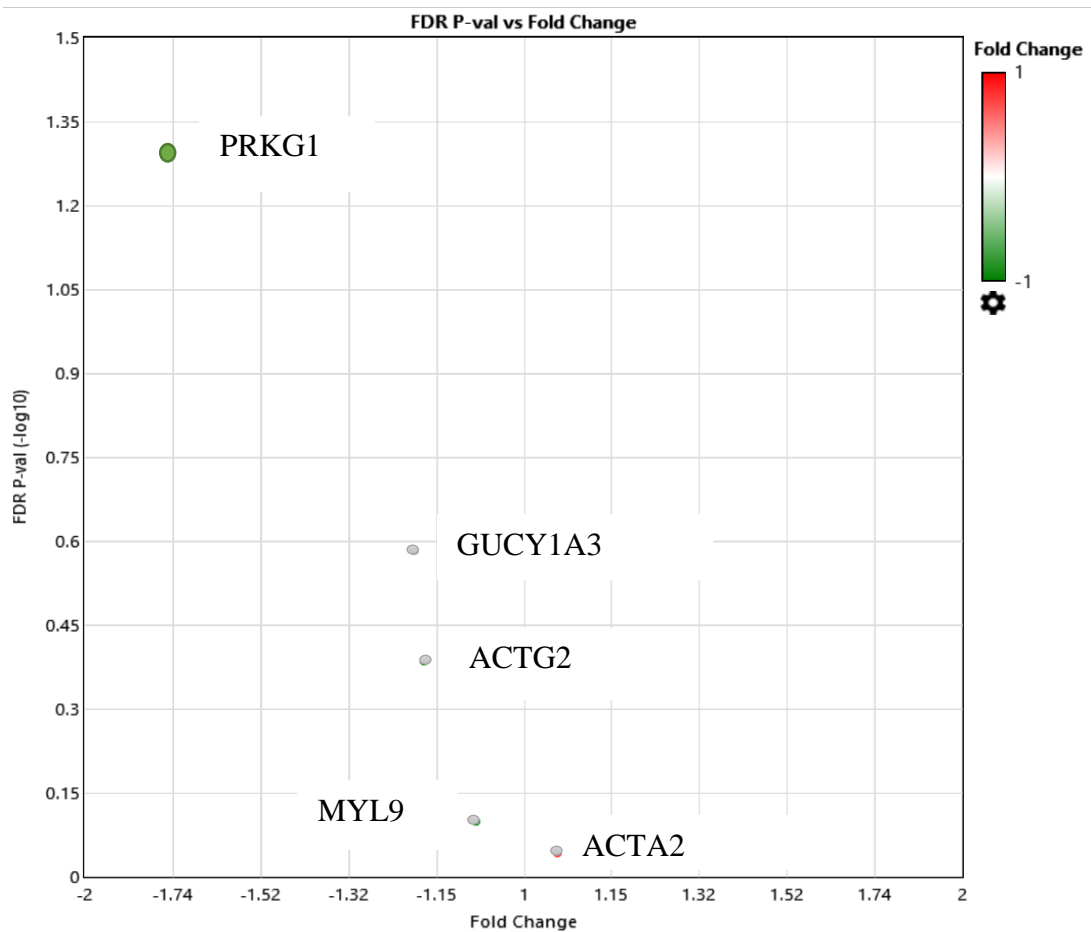
Figure 54: Volcano plot of gene expression fold changes vs. FDR p-value encoding smooth muscle contractile proteins in 20-HE treated SKM arteries.

PRKG gene was down-regulated in SKM 20-HE treated arteries (indicated in green). Genes that were not different are indicated in gray.

Expression of genes encoding proteins involved in inflammation and oxidative stress pathways regulation in SKM and ME arteries treated with 20-HE

Transcripts of genes that encode proteins that regulate inflammatory response and oxidative stress that were mentioned in chapter 3 and up-regulated in 20-HE SKM arteries; EGR1, HSPB1, JUNB, FOS, NFKBIB, snail family zinc finger 1 (SNAI2) and DUSP10 (Figure 55). JUNB gene was up-regulated in 20-HE treated ME arteries while all other genes in this category were not changed (Figure 56).
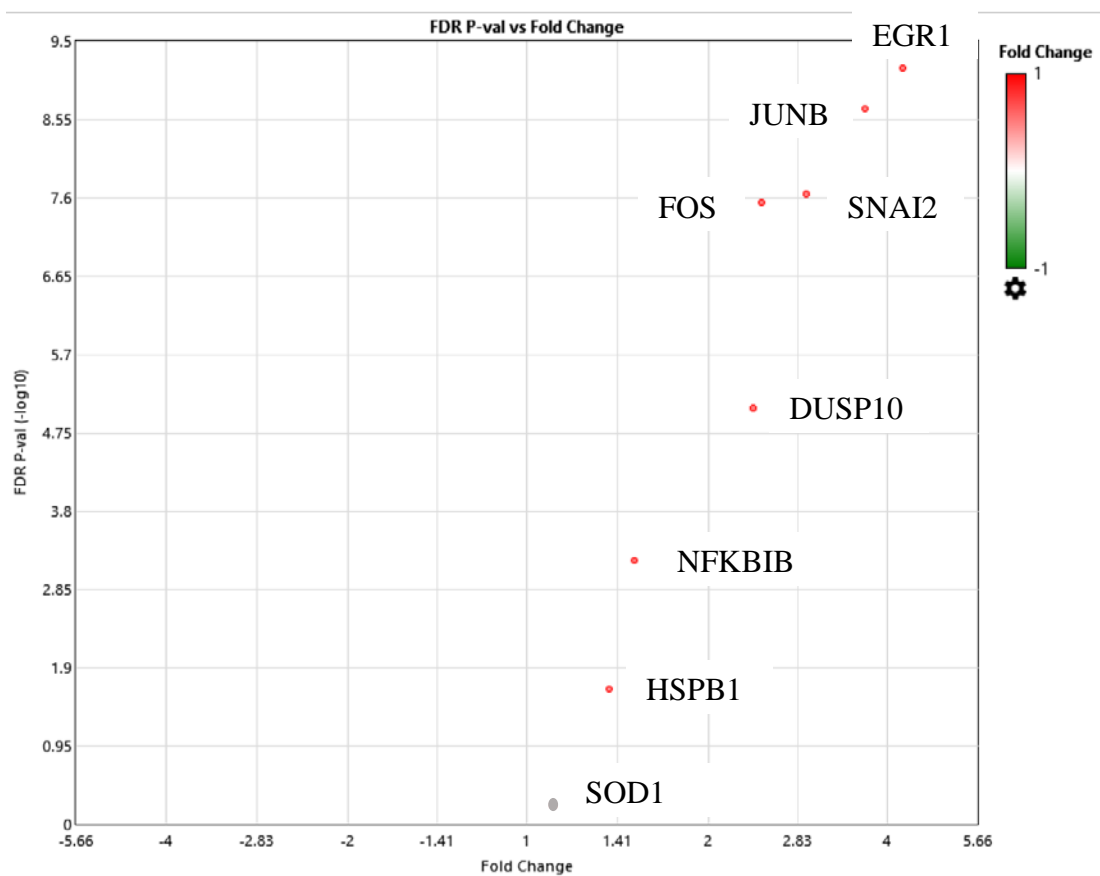
Figure 55: Volcano plot of gene expression fold change vs. FDR-p-value encoding proteins involved in inflammation and oxidative stress pathway regulation in 20-HE treated SKM arteries.

EGR1, HSPB1, JUNB, FOS, NFKBIB, SNAI2 and DUSP10 were up-regulated genes in SKM 20-HE arteries (indicated in red). SOD1 gene was not changed (indicated in gray).
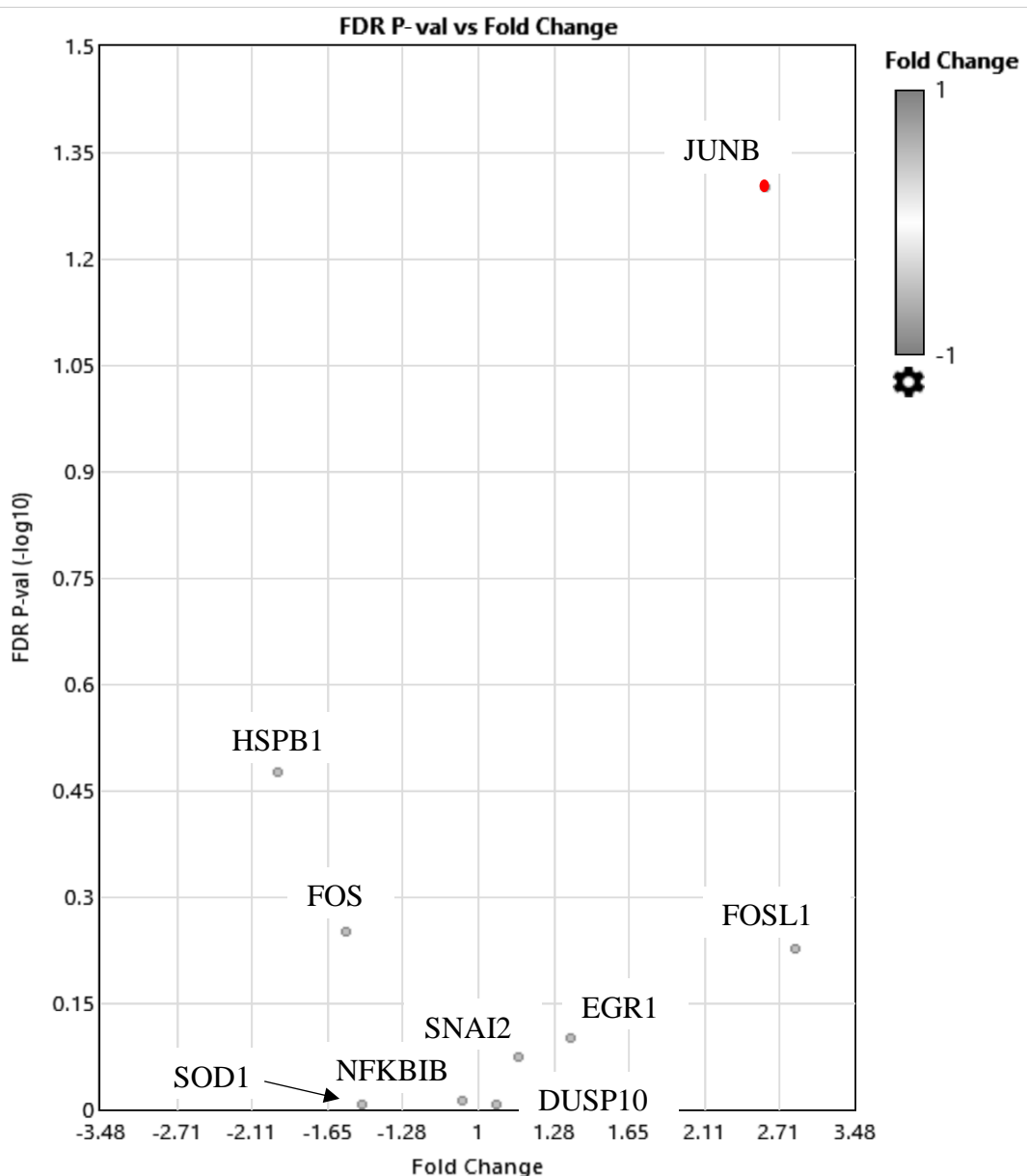
Figure 56: Volcano plot of gene expression fold change vs. FDR-p-value encoding proteins involved in inflammation and oxidative stress pathway regulation in 20-HE treated ME arteries.

JUNB gene was up-regulated in ME 20-HE arteries (indicated in red). EGR1, HSPB1, FOS, FOSL1, NFKBIB, SNAI2, DUSP10 and SOD1 were not changed (indicated in gray).

Estrogen receptor pathway regulation in SKM and ME arteries treated with 20-HE

Estrogen receptor ESR1 (ERα) and ESR2 (ERβ) genes were not changed with 20-HE treatment in either SKM or ME arteries. However, genes that encode estrogen receptor regulation proteins were changed including H2A histone family, member Z (H2AFZ), DEAD (Asp-Glu-Ala-Asp) box helicase 5 (DDX5), annexin A1 (ANXA1) and caspase 3 (CASP3), which were up-regulated in SKM arteries treated with 20-HE. TEK tyrosine kinase, endothelial (TEK) and nuclear receptor subfamily 2, group F, member 2 (NR2F2) were down-regulated in the same arteries (Figure 57, Table 11). In ME arteries treated with 20-HE, there were no significant gene change in this category.
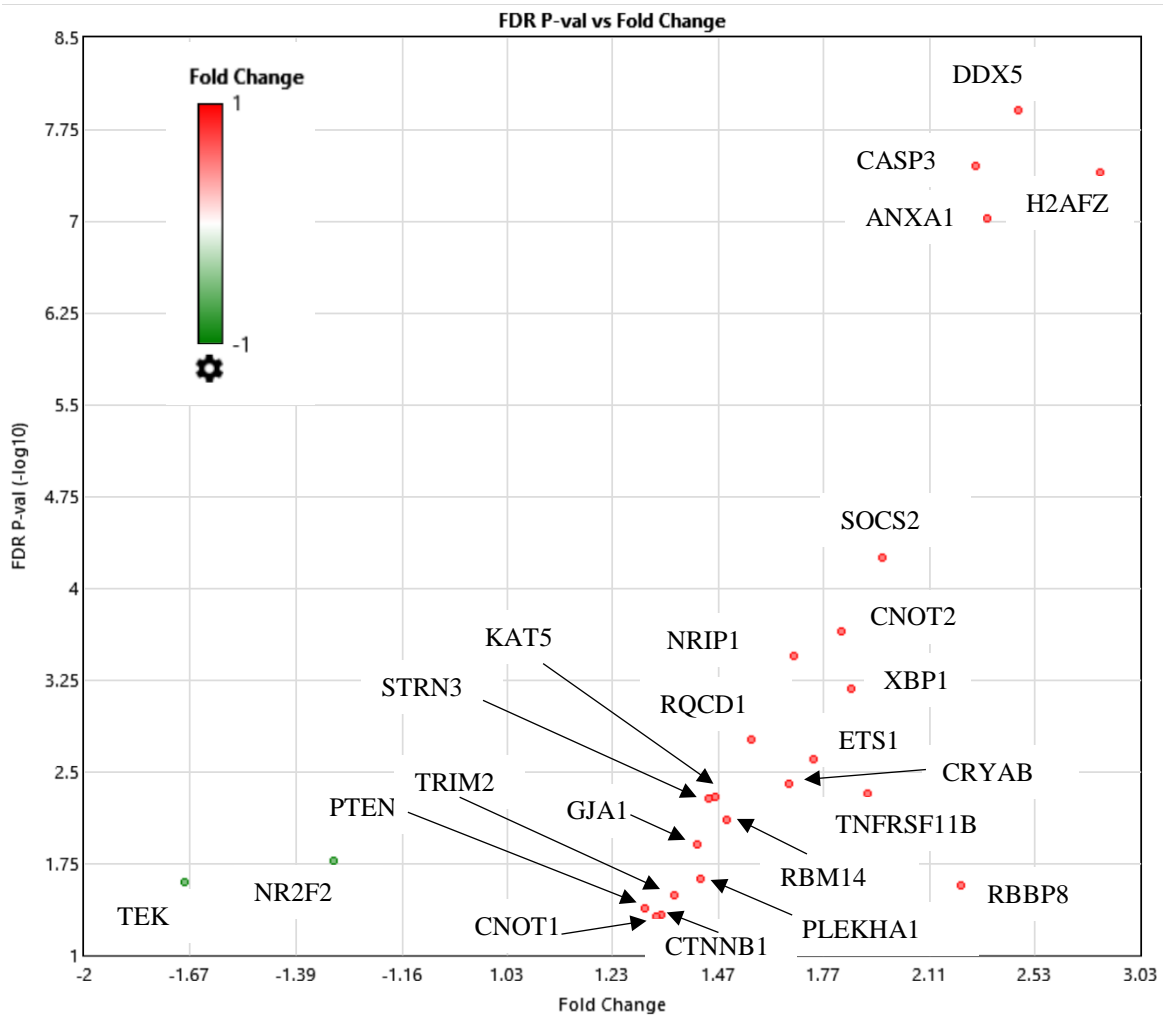
Figure 57: Volcano plot of gene expression fold change vs. FDR p-value encoding proteins involved in estrogen receptor regulation in 20-HE treated SKM arteries.

Up-regulated genes in SKM 20-HE arteries were indicated in red. Down-regulated genes were indicated in green.

Table 11: List of differentially expressed genes encoding proteins involved in estrogen receptor pathway regulation in SKM arteries in response to 20-hydroxyecdysone.

The genes were classified according to molecular functions. 22 Up-regulated genes in SKM arteries that encode proteins that positively regulate estrogen receptors, while 2 down-regulated genes in SKM arteries that encode protein that function as negative regulators of estrogen receptors. (FDR-P value < 0.05).

Gene Symbol	Fold Change	Regulation	GO Biological Process Term	P-val	FDR P-val
H2AFZ	2.82	Up-regulated	Cellular response to estradiol stimulus	7.53E-11	1.24E-08
DDX5	2.46	Up-regulated	Positive regulation of intracellular estrogen receptor signaling pathway	2.39E-10	3.48E-08
ANXA1	2.33	Up-regulated	Response to estradiol	2.77E-10	3.93E-08
CASP3	2.29	Up-regulated	Response to estradiol	7.66E-10	9.53E-08
RBBP8	2.23	Up-regulated	Response to estradiol	1.06E-06	5.60E-05
SOCS2	1.95	Up-regulated	Response to estradiol; cellular response to hormone stimulus	5.50E-06	0.0002
TNFRSF11B	1.9	Up-regulated	Response to estrogen	9.61E-06	0.0004
XBP1	1.85	Up-regulated	Fatty acid Sterol homeostasis; cellular response to peptide hormone stimulus	2.06E-05	0.0007
CNOT2	1.82	Up-regulated	Negative regulation of intracellular estrogen receptor signaling pathway	6.76E-05	0.0017
ETS1	1.73	Up-regulated	Female pregnancy; estrous cycle	0.0001	0.0025
NRIP1	1.67	Up-regulated	Androgen receptor; cellular response to estradiol stimulus; ovulation	0.0002	0.0039
CRYAB	1.66	Up-regulated	Response to estradiol	0.0002	0.0047
RQCD1	1.56	Up-regulated	Negative regulation of intracellular estrogen receptor signaling pathway	0.0003	0.005
RBM14	1.49	Up-regulated	Response to hormone; intracellular estrogen receptor signaling pathway; glucocorticoid receptor signaling pathway	0.0003	0.0052

148

KAT5	1.47	Up-regulated	Cellular response to estradiol stimulus	0.0005	0.0078
STRN3	1.45	Up-regulated	Response to estradiol; negative regulation of intracellular estrogen receptor signaling pathway	0.0009	0.0122
PLEKHA1	1.43	Up-regulated	Spermatogenesis; androgen metabolic process; estrogen metabolic process; female gonad development	0.002	0.0233
GJA1	1.42	Up-regulated	Response to peptide hormone	0.0024	0.0263
TRIM24	1.37	Up-regulated	Regulation of vitamin D receptor signaling pathway; cellular response to estrogen stimulus	0.0031	0.0317
CTNNB1	1.34	Up-regulated	Response to estradiol	0.0043	0.0407
CNOT1	1.33	Up-regulated	Negative regulation of intracellular estrogen receptor signaling pathway	0.0053	0.0468
PTEN	1.3	Up-regulated	Response to estradiol	0.0055	0.0483
TEK	-1.69	Down-regulated	Response to estrogen	0.0022	0.0246
NR2F2	-1.31	Down-regulated	Response to estradiol; steroid hormone mediated signaling pathway	0.0013	0.017

5.3.5.2 Expression of COX-1/2 and eNOS mRNA determined by q-PCR in SKM and ME treated with 20-HE

COX-1 expression was significantly higher in untreated SKM compared with untreated ME arteries (Figure 58, A, $P<0.05$, n=8). There was no difference in COX-1 expression in untreated SKM compared with treated SKM arteries (Figure 58, C, n=8). Treatment with 20-HE resulted in the up regulation of COX-1 in ME arteries (Figure 58, D, $P<0.05$, n=8). There was no difference in COX-2 expression between the untreated SKM and ME arteries (Figure 59, A, n=8). However, 20-HE treatment significantly down regulated COX-2 gene expression in ME (Figure 59, D, $P<0.05$, n=8) compared with SKM (Figure 59, C, n=8) arteries. There were no significant differences in eNOS gene

expression, between SKM and ME arteries, without or with 20-HE treatment (Figure 60, A, B, C, D, n=8).
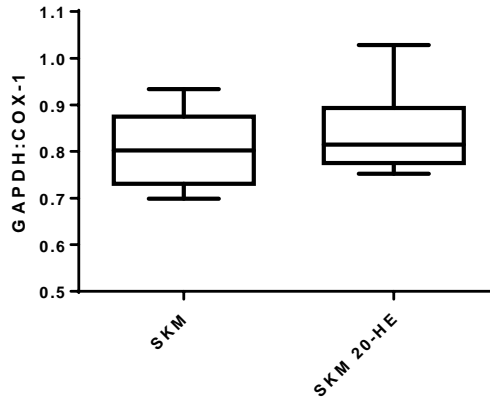
Figure 58: COX-1 mRNA expression determined by single q-PCR in SKM and ME arteries treated with 20-HE.

(A) COX-1 was relatively more abundant in SKM compared with ME arteries ($P<0.05$). (B) Comparable expressions of COX-1 in SKM and ME arteries treated with 20-HE. (C) Comparable COX-1 expression in untreated and 20-HE-treated SKM arteries. (D) COX-1 expression in 20-HE treated ME arteries was significantly increased compared with untreated ME arteries ($P<0.05$). Data normalized and represented as ratio of GAPDH to target gene expression, n=8, paired t-test was used.
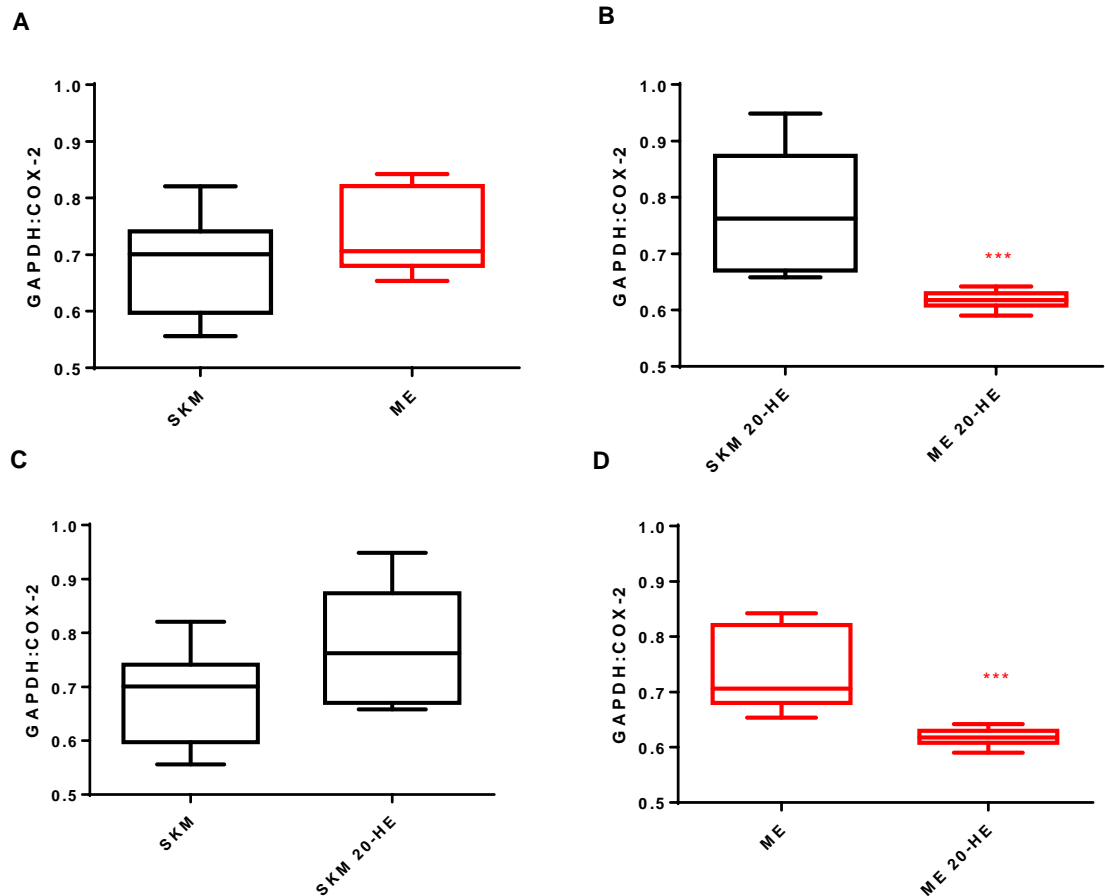
Figure 59: COX-2 mRNA expression determined by single q-PCR in SKM and ME arteries treated with 20-HE.

(A) COX-2 expression in untreated SKM and ME arteries were comparable (B) COX-2 expression in 20-HE treated ME arteries was significantly lower compared with 20-HE treated SKM (P<0.05). (C) Comparable expressions of COX-2 in untreated and 20-HE treated SKM arteries. (D) COX-2 expression in 20-HE treated ME arteries was significantly decreased compared with untreated ME arteries (P<0.05). Data represented as ratio of GAPDH to target gene expression, n=8, paired t-test was used.
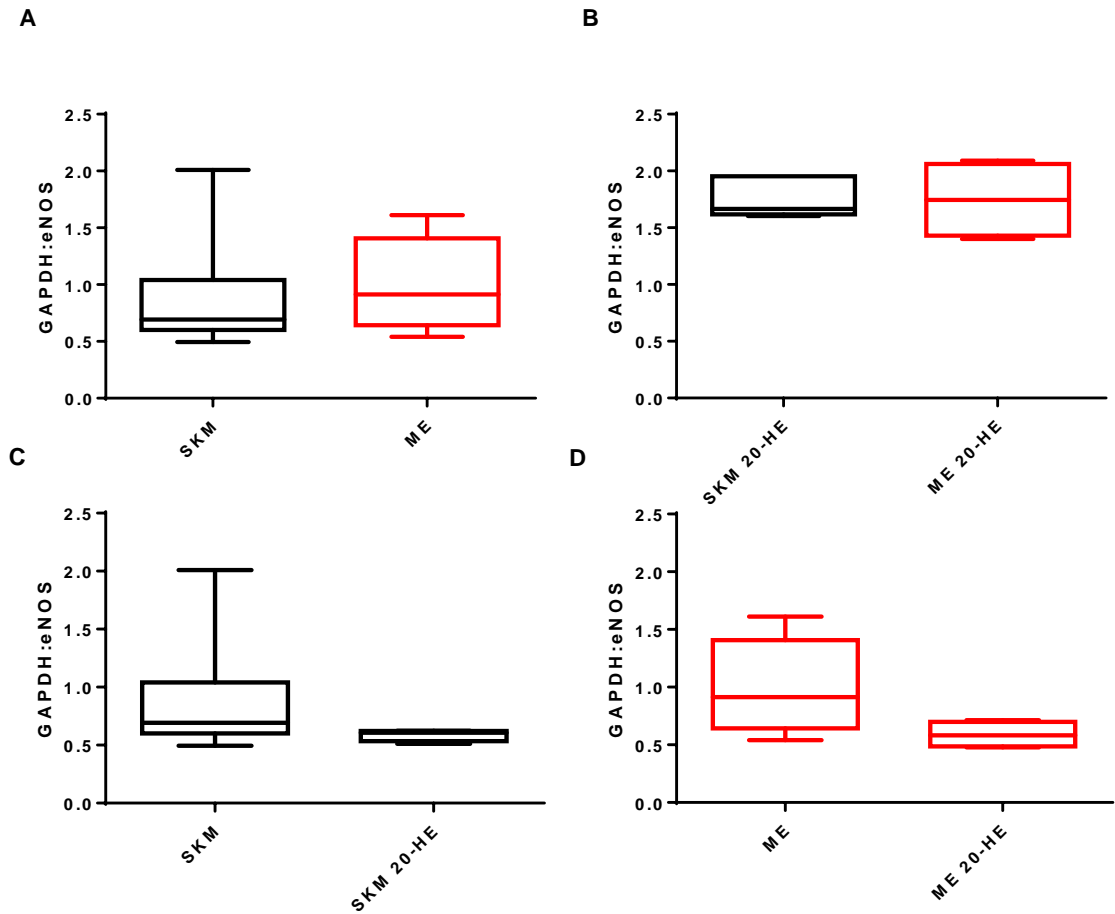
Figure 60: eNOS mRNA expression in SKM and ME arteries.

(A) Comparable eNOS expression in SKM and ME arteries (B) Comparable eNOS expression in SKM and ME arteries treated with 20-HE. (C) Comparable eNOS expression in untreated and 20-HE treated SKM arteries. (D) Comparable eNOS expression in untreated and 20-HE treated ME arteries. Data represented as ratio of GAPDH to target gene expression, n=8, paired t-test was used.

5.3.5.3 Expression of ERα and ERβ mRNA determined by q-PCR in SKM and ME treated with 20-HE

ERβ mRNA was more abundant than ERα in SKM arteries (Figure 61, p<0.05, n=7). There was no difference in ERα expression between the untreated SKM and ME arteries (Figure 62, A, n=8). Also, there was no difference between the untreated and 20-HE treated SKM or ME arteries (Figure 62, C, D, n=8). In contrast, ERβ expression was significantly less in untreated SKM compared with untreated ME arteries (Figure 63, A) and the difference remained with treatment 20-HE (Figure 63, B). Treatment with 20-HE made no difference in the expression of ERβ in both arteries (Figure 63, C and D).
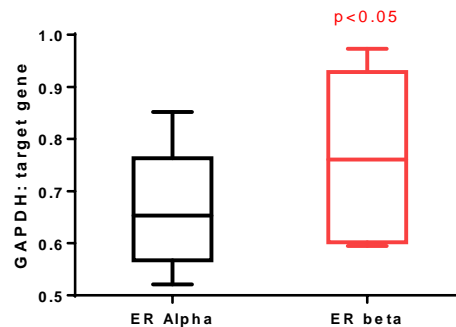
Figure 61: ER-α and ER-β mRNA expression in SKM arteries.

ER-β was more abundant in the arteries compared with ER-α (p<0.05). Data represented as ratio of GAPDH to target gene expression, n=7, paired t-test was used.
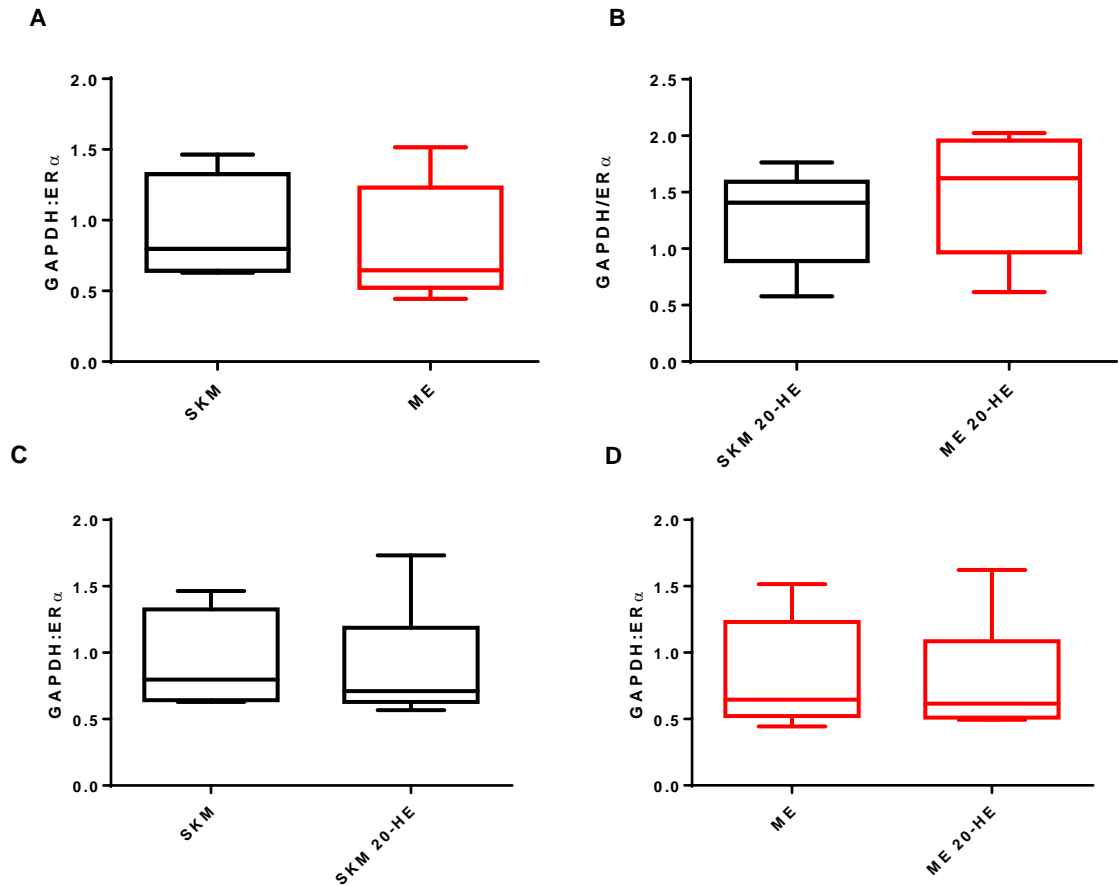
Figure 62: ERα mRNA expression determined by single q-PCR in SKM and ME arteries treated with 20-HE.

(A) Comparable ERα expression in untreated SKM and ME arteries. (B) Comparable ERα expression in treated SKM and ME arteries. (C) 20-HE treatment did not change ERα expression in SKM arteries. (D) 20-HE treatment did not change ERα expression in ME arteries. Data represented as ratio of GAPDH to target gene expression, n=8, paired t-test was used.
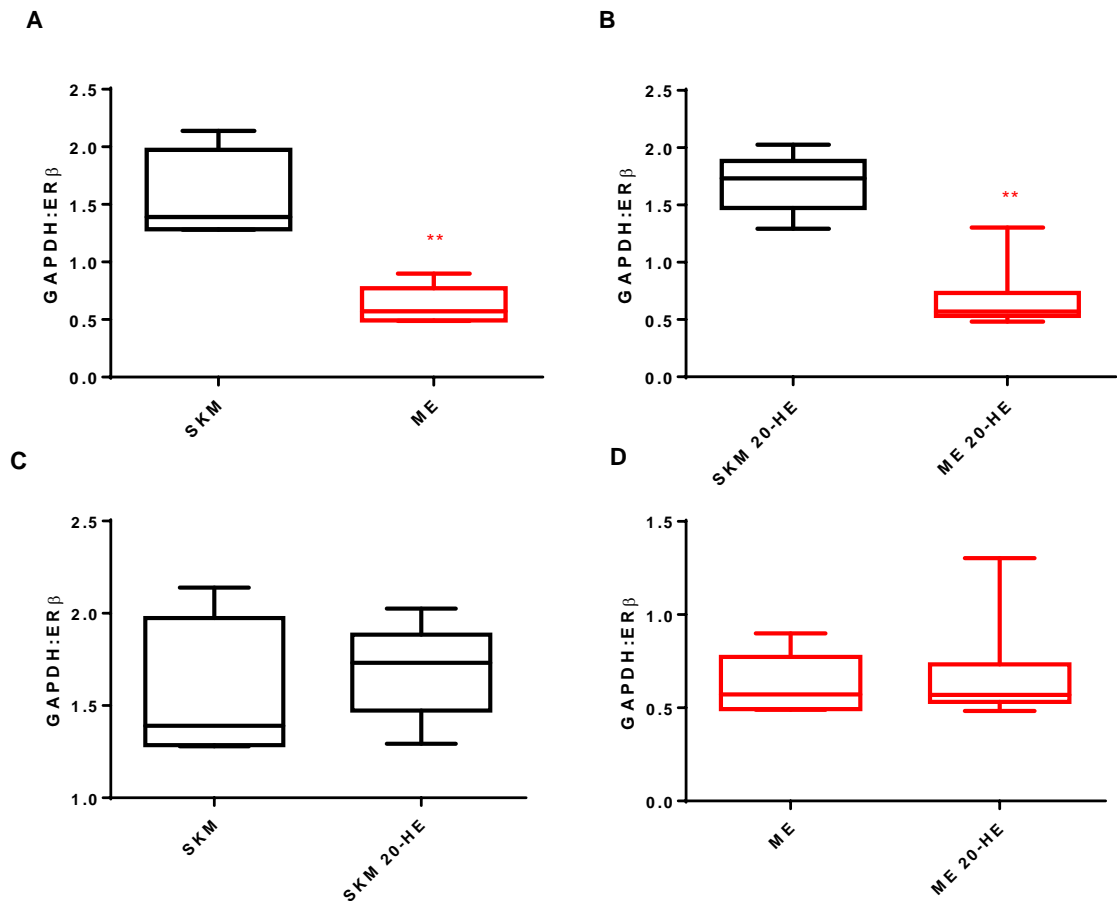
Figure 63: ERβ mRNA expression determined by single q-PCR in SKM and ME arteries treated with 20-HE.

(A) ERβ mRNA expression in untreated SKM arteries was significantly higher than in untreated ME arteries (P<0.05) (B) The difference in ERβ mRNA expression between both arteries remained with 20-HE treatment. (C) 20-HE treatment did not change ERβ expression in SKM arteries. (D) 20-HE treatment did not change ERβ expression in ME arteries. Data represented as ratio of GAPDH to target gene expression, n=8, paired t-test was used.

5.3.6   Protein expression studies

5.3.6.1 20-HE effects on COX isoforms protein expression in arterial tissues and endothelial cells

To determine whether the vasodilatory effects of 20-HE were associated with changes in COX isoform protein expressions, the arteries as well as cultured human endothelial cells exposed to 1 µM 20-HE for 1 hour were analyzed (Figure 64, A, B). Both COX-1 and COX-2 were unchanged by the treatment in both arteries, SKM (Figure 65, A, B, n=4) and ME arteries (Figure 66, A, B, n=4) as well as in HCAECs (Figure 67, A, B, n=3).
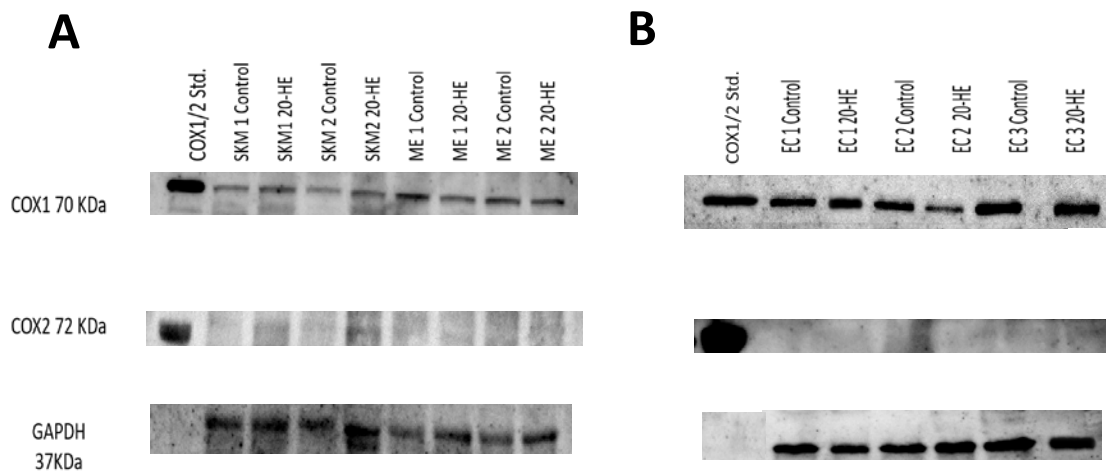
Figure 64: Representative blots of SKM and ME arteries treated with 20-HE.

Western blot of 1 µM 20-HE-treated and untreated SKM and ME arteries. Samples were analyzed for levels of COX-1(70 KDa), COX-2 (72 KDa) and GAPDH (37 KDa) proteins by western blot. All lanes were loaded with 50 µg of total protein, and loading was consistent across all lanes.
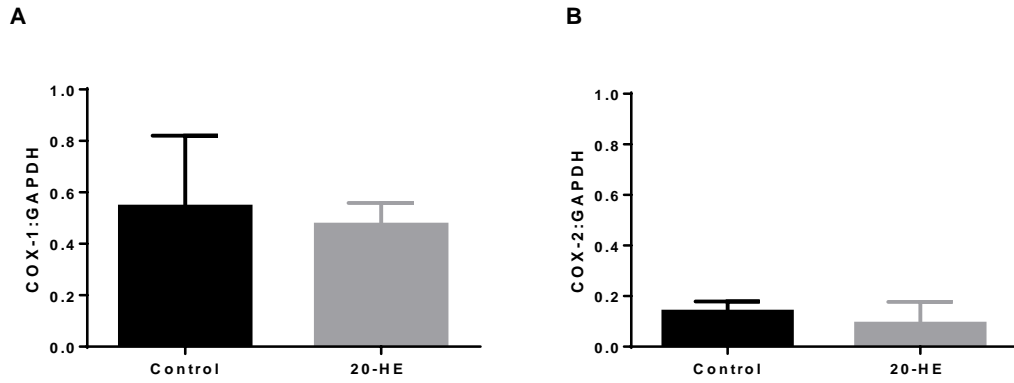
Figure 65: COX-1 and COX-2 protein expression in SKM arteries treated with 20-HE.

(A) Comparable COX-1 expression between untreated and 20-HE treated SKM arteries. (B) Comparable COX-2 expression between untreated and 20-HE treated SKM arteries. Data are reported as ratio of target protein to GAPDH of n=4, paired t-test was used.
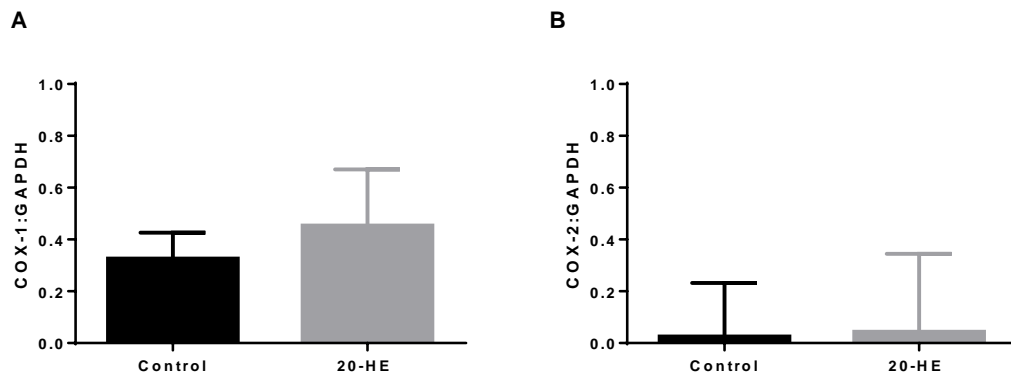
Figure 66: COX-1 and COX-2 protein expression in ME arteries treated with 20-HE.

(A) Comparable COX-1 expression between untreated ME arteries and treated with 20-HE. (B) Comparable COX-2 expression between untreated and 20-HE treated ME arteries. Data are reported as ratio of target protein to GAPDH of n=4, paired t-test was used.
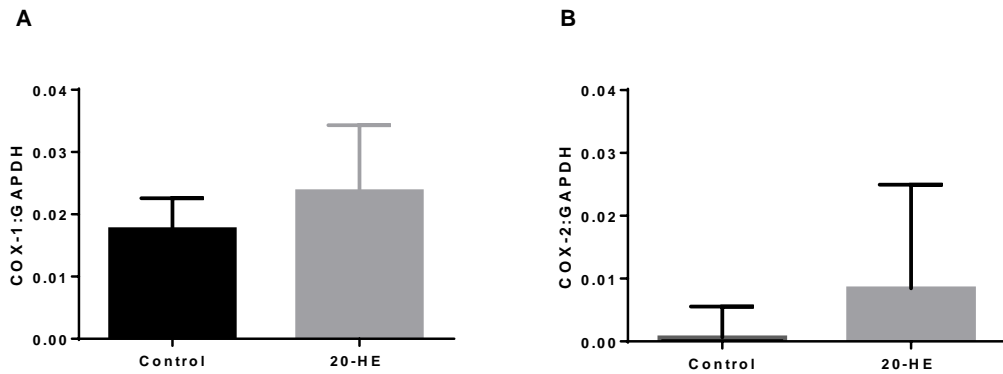
Figure 67: COX-1 and COX-2 protein expression in HACEC treated with 20-HE.

(A) Comparable COX-1 expression between untreated HACEC and treated with 20-HE. (B) Comparable COX-2 expression between untreated HACEC and treated with 20-HE. Data are reported as ratio of target protein to GAPDH of n=3, paired t-test was used.

5.3.6.2   20-HE effects on eNOS protein expression in arterial tissues and endothelial cells

Although eNOS protein was unchanged in 1 µM 20-HE treated SKM (Figure 69, A, n=4) and ME (Figure 69, B, n=4) arteries, it was significantly increased in HCAECs treated with same concentration of 20-HE (Figure 70, B, $P<0.05$, n=3) compared with respective untreated controls.
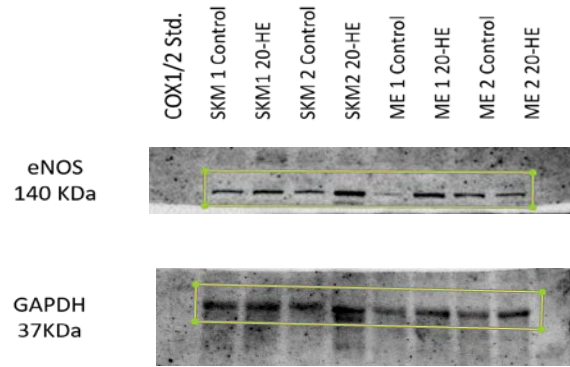
Figure 68: Representative blots of eNOS in SKM and ME arteries treated with 20-HE.

Western blot of 1 μM 20-HE-treated and untreated SKM and ME arteries. Arteries were analyzed for levels of eNOS (140 KDa) and GAPDH (37 KDa) proteins by Western blot. All lanes were loaded with 50 μg of total protein and loading was consistent across all lanes.
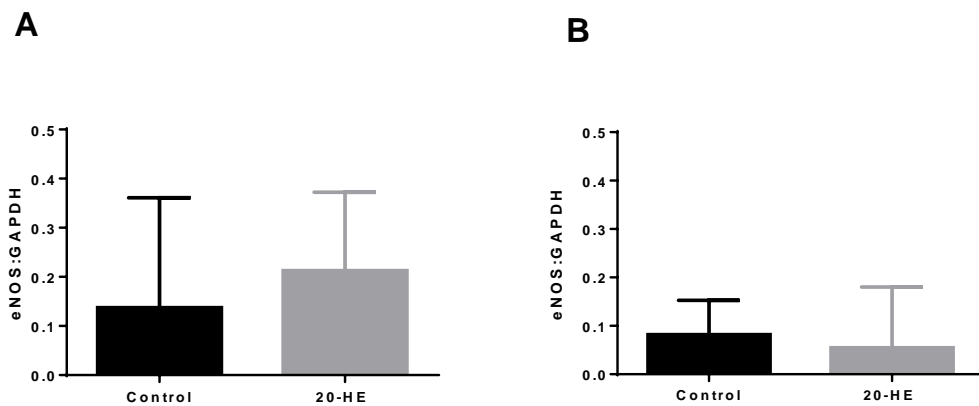
Figure 69: eNOS protein expression in SKM arteries treated with 20-HE.

(A) Comparable eNOS expression between untreated and 20-HE treated SKM arteries. (B) Comparable eNOS expression between untreated and 20-HE treated ME arteries. Data are reported as ratio of target protein to GAPDH of n=4, paired t-test was used.
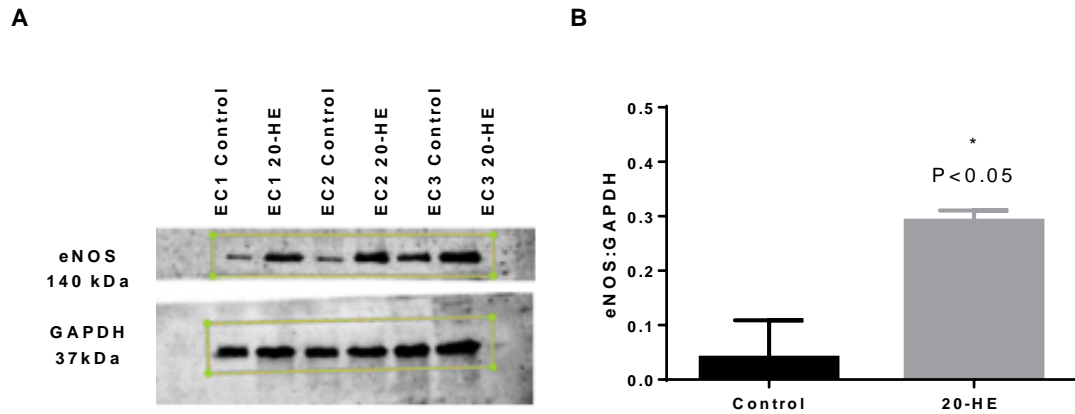
Figure 70: eNOS protein expression in HCAEC treated with 20-HE.

(A) Representative western blot of eNOS in untreated and 1 µM 20-HE-treated HCAECs. Cells were analyzed for levels of eNOS (140 kDa) and GAPDH (37 kDa) proteins. (B) eNOS was more abundant in cells treated with 20-HE compared with untreated cells. Data are reported as ratio of target protein to GAPDH of n=3, paired t-test was used. All lanes were loaded with 50 µg of total protein, and loading was consistent across all lanes.

5.3.6.3 20-HE effects on ER protein expression in arterial tissues

To determine whether the vasodilatory effects of 20-HE were associated with changes in ER protein expressions, the arteries exposed to 1 µM 20-HE for 1 hour were analyzed (Figure 71). There was no difference in ERα expression between the treated and untreated SKM or ME arteries (Figure 72, A, B, n=4). Also, there was no difference in ERβ expression between the treated and untreated SKM or ME arteries (Figure 73, A, B, n=4).

160
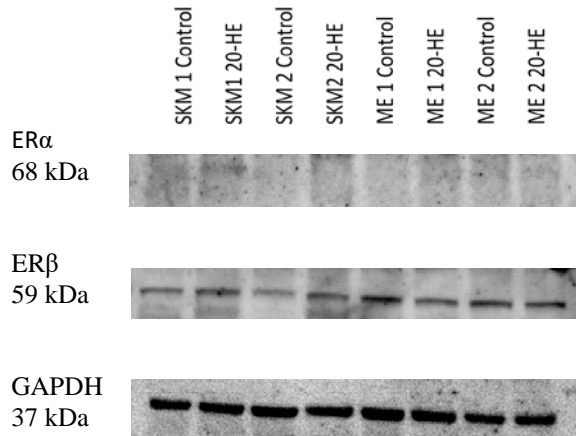
Figure 71: Representative blots of ERα and ERβ in SKM and ME arteries treated with 20-HE.

Western blot of 1 μM 20-HE-treated and untreated SKM and ME arteries. Arteries were analyzed for levels of ERα (68 kDa) ,ERβ (59 kDa) and GAPDH (37 kDa) proteins by Western blot. All lanes were loaded with 50 μg of total protein, and loading was consistent across all lanes.
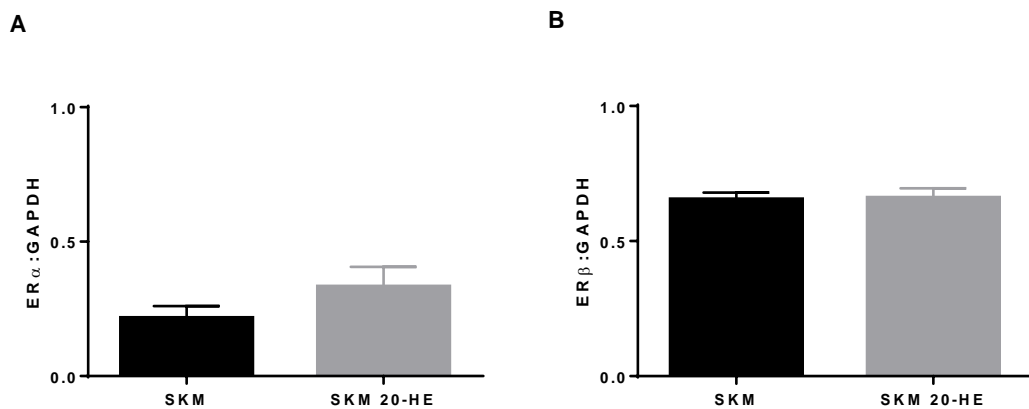
Figure 72: ERα and ERβ protein expression in SKM arteries treated with 20-HE.

(A) Comparable ERα expression between untreated and 20-HE treated SKM arteries. (B) Comparable ERβ expression between untreated SKM arteries and treated with 20-HE. Data are reported as ratio of target protein to GAPDH of n=4.
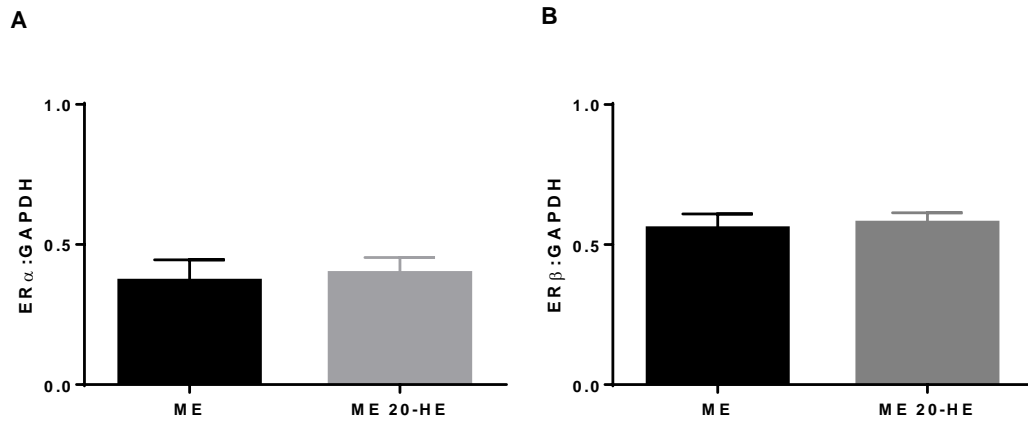
161

Figure 73: ERα and ERβ protein expression in ME arteries treated with 20-HE.

(A) Comparable ERα expression between untreated ME arteries and treated with 20-HE. (B) Comparable ERβ expression between untreated and 20-HE treated ME arteries. Data are reported as ratio of target protein to GAPDH of n=4.

5.4 Discussion

Dietary supplementation is an important aspect of sports nutrition. It ensures that elite athletes can meet their essential nutritional needs and avoid deficiencies that would impact their health and performance. In recent years, increasing number of available supplements have been contaminated with substances such as 20-hydroxyecdysone, an ecdysteroid that could potentially enhance performance (372). The data show that 20-hydroxyecdysone induces relaxation in both ME and SKM arteries in a NO-dependent manner. To my knowledge, this is the first study to describe the endothelium-dependence of the vascular effects of this compound.

Although eNOS protein expression was not altered by 20-hydroxyecdysone treatment in both arteries, it was markedly increased in the HCAECs. This suggests that 20-hydroxyecdysone might both increase eNOS protein and its activity consistent with the endothelium-dependence of its effect and previous reports (221, 368).

COX appeared to play no apparent role in the vasodilatory effect of 20-hydroxyecdysone in both SKM and ME arteries. Both pharmacological inhibition and protein expression analysis failed to demonstrate a role for COX in the actions of 20-HE in this study. Although COX was not expected to contribute to relaxation in ME arteries due to inherent opposition reported in chapter 3, the lack of a role in the SKM arteries was surprising, although this could have been masked by the functional redundancy between eNOS and COX reported in chapter 3.

The receptor mechanisms of ecdysteroid actions are not yet known. One of the predictions is that they act through estrogen receptors (187, 193), which make them potentially vasodilatory. Estrogen receptors, particularly ER-β was expressed in these arteries, consistent with ER-β being the predominant isoform expressed in blood vessels (373). Although the ER antagonist ICI.182.780 with stronger affinity for ERα compared with ER-β, had no effect on 20-hydroxyecdysone relaxation, specific blockers of ER-α or ER-β failed to

reduce the response. Worryingly, the same antagonists could not alter β-estradiol-induced relaxation in these arteries either, making it difficult to draw the right conclusions about the roles of estrogen receptors in the vasodilatory actions of 20-HE. Interestingly, several genes that positively influence estrogen signaling such as H2AFZ and DDX5 were upregulated in 20-hydroxyecdysone-treated arteries, even without noticeable change in the expression of ERα or ERβ. Moreover, ERα or ERβ activation can increase eNOS phosphorylation (without necessarily increasing the protein) leading to increase in NO levels (361).

Evaluation of the molecular mechanisms modulated by 20-hydroxyecdysone treatment was important to understand the networks that could explain its biological actions. Hence the use of microarray analysis to gain deeper insights into multi-target effects of 20-hydroxyecdysone on arteries and cells. Several genes that negatively influence inflammation and oxidative stress such as DUSP10 and NFKBIB were upregulated, indicating 20-hydroxyecdysone may protect vascular tissues against inflammation and oxidative stress. Inflammatory response increases the production of reactive oxygen species and modifies the production/activity of vasodilatory mediators including prostacyclin and NO (374). Thus, 20-hydroxyecdysone anti-inflammatory and antioxidative properties might benefit vasodilation, by inhibiting ROS production and preventing oxidant-induced injury (221, 241).

The lack of selective effect of 20-HE on SKM arteries could have implication for sports performance. SKM circulation is unique in accommodating up to 80 % of cardiac output during exercise following redistribution of blood from other tissues, notably from the gastrointestinal circulation (375). This essential adaptation to exercise could therefore be compromised if ecdysteroids consumed by the athlete were to cause other vessels such as the mesenteric arteries to dilate at this critical time.

5.5 Limitation

The ovine SKM and ME tissue samples were obtained from the abattoir for human consumption with limited knowledge of the animal condition that could affect the uniformity of samples. However, this were overcome by collecting SKM and ME arteries from the same animal in some experiments.

5.6 Conclusion

The data show that 20-hydroxyecdysone containing supplements have vasodilatory properties, which are, in large part endothelium-dependent in specific NO-dependent. This could increase skeletal muscle blood flow and enhance muscle function. However, this benefit could be limited by the ability of this compound to dilate other vessels such as the mesenteric arteries, which could affect the essential blood redistribution required during exercise.

CHAPTER 6: Discussion

6.1 Summary of Findings

This study made several key and novel findings. These include: (1) COX activities in resistance arteries were double-edged in both health and disease, were isoform-specific and the net effects were dependent on the vasculature. COX-1 activity was generally vasodilatory in both SKM and ME arteries obtained from apparently healthy sheep but opposed relaxation in OM arteries obtained from obese humans. On the other hand, COX-2 activity was either opposed to relaxation in ME arteries obtained from healthy sheep or played no measurable part in vasomotor regulation in SKM from healthy sheep and OM and SC arteries from obese humans. (2) COX opposition to relaxation in all small arteries studied was in large part driven by enhanced TXA2 activity, irrespective of health status and the COX isoform involved. TXA2 vasoactivity was coupled to COX-2 in ME arteries from healthy but to COX-1 OM arteries in human obesity. (3) COX displayed a redundant relationship with eNOS, which was both dependent on vasculature and agonist. This functional redundancy was observed in SKM arteries but not in ME arteries, and with acetylcholine but not in bradykinin relaxation. (4) The data confirmed EDH as the main mechanism of microvascular endothelial dilatory function and demonstrated that its deficiency accounted for OM arteriolar endothelial dysfunction in obesity. While the trio of eNOS, COX and EDH could completely explain endothelium-dependent relaxation in healthy SKM arteries, only eNOS and EDH could explain the limited acetylcholine relaxation in ME arteries in health and OM and SC arteries in obesity. (5) Demonstrated that eNOS but not COX accounted for the endothelium-dependent vasodilation induced by 20-hydroxyecdysone, a supplement-derived ecdysteroid and novel anabolic agent, in resistance arteries. These findings have shed more light on COX's roles in the regulation of microvascular endothelial dilator functions in both health and disease.

6.2 COX's role in tone regulation in healthy resistance arteries

The data supports the hypothesis that the role of COX in microvascular endothelial dilator function is isoform-specific. While COX-1 activity was vasodilatory in healthy SKM and ME arteries, COX-2 activity was either not detectable (as in SKM arteries) or opposed vasodilation (as in ME arteries). The opposition to vasodilation in these apparently healthy mesenteric arteries by COX was consistent with enhanced relaxation to acetylcholine in the presence of either the general COX inhibitor, indomethacin, or the selective COX-1 inhibitor, FR122047. The data not only confirms COX involvement in negative tone regulation in healthy arteries but also identifies COX-2 isoform activity as the driver of this role in mesenteric arteries, consistent with similar role reported in mice small mesenteric artery (289). However, COX isoform roles in vascular function have not always been inconsistent. For instance, COX-1 is thought to mediate vasorelaxation in human forearm arteries (278), but contraction in rat aorta and coronary arteries (244, 281). On its part, COX-2 is reported to support the production of vasorelaxant prostaglandins in healthy human subjects (282), canine coronary arteries (283), mice aortic rings (287) and gracilis muscle arterioles (284, 285) but to mediate contraction in mice small mesenteric artery and aorta as well as aortae of aged hamsters (288-290). Furthermore, both COX-1 and COX-2 could synthesize TXA_2, the main constrictor prostanoid, under physiological conditions in rat (266) and mice (291).

COX main product in the vasculature is prostacyclin (PGI_2, (89)), which is generally vasodilatory under physiological conditions. PGI_2 synthesis is triggered by increased intracellular Ca^{2+} concentrations in endothelial cells, which initiates Ca^{2+}-sensitive hydrolysis of arachidonic acid by COX. PGI_2 induces vasodilation by activating prostanoid IP, EP2 or EP4 receptors on the vascular smooth muscle (84). These prostanoid receptors belong to G protein-coupled receptors (GPCRs) and therefore are coupled to the GTP-binding protein Gs, which mediate increases in cyclic adenosine monophosphate (cAMP) (85-88). cAMP is a ubiquitous second messenger, which controls multiple physiological processes, including smooth muscle tone regulation

(376). The mechanisms underlying cyclic nucleotide-induced smooth muscle relaxation include: (a) decreased cytosolic calcium concentration ($[Ca^{2+}]i$) involving the activation of plasmalemmal and sarcoplasmic Ca^{2+}-ATPases (377, 378) or inactivation of voltage-dependent Ca^{2+} channels caused by hyperpolarization via the activation of K^+ channels (379, 380); and (b) decreased contractile protein Ca^{2+} sensitivity, even at constant $[Ca^{2+}]i$ by activation of protein kinase A (PKA) (i.e. inhibition of Ca^{2+} sensitization that modulates the activity of myosin light chain kinase [MLCK] or myosin light chain phosphatase [MLCP]) (381, 382). PGI_2 may also act via cAMP-independent pathways to control various cellular processes (87, 90), including direct activation of K^+ channels located on the vascular smooth muscle membrane, which lead to hyperpolarization and relaxation (91).

COX opposition to relaxation in ME arteries was mediated by TP receptor activities, as blocking of these receptors restored maximum relaxation to acetylcholine. TP receptor-mediated enhancement of contractions has been reported in rat mesenteric resistance arteries (292) and COX-2 ability to produce TXA_2 has been demonstrated in mice mesenteric arteries (383). TXA_2 binds TP receptor to activate phospholipase Cβ (PLCβ) through coupling to either Gq/11 or G12/13 (384). Activated PLCβ hydrolyzes phospho inositol diphosphate (PIP2) to inositol-1,4,5-trisphosphate (IP3) and diacyl-glycerol (DAG). IP3 binds to IP3 receptor on the sarcoplasmic reticulum to release Ca^{2+}, while DAG activates protein kinase C (PKC). PKC phosphorylates protein kinase C-potentiated inhibitory protein (CPI-17), which inhibits myosin light chain phosphatase (MLCP) (385), to enhance contraction. TP receptor also signals through specific RhoA guanine nucleotide exchange factors, which activate Rho kinase (ROK). ROK phosphorylates myosin-targeting subunit of MLCP (MYPT1) (386), to inhibit it and enhance contraction. Together, these events increase cytosolic Ca^{2+} and sensitization of the contractile machinery to Ca^{2+}, leading to increased myosin light chain (MLC) phosphorylation (387) and contraction. It was unlikely that any other contractile prostanoid receptors such as EP1 and EP3 receptors was involved in COX opposition to vasodilation observed in this study. This conclusion was based on the fact that both PGI2

168

and PGE2 which are agonists on these receptors caused relaxation and not contraction of these arteries.

COX-1 protein expression was higher in both SKM and ME arteries compared with COX-2, consistent with both tissues being obtained from healthy donors (296) and COX-2 being relatively undetectable under physiological conditions (297). Although the expression levels of COX-2 in both arteries were comparable, this isoform was relatively more active in ME compared with SKM arteries and was responsible for the COX-mediated opposition to endothelium-dependent relaxation in ME arteries as discussed above. It is not clear why the expression level of COX-2 did not increase noticeably with its activity in ME arteries. However, mRNA levels of genes associated with inflammation such as HSPB1 and FOS, were increased in ME compared with SKM arteries and may have impacted the enzyme activity. HSPB1 and FOS enhance mRNA Stability signaled by the Mitogen-Activated Protein Kinase p38 Signaling Cascade (388-391). Genes such as ZFP36 and DPM2, which are related to cytokine protein stability were also higher in ME compared with SKM arteries and might have contributed to the differential regulation of COX activities in these arteries (392-395). Moreover, the mesenteric arterial bed is a primary toxicity target organ (299) apparently more exposed to inflammatory cytokines such as tumor necrosis factor (TNF)-α and proteins such as DAPK3 (300), C reactive protein (CRP) (301), and phosphodiesterase 4 (PDE4), which are known to activate endothelium-derived contracting factors (EDCFs) (299-301). In addition to pro-inflammatory genes, there was also enhanced expression of hypoxic response genes such as 1 HSPB1, NFKBIB, EGR1, FOS, CCL21 and IL15 in ME compared with SKM arteries. In contrast, genes involved in anti-inflammatory and antioxidant activity such as GUCY1A3, SOD1, SNAI2, AKT1S1 and FKBP1A were higher in SKM compared with ME arteries. It is therefore reasonable to suggest that the local tissue environment may have played a critical role in shifting the activities of the isoforms and in turn the balance of prostanoids produced in each arterial bed.

The data revealed a unique functional relationship between COX and eNOS in the endothelium-dependent relaxation of SKM arteries, which was not observed in ME arteries. COX could compensate for the absence of eNOS and vice versa – a state of functional redundancy between the 2 key enzymes in endothelial functions. This phenomenon might explain some of the inconsistencies in the use of inhibitors of either enzyme to define their respective contributions to muscle vascular tone regulation (284, 314, 315). Interestingly, this phenomenon was agonist-dependent as it was observed with acetylcholine but not with bradykinin-induced relaxation of these arteries, even though both agonists acted in ways that involved COX and eNOS. The reason for this agonist-dependence is not clear but might be related to the differences in the manner of activation and degree of involvement of COX and eNOS in the mechanisms of actions of these agonists. Acetylcholine relaxation is mediated by muscarinic (M1 and M3) receptors and appears to be more eNOS-dependent, while bradykinin relaxation is mediated by bradykinin (B2) Receptor (46) and appears to be equally dependent on eNOS and COX (46).

Endothelial NOS synthesizes NO from L-arginine. NO diffuses into the vascular smooth muscle cells adjacent to the endothelium where it binds to and activates guanylyl cyclase. This enzyme catalyzes the dephosphorylation of GTP to cGMP, which serves as a second messenger for many important cellular functions, particularly for signaling smooth muscle relaxation by multiple mechanisms. cGMP activates GMP-dependent kinase (PKG), which among other effects, activates the large-conductance Ca^{2+}-activated potassium (K^+) channels leading to K^+ efflux, hyperpolarization and closure of Ca^{2+} channels (396, 397). PKG also activates plasma and sarcoplasmic reticulum Ca^{2+}-ATPase pumps to promote Ca^{2+} uptake and extrusion (398), and activates MLCP (385), which causes Ca^{2+} desensitization of the actin-myosin contractile system (41). Eventually, all these molecular targets inhibit calcium entry into the cell, decreases cytosolic calcium concentrations and lead to smooth muscle relaxation (32).

EDH was the dominant mechanism of endothelium-dependent relaxation recorded in all arteries studied, accounting for as much as 70 % of the relaxation in SKM arteries. The major role played by EDH in these arteries is consistent with previous reports (145, 308-310) all of which demonstrated its predominant role in endothelium-dependent vasodilation in small arteries. Its role increases as vessel size decreases and the role of NO decreases along the vascular tree (95, 96). This mechanism involves the release from the endothelium of yet-to-be identified factor(s) generally referred to as endothelium-derived hyperpolarizing factor(s) [EDHF(s)], which open K^+ channels on the underlying vascular smooth muscle leading to vasodilation. EDHF release from the endothelial cell occurs following the opening of endothelial small conductance calcium-activated potassium channel (SKCa) and intermediate conductance calcium-activated potassium channel (IKCa) (97). However, the identity of this factor(s) remains uncertain. The candidate factors so far proposed include, hydrogen peroxide (H_2O_2; (98)), hydrogen sulfide (H_2S; (99)), metabolites of arachidonic acid such as epoxyeicosatrienoic acids (EETs; (100)), potassium ions (K^+; (101)), and C-type natriuretic peptide (CNP; (102)) and vary according to vasculature. There have also been suggestions that EDH may involve an electrical coupling through myoendothelial junctions (103). The identity of the candidate EDHF in the vessels studied could not be determined and would be subject of future investigations.

6.3 COX's role in tone regulation in adipose tissue resistance arteries in obesity

It is widely recognized that the microvascular circulation is a major target for obesity-related endothelial dysfunction (322). The data showed for the first time that reduction in EDHF rather than NO per se accounts for decreased endothelial dilatory capacity of OM compared with SC arteries in morbid obesity (142, 331). The data also supports the hypothesis that decreased dilatory capacity of OM arteries is orchestrated by increased but altered COX-1 and thromboxane TP receptor activities which oppose endothelium-dependent relaxation of these arteries. The depot-specific difference in endothelial dilatory

capacity between OM and SC arteries is in agreement with previous reports albeit for a different (North American) obese population (332) that also suggested that COX-1-derived vasoconstrictor prostanoids were partly responsible for this abnormality (159). The current data has gone further to demonstrate that the OM arteries which suffer reduced endothelial dilatory capacity, also displayed enhanced TP receptor activity, demonstrated by the enhanced contractile response to the TP receptor agonist U46619 compared with SC arteries. This provides the first direct evidence for the greater vulnerability of human OM arteries to exaggerated contractile prostanoid activity that has the potential to limit their endothelium-dependent dilatory capacity in obesity. This is also consistent with COX-1 being the primary isoform related to endothelium-dependent contractions (244, 333-335) and enhanced TP receptor-dependent vascular contractions being associated with metabolic diseases (336, 337). Moreover, COX-1/TXA$_2$ pathway has been shown to mediate vascular hypercontractility linked to endothelial dysfunction in obesity (337) and experimental model of hyperlipidemia (338). TP receptor is coupled to guanine nucleotide-binding protein G$_q$ in vascular smooth muscle (VSM) (339). Activation of the receptor stimulates membrane-bound G$_q$-dependent phospholipase C (PLC) β to hydrolyze Phosphatidylinositol 4,5-bisphosphate (PIP$_2$) to inositol triphosphate (IP$_3$) and diacyl glycerol (DAG) (340). IP3 activates the mobilization of intracellular Ca^{2+}, and DAG activates PKC, to initiate and promote vasoconstriction respectively.

The OM depot is more heavily implicated in metabolic syndrome compared with SC. Obese individuals with excess fat stored in visceral adipose depots generally suffer greater adverse metabolic consequences compared with similarly overweight subjects with excess fat stored predominantly in subcutaneous sites (341). OM being more extensively infiltrated with immune-inflammatory cells, such as macrophages and T-lymphocytes (155) and have the capacity to secrete more interlukin-6 (IL-6), (342) and tumor necrosis factor-alpha (TNF-α) (322, 343) which could modulate the deleterious impact of local fat on vasomotor function. TNF-α downregulates endothelial NO synthase (eNOS) expression at the posttranscriptional level (322, 344) and IL-6

attenuates EDHF-mediated vasodilation (345) and can induce monocyte chemoattractant protein-1 (MCP-1) formation in the vascular smooth muscle via JAK (janus-activated kinase)/STAT (signal and transducers and activators of transcription) signaling pathway (346) to further disrupt vascular tone. Thus, as an important source of low-grade inflammation, visceral fat can directly contribute to the local development of endothelial dysfunction (322). The current study shows that this micro environmental change alters endothelial COX-1 and vascular smooth muscle TP receptor activity in such a way that leads to reduction in the endothelial dilatory capacities of local vessels.

6.4   Lack of role for COX in 20-hydroxyecdysone-induced vasodilation

Dietary supplementation is an important aspect of sports nutrition. It ensures that elite athletes can meet their essential nutritional needs and avoid deficiencies that would impact their health and performance. In recent years, increasing number of available supplements have been contaminated with substances such as 20-hydroxyecdysone, which are thought to have the potential to enhance performance (372). The data supports the hypothesis that 20-hydroxyecdysone induces vasorelaxation as recorded in both ME and SKM arteries. The data also supports the hypothesis that this vasodilation is partly NO-dependent. Although eNOS expression in intact arteries were not noticeably changed by 20-hydroxyecdysone treatment, they were markedly increased in cultured human coronary artery endothelial cells (HCAECs), consistent with the observed endothelium-dependence of its effect. To my knowledge, this is the first study to describe the endothelium-dependence of the vascular effects of this supplement-derived novel anabolic compound.

However, the results do not support the hypothesis that the vasodilation is COX-dependent. There was no evidence that COX played any role in the vasodilatory effect of 20-hydroxyecdysone in both SKM and ME arteries. It is not clear whether COX's inherent opposition to ME arteriolar relaxation and the functional redundancy with eNOS in SKM arteries played any part in obscuring its role in 20-hydroxyecdysone vasodilation.

20-hydroxyecdysone was hypothesized to have vasodilatory properties, in part, because of its reported affinity for estrogen receptors (187, 193). Estrogen receptors, particularly ER-β were expressed in these arteries, consistent with ER-β being the predominant isoform expressed in blood vessels (373). However, the ER-β antagonist, PHTPP failed to alter the response to 20-hydroxyecdysone. A small but insignificant reduction in response was recorded with the ER antagonist ICI.182.780. which has stronger affinity for ER-α compared with ER-β, but selective antagonism of ER-α alone did not alter the response. Unfortunately, the same antagonists also failed to significantly alter the relaxation induced by β-estradiol, the agonist for both ER-receptors, in these arteries. The later made it difficult to draw a definitive conclusion about the roles of estrogen receptors in the vasodilatory actions of 20-hydroxyecdysone. Interestingly, several genes that positively influence estrogen signaling such as H2AFZ and DDX5 were upregulated in 20-hydroxyecdysone-treated arteries, even without noticeable change in the expression of ERα or ERβ. Moreover, rapid effects of estrogen do not require changes in NOS gene expression but may involve proteins that interact with the receptors, such as heat-shock protein 90, which also binds to and activates eNOS (39). ERα or ERβ activation can increase eNOS phosphorylation via phosphatidylinositol 3 (PI3)-kinase-Akt pathway (180, 213-216), without necessarily increasing the protein, leading to increase in NO levels (361).

To further characterize the molecular mechanisms modulated by 20-hydroxyecdysone treatment in these arteries, microarray analysis was performed. Interestingly, genes that counteract inflammation and oxidative stress such as DUSP10 and HSPB1 were up-regulated in arteries treated with 20-hydroxyecdysone, consistent with its ability to modulate oxidant and inflammatory signal transduction pathways (221, 241). Inflammation increases the production of reactive oxygen species, which is known to modify the production/activity of vasodilatory mediators including prostacyclin and NO (374). The anti-inflammatory and anti-oxidant properties of 20-hydroxyecdysone would therefore potentially benefit endothelial function.

The lack of selective effect of 20-hydroxyecdysone on SKM arteries could have implication for sports performance. SKM circulation is unique in accommodating up to 80 % of cardiac output during exercise following redistribution of blood from other tissues, notably from the gastrointestinal circulation (375). This essential adaptation to exercise could therefore be compromised if vasodilation is generalized and not limited to the muscle circulations at this critical time.

6.5 Limitations of the study

The ovine SKM and ME tissue samples were obtained from sheep farmed and euthanized in the public abattoir. Although the animals were certified as healthy for human consumption before they were slaughtered for meat, their health conditions could not be completely guaranteed. To mitigate this limitation, SKM and ME arteries were obtained from same animals and compared.

The human adipose tissue samples were obtained from patients who were morbidly obese, which could limit the applicability of the data to the general obese population. However, this limitation is outweighed by the clinical feasibility of accessing both OM and SC simultaneously in same patients to ensure a more robust comparison between the two depots. By comparing arteries from two depots in the same obese individual, the study reduced the potential cofounding effects of medications and comorbidities and highlight the depot-specific differences, which could apply to all degrees of obesity. To avoid the confounding effects of ethnicity, only patients of Arab origin were studied. Thus, the relevance of the specific mechanisms revealed by this study in other ethnic obese populations might require further studies in those populations.

6.6 Future directions

One of the key findings of this study is the apparent switch in COX-1 activity from being generally vasodilatory in arteries from healthy ovine donors, to opposing vasodilation in omental arteries from obese individuals. This change

in activity was depot-specific and therefore appears to relate to the adipose tissue microenvironment. Identification of the factor(s) within the fat tissue, which drive this change in COX-1 enzymatic activity would be an important future study. If the factor (s) can be identified, the next logical step would be to investigate the possibility of reversing the enzyme activity by targeted interventions.

The receptor mechanism for 20-hydroxyecdysone vasodilation could not be determined and requires further investigation. More tools are necessary to confirm or reject the involvement of estrogen receptors in the actions of the compound. In addition, it would be important to determine whether the vascular sensitivity to this supplement-derived compound is different in athletes vs. non-athletes, particularly whether the sensitivity of the muscle vasculature is different, to strengthen the implication of its consumption by athletes. This is more so important now that the compound has been added to the list of compounds being monitored by the world anti-doping agency for a possible ban.

References

1.   Mazurek R, Dave JM, Chandran RR, Misra A, Sheikh AQ, Greif DM. Vascular Cells in Blood Vessel Wall Development and Disease. Advances in Pharmacology (San Diego, Calif). 2017;78:323-50.

2.   Ponticos M, Smith BD. Extracellular matrix synthesis in vascular disease: hypertension, and atherosclerosis. Journal of biomedical research. 2014;28(1):25-39.

3.   Haurani MJ, Pagano PJ. Adventitial fibroblast reactive oxygen species as autacrine and paracrine mediators of remodeling: bellwether for vascular disease? Cardiovascular research. 2007;75(4):679-89.

4.   Galkina E, Kadl A, Sanders J, Varughese D, Sarembock IJ, Ley K. Lymphocyte recruitment into the aortic wall before and during development of atherosclerosis is partially L-selectin dependent. The Journal of experimental medicine. 2006;203(5):1273-82.

5.   Swedenborg J, Mäyränpää MI, Kovanen PT. Mast Cells: important players in the orchestrated pathogenesis of abdominal aortic aneurysms. Arterioscler Thromb Vasc Bio. 2011;31(4):734.

6.   Tieu BC, Lee C, Sun H, Lejeune W, Recinos A, Ju X, et al. An adventitial IL-6/MCP1 amplification loop accelerates macrophage-mediated vascular inflammation leading to aortic dissection in mice. The Journal of clinical investigation. 2009;119(12):3637-51.

7.   Pugsley MK, Tabrizchi R. The vascular system: An overview of structure and function. Methods in Vascular Pharmacology. 2000;44(2):333-40.

8.   Martinez-Lemus LA. The dynamic structure of arterioles. Basic & clinical pharmacology & toxicology. 2012;110(1):5-11.

9.   Christensen KL, Mulvany MJ. Location of Resistance Arteries. Journal of vascular research. 2001;38(1):1-12.

10.   Bush PC, Owen WG. Interactions of thrombin with endothelium. In: Nossel Hl VHJ, editor. Pathophysiology of the endothelial cell. New York: Academic Press; 1982. p. 97-101.

11.   Van Hinsbergh VWM. The endothelium: vascular control of haemostasis. Proceedings of the Third Symposium of the Wim Schellekens Foundation "Thrombophilia and Reproduction". 2001;95(2):198-201.

12.   Van Hinsbergh VWM. Endothelial Permeability for Macromolecules. Arteriosclerosis, Thrombosis, and Vascular Biology. 1997;17(6):1018-23.

13.   Brasier AR, Recinos A, Eledrisi MS. Vascular Inflammation and the Renin-Angiotensin System. Arteriosclerosis, Thrombosis, and Vascular Biology. 2002;22(8):1257-66.

14.   Etzioni A, Doerschuk CM, Harlan JM. Of Man and Mouse: Leukocyte and Endothelial Adhesion Molecule Deficiencies. Blood. 1999;94(10):3281-8.

15.   Mantovani A, Bussolino F, Introna M. Cytokine regulation of endothelial cell function: from molecular level to the bedside. 1997. p. 231-40.

16.   Bassenge E. Endothelial function in different organs. The Endothelium and Cardiocirculatory Function, Part I. 1996;39(3):209-28.

17.   Wray DW. Interaction of neural and local mechanisms in the control of skeletal muscle blood flow. ProQuest Dissertations Publishing; 2003.

18.   Davis MJ, Hill MA. Signaling mechanisms underlying the vascular myogenic response. Physiol Rev. 1999 Apr;79(2):387-423.

19.   Narayanan J, Imig M, Roman RJ, Harder DR. Pressurization of isolated renal arteries increases inositol trisphosphate and diacylglycerol. AJP - Heart and Circulatory Physiology. 1994;266(5):H1840-H5.

20.   Coats P, Johnston F, MacDonald J, McMurray JJ, Hillier C. Signalling mechanisms underlying the myogenic response in human subcutaneous resistance arteries. Cardiovascular Research. 2001;49(4):828-37.

21.   Jackson WF, Boerman EM. Regional heterogeneity in the mechanisms of myogenic tone in hamster arterioles. American Journal of Physiology-Heart and Circulatory Physiology. 2017;313(3):H667-H75.

22.   Hill MA, Falcone JC, Meininger GA. Evidence for protein kinase C involvement in arteriolar myogenic reactivity. American Journal of Physiology-Heart and Circulatory Physiology. 1990;259(5):H1586-H94.

23.   JOHNSON PC. Autoregulatory Responses of Cat Mesenteric Arterioles Measured in Vivo. Circulation Research. 1968;22(2):199-212.

24.   Bouskela E, Wiederhielm CA. Microvascular myogenic reaction in the wing of the intact unanesthetized bat. American Journal of Physiology-Heart and Circulatory Physiology. 1979;237(1):H59-H65.

25.   Aukland K. Myogenic mechanisms in the kidney. J Hypertens Suppl. 1989 Sep;7(4):S71-6; discussion S7.

26.   Rembold CM, Murphy RA. Myoplasmic [Ca2+] Determines Myosin Phosphorylation and Isometric Stress in Agonist-Stimulated Swine Arterial Smooth Muscle. Journal of cardiovascular pharmacology. 1988;12(Supplement 5):38-42.

27.   Hai C, Murphy RA. Ca2+ Crossbridge Phosphorylation, and Contraction. Annual Review of Physiology. 1989;51(1):285-98.

28.   Du W, McMahon TJ, Zhang Z-S, Stiber JA, Meissner G, Eu JP. Excitation-Contraction Coupling in Airway Smooth Muscle. Journal of Biological Chemistry. 2006;281(40):30143-51.

29.   Khalil R, Lodge N, Saida K, van Breemen C. Mechanism of Calcium Activation in Vascular Smooth Muscle. Journal of hypertension. 1987;5(Supplement 4):S5-S15.

30.   Ashida T, Blaustein MP. Regulation of cell calcium and contractility in mammalian arterial smooth muscle: the role of sodium-calcium exchange. The Journal of physiology. 1987;392:617-35.

31.   Webb RC. SMOOTH MUSCLE CONTRACTION AND RELAXATION. Advances in Physiology Education. 2003;27(4):201-6.

32.   Al-Shboul O. Contraction and Relaxation Signaling in Gastrointestinal Smooth Muscle. 2018 04/17:315-21.

33.   Somlyo AP, Somlyo AV. Signal transduction and regulation in smooth muscle. Nature. 1994 Nov 17;372(6503):231-6.

34.   Fukata Y, Amano M, Kaibuchi K. Rho-Rho-kinase pathway in smooth muscle contraction and cytoskeletal reorganization of non-muscle cells. Trends in pharmacological sciences. 2001;22(1):32-9.

35.   Chitaley K, Weber D, Webb RC. RhoA/Rho-kinase, vascular changes, and hypertension. Curr Hypertens Rep. 2001 Apr;3(2):139-44.

36.   Murthy KS, Zhou H, Grider JR, Makhlouf GM. Inhibition of sustained smooth muscle contraction by PKA and PKG preferentially mediated by phosphorylation of RhoA. American Journal of Physiology-Gastrointestinal and Liver Physiology. 2003;284(6):G1006-G16.

37.   Wooldridge AA, MacDonald JA, Erdodi F, Ma C, Borman MA, Hartshorne DJ, et al. Smooth Muscle Phosphatase Is Regulated in Vivo by Exclusion of Phosphorylation of Threonine 696 of MYPT1 by Phosphorylation of Serine 695 in Response to Cyclic Nucleotides. Journal of Biological Chemistry. 2004 August 13, 2004;279(33):34496-504.

38.   MacDonald JA, Walker LA, Nakamoto RK, Gorenne I, Somlyo AV, Somlyo AP, et al. Phosphorylation of telokin by cyclic nucleotide kinases and the identification of in vivo phosphorylation sites in smooth muscle. FEBS Letters. 2000;479(3):83-8.

39.   Alderton WK, Cooper CE, Knowels RG. Nitric oxide synthases: structure, function and inhibition. Biochemical Journal. 2001;357(3):593-615.

40.   Palmer RMJ, Ashton DS, Moncada S. Vascular endothelial cells synthesize nitric oxide from L-arginine. Nature. 1988;333(6174):664-6.

41.   Moncada S, Palmer RM, Higgs EA. Nitric oxide: physiology, pathophysiology, and pharmacology. Pharmacol Rev. 1991;43(2):109.

42.   Bourque SL, Davidge ST, Adams MA. The interaction between endothelin-1 and nitric oxide in the vasculature: new perspectives. Am J Physiol Regul Integr Comp Physiol. 2011 Jun;300(6):R1288-95.

43.   Cannon RO. Role of nitric oxide in cardiovascular disease: focus on the endothelium. Clinical chemistry. 1998;44(8):1809-19.

44.   Schwarz P, Diem R, Dun NJ, Förstermann U. Endogenous and exogenous nitric oxide inhibits norepinephrine release from rat heart sympathetic nerves. Circulation research. 1995;77(4):841-8.

45.   Furchgott RF, Zawadzki JV. The obligatory role of endothelial cells in the relaxation of arterial smooth muscle by acetylcholine. Nature. 1980;288(5789):373-6.

46.   Groves P, Kurz S, Just H, Drexler H. Role of endogenous Bradykinin in human coronary vasomotor control. Circulation. 1995;92(12):3424-30.

47.   Joannides R, Haefeli WE, Linder L, Richard V, Bakkali EH, Thuillez C, et al. Nitric Oxide Is Responsible for Flow-Dependent Dilatation of Human Peripheral Conduit Arteries In Vivo. Circulation. 1995;91(5):1314-9.

48.   Rubanyi GM, Romero JC, Vanhoutte PM. Flow-induced release of endothelium-derived relaxing factor. American Journal of Physiology - Heart and Circulatory Physiology. 1986;250(6):H1145-H9.

49.   Klabunde RE. Nitric Oxide. CVphysiology; 2018.

50.   Smith WL, DeWitt DL, Garavito RM. Cyclooxygenases: Structural, Cellular, and Molecular Biology. Annual Review of Biochemistry. 2000;69(1):145-82.

51.   Blobaum AL, Marnett LJ. Structural and Functional Basis of Cyclooxygenase Inhibition. Journal of Medicinal Chemistry. 2007;50(7):1425-41.

52.   Picot D, Loll PJ, Garavito RM. The X-ray crystal structure of the membrane protein prostaglandin H2 synthase-1. Nature. 1994;367(6460):243-9.

53.   Yuan C, Rieke CJ, Rimon G, Wingerd BA, Smith WL. Partnering between monomers of cyclooxygenase-2 homodimers. Proceedings of the National Academy of Sciences. 2006;103(16):6142-7.

54.   Chandrasekharan NV, Simmons DL. The cyclooxygenases. Genome biology. 2004;5(9):241.

55.   Varvas K, Kasvandik S, Hansen K, Järving I, Morell I, Samel N. Structural and catalytic insights into the algal prostaglandin H synthase reveal atypical features of the first non-animal cyclooxygenase. Biochimica et Biophysica Acta - Molecular and Cell Biology of Lipids. 2013;1831(4):863-71.

56.   Davidge ST. Prostaglandin H Synthase and Vascular Function. Circulation research. 2001;89(8):650-60.

57.   Félétou M, Huang Y, Vanhoutte PM. Endothelium-mediated control of vascular tone: COX-1 and COX-2 products. British journal of pharmacology. 2011;164(3):894-912.

58.   Snipes JA, Kis B, Shelness GS, Hewett JA, Busija DW. Cloning and characterization of cyclooxygenase-1b (putative cyclooxygenase-3) in rat. The Journal of pharmacology and experimental therapeutics. 2005;313(2):668-76.

59.   Rao P, Knaus E. Evolution of Nonsteroidal Anti-Inflammatory Drugs (NSAIDs): Cyclooxygenase (COX) Inhibition and Beyond. Journal of pharmacy & pharmaceutical sciences. 2008;11(2):81.

60.   Langenbach R, Morham SG, Tiano HF, Loftin CD, Ghanayem BI, Chulada PC, et al. Prostaglandin synthase 1 gene disruption in mice reduces arachidonic acid-induced inflammation and indomethacin-induced gastric ulceration. Cell. 1995;83(3):483-92.

61.   Loftin CD, Tiano HF, Langenbach R. Phenotypes of the COX-deficient mice indicate physiological and pathophysiological roles for COX-1 and COX-2. Prostaglandins & other lipid mediators. 2002;68-69:177-85.

62.   Morita I. Distinct functions of COX-1 and COX-2. Molecular Biology of the Arachidonate Cascade. 2002;68–69:165-75.

63.   Smyth EM, Grosser T, Wang M, Yu Y, FitzGerald GA. Prostanoids in health and disease. Journal of lipid research. 2009;50 Suppl:S423-8.

64.   McClelland S, Gawaz M, Kennerknecht E, Konrad CSI, Sauer S, Schuerzinger K, et al. Contribution of cyclooxygenase-1 to thromboxane formation, platelet–vessel wall interactions and atherosclerosis in the ApoE null mouse. Atherosclerosis. 2009;202(1):84-91.

65.   Claria J. Cyclooxygenase-2 Biology. Current pharmaceutical design. 2003;9(27):2177-90.

66.   Funk CD, FitzGerald GA. COX-2 inhibitors and cardiovascular risk. Journal of cardiovascular pharmacology. 2007;50(5):470-9.

67.   Grosser T, Fries S, FitzGerald GA. Biological basis for the cardiovascular consequences of COX-2 inhibition: therapeutic challenges and opportunities. Journal of Clinical Investigation. 2006;116(1):4-15.

68.   Sun D, Liu H, Yan C, Jacobson A, Ojaimi C, Huang A, et al. COX-2 contributes to the maintenance of flow-induced dilation in arterioles of eNOS-knockout mice. American journal of physiologyHeart and circulatory physiology. 2006;291(3):H1429-35.

69.   Zhang J, Ding EL, Song Y. Adverse effects of cyclooxygenase 2 inhibitors on renal and arrhythmia events: meta-analysis of randomized trials. Jama. 2006;296(13):1619-32.

70.   Kirkby NS, Sampaio W, Etelvino G, Alves DT, Anders KL, Temponi R, et al. Cyclooxygenase-2 Selectively Controls Renal Blood Flow Through a Novel PPARβ/δ-Dependent Vasodilator Pathway. Hypertension (Dallas, Tex: 1979). 2018;71(2):297-305.

71.   Loftin CD, Trivedi DB, Tiano HF, Clark JA, Lee CA, Epstein JA, et al. Failure of ductus arteriosus closure and remodeling in neonatal mice deficient in cyclooxygenase-1 and cyclooxygenase-2. Proceedings of the National Academy of Sciences of the United States of America. 2001;98(3):1059-64.

72.   Morham SG, Langenbach R, Loftin CD, Tiano HF, Vouloumanos N, Jennette JC, et al. Prostaglandin synthase 2 gene disruption causes severe renal pathology in the mouse. Cell. 1995;83(3):473-82.

73.   Yu Y, Funk CD. A novel genetic model of selective COX-2 inhibition: Comparison with COX-2 null mice. John C McGiff: Four decades of contributions to the study of eicosanoid-mediated regulation of vascular and renal function. 2007;82(1–4):77-84.

74.   Félétou M. The Endothelium: Part 1: Multiple Functions of the Endothelial Cells—Focus on Endothelium-Derived Vasoactive Mediators. San Rafael (CA): Morgan & Claypool Life Sciences; 2011. p. 281.

75.   Narumiya S. Physiology and pathophysiology of prostanoid receptors. Proceedings of the Japan Academy, Series B. 2007;83(9):296-319.

76.   Helliwell RJA, Adams LF, Mitchell MD. Prostaglandin synthases: recent developments and a novel hypothesis. Prostaglandins, Leukotrienes and Essential Fatty Acids. 2004;70(2):101-13.

77.   Bock A, Kostenis E, Tränkle C, Lohse MJ, Mohr K. Pilot the pulse: controlling the multiplicity of receptor dynamics. Trends in Pharmacological Sciences. 2014;35(12):630-8.

78.   Coleman RA, Smith WL, Narumiya S. International Union of Pharmacology classification of prostanoid receptors: properties, distribution, and structure of the receptors and their subtypes. Pharmacological reviews. 1994;46(2):205-29.

79.   Norel X. Prostanoid Receptors in the Human Vascular Wall. ScientificWorldJournal. 2007;7:1359-74.

80.   Norel X, Breyer RM, Clapp L, Coleman RA, Giembycz M, Heinemann A, et al. Prostanoid receptors | G protein-coupled receptors. 2019.

81.   Moreno JJ. Eicosanoid receptors: Targets for the treatment of disrupted intestinal epithelial homeostasis. European Journal of Pharmacology. 2017;796:7-19.

82.   Caughey GE, Cleland LG, Penglis PS, Gamble JR, James MJ. Roles of Cyclooxygenase (COX)-1 and COX-2 in Prostanoid Production by Human Endothelial Cells: Selective Up-Regulation of Prostacyclin Synthesis by COX-2. The Journal of Immunology. 2001;167(5):2831-8.

83.   Pearson JD. Endothelial cell function and thrombosis. Best Practice & Research Clinical Haematology. 1999;12(3):329-41.

84.   Orie NN, Ledwozyw A, Williams DJ, Whittle BJ, Clapp LH. Differential actions of the prostacyclin analogues treprostinil and iloprost and the selexipag metabolite, MRE-269 (ACT-333679) in rat small pulmonary arteries and veins. Prostaglandins & other lipid mediators. 2013;106:1-7.

85.   Vegesna RVK, Diamond J. Elevation of cyclic AMP by prostacyclin is accompanied by relaxation of bovine coronary arteries and contraction of rabbit aortic rings. 1986. p. 25-31.

86.   Turcato S, Clapp LH. Effects of the adenylyl cyclase inhibitor SQ22536 on iloprost-induced vasorelaxation and cyclic AMP elevation in isolated guinea-pig aorta. British journal of pharmacology. 1999;126(4):845-7.

87.   Yamaki F, Kaga M, Horinouchi T, Tanaka H, Koike K, Shigenobu K, et al. MaxiK channel-mediated relaxation of guinea-pig aorta following stimulation of IP receptor with beraprost via cyclic AMP-dependent and -independent mechanisms. Naunyn-Schmiedeberg's archives of pharmacology. 2001;364(6):538-50.

88.   Clapp LH, Finney P, Turcato S, Tran S, Rubin LJ, Tinker A. Differential effects of stable prostacyclin analogs on smooth muscle proliferation and cyclic AMP

generation in human pulmonary artery. Am J Respir Cell Mol Biol. 2002;26(2):194-201.

89.   Majed BH, Khalil RA. Molecular mechanisms regulating the vascular prostacyclin pathways and their adaptation during pregnancy and in the newborn. Pharmacological reviews. 2012;64(3):540-82.

90.   Wise H. Multiple signalling options for prostacyclin. Acta Pharmacologica Sinica. 2003;24(7):625-30.

91.   Orie NN, Fry CH, Clapp LH. Evidence that inward rectifier K+ channels mediate relaxation by the PGI2 receptor agonist cicaprost via a cyclic AMP-independent mechanism. Cardiovascular Research. 2006;69(1):107-15.

92.   Lim H, Dey SK. A novel pathway of prostacyclin signaling-hanging out with nuclear receptors. Endocrinology. 2002;143(9):3207-10.

93.   Li Y, Connolly M, Nagaraj C, Tang B, Bálint Z, Popper H, et al. Peroxisome Proliferator–Activated Receptor–β/δ, the Acute Signaling Factor in Prostacyclin-Induced Pulmonary Vasodilation. Am J Respir Cell Mol Biol. 2012;46(3):372-9.

94.   McGuire JJ, Ding H, Triggle CR. Endothelium-derived relaxing factors: A focus on endothelium-derived hyperpolarizing factor(s). Canadian journal of physiology and pharmacology. 2001;79(6):443-70.

95.   Shimokawa H, Yasutake H, Fujii K, Owada MK, Nakaike R, Fukumoto Y, et al. The importance of the hyperpolarizing mechanism increases as the vessel size decreases in endothelium-dependent relaxations in rat mesenteric circulation. Journal of cardiovascular pharmacology. 1996 Nov;28(5):703-11.

96.   Luksha L, Agewall S, Kublickiene K. Endothelium-derived hyperpolarizing factor in vascular physiology and cardiovascular disease. Atherosclerosis. 2009;202(2):330-44.

97.   Busse R, Edwards G, Félétou M, Fleming I, Vanhoutte PM, Weston AH. EDHF: bringing the concepts together. Trends in Pharmacological Sciences. 2002;23(8):374-80.

98.   Shimokawa H, Morikawa K. Hydrogen peroxide is an endothelium-derived hyperpolarizing factor in animals and humans. Journal of Molecular and Cellular Cardiology. 2005;39(5):725-32.

99.   Mustafa AK, Sikka G, Gazi SK, Steppan J, Jung SM, Bhunia AK, et al. Hydrogen Sulfide as Endothelium-Derived Hyperpolarizing Factor Sulfhydrates Potassium Channels Novelty and Significance. Circ Res. 2011;109(11):1259.

100.   Fleming I, Busse R. Endothelium-Derived Epoxyeicosatrienoic Acids and Vascular Function. Hypertension. 2006;47(4):629-33.

101.   Edwards G, Weston AH. Potassium and potassium clouds in endothelium-dependent hyperpolarizations. Endothelium-dependent hyperpolarizations. 2004;49(6):535-41.

102.   Ahluwalia A, Hobbs AJ. Endothelium-derived C-type natriuretic peptide: more than just a hyperpolarizing factor. Trends in Pharmacological Sciences. 2005;26(3):162-7.

103.   Félétou M, Vanhoutte PM. Endothelium-Derived Hyperpolarizing Factor. Arteriosclerosis, Thrombosis, and Vascular Biology. 2006;26(6):1215-25.

104.   Lüscher TF, Boulanger CM, Dohi Y, Yang ZH. Endothelium-derived contracting factors. Hypertension. 1992;19(2):117-30.

105.   Nasr A, Breckwoldt M. Estrogen replacement therapy and cardiovascular protection: lipid mechanisms are the tip of an iceburg. Gynecol Endocrinol. 1998;12:43-59.

106.   Katusic ZS, Shepherd JT. Endothelium-derived vasoactive factors: II. Endothelium-dependent contraction. Hypertension. 1991;18:III86-III92.
107.   Moncada S, Higgs EA. Arachidonate metabolism in blood cells and the vessel wall. Clin Haematol. 1986;15:273-87.
108.   Asano H, Shimizu K, Muramatsu M, Iwama Y, Toki Y, Miyazaki Y, et al. Prostaglandin H2 as an endothelium-derived contracting factor modulates endothelin-1-induced contraction. J Hypertens. 1994;12(4):383-90.
109.   Ge T, Hughes H, Junquero DC, Wu KK, Vanhoutte PM, Boulanger CM. Endothelium-dependent contractions are associated with both augmented expression of prostaglandin H synthase-1 and hypersensitivity to prostaglandin H2 in the SHR aorta. Circulation research. 1995;76(6):1003-10.
110.   Gluais P, Lonchampt M, Morrow JD, Vanhoutte PM, Feletou M. Acetylcholine-induced endothelium-dependent contractions in the SHR aorta: the Janus face of prostacyclin. British journal of pharmacology. 2005;146(6):834-45.
111.   Auch-Schwelk W, Katusic ZS, Vanhoutte PM. Thromboxane A2 receptor antagonists inhibit endothelium-dependent contractions. Hypertension. 1990;15(6 Pt 2):699-703.
112.   Ito T, Kato T, Iwama Y, Muramatsu M, Shimizu K, Asano H, et al. Prostaglandin H2 as an endothelium-derived contracting factor and its interaction with endothelium-derived nitric oxide. J Hypertens. 1991;9(8):729-36.
113.   Wong MS-K, Vanhoutte PM. COX-mediated endothelium-dependent contractions: from the past to recent discoveries. Acta Pharmacologica Sinica. 2010;31(9):1095-102.
114.   Henze D, Menzel M, Soukup J, Scharf A, Holz C, Németh N, et al. Endothelin-1 and cerebral blood flow in a porcine model. Journal of Clinical Neuroscience. 2007;14(7):650-7.
115.   Hirose H, Ide K, Sasaki T, et al. The role of endothelin and nitric oxide in modulation of normal and spastic cerebral vascular tone in the dog. Eur J Pharmacol. 1995;277:77-87.
116.   De Nucci G, Thomas R, D'Orleans-Juste P, et al. Pressor effects of circulating endothelin are limited by its removal in the pulmonary circulation and by the release of prostacyclin and endothelium-derived relaxing factor. Proc Natl Acad Sci USA. 1988;85:9797-800.
117.   Lin HY, Kaji EH, Winkel GK, et al. Cloning and functional expression of a vascular smooth muscle endothelin 1 receptor. Proc Natl Acad Sci USA. 1991;88:3185-9.
118.   Spinella MJ, Malik AB, Everitt J, et al. Design and synthesis of a specific endothelin 1 antagonist: effects on pulmonary vasoconstriction. Proc Natl Acad Sci USA. 1991;88:7443-6.
119.   Wynne BM, Chiao C-W, Webb RC. Vascular Smooth Muscle Cell Signaling Mechanisms for Contraction to Angiotensin II and Endothelin-1. Journal of the American Society of Hypertension. 2009;3(2):84-95.
120.   Jun F, Chu LM, Robich MP, Clements RT, Khabbaz KR, Robert H, et al. Effects of Cardiopulmonary Bypass on Endothelin-1-Induced Contraction and Signaling in Human Skeletal Muscle Microcirculation. Circulation. 2010;122(11):S150-S5.
121.   Feng J. Invited Commentary. The Annals of Thoracic Surgery. 2011;92(4):1307-.

122.   Takayama H, Hamner CE, Caccitolo JA, Hisamochi K, Pearson PJ, Schaff HV. A Novel Antioxidant, EPC-K1, Stimulates Endothelial Nitric Oxide Production and Scavenges Hydroxyl Radicals. Circulation Journal. 2003;67(12):1046-52.

123.   Yamada T, Egashira N, Imuta M, Yano T, Yamauchi Y, Watanabe H, et al. Role of oxidative stress in vinorelbine-induced vascular endothelial cell injury. Free Radical Biology and Medicine. 2010;48(1):120-7.

124.   Ott M, Gogvadze V, Orrenius S, Zhivotovsky B. Mitochondria, oxidative stress and cell death. Apoptosis. 2007;12(5):913-22.

125.   Jones RD, Berne RM. Intrinsic Regulation of Skeletal Muscle Blood Flow. Circulation research. 1964;14(2):126-38.

126.   Burrows ME, Johnson PC. Diameter, wall tension, and flow in mesenteric arterioles during autoregulation. American Journal of Physiology-Heart and Circulatory Physiology. 1981;241(6):H829-H37.

127.   Khalid M, Jacques M, Levy BI, Daniel H. Impaired Nitric Oxide-and Prostaglandin-Mediated Responses to Flow in Resistance Arteries of Hypertensive Rats. Hypertension. 1997;30(4):942-7.

128.   Koller A, Sun D, Huang A, Kaley G. Corelease of nitric oxide and prostaglandins mediates flow-dependent dilation of rat gracilis muscle arterioles. American Journal of Physiology-Heart and Circulatory Physiology. 1994;267(1):H326-H32.

129.   Koller A, Sun D, Kaley G. Role of shear stress and endothelial prostaglandins in flow- and viscosity-induced dilation of arterioles in vitro. Circulation research. 1993;72(6):1276-84.

130.   Sun D, Huang A, Koller A, Kaley G. Endothelial KCa Channels Mediate Flow-Dependent Dilation of Arterioles of Skeletal Muscle and Mesentery. Microvascular Research. 2001;61(2):179-86.

131.   Dube S, Canty JM. Shear stress-induced vasodilation in porcine coronary conduit arteries is independent of nitric oxide release. American Journal of Physiology-Heart and Circulatory Physiology. 2001;280(6):H2581-H90.

132.   Huang A, Sun D, Carroll MA, Jiang H, Smith CJ, Connetta JA, et al. EDHF mediates flow-induced dilation in skeletal muscle arterioles of female eNOS-KO mice. American Journal of Physiology-Heart and Circulatory Physiology. 2001;280(6):H2462-H9.

133.   Huang A, Koller A. Endothelin and Prostaglandin H2 Enhance Arteriolar Myogenic Tone in Hypertension. Hypertension. 1997 1997/11/01;30(5):1210-5.

134.   Marti-nez-Revelles S, Caracuel L, Marquez-Marta-n A, Dantas A, Oliver E, D'Ocon P, et al. Increased endothelin-1 vasoconstriction in mesenteric resistance arteries after superior mesenteric ischaemia-reperfusion. British journal of pharmacology. 2012;165(4):937-50.

135.   Touyz RM, Yuan DL, Schiffrin EL. Endothelin Subtype B Receptor-Mediated Calcium and Contractile Responses in Small Arteries of Hypertensive Rats. Hypertension. 1995;26(6):1041-5.

136.   Csongor C, Bagi Z, Koller A. Biphasic effect of hydrogen peroxide on skeletal muscle arteriolar tone via activation of endothelial and smooth muscle signaling pathways. Journal of applied physiology. 2004;97(3):1130-7.

137.   Gao YJ, Hirota S, Zhang DW, Janssen LJ, Lee RM. Mechanisms of hydrogen-peroxide-induced biphasic response in rat mesenteric artery. British journal of pharmacology. 2003;138(6):1085-92.

138.   Goodwill AG, Stapleton PA, James ME, D'Audiffret AC, Frisbee JC. Increased Arachidonic Acid-Induced Thromboxane Generation Impairs Skeletal Muscle Arteriolar Dilation with Genetic Dyslipidemia. Microcirculation. 2008;15(7):621-31.

139.   Deanfield JE, Halcox JP, Rabelink TJ. Endothelial Function and Dysfunction. Circulation. 2007;115(10):1285.

140.   Sena CM, Pereira AM, Seiça R. Endothelial dysfunction — A major mediator of diabetic vascular disease. Biochimica et Biophysica Acta (BBA) - Molecular Basis of Disease. 2013;1832(12):2216-31.

141.   Matz RL, de Sotomayor MA, Schott C, Stoclet J-C, Andriantsitohaina R. Vascular bed heterogeneity in age-related endothelial dysfunction with respect to NO and eicosanoids. British Journal of Pharmacology. 2000;131:303-11.

142.   Raees A, Backhamis A, Mohamed-Ali V, Bashah M, Al-Jaber M, Abraham D, et al. Altered cyclooxygenase-1 and enhanced thromboxane receptor activities underlie attenuated endothelial dilatory capacity of omental arteries in obesity. Life Sciences. 2019;239:117039.

143.   Dan W, Zaiming L, Xiaoyan W, Jose PA, Falck JR, Welch WJ, et al. Impaired Endothelial Function and Microvascular Asymmetrical Dimethylarginine in Angiotensin II–Infused Rats. Hypertension. 2010;56(5):950-5.

144.   Dan W, Cheng W, Xie W, Wei Z, Kathryn S, Hong J, et al. Endothelial Dysfunction and Enhanced Contractility in Microvessels From Ovariectomized Rats. Hypertension. 2014;63(5):1063-9.

145.   Dunn SM, Hilgers R, Das KC. Decreased EDHF-mediated relaxation is a major mechanism in endothelial dysfunction in resistance arteries in aged mice on prolonged high-fat sucrose diet. Physiological reports. 2017;5(23):e13502-e618.

146.   Michel FS, Man GS, Man RYK, Vanhoutte PM. Hypertension and the absence of EDHF-mediated responses favour endothelium-dependent contractions in renal arteries of the rat. British journal of pharmacology. 2008;155(2):217-26.

147.   Morikawa K, Matoba T, Kubota H, Hatanaka M, Fujiki T, Takahashi S, et al. Influence of diabetes mellitus, hypercholesterolemia, and their combination on EDHF-mediated responses in mice. Journal of cardiovascular pharmacology. 2005;45(5):485-90.

148.   Ruggeri ZM, Loredana MG. Adhesion Mechanisms in Platelet Function. Circulation research. 2007;100(12):1673-85.

149.   Hidekazu S, Zweifach BW, Schmid-Schonbein GW. Vasodilator Response of Mesenteric Arterioles to Histamine in Spontaneously Hypertensive Rats. Hypertension. 1995;26(3):397-400.

150.   Abou Abbas L, Salameh P, Nasser W, Nasser Z, Godin I. Obesity and symptoms of depression among adults in selected countries of the Middle East: a systematic review and meta-analysis. Clinical Obesity. 2015;5(1):2-11.

151.   Fantuzzi G. Adipose tissue, adipokines, and inflammation. Journal of Allergy and Clinical Immunology. 2005;115(5):911-9.

152.   Lundgren CH, Brown SL, Nordt TK, Sobel BE, Fujii S. Elaboration of Type-1 Plasminogen Activator Inhibitor From Adipocytes. Circulation. 1996;93(1):106-10.

153.   Kershaw EE, Flier JS. Adipose Tissue as an Endocrine Organ. The Journal of Clinical Endocrinology & Metabolism. 2004;89(6):2548-56.

154.   Jensen MD. Role of Body Fat Distribution and the Metabolic Complications of Obesity. The Journal of Clinical Endocrinology & Metabolism. 2008;93(11_supplement_1):s57-s63.

155.   Madani R, Karastergiou K, Ogston NC, Miheisi N, Bhome R, Haloob N, et al. RANTES release by human adipose tissue in vivo and evidence for depot-specific differences. American Journal of Physiology-Endocrinology and Metabolism. 2009;296(6):E1262-E8.

156.   Marchesi S, Lupattelli G, Schillaci G, Pirro M, Siepi D, Roscini AR, et al. Impaired flow-mediated vasoactivity during post-prandial phase in young healthy men. Atherosclerosis. 2000;153(2):397-402.

157.   Wajchenberg BL. Subcutaneous and Visceral Adipose Tissue: Their Relation to the Metabolic Syndrome. Endocrine reviews. 2000;21(6):697-738.

158.   Herz J, Hui DY. Lipoprotein receptors in the vascular wall. Curr Opin Lipidol. 2004;15(2):175-81.

159.   Farb MG, Tiwari S, Karki S, Ngo DTM, Carmine B, Hess DT, et al. Cyclooxygenase inhibition improves endothelial vasomotor dysfunction of visceral adipose arterioles in human obesity. Obesity. 2014;22(2):349-55.

160.   Bunting S, Moncada S, Vane JR. The prostacyclin--thromboxane A2 balance: pathophysiological and therapeutic implications. British medical bulletin. 1983;39(3):271-6.

161.   Moncada S. Prostacyclin and arterial wall biology. Arteriosclerosis (Dallas, Tex). 1982;2(3):193-207.

162.   Okahara K, Sun B, Kambayashi J-i. Upregulation of prostacyclin synthesis-related gene expression by shear stress in vascular endothelial cells. Arteriosclerosis, Thrombosis, and Vascular Biology. 1998;18(12):1922-6.

163.   Topper JN, Cai J, Falb D, Gimbrone MA. Identification of vascular endothelial genes differentially responsive to fluid mechanical stimuli: cyclooxygenase-2, manganese superoxide dismutase, and endothelial cell nitric oxide synthase are selectively up-regulated by steady laminar shear stress. Proceedings of the National Academy of Sciences. 1996;93(19):10417-22.

164.   Camacho M, Lopez-Belmonte J, Vila L. Rate of Vasoconstrictor Prostanoids Released by Endothelial Cells Depends on Cyclooxygenase-2 Expression and Prostaglandin I Synthase Activity. Circulation research. 1998;83(4):353-65.

165.   Meyer MR, Fredette NC, Barton M, Prossnitz ER. Regulation of vascular smooth muscle tone by adipose-derived contracting factor. PloS one. 2013;8(11):e79245.

166.   Saraswathi V, Ramnanan CJ, Wilks AW, Desouza CV, Eller AA, Murali G, et al. Impact of hematopoietic cyclooxygenase-1 deficiency on obesity-linked adipose tissue inflammation and metabolic disorders in mice. Metabolism: clinical and experimental. 2013;62(11):1673-85.

167.   Muñoz M, Sánchez A, Pilar Martínez M, Benedito S, López-Oliva M-E, García-Sacristán A, et al. COX-2 is involved in vascular oxidative stress and endothelial dysfunction of renal interlobar arteries from obese Zucker rats. Free Radical Biology and Medicine. 2015;84:77-90.

168.   Fain JN, Ballou LR, Bahouth SW. Obesity is induced in mice heterozygous for cyclooxygenase-2. Prostaglandins & Other Lipid Mediators. 2001;65(4):199-209.

169.   Hodgkinson CP, Laxton RC, Patel K, Ye S. Advanced Glycation End-Product of Low Density Lipoprotein Activates the Toll-Like 4 Receptor Pathway Implications for Diabetic Atherosclerosis. Arterioscler Thromb Vasc Bio. 2008;28(12):2275.

170.   Sterin-Borda L, Franchi AM, Borda ES, Castillo ED, Gimeno MF, Gimeno AL. Augmented thromboxane generation by mesenteric arteries from pancreatectomized diabetic dogs is coincident with the vascular tone enhancement

evoked by Na arachidonate and prostacyclin. European Journal of Pharmacology. 1984;103(3):211-21.

171.   Shi Y, Ku DD, Man RYK, Vanhoutte PM. Augmented Endothelium-Derived Hyperpolarizing Factor-Mediated Relaxations Attenuate Endothelial Dysfunction in Femoral and Mesenteric, but Not in Carotid Arteries from Type I Diabetic Rats. Journal of Pharmacology and Experimental Therapeutics. 2006;318(1):276-81.

172.   Zhang H, Dellsperger KC, Zhang C. The link between metabolic abnormalities and endothelial dysfunction in type 2 diabetes: an update. Basic research in cardiology. 2012;107(1):1-237.

173.   John E, John S, Schmieder R. Impaired endothelial function in arterial hypertension and hypercholesterolemia. Journal of hypertension. 2000;18(4):363-74.

174.   Taddei S, Taddei S, Virdis A, Ghiadoni L, Salvetti A. The role of endothelium in human hypertension. Current opinion in nephrology and hypertension. 1998;7(2):203-10.

175.   Panza JA, García CE, Kilcoyne CM, Quyyumi AA, Cannon RO. Impaired endothelium-dependent vasodilation in patients with essential hypertension. Circulation. 1995;91(6):1732-8.

176.   Taddei S, Virdis A, Ghiadoni L, Magagna A, Salvetti A. Vitamin C Improves Endothelium-Dependent Vasodilation by Restoring Nitric Oxide Activity in Essential Hypertension. Circulation. 1998;97(22):2222-9.

177.   Perticone F, Sciacqua A, Maio R, Perticone M, Galiano Leone G, Bruni R, et al. Endothelial dysfunction, ADMA and insulin resistance in essential hypertension. International Journal of Cardiology. 2010;142(3):236-41.

178.   Vanhoutte PM. Endothelium and control of vascular function. Hypertension. 1989;13(6):658-67.

179.   Versari D, Daghini E, Virdis A, Ghiadoni L, Taddei S. Endothelium-dependent contractions and endothelial dysfunction in human hypertension. British journal of pharmacology. 2009;157(4):527-36.

180.   Gorelick-Feldman J, Cohick W, Raskin I. Ecdysteroids elicit a rapid Ca2+ flux leading to Akt activation and increased protein synthesis in skeletal muscle cells. Steroids. 2010;75(10):632-7.

181.   Dinan L. Phytoecdysteroids: biological aspects. Phytochemistry. 2001;57(3):325-39.

182.   Lafont R, Harmatha J, Marion-Poll F, Dinan L, Wilson I. Ecdybase (The Ecdysone Handbook) - a free online ecdysteroids database. 2019.

183.   Gorelick Feldman J. Phytoecdysteroids: Understanding their anabolic activity. New Jersey: Graduate School-New Brunswick Rutgers, The State University of New Jersey; 2009.

184.   Dinan L, Harmatha J, Volodin V, Lafont R. Phytoecdysteroids: Diversity, Biosynthesis and Distribution. In: Smagghe G, editor. Ecdysone: Structures and Functions: © Springer Science + Business Media B.V.; 2009. p. 3-45.

185.   Lafont R, Dinan L. Practical uses for ecdysteroids in mammals including humans: and update. Journal of Insect Science. 2003;3(7):1-30.

186.   Gadzhieva RM, Portugalov SN, Paniushkin VV, Kondrat'eva II. A comparative study of the anabolic action of ecdysten, leveton and Prime Plus, preparations of plant origin. Eksperimental'naia i klinicheskaia farmakologiia. 1995;58(5):46-8.

187.   Parr MK, Botrè F, Naß A, Hengevoss J, Diel P, Wolber G. Ecdysteroids: A novel class of anabolic agents? Biology of Sport. 2015;32(2):169-73.

188.   Simakin SY. The combined use of ecdisten and the product 'bodrost' during training in cyclical types of sport. Scientific Sports Bulletin. 1988;2.

189.   Syrov VN, Saatov Z, Sagdullaev SS, Mamatkhanov AU. Study of the Structure-Anabolic Activity Relationship for Phytoecdysteroids Extracted from Some Plants of Central Asia. Pharmaceutical Chemistry Journal. 2001;35(12):667-71.

190.   Le Bizec B, Antignac J-P, Monteau F, Andre F. Ecdysteroids: one potential new anabolic family in breeding animals. Papers presented at the 4th International Symposium on Hormone and Veterinary Drug Residue Analysis Antwerp,Belgium,4-7 June 2002 Part I. 2002;473(1):89-97.

191.   Phungphong S, Kijtawornrat A, Chaiduang S, Saengsirisuwan V, Bupha-Intr T. 20-Hydroxyecdysone attenuates cardiac remodeling in spontaneously hypertensive rats. 2017. p. 79-84.

192.   Zwetsloot KA, Shanely AR, Merritt EK, McBride JM. Phytoecdysteroids: A Novel, Non-Androgenic Alternative for Muscle Health and Performance. J Steroids Hormon Sci. 2014;S12:e001.

193.   Parr MK, Zhao P, Haupt O, Ngueu ST, Hengevoss J, Fritzemeier KH, et al. Estrogen receptor beta is involved in skeletal muscle hypertrophy induced by the phytoecdysteroid ecdysterone. Molecular Nutrition & Food Research. 2014;58(9):1861-72.

194.   Syrov VN, Kurmukov AG. Anabolic activity of phytoecdysone-ecdysterone isolated from Rhaponticum carthamoides (Willd.) Iljin. Farmakol Toksikol. 1976;39(6):690-3.

195.   Tóth N, Szabó A, Kacsala P, Héger J, Zádor E. 20-Hydroxyecdysone increases fiber size in a muscle-specific fashion in rat. Phytomedicine. 2008;15(9):691-8.

196.   Chermnykh NS, Shimanovskii NL, Shutko GV, Syrov VN. The action of methandrostenolone and ecdysterone on the physical endurance of animals and on protein metabolism in the skeletal muscles. Farmakol Toksikol. 1988;51(6):57-60.

197.   Hikino H, Nabetani S, Nomoto K, Arai T, Takemoto T. Effect of Long Term Administration of Insect-Metamorphosing Substances on Higher Animals. YAKUGAKU ZASSHI. 1969;89(2):235-40.

198.   Xu H, Cheng X, Cui Z, Wang B. Androgen-like and anabolic action of Antheraea pernyi Guerin-Meneville Pas. Zhongguo zhong yao za zhi = Zhongguo zhongyao zazhi = China journal of Chinese materia medica. 1991;16(4):237-40, 56.

199.   Dinan L, Lafont R. Effects and applications of arthropod steroid hormones (ecdysteroids) in mammals. Journal of Endocrinology. 2006;191(1):1-8.

200.   Koudela K, Tenora J, Bajer J, Mathova A, Slama K. Stimulation of growth and development in Japanase quails after oral administration of ecdysteroid-containing diet. EJE. 1995;92(1):349-54.

201.   Kratky F, Opletal L, Hejhalek J, Kucharova S. Vliv 20-hydroxyekdysonu na proteosyntezu u prasat; Effect of 20-hydroxyecdysone on the protein synthesis in pigs. Zivočišná Výroba. 1997;42(10):445-51.

202.   Purser D, Baker S. Ecdysones used to improve productivity of ruminants. Chemical Abstract. 1994;121,254587u.

203.   Todorov IN, Mitrokhin YI, Efremova OI, Sidorenko LI. The Effect of Ecdysterone on the Biosynthesis of Proteins and Nucleic Acids in Mice. Pharmaceutical Chemistry Journal. 2000;34(9):455-8.

204.   Hirunsai M, Yimlamai T, Suksamrarn A. Effect of 20-Hydroxyecdysone on Proteolytic Regulation in Skeletal Muscle Atrophy. In vivo (Athens, Greece). 2016;30(6):869-77.

205.   Wilborn CD, Taylor LW, Campbell BI, Kerksick C, Rasmussen CJ, Greenwood M, et al. Effects of methoxyisoflavone, ecdysterone, and sulfo-polysaccharide supplementation on training adaptations in resistance-trained males. Journal of the International Society of Sports Nutrition. 2006;3(2):19.

206.   Chaudhary KD, Lupien PJ, Hinse C. Effect of ecdysone on glutamic decarboxylase in rat brain. Experientia. 1969;25:250-1.

207.   Bathori M, Toth N, Hunyadi A, Marki A, Zador E. Phytoecdysteroids and anabolic-androgenic steroids-structure and effects on humans. Current medicinal chemistry. 2008;15(-):75-91.

208.   Issaadi HM, Csábi J, Hsieh T-J, Gáti T, Tóth G, Hunyadi A. Side-chain cleaved phytoecdysteroid metabolites as activators of protein kinase B. Bioorganic Chemistry. 2019 2019/02/01/;82:405-13.

209.   Toth N, Hunyadi A, Bathori M, Zador E. Phytoecdysteroids and vitamin D analogues--similarities in structure and mode of action. Current medicinal chemistry. 2010;17(18):1974-94.

210.   Danik JS, Manson JE. Vitamin d and cardiovascular disease. Current treatment options in cardiovascular medicine. 2012;14(4):414-24.

211.   Sobrino A, Pilar JO, Novella S, Laguna-Fernandez A, Bueno C, Miguel AG, et al. Estradiol selectively stimulates endothelial prostacyclin production through estrogen receptor alpha. Journal of Molecular Endocrinology. 2010;44(4):237-46.

212.   Sobrino A, Mata M, Laguna-Fernandez A, Novella S, Oviedo PJ, García-Pérez MA, et al. Estradiol Stimulates Vasodilatory and Metabolic Pathways in Cultured Human Endothelial Cells (Estradiol and Gene Expression). PLoS ONE. 2009;4(12):e8242.

213.   Constantino S, Santos R, Gisselbrecht S, Gouilleux F. The ecdysone inducible gene expression system: unexpected effects of muristerone A and ponasterone A on cytokine signaling in mammalian cells. European Cytokine Network. 2001;12(2):365-7.

214.   Gorelick-Feldman J, MacLean D, Ilic N, Poulev A, Lila MA, Cheng D, et al. Phytoecdysteroids Increase Protein Synthesis in Skeletal Muscle Cells. Journal of Agricultural and Food Chemistry. 2008;56(10):3532-7.

215.   Kizelsztein P, Govorko D, Komarnytsky S, Evans A, Wang Z, Cefalu WT, et al. 20-Hydroxyecdysone decreases weight and hyperglycemia in a diet-induced obesity mice model. American journal of physiologyEndocrinology and metabolism. 2009;296(3):E433-9.

216.   Oehme I, Bosser S, Zornig M. Agonists of an ecdysone-inducible mammalian expression system inhibit Fas Ligand- and TRAIL-induced apoptosis in the human colon carcinoma cell line RKO. Cell death and differentiation. 2005;13(2):189-201.

217.   Jian C-X, Liu X-F, Hu J, Li C-J, Zhang G, Li Y, et al. 20-hydroxyecdysone-induced bone morphogenetic protein-2-dependent osteogenic differentiation through the ERK pathway in human periodontal ligament stem cells. European Journal of Pharmacology. 2013 2013/01/05/;698(1):48-56.

218.   Syrov VN, Khushbaktova ZA, Abzalova MK, Sultanov MB. On the hypolipidemic and antiatherosclerotic action of phytoecdysteroids. Doklady Akademii Nauk Uzbeckoy SSR. 1983;9:44-5.

219.   Kurmukov AG, Yermishina OA. Effect of ecdysterone on experimental arrhythmias, changes in hemodynamics and contractility of the myocardium produced by a coronary artery occlusion. Farmakologiya i Toksikologiya. 1991;54:27-9.

220.   Yang C, Xu J, Dong Y, Liu X. Studies on the isolation and identification of 20-ecdysone from Zebrina pendula Schnizl. and its antiarrhythmic effect. Tianran Chanwu Yanjiu Yu Kaifa. 1996;8:17-9.

221.   Sun Y, Zhao DL, Liu ZX, Sun XH, Li Y. Beneficial effect of 20hydroxyecdysone exerted by modulating antioxidants and inflammatory cytokine levels in collageninduced arthritis: A model for rheumatoid arthritis. Molecular medicine reports. 2017;16(5):6162-9.

222.   Wu X, Lin S, Yang Y, Feng S. Effects of ecdysterone on human umbilical vein endothelial cells injuried by tumor necrosis factor. Chinese Journal of Pathophysiology. 1998;14:58-62.

223.   Prabhu VKK, Nayar KK. Crustecdysone is without estrogenic or antiestrogenic activity in the rat. Experientia. 1974;30(7):821-.

224.   Tashmukhamedova MA, Almatov KT, Syrov VN, Sultanov MB, Abidov AA. Comparative study of the effect of ecdysterone, turkesterone and nerobol on the function of rat liver mitochondria in experimental diabetes. Voprosy meditsinskoi khimii. 1986;32(5):24-8.

225.   Lu M, Wang P, Ge Y, Dworkin L, Brem A, Liu Z, et al. Activation of mineralocorticoid receptor by ecdysone, an adaptogenic and anabolic ecdysteroid, promotes glomerular injury and proteinuria involving overactive GSK3β pathway signaling. Scientific Reports. 2018 2018/08/15;8(1):12225.

226.   Lu M, Wang P, Zhou S, Flickinger B, Malhotra D, Ge Y, et al. Ecdysone Elicits Chronic Renal Impairment via Mineralocorticoid-Like Pathogenic Activities. Cellular Physiology and Biochemistry. 2018;49(4):1633-45.

227.   Khimiko IN, Mitrokin YI, Efremova OI, Sidorenko LI. The influence of ecdysterone on the biosynthesis of proteins and nucleic acids in mouse organs. Khimiko-Farmatsevticheskii Zhurnal. 2000;34:3-5.

228.   Kuzmenko AI, Morozova RP, Nikolenko IA, Korniets GV, YuD K. Effects of vitamin D3 and ecdysterone on free-radical lipid peroxidation. BiochemistryBiokhimiia. 1997;62(6):609-12.

229.   Lupien PJ, Hinse C, Chaudhary KD. Ecdysone as a hypocholesterolemic agent. Archives Internationales de Physiologie et de Biochimie. 1969;77(2):206-12.

230.   Naresh Kumar R, Sundaram R, Shanthi P, Sachdanandam P. Protective role of 20-OH ecdysone on lipid profile and tissue fatty acid changes in streptozotocin induced diabetic rats. Eur J Pharmacol. 2013 Jan 5;698(1-3):489-98.

231.   Chen Q, Xia Y, Qiu Z. Effect of ecdysterone on glucose metabolism in vitro. Life Sciences. 2006;78(10):1108-13.

232.   Syrov VN, Iuldasheva NK, Egamova FR, Ismailova GI, Abdullaev ND, Khushbaktova ZA. Estimation of the hypoglycemic effect of phytoecdysteroids. Eksperimental'naia i klinicheskaia farmakologiia. 2012;75(5):28-31.

233.   Syrov VN, Khushbaktova ZA, Nabiev AN. An experimental study of the hepatoprotective properties of phytoecdysteroids and nerobol in carbon tetrachloride-induced liver lesion. Eksperimental'naia i klinicheskaia farmakologiia. 1992;55(3):61-5.

234.   Syrov VN, Khushbaktova ZA. The pharmacokinetics of phytoecdysteroids and nerobol on anaimals with experimental toxic renal damage. Eksperimentalnaya in Klinicheskaya Farmakologiya. 2001;64:56-8.

235.   Shakhmurova GA, Syrov VN, Khushbaktova ZA. Immunomodulating and antistress activity of ecdysterone and turkesterone under immobilization-induced stress conditions in mice. Pharmaceutical Chemistry Journal. 2010;44(1):7-9.

236.   Syrov VN, Shakhmurova GA, Khushbaktova ZA. Effects of phytoecdysteroids and bemithyl on functional, metabolic, and immunobiological parameters of working capacity in experimental animals. Eksperimental'naia i klinicheskaia farmakologiia. 2008;71(5):40-3.

237.   Lamia A, Habiba L, Amel A, Francisco L, Ignacio B, Samir B, et al. Isolation, Antioxidant and Antimicrobial Activities of Ecdysteroids from Serratula cichoracea. Current Bioactive Compounds. 2018;14(1):60-6.

238.   Ehrhardt C, Wessels JT, Wuttke W, Seidlová-Wuttke D. The effects of 20-hydroxyecdysone and 17ß-estradiol on the skin of ovariectomized rats. Menopause. 2011;18(3):323-7.

239.   Seidlova-Wuttke D, Ehrhardt C, Wuttke W. Metabolic effects of 20-OH-Ecdysone in ovariectomized rats. The Journal of Steroid Biochemistry and Molecular Biology. 2010;119(3):121-6.

240.   Detmar M, Dumas M, Bonte´ F, Meybeck A, Orfanos CE. Effects of ecdysterone on the differentiation of normal human keratinocytes in vitro. European journal of dermatology. 1994 (4):558-69.

241.   Hu J, Luo CX, Chu WH, Shan YA, Qian Z-M, Zhu G, et al. 20-Hydroxyecdysone Protects against Oxidative Stress-Induced Neuronal Injury by Scavenging Free Radicals and Modulating NF-κB and JNK Pathways. PLOS ONE. 2012;7(12):e50764.

242.   Ochi T, Motoyama Y, Goto T. The analgesic effect profile of FR122047, a selective cyclooxygenase-1 inhibitor, in chemical nociceptive models. Eur J Pharmacol. 2000 Mar 10;391(1-2):49-54.

243.   Liu B, Luo W, Zhang Y, Li H, Zhu N, Huang D, et al. Effect of celecoxib on cyclooxygenase-1-mediated prostacyclin synthesis and endothelium-dependent contraction in mouse arteries. European Journal of Pharmacology. 2013;698(1):354-61.

244.   Tang EHC, Ku DD, Tipoe GL, Feletou M, Man RYK, Vanhoutte PM. Endothelium-dependent contractions occur in the aorta of wild-type and COX2-/- knockout but not COX1-/- knockout mice. Journal of cardiovascular pharmacology. 2005;46(6):761-5.

245.   Nelson MT, Quayle JM. Physiological roles and properties of potassium channels in arterial smooth muscle. American Journal of Physiology-Cell Physiology. 1995;268(4):C799-C822.

246.   Tsukiyama Y, Iranami H, Kinoshita H, Ogawa K, Hatano Y. Effects of halothane and isoflurane on acetylcholine-induced, endothelium-dependent vasodilation in perfused rat mesenteric arterial beds. Journal of Anesthesia. 2003;17(1):13-21.

247.   Zhang HH, Feng L, Wang W, Magness RR, Chen DB. Estrogen-responsive nitroso-proteome in uterine artery endothelial cells: role of endothelial nitric oxide synthase and estrogen receptor-beta. J Cell Physiol. 2012 Jan;227(1):146-59.

248.   Zuloaga KL, O'Connor DT, Handa RJ, Gonzales RJ. Estrogen receptor beta dependent attenuation of cytokine-induced cyclooxygenase-2 by androgens in human brain vascular smooth muscle cells and rat mesenteric arteries. Steroids. 2012 Jul;77(8-9):835-44.

249.   Saleh MC, Connell BJ, Saleh TM. Resveratrol induced neuroprotection is mediated via both estrogen receptor subtypes, ERα and ERβ. Neuroscience Letters. 2013 2013/08/26/;548:217-21.

250.   Pastore MB, Talwar S, Conley MR, Magness RR. Identification of Differential ER-Alpha Versus ER-Beta Mediated Activation of eNOS in Ovine Uterine Artery Endothelial Cells. Biol Reprod. 2016 Jun;94(6):139.

251.   Bajla I, Holländer I, Minichmayr M, Gmeiner G, Reichel C. GASepo—a software solution for quantitative analysis of digital images in Epo doping control. Computer Methods and Programs in Biomedicine. 2005;80(3):246-70.

252.   Irizarry RA, Hobbs B, Collin F, Beazer-Barclay YD, Antonellis KJ, Scherf U, et al. Exploration, normalization, and summaries of high density oligonucleotide array probe level data. Biostatistics (Oxford, England). 2003;4(2):249-64.

253.   Bolstad BM, Irizarry RA, Astrand M, Speed TP. A comparison of normalization methods for high density oligonucleotide array data based on variance and bias. Bioinformatics (Oxford, England). 2003;19(2):185-93.

254.   Barash Y, Dehan E, Krupsky M, Franklin W, Geraci M, Friedman N, et al. Comparative analysis of algorithms for signal quantitation from oligonucleotide microarrays. Bioinformatics. 2004;20(6):839-46.

255.   Benjamini Y, Hochberg Y. Controlling the False Discovery Rate: A Practical and Powerful Approach to Multiple Testing. Journal of the Royal Statistical Society Series B (Methodological). 1995;57(1):289-300.

256.   Glickman ME, Rao SR, Schultz MR. False discovery rate control is a recommended alternative to Bonferroni-type adjustments in health studies. Journal of clinical epidemiology. 2014;67(8):850-7.

257.   Narumiya S, Sugimoto Y, Ushikubi F. Prostanoid Receptors: Structures, Properties, and Functions. Physiological Reviews. 1999;79(4):1193-226.

258.   Habib A, Vezza R, Créminon C, Maclouf J, FitzGerald GA. Rapid, Agonist-dependent Phosphorylation in Vivo of Human Thromboxane Receptor Isoforms: Minimal involvement of protein kinase C. Journal of Biological Chemistry. 1997;272(11):7191-200.

259.   Evett GE, Xie W, Chipman JG, Robertson DL, Simmons DL. Prostaglandin G/H synthase isoenzyme 2 expression in fibroblasts: regulation by dexamethasone, mitogens, and oncogenes. Archives of Biochemistry and Biophysics. 1993;306(1):169-77.

260.   Jones DA, Carlton DP, McIntyre TM, Zimmerman GA, Prescott SM. Molecular cloning of human prostaglandin endoperoxide synthase type II and demonstration of expression in response to cytokines. The Journal of biological chemistry. 1993;268(12):9049-54.

261.   O'Sullivan MG, Huggins EM, Meade EA, DeWitt DL, McCall CE. Lipopolysaccharide induces prostaglandin H synthase-2 in alveolar macrophages. 1992. p. 1123-7.

262.   Hla T, Neilson K. Human cyclooxygenase-2 cDNA. Proceedings of the National Academy of Sciences. 1992;89(16):7384-8.

263.   Masferrer JL, Zweifel BS, Seibert K, Needleman P. Selective regulation of cellular cyclooxygenase by dexamethasone and endotoxin in mice. The Journal of clinical investigation. 1990;86(4):1375-9.

264.   Niiro H, Otsuka T, Izuhara K, Yamaoka K, Ohshima K, Tanabe T, et al. Regulation by Interleukin-10 and Interleukin-4 of Cyclooxygenase-2 Expression in Human Neutrophils. Blood. 1997;89(5):1621-8.

265.   McAdam BF, Catella-Lawson F, Mardini IA, Kapoor S, Lawson JA, Fitzgerald GA. Systemic biosynthesis of prostacyclin by cyclooxygenase (COX)-2:

The human pharmacology of a selective inhibitor of COX-2. Proceedings of the National Academy of Sciences of the United States of America. 1999;96(1):272-7.

266.   Baber SR, Champion HC, Bivalacqua TJ, Hyman AL, Kadowitz PJ. Role of Cyclooxygenase-2 in the Generation of Vasoactive Prostanoids in the Rat Pulmonary and Systemic Vascular Beds. Circulation. 2003;108(7):896-901.

267.   Mitchell JA, Warner TD. COX isoforms in the cardiovascular system: understanding the activities of non-steroidal anti-inflammatory drugs. Nature Reviews Drug Discovery. 2006;5:75-86.

268.   Qi Z, Cai H, Morrow JD, Breyer MD. Differentiation of cyclooxygenase 1- and 2-derived prostanoids in mouse kidney and aorta. Hypertension. 2006;48(2):323-8.

269.   Luo W, Liu B, Zhou Y. The endothelial cyclooxygenase pathway: Insights from mouse arteries. European journal of pharmacology. 2016;780:148-58.

270.   Knoepp L, Beall A, Woodrum D, Mondy JS, Shaver E, Dickinson M, et al. Cellular stress inhibits vascular smooth muscle relaxation. Journal of Vascular Surgery. 2000;31(2):343-53.

271.   Larsen JK, Yamboliev IA, Weber LA, Gerthoffer WT. Phosphorylation of the 27-kDa heat shock protein via p38 MAP kinase and MAPKAP kinase in smooth muscle. American Journal of Physiology-Lung Cellular and Molecular Physiology. 1997;273(5):L930-L40.

272.   Tsatsanis C, Androulidaki A, Venihaki M, Margioris AN. Signalling networks regulating cyclooxygenase-2. The international journal of biochemistry & cell biology. 2006;38(10):1654-61.

273.   Blanco-Rivero J, Victoria C, Vicente L, Aras-Lopez R, Márquez-Rodas I, Mercedes S, et al. Participation of Prostacyclin in Endothelial Dysfunction Induced by Aldosterone in Normotensive and Hypertensive Rats. Hypertension. 2005;46(1):107-12.

274.   Chenevard R, Hurlimann D, Bechir M, Enseleit F, Spieker L, Hermann M, et al. Selective COX-2 Inhibition Improves Endothelial Function in Coronary Artery Disease. Circulation. 2003;107(3):405-9.

275.   Heymes C, Habib A, Yang D, Mathieu E, Marotte Fo, Samuel J, et al. Cyclo-oxygenase-1 and -2 contribution to endothelial dysfunction in ageing. British Journal of Pharmacology. 2000;131:804-10.

276.   Mittal N, Sanyal SN. Cycloxygenase Inhibition Enhances the Effects of Surfactant Therapy in Endotoxin-Induced Rat Model of ARDS. Inflammation. 2011;34(2):92-8.

277.   Virdis A, Colucci R, Versari D, Ghisu N, Fornai M, Antonioli L, et al. Atorvastatin prevents endothelial dysfunction in mesenteric arteries from spontaneously hypertensive rats: role of cyclooxygenase 2-derived contracting prostanoids. Hypertension (Dallas, Tex: 1979). 2009;53(6):1008-16.

278.   Verma S, Raj SR, Shewchuk L, Mather KJ, Anderson TJ. Cyclooxygenase-2 blockade does not impair endothelial vasodilator function in healthy volunteers: randomized evaluation of rofecoxib versus naproxen on endothelium-dependent vasodilatation. Circulation. 2001;104(24):2879-82.

279.   Kirkby NS, Lundberg MH, Harrington LS, Leadbeater PDM, Milne GL, Potter CMF, et al. Cyclooxygenase-1, not cyclooxygenase-2, is responsible for physiological production of prostacyclin in the cardiovascular system. Proceedings of the National Academy of Sciences. 2012;109(43):17597-602.

280.   Liu B, Li Z, Zhang Y, Luo W, Zhang J, Li H, et al. Vasomotor Reaction to Cyclooxygenase-1-Mediated Prostacyclin Synthesis in Carotid Arteries from Two-Kidney-One-Clip Hypertensive Mice. PLOS ONE. 2015;10(8):e0136738.
281.   Wang A, Nishihashi T, Murakami S, Trandafir CC, Ji X, Shimizu Y, et al. Noradrenaline-induced contraction mediated by endothelial COX-1 metabolites in the rat coronary artery. Journal of cardiovascular pharmacology. 2003;42 Suppl 1:S39-42.
282.   Catella-Lawson F, McAdam B, Morrison BW, Kapoor S, Kujubu D, Antes L, et al. Effects of Specific Inhibition of Cyclooxygenase-2 on Sodium Balance, Hemodynamics, and Vasoactive Eicosanoids. Journal of Pharmacology and Experimental Therapeutics. 1999;289(2):735-41.
283.   Hennan James K, Jinbao H, Barrett Terrance D, Driscoll Edward M, Willens David E, Park Andrew M, et al. Effects of Selective Cyclooxygenase-2 Inhibition on Vascular Responses and Thrombosis in Canine Coronary Arteries. Circulation. 2001;104(7):820-5.
284.   Sun D, Liu H, Yan C, Jacobson A, Ojaimi C, Huang A, et al. COX-2 contributes to the maintenance of flow-induced dilation in arterioles of eNOS-knockout mice. American journal of physiologyHeart and circulatory physiology. 2006;291(3):H1429-H35.
285.   Yingbi Z, Srabani M, Saradhadevi V, Narasimham P, Zweier Jay L, Flavahan Nicholas A. Increased Expression of Cyclooxygenase-2 Mediates Enhanced Contraction to Endothelin ETA Receptor Stimulation in Endothelial Nitric Oxide Synthase Knockout Mice. Circulation research. 2006;98(11):1439-45.
286.   Cheng Y, Wang M, Yu Y, Lawson J, Funk CD, Fitzgerald GA. Cyclooxygenases, microsomal prostaglandin E synthase-1, and cardiovascular function. The Journal of clinical investigation. 2006;116(5):1391-9.
287.   Ahmetaj-Shala B, Kirkby NS, Knowles R, Al'Yamani M, Mazi S, Wang Z, et al. Evidence that links loss of cyclooxygenase-2 with increased asymmetric dimethylarginine: novel explanation of cardiovascular side effects associated with anti-inflammatory drugs. Circulation. 2015;131(7):633-42.
288.   Feng J, Anderson K, Singh AK, Ehsan A, Mitchell H, Liu Y, et al. Diabetes Upregulation of Cyclooxygenase 2 Contributes to Altered Coronary Reactivity After Cardiac Surgery2017; 104(2):[568-76 pp.].
289.   Guo Z, Su W, Allen S, Pang H, Daugherty A, Smart E, et al. COX-2 up-regulation and vascular smooth muscle contractile hyperreactivity in spontaneous diabetic db/db mice. Cardiovascular research. 2005;67(4):723-35.
290.   Wong SL, Leung FP, Lau CW, Au CL, Yung LM, Xiaoqiang Y, et al. Cyclooxygenase-2–Derived Prostaglandin F2α Mediates Endothelium-Dependent Contractions in the Aortae of Hamsters With Increased Impact During Aging. Circulation research. 2009;104(2):228-35.
291.   Baber SR, Deng W, Rodriguez J, Master RG, Bivalacqua TJ, Hyman AL, et al. Vasoactive prostanoids are generated from arachidonic acid by COX-1 and COX-2 in the mouse. American Journal of Physiology-Heart and Circulatory Physiology. 2005;289(4):H1476-H87.
292.   Bolla M, You D, Loufrani L, Levy BI, Levy-Toledano S, Habib A, et al. Cyclooxygenase involvement in thromboxane-dependent contraction in rat mesenteric resistance arteries. Hypertension (Dallas, Tex: 1979). 2004;43(6):1264-9.
293.   Félétou M, Verbeuren TJ, Vanhoutte PM. Endothelium-dependent contractions in SHR: a tale of prostanoid TP and IP receptors. British journal of pharmacology. 2009;156(4):563-74.

294.	Kawada N, Dennehy K, Solis G, Modlinger P, Hamel R, Kawada JT, et al. TP receptors regulate renal hemodynamics during angiotensin II slow pressor response. American Journal of Physiology-Renal Physiology. 2004;287(4):F753-F9.

295.	Matsumoto T, Watanabe S, Kawamura R, Taguchi K, Kobayashi T. Enhanced uridine adenosine tetraphosphate-induced contraction in renal artery from type 2 diabetic Goto-Kakizaki rats due to activated cyclooxygenase/thromboxane receptor axis. Pflügers Archiv - European Journal of Physiology. 2014;466(2):331-42.

296.	Parente L, Perretti M. Advances in the pathophysiology of constitutive and inducible cyclooxygenases: two enzymes in the spotlight. Biochemical Pharmacology. 2003;65(2):153-9.

297.	Öst M, Uhl E, Carlsson M, Gidlöf A, Söderkvist P, Sirsjö A. Expression of mRNA for Phospholipase A2, Cyclooxygenases, and Lipoxygenases in Cultured Human Umbilical Vascular Endothelial and Smooth Muscle Cells and in Biopsies from Umbilical Arteries and Veins. Journal of vascular research. 1998;35(3):150-5.

298.	Bishop-Bailey D, Mitchell Jane A, Warner Timothy D. COX-2 in Cardiovascular Disease. Arteriosclerosis, Thrombosis, and Vascular Biology. 2006;26(5):956-8.

299.	Korkmaz S, Maupoil V, Sobry C, Brunet C, Chevalier S, Freslon J-L. An Increased Regional Blood Flow Precedes Mesenteric Inflammation in Rats Treated by a Phosphodiesterase 4 Inhibitor. Toxicological Sciences. 2008;107(1):298-305.

300.	Tatsuya U, Muneyoshi O, Yukio H, Hideyuki Y. Death-Associated Protein Kinase 3 Mediates Vascular Inflammation and Development of Hypertension in Spontaneously Hypertensive Rats. Hypertension. 2012;60(4):1031-9.

301.	Peyrin-Biroulet L, Gonzalez F, Dubuquoy L, Rousseaux C, Dubuquoy C, Decourcelle C, et al. Mesenteric fat as a source of C reactive protein and as a target for bacterial translocation in Crohn's disease. Gut. 2012;61(1):78-85.

302.	Boerman EM, Sen S, Shaw RL, Joshi T, Segal SS. Gene expression profiles of ion channels and receptors in mouse resistance arteries: Effects of cell type, vascular bed, and age. Microcirculation (New York, NY: 1994). 2018;25(4):e12452.

303.	Yajima N, Masuda M, Miyazaki M, Nakajima N, Chien S, Shyy JY. Oxidative stress is involved in the development of experimental abdominal aortic aneurysm: a study of the transcription profile with complementary DNA microarray. Journal of vascular surgery. 2002;36(2):379-85.

304.	Hiltunen MO, Tuomisto TT, Niemi M, Bräsen JH, Rissanen TT, Törönen P, et al. Changes in gene expression in atherosclerotic plaques analyzed using DNA array. Atherosclerosis. 2002;165(1):23-32.

305.	Chen BP, Li YS, Zhao Y, Chen KD, Li S, Lao J, et al. DNA microarray analysis of gene expression in endothelial cells in response to 24-h shear stress. Physiological Genomics. 2001;7(1):55-63.

306.	Neilsen PO, Zimmerman GA, McIntyre TM. Escherichia coli Braun Lipoprotein Induces a Lipopolysaccharide-Like Endotoxic Response from Primary Human Endothelial Cells. The Journal of Immunology. 2001;167(9):5231-9.

307.	Zhao B, Bowden RA, Stavchansky SA, Bowman PD. Human endothelial cell response to gram-negative lipopolysaccharide assessed with cDNA microarrays. American Journal of Physiology-Cell Physiology. 2001;281(5):C1587-C95.

308.	Brandes RP, Schmitz-Winnenthal F-H, Félétou M, Gödecke A, Huang PL, Vanhoutte PM, et al. An endothelium-derived hyperpolarizing factor distinct from NO and prostacyclin is a major endothelium-dependent vasodilator in resistance vessels of

wild-type and endothelial NO synthase knockout mice. Proceedings of the National Academy of Sciences. 2000;97(17):9747-52.

309.   Julian PJH, Narayanan S, Laura C-J, Mincemoyer R, Quyyumi AA. Characterization of endothelium-derived hyperpolarizing factor in the human forearm microcirculation. American Journal of Physiology-Heart and Circulatory Physiology. 2001;280(6):H2470-H7.

310.   Kosuke I, Yoshitaka H, Hiroaki S, Koji S, Takuya K, Koji I, et al. Role of Endothelium-Derived Hyperpolarizing Factor in Human Forearm Circulation. Hypertension. 2003;42(5):919-24.

311.   Schrage WG, Dietz NM, Eisenach JH, Joyner MJ. Agonist-dependent variablity of contributions of nitric oxide and prostaglandins in human skeletal muscle. Journal of applied physiology. 2005;98(4):1251-7.

312.   Wang D, Borrego-Conde L, Falck JR, Sharma KK, Wilcox CS, Umans JG. Contributions of nitric oxide, EDHF, and EETs to endothelium-dependent relaxation in renal afferent arterioles. Kidney international. 2003;63(6):2187-93.

313.   Hellsten Y, Nyberg M, Jensen LG, Mortensen SP. Vasodilator interactions in skeletal muscle blood flow regulation. The Journal of Physiology. 2012;590(24):6297-305.

314.   Laemmel E, Bonnardel-Phu E, Hou X, Seror J, Vicaut E. Interaction between nitric oxide and prostanoids in arterioles of rat cremaster muscle in vivo. American Journal of Physiology-Heart and Circulatory Physiology. 2003;285(3):H1254-H60.

315.   Osanai T, Fujita N, Fujiwara N, Nakano T, Takahashi K, Guan W, et al. Cross talk of shear-induced production of prostacyclin and nitric oxide in endothelial cells. American Journal of Physiology-Heart and Circulatory Physiology. 2000;278(1):H233-H8.

316.   Boushel R, Langberg H, Gemmer C, Olesen J, Crameri R, Scheede C, et al. Combined inhibition of nitric oxide and prostaglandins reduces human skeletal muscle blood flow during exercise. The Journal of physiology. 2002;543:691-8.

317.   Förstermann U, Hertting G, Neufang B. The role of endothelial and non-endothelial prostaglandins in the relaxation of isolated blood vessels of the rabbit induced by acetylcholine and bradykinin. British journal of pharmacology. 1986;87(3):521-32.

318.   Gambone LM, Murray PA, Flavahan NA. Synergistic interaction between endothelium-derived NO and prostacyclin in pulmonary artery: potential role for K+ATP channels. British journal of pharmacology. 1997;121(2):271-9.

319.   Peredo HA, Feleder EC, Adler-Graschinsky E. Differential effects of acetylcholine and bradykinin on prostanoid release from the rat mesenteric bed: role of endothelium and of nitric oxide. Prostaglandins, leukotrienes, and essential fatty acids. 1997;56(4):253-8.

320.   Wirth KJ, Linz W, Wiemer G, Scholkens BA. Differences in acetylcholine- and bradykinin-induced vasorelaxation of the mesenteric vascular bed in spontaneously hypertensive rats of different ages. Naunyn-Schmiedeberg's archives of pharmacology. 1996;354(1):38-43.

321.   Tesfamariam B, Brown ML, Cohen RA. 15-Hydroxyeicosatetraenoic acid and diabetic endothelial dysfunction in rabbit aorta. Journal of cardiovascular pharmacology. 1995;25(5):748-55.

322.   Virdis A, Colucci R, Bernardini N, Blandizzi C, Taddei S, Masi S. Microvascular endothelial dysfunction in human obesity: role of TNF-alpha. The Journal of clinical endocrinology and metabolism. 2018;104(2):341-8.

323.   Doroudi R, Gan L-m, Selin Sj╟gren L, Jern S. Effects of Shear Stress on Eicosanoid Gene Expression and Metabolite Production in Vascular Endothelium as Studied in a Novel Biomechanical Perfusion Model. Biochemical and Biophysical Research Communications. 2000;269:257-64.

324.   Morita I. Distinct functions of COX-1 and COX-2. Prostaglandins & Other Lipid Mediators. 2002;68ΓÇô69:165-75.

325.   Morteau O, Morham SG, Sellon R, Dieleman LA, Langenbach R, Smithies O, et al. Impaired mucosal defense to acute colonic injury in mice lacking cyclooxygenase-1 or cyclooxygenase-2. The Journal of clinical investigation. 2000;105(4):469-78.

326.   Jaimes EA, Ming-Sheng Z, Pearse DD, Puzis L, Raij L. Upregulation of cortical COX-2 in salt-sensitive hypertension: role of angiotensin II and reactive oxygen species. American Journal of Physiology-Renal Physiology. 2008;294(2):F385-F92.

327.   Wong WT, Tian XY, Chen Y, Leung FP, Liu L, Lee HK, et al. Bone morphogenic protein-4 impairs endothelial function through oxidative stress-dependent cyclooxygenase-2 upregulation: implications on hypertension. Circulation research. 2010;107(8):984-91.

328.   Vessières E, Guihot AL, Bertrand T, Maud M, Fassot C, Laurent L, et al. COX-2-derived prostanoids and oxidative stress additionally reduce endothelium-mediated relaxation in old type 2 diabetic rats. PLoS ONE. 2013;8(7):e68217.

329.   Chan P-C, Wu T-N, Chen Y-C, Lu C-H, Wabitsch M, Tian Y-F, et al. Targeted inhibition of CD74 attenuates adipose COX-2-MIF-mediated M1 macrophage polarization and retards obesity-related adipose tissue inflammation and insulin resistance. Clin Sci. 2018;132(14):1581-96.

330.   Xu L, Miyoshi H, Nishimura K, Jisaka M, Nagaya T, Yokota K. Gene expression of isoformic enzymes in arachidonate cyclooxygenase pathway and the regulation by tumor necrosis factor α during life cycle of adipocytes. Proceedings of the International Eicosanoids Conference. 2007;83(3):213-8.

331.   Bakhamis A. Investigation of effect of hyperinsulinaemia on adipose tissue microvasculature / Aysha Bakhamis 2015.

332.   Farb MG, Ganley-Leal L, Mott M, Liang Y, Ercan B, Widlansky ME, et al. Arteriolar Function in Visceral Adipose Tissue Is Impaired in Human Obesity. Arteriosclerosis, Thrombosis, and Vascular Biology. 2012;32(2):467-73.

333.   Tang EHC, Vanhoutte PM. Gene expression changes of prostanoid synthases in endothelial cells and prostanoid receptors in vascular smooth muscle cells caused by aging and hypertension. Physiological Genomics. 2008;32(3):409-18.

334.   Vanhoutte PM. COX-1 and Vascular Disease. Clinical Pharmacology & Therapeutics. 2009;86(2):212-5.

335.   Zhu N, Liu B, Luo W, Zhang Y, Li H, Li S, et al. Vasoconstrictor role of cyclooxygenase-1-mediated prostacyclin synthesis in non-insulin-dependent diabetic mice induced by high-fat diet and streptozotocin. American Journal of Physiology. 2014;307(3):H319-H27.

336.   Michel F, Simonet S, Vayssettes-Courchay C, Bertin F, Sansilvestri-Morel P, Bernhardt F, et al. Altered TP receptor function in isolated, perfused kidneys of nondiabetic and diabetic ApoE-deficient mice. American journal of physiologyRenal physiology. 2008;294(1):F120-9.

337. Traupe T, Lang M, Goettsch W, Münter K, Morawietz H, Vetter W, et al. Obesity increases prostanoid-mediated vasoconstriction and vascular thromboxane receptor gene expression. Journal of hypertension. 2002;20(11):2239-45.

338. Leal Marcos aS, Dias Ananda t, Porto Marcella l, Brun Bruna f, Gava Agata l, Meyrelles Silvana s, et al. Sildenafil (Viagra®) Prevents Cox-1/ TXA2 Pathway-Mediated Vascular Hypercontractility in ApoE-/- Mice. Cellular Physiology and Biochemistry. 2018;44(5):1796-809.

339. Sellers MM, Stallone J. Sympathy for the devil: the role of thromboxane in the regulation of vascular tone and blood pressure. American Journal Of Physiology-Heart And Circulatory Physiology; AmJPhysiol-Heart CirculPhysiol. 2008;294(5):H1978-H86.

340. Hata AN, Breyer RM. Pharmacology and signaling of prostaglandin receptors: Multiple roles in inflammation and immune modulation. Pharmacology and Therapeutics. 2004;103(2):147-66.

341. Montague C, O'Rahilly S. The perils of portliness causes and consequences of visceral adiposity. Diabetes. 2000;49(6):883-8.

342. Fontana L, Eagon J, Trujillo M, Scherer P, Klein S. Visceral Fat Adipokine Secretion Is Associated With Systemic Inflammation in Obese Humans. Diabetes. 2007;56(4):1010-3.

343. Hotamisligil GS, Arner P, Caro JF, Atkinson RL, Spiegelman BM. Increased adipose tissue expression of tumor necrosis factor-alpha in human obesity and insulin resistance. The Journal of clinical investigation. 1995;95(5):2409-15.

344. Yan KG, You KB, Chen KS, Liao KJ, Sun KJ. Tumor Necrosis Factor-α Downregulates Endothelial Nitric Oxide Synthase mRNA Stability via Translation Elongation Factor 1-α 1. Circulation research. 2008;103(6):591-7.

345. Park Y, Capobianco S, Gao X, Falck JR, Dellsperger KC, Zhang C. Role of EDHF in type 2 diabetes-induced endothelial dysfunction. American journal of physiologyHeart and circulatory physiology. 2008;295(5):H1982-H8.

346. Watanabe S, Mu W, Kahn A, Jing N, Li JH, Lan HY, et al. Role of JAK/STAT Pathway in IL-6-Induced Activation of Vascular Smooth Muscle Cells. American journal of nephrology. 2004;24(4):387-92.

347. Isenmann E, Ambrosio G, Joseph JF, Mazzarino M, de la Torre X, Zimmer P, et al. Ecdysteroids as non-conventional anabolic agent: performance enhancement by ecdysterone supplementation in humans. Archives of Toxicology. 2019;93(7):1807-16.

348. World anti-doping a. Monitoring program. 2020.

349. Fallon AM, Gerenday A. Ecdysone and the cell cycle: Investigations in a mosquito cell line. Insect Molecular Physiology - Basic Science to Applications A Special Issue in Honour of Dr Judith H Willis. 2010;56(10):1396-401.

350. Iga M, Sakurai S. Genomic and Nongenomic Actions of 20-Hydroxyecdysone in Programmed Cell Death. In: Smagghe G, editor. Ecdysone: Structures and Functions. Dordrecht: Springer Netherlands; 2009. p. 411-23.

351. Gao L, Cai G, Shi X. Beta-Ecdysterone Induces Osteogenic Differentiation in Mouse Mesenchymal Stem Cells and Relieves Osteoporosis. Biological and Pharmaceutical Bulletin. 2008;31(12):2245-9.

352. Manaboon M, Masatoshi I, Sakurai S. Nongenomic and genomic actions of an insect steroid coordinately regulate programmed cell death of anterior silk glands of Bombyx mori. Invertebr Surviv J. 2008;5(1):1-22.

353.   Schlattner U, Vafopoulou X, Steel CGH, Hormann RE, Lezzi M. Non-genomic ecdysone effects and the invertebrate nuclear steroid hormone receptor EcR—new role for an "old" receptor? Molecular and Cellular Endocrinology. 2006;247(1):64-72.

354.   Srivastava DP, Yu EJ, Kennedy K, Chatwin H, Reale V, Hamon M, et al. Rapid, Nongenomic Responses to Ecdysteroids and Catecholamines Mediated by a Novel Drosophila G-Protein-Coupled Receptor. The Journal of Neuroscience. 2005;25(26):6145-55.

355.   Vafopoulou X, Steel CGH. Cytoplasmic Travels of the Ecdysteroid Receptor in Target Cells: Pathways for Both Genomic and Non-Genomic Actions. Frontiers in Endocrinology. 2012;3:43.

356.   Zhang K-l, Qi M-x, Huang X-r, Guo N. Effect of ecdysterone on the expression of estrogen receptor in oxidative stress-induced human lens epithelial cells. Chin J Ophthalmol and Otorhinolaryngol. 2013;13(1):14.

357.   Hermenegildo C, Oviedo PJ, Cano A. Cyclooxygenases regulation by estradiol on endothelium. Current pharmaceutical design. 2006;12(2):205-15.

358.   Jun SS, Chen Z, Pace MC, Shaul PW. Estrogen upregulates cyclooxygenase-1 gene expression in ovine fetal pulmonary artery endothelium. The Journal of clinical investigation. 1998;102(1):176-83.

359.   Sherman T, Chambliss K, Gibson L, Pace M. Estrogen acutely activates prostacyclin synthesis in ovine fetal pulmonary artery endothelium. American Journal of Respiratory Cell and Molecular Biology. 2002;26(5):610-6.

360.   Álvarez CÁ, Hermenegildo VC, Issekutz VA, Esplugues VJ, Sanz VM. Estrogens Inhibit Angiotensin II–Induced Leukocyte–Endothelial Cell Interactions In Vivo via Rapid Endothelial Nitric Oxide Synthase and Cyclooxygenase Activation. Circulation Research: Journal of the American Heart Association. 2002;91(12):1142-50.

361.   Pastore MB, Talwar S, Conley MR, Magness RR. Identification of Differential ER-Alpha Versus ER-Beta Mediated Activation of eNOS in Ovine Uterine Artery Endothelial Cells. Biology of reproduction. 2016;94(6):139.

362.   Montgomery S, Shaw L, Pantelides N, Taggart M, Austin C. Acute effects of oestrogen receptor subtype-specific agonists on vascular contractility. British journal of pharmacology. 2003;139(7):1249-53.

363.   Zhu Y, Bian Z, Lu P, Karas RH, Bao L, Cox D, et al. Abnormal Vascular Function and Hypertension in Mice Deficient in Estrogen Receptor β. Science. 2002;295(5554):505-8.

364.   Kim S, Hamblin M. Estrogen Receptor-Alpha Activation of AMPK in Vascular Smooth Muscle Cells and Vascular Tone. The FASEB Journal. 2015;29(1):1052.9.

365.   Kim SC, Boese AC, Moore MH, Cleland RM, Chang L, Delafontaine P, et al. Rapid estrogen receptor-alpha signaling mediated by ERK activation regulates vascular tone in male and ovary-intact female mice. American journal of physiologyHeart and circulatory physiology. 2018;314(2):H330-H42.

366.   Oviedo PJ, Hermenegildo C, Tarín JJ, Cano A. Raloxifene promotes prostacyclin release in human endothelial cells through a mechanism that involves cyclooxygenase-1 and -2. Fertility and Sterility. 2005;83(6):1822-9.

367.   Lantin-Hermoso RL, Rosenfeld CR, Yuhanna IS, German Z, Chen Z, Shaul PW. Estrogen acutely stimulates nitric oxide synthase activity in fetal pulmonary

artery endothelium. American Journal of Physiology - Lung Cellular and Molecular Physiology. 1997;273(1):L119-L26.

368.   Omanakuttan A, Bose C, Pandurangan N, Kumar GB, Banerji A, Nair BG. Nitric Oxide and ERK mediates regulation of cellular processes by Ecdysterone. Experimental Cell Research. 2016;346(2):167-75.

369.   Liu W, Cai M-J, Wang J-X, Zhao X-F. In a Nongenomic Action, Steroid Hormone 20-Hydroxyecdysone Induces Phosphorylation of Cyclin-Dependent Kinase 10 to Promote Gene Transcription. Endocrinology. 2014;155(5):1738-50.

370.   Wehling M, Neylon CB, Fullerton M, Bobik A, Funder JW. Nongenomic effects of aldosterone on intracellular Ca2+ in vascular smooth muscle cells. Circ Res. 1995 Jun;76(6):973-9.

371.   Deng Q, Zhang Z, Wu Y, Yu W, Zhang J, Jiang Z, et al. Non-Genomic Action of Androgens is Mediated by Rapid Phosphorylation and Regulation of Androgen Receptor Trafficking. Cellular Physiology and Biochemistry. 2017;43(1):223-36.

372.   Slama K, Lafont R. Insect hormones - ecdysteroids: their presence and actions in vertebrates. EJE. 1995;92(1):355-77.

373.   Gustafsson JÃ. Novel aspects of estrogen action. Journal of the Society for Gynecologic Investigation. 2000;7(1):S8-S9.

374.   Sprague AH, Khalil RA. Inflammatory cytokines in vascular dysfunction and vascular disease. Biochemical pharmacology. 2009;78(6):539-52.

375.   Delp MD, O'Leary DS. Integrative control of the skeletal muscle microcirculation in the maintenance of arterial pressure during exercise. Journal of applied physiology. 2004;97(3):1112-8.

376.   Hayashi M, Kajioka S, Itsumi M, Takahashi R, Shahab N, Ishigami T, et al. Actions of cAMP on calcium sensitization in human detrusor smooth muscle contraction. BJU International. 2016;117(1):179-91.

377.   Raeymaekers L, Eggermont JA, Wuytack F, Casteels R. Effects of cyclic nucleotide dependent protein kinases on the endoplasmic reticulum Ca2+ pump of bovine pulmonary artery. Cell Calcium. 1990 1990/04/01/;11(4):261-8.

378.   Mundiña-Weilenmann C, Vittone L, Rinaldi G, Said M, Cingolani GCd, Mattiazzi A. Endoplasmic reticulum contribution to the relaxant effect of cGMP- and cAMP-elevating agents in feline aorta. American Journal of Physiology-Heart and Circulatory Physiology. 2000;278(6):H1856-H65.

379.   Robertson BE, Schubert R, Hescheler J, Nelson MT. cGMP-dependent protein kinase activates Ca-activated K channels in cerebral artery smooth muscle cells. American Journal of Physiology-Cell Physiology. 1993;265(1):C299-C303.

380.   Xin W, Li N, Cheng Q, Petkov GV. BK Channel-Mediated Relaxation of Urinary Bladder Smooth Muscle: A Novel Paradigm for Phosphodiesterase Type 4 Regulation of Bladder Function. Journal of Pharmacology and Experimental Therapeutics. 2014;349(1):56-65.

381.   Conti MA, Adelstein RS. The relationship between calmodulin binding and phosphorylation of smooth muscle myosin kinase by the catalytic subunit of 3':5' cAMP-dependent protein kinase. The Journal of biological chemistry. 1981 Apr 10;256(7):3178-81.

382.   Rembold CM. Regulation of contraction and relaxation in arterial smooth muscle. Hypertension. 1992;20(2):129-37.

383.   Alvarez de Sotomayor M, Mingorance C, Andriantsitohaina R. Fenofibrate improves age-related endothelial dysfunction in rat resistance arteries. Atherosclerosis. 2007 2007/07/01/;193(1):112-20.

384.   Ellinsworth DC, Shukla N, Fleming I, Jeremy JY. Interactions between thromboxane A2, thromboxane/prostaglandin (TP) receptors, and endothelium-derived hyperpolarization. Cardiovascular Research. 2014;102(1):9-16.

385.   Lee MR, Li L, Kitazawa T. Cyclic GMP Causes Ca2+ Desensitization in Vascular Smooth Muscle by Activating the Myosin Light Chain Phosphatase. Journal of Biological Chemistry. 1997 February 21, 1997;272(8):5063-8.

386.   Momotani K, Artamonov MV, Utepbergenov D, Derewenda U, Derewenda ZS, Somlyo AV. p63RhoGEF Couples Gαq/11-mediated Signaling to Ca2+ Sensitization of Vascular Smooth Muscle Contractility. Circulation Research. 2011;109(9):993-1002.

387.   Grann M, Comerma-Steffensen S, Arcanjo DDR, Simonsen U. Mechanisms Involved in Thromboxane A2-induced Vasoconstriction of Rat Intracavernous Small Penile Arteries. Basic & Clinical Pharmacology & Toxicology. 2016;119(S3):86-95.

388.   Hoffman L, Jensen CC, Yoshigi M, Beckerle M. Mechanical signals activate p38 MAPK pathway-dependent reinforcement of actin via mechanosensitive HspB1. Mol Biol Cell. 2017;28(20):2661-75.

389.   Lasa M, Mahtani KR, Finch A, Brewer G, Saklatvala J, Clark AR. Regulation of cyclooxygenase 2 mRNA stability by the mitogen-activated protein kinase p38 signaling cascade. Molecular and cellular biology. 2000;20(12):4265-74.

390.   Winzen R, Kracht M, Ritter B, Wilhelm A, Chen CY, Shyu AB, et al. The p38 MAP kinase pathway signals for cytokine-induced mRNA stabilization via MAP kinase-activated protein kinase 2 and an AU-rich region-targeted mechanism. The EMBO journal. 1999;18(18):4969-80.

391.   Rösch S, Ramer R, Brune K, Hinz B. Prostaglandin E2 induces cyclooxygenase-2 expression in human non-pigmented ciliary epithelial cells through activation of p38 and p42/44 mitogen-activated protein kinases. 2005. p. 1171-8.

392.   Barone R, Aiello C, Race V, Morava E, Foulquier F, Riemersma M, et al. DPM2-CDG: A muscular dystrophy–dystroglycanopathy syndrome with severe epilepsy. Annals of Neurology. 2012;72(4):550-8.

393.   Jin W-J, Chen C-F, Liao H-Y, Gong L-L, Yuan X-H, Zhao B-B, et al. Downregulation of the AU-Rich RNA-Binding Protein ZFP36 in Chronic HBV Patients: Implications for Anti-Inflammatory Therapy. PLOS ONE. 2012;7(3):e33356.

394.   Watanabe R, Murakami Y, Marmor MD, Inoue N, Maeda Y, Hino J, et al. Initial enzyme for glycosylphosphatidylinositol biosynthesis requires PIG-P and is regulated by DPM2. The EMBO journal. 2000;19(16):4402-11.

395.   Pisapia L, Hamilton RS, Farina F, D'Agostino V, Barba P, Strazzullo M, et al. Tristetraprolin/ZFP36 regulates the turnover of autoimmune-associated HLA-DQ mRNAs. bioRxiv. 2019:337907.

396.   Hashimoto M, Close LA, Ishida Y, Paul RJ. Dependence of endothelium-mediated relaxation on oxygen and metabolism in porcine coronary arteries. American Journal of Physiology-Heart and Circulatory Physiology. 1993;265(1):H299-H306.

397.   Stockand JD, Sansom SC. Mechanism of activation by cGMP-dependent protein kinase of large Ca(2+)-activated K+ channels in mesangial cells. American Journal of Physiology-Cell Physiology. 1996;271(5):C1669-C77.

398.   Yoshida Y, Sun HT, Cai JQ, Imai S. Cyclic GMP-dependent protein kinase stimulates the plasma membrane Ca2+ pump ATPase of vascular smooth muscle via

phosphorylation of a 240-kDa protein. The Journal of biological chemistry. 1991 Oct 15;266(29):19819-25.

Appendix

Appendix 1: Patient consent form

1. Title of research	1. عنوان البحث
Role of fat stem cells in the development of insulin resistance The role of preadipocyte differentiation in site-specific adipocyte dysfunction and development of obesity-induced insulin resistance	دور تمايز الخلايا الدهنية الجذعية في الاختلال الوظيفي للانسولين دور تمايز الخلايا الدهنية الجذعية في اختلالها الوظيفي والتسبب في الاختلال الوظيفي للانسولين المرافق للسمنة المفرطة
2. Principal Investigator	2. الباحث الرئيسي
Dr Moataz Bashah, HMC Dr Mohamed Elrayess, Anti-Doping Lab Qatar	د. معتز باشا (مؤسسة حمد الطبية) د. محمد الريس (مختبر مكافحة المنشطات-قطر)
3. Why are we inviting you to join this research?	3. لماذا ندعوك للإنضمام إلى هذا البحث؟
The investigator and colleagues at Hamad Medical Corporation (HMC) and AntiDoping Lab Qatar are conducting this research. We are inviting you to join because you are over 18 and below 65 years old and are going to have weight reduction surgery and we would like to collect blood sample and fat tissue during this procedure to study the role of fat stem cells in the development of insulin resistance	الباحث وزملائه في مؤسسة حمد الطبية ومختبر مكافحة المنشطات-قطر ينوون اجراء هذا البحث. أنت مدعو/ة للمشاركة لأنك فوق 18 سنة وتحت 65 سنة وكونك ستخضع لجراحة تخفيف الوزن ونحن نرغب بالحصول على عينة دم و نسيج دهني أثناء هذه الجراحة لدراسة دور تمايز الخلايا الدهنية الجذعية في الاختلال الوظيفي للانسولين.
4. What should you know about the invitation?	4. ما الذي يجب أن تعرفه عن هذا البحث؟
• We will explain the research to you • Whether or not you join is your decision (you can accept or refuse no matter who is inviting you to participate)	• سنقوم بشرح البحث لك بشكل وافٍ • قرار انضمامك للمشاركة بهذا البحث أو عدمه يعود لك (يمكنم قبول أو رفض المشاركة بغض النظر عن من يدعوك للمشاركة)

English	العربية
• You are free to ask any questions you want before deciding • You can say yes but change your mind later • We will not hold your decision against you • Please ask questions or mention concerns before, during or after the research	• لك مطلق الحرية بأن تسأل أي سؤال قبل اتخاذ قرارك • إذا وافقت على المشاركة, بإمكانك أن تغير رأيك لاحقاً وبأي وقت • لن يستخدم قرارك ضدك بأي حال من الأحوال • لطفاً, اطرح أية أسئلة أو مخاوف قبل, خلال, أو بعد البحث
5. Who can you talk to?	**5. مع من يمكنك التحدث؟**
If you have questions or concerns, or if you think the research has hurt you, talk to Dr Moataz Bashah Office number: 44396795 Bleep number: 44346111 If you have questions about your rights as a volunteer, or you want to talk to someone outside the research team, please contact: HMC Medical Research Centre at 44392440 or research@hmc.org.qa	لطرح أية أسئلة أو مناقشة أي مخاوف, أو إذا كنت تعتقد أن البحث قد أضر/يضر بك, قم بالتحدث مع الدكتور معتز باشا رقم المكتب: 44396795 رقم جهاز الإخطار: 44346111 إذا كان لديك أسئلة حول حقوقك كمشارك بالبحث، أو كنت ترغب في التحدث مع شخص من خارج فريق البحث، يرجى الإتصال ب: مركز الأبحاث, مؤسسة حمد الطبية تلفون: 44392440 أو إيميل: research@hmc.org.qa
6. Why are we doing the research?	**6. لماذا نقوم بهذا البحث؟**
Obesity is associated with diseases such as type 2 diabetes and coronary artery disease. However not all obese people develop these problems. This may be due to different functions of fat tissue. In this project, we want to assess if stem cells from fat cells can regenerate differently among various obese patients and how this is related to the development of pre-diabetes insulin resistance. We believe that stem cells that can regenerate can protect people from the complications of obesity. We want to understand these mechanisms better and develop better therapies for obesity associated diseases in the future.	هناك ترابط وثيق بين السمنة وبعض الامراض المزمنة كمرض السكري من النوع الثاني وأمراض القلب. إلا ان الزيادة المفرطة في الوزن لا تودي دائماً الى هذه المضاعفات. قد يرجع هذا الإختلاف إلى تباين وظائف الانسجة الدهنية بين الافراد. في هذا المشروع نود أن نقيّم ما إذا كانت قدرة الخلايا الجذعية المستخلصة من الخلايا الدهنية على التجديد مختلفة بين مرضى السمنة المفرطة، وكيف يمكن أن يتطور هذا الإختلاف إلى اختلاف القابلية للإصابة بمرض السكري من النوع الثاني. نعتقد أنه بإمكان الخلايا الجذعية المتجددة أن تحمي الناس من مضاعفات السمنة وأن دراسة آليات هذه الظاهرة من شأنها ان تساعدنا على تطوير علاجات أفضل للبدانة والأمراض المرتبطة بها في المستقبل.
7. How long will the research take?	**7. كم من الوقت سيستغرق هذا البحث؟**
We think that you will be in the research for 12 months	نعتقد أنك ستكون في الدراسة مدة 12 شهراً.

English	Arabic
We expect the research to last for 3 years	نتوقع أن يستمر البحث مدة ثلاث سنوات.
8. How many people will take part?	**8. كم عدد الأشخاص الذين سيشاركون بهذا البحث؟**
We plan to stud around 120 people distributed among HMC and other hospitals.	نحن نخطط لدراسة حوالي 120 شخصاً موزعين بين مرضى مؤسسة حمد الطبية ومستشفيات أخرى.
9. What happens if you take part?	**9. ما الذي سيحدث اذا قررت الاشتراك بهذا البحث؟**
If you agree to join, we will ask you to do the following: First appointment: You will be asked to attend your pre-assessment appointment "fasting" which means that we shall ask you to take nothing by mouth from midnight. We shall take a blood sample by inserting a small needle, called a "butterfly needle" into a vein. We shall measure your blood pressure, height, weight, and circumference. The research team may ask you some questions about your general health and lifestyle, this will take about 30 minutes. We shall ask you whether you would be willing to take other **OPTIONAL** tests including: 1. Glucose tolerance test (2.30 hours) that involves taking a sweet drink to determine how quickly it is cleared from the blood. If you agree to this you will be given a glucose drink and two more blood samples will be taken from the butterfly needle after 45 minutes and two hours, so that there is only one needle prick. 2. Determine body bone density and fat composition by DEXA scanning (30 minutes). This includes lying down on an examining table, and the scanner rapidly directing low does x-ray on your body.	اذا وافقت على المشاركة, سنطلب منك القيام بما يلي: **الموعد الأول:** سوف يطلب منك حضور موعدك الأول صائماً مما يعني امتناعك عن الطعام والشراب اعتباراً من منتصف الليل السابقة. سيتم أخذ عينة دم بواسطة ادخال ابرة صغيرة تسمى "إبرة الفراشة" في الوريد. سيتم أيضاً قياس ضغط الدم، الطول، الوزن، محيط الخصر، بالإضافة إلى بعض الأسئلة حول الصحة العامة وأسلوب حياتك. وقد يقوم فريق البحث بمراجعة سجلاتك الصحية للتحقق من بعض التفاصيل ذات العلاقة بالبحث. (سيستغرق حوالي 30 دقيقة). وستسأل إذا كنت على استعداد للخضوع لاختبارات إضافية **اختيارية** تتضمن التالي: 1. إختبار تحمل الغلوكوز (ساعتان ونصف) الذي يتضمن إعطاءك شراب سكري وتحديد سرعة تصفيته من الدم. في حال موافقتك على هذا سوف تعطى شراب الجلوكوز و تؤخذ عينتين دم أخريين بواسطة نفس إبرة الفراشة (حتى لا يكون هناك أكثر من وخز واحد للإبرة) بعد 45 دقيقة وساعتين. 2. تحديد نسبة الدهون وكثافة العظام في الجسم عن طريق جهاز DEXA (30 دقيقة). ويشمل مسح DEXA الاستلقاء على طاولة فحص، والماسح الضوئي السريع بتوج يه جرعات منخفضة من الأشعة السينية على جسمك **الموعد الثاني:**

Second appointment:
 	
You will next be seen at the time of your operation and will involve the following:
 	
  1. Before the operation a blood sample will be taken from the lines the anesthetist inserts in your arm. (5 minutes)
 	
  2. During the main procedure two fat samples (1 to 4 gm. each) will be taken; one from the fat tissue immediately under the skin of the abdomen and one from a site deeper in the abdominal cavity from some tissue called "omental fat". You will not feel anything while obtaining these samples as you will be under anesthetic. (this will add 15 extra minutes to your surgery)
 	
Third, fourth and fifth appointments (<u>OPTIONAL</u>):
 	
After your surgery, we shall ask to see you again at three, six and twelve months after the operation when you attend for follow-up in outpatients. We should like to conduct the same tests as at your first visit, including the glucose tolerance test and DEXA.
	سيكون الموعد الثاني وقت العملية الخاصة بك وسيتضمن التالي:
	
	1. قبل العملية سوف يتم أخذ عينة دم من نفس انبوب التخدير في ذراعك. (5 دقائق)
	
	2. أثناء العملية سيتم أخذ عينتين من الدهون (1-4 جرام لكل منهما)؛ واحد من الأنسجة الدهنية تحت الجلد مباشرة من البطن وآخر من موقع أعمق في تجويف البطن من بعض الأنسجة المسماة ب "الدهون الثربية". لن تشعر مطلقاً باخذ هذه العينات حيث ستكون تحت تأثير المخدر. (وهذا سيضيف 15 دقيقة إضافية إلى الجراحة)
	
	الموعد الثالث والرابع والخامس (<u>اختياري</u>):
	
	نود مقابلتك بعد الجراحة خلال ثلاثة ، ستة واثني عشر شهراً عند حضورك للمتابعة في العيادات الخارجية لإجراء نفس الاختبارات كما في زيارتك الأولى، بما في ذلك اختبار تحمل الجلوكوز وتحديد نسبة الدهون عن طريق جهاز DEXA.

10. Could the research be bad for you?	**10. هل يمكن لهذا البحث أن يضرك؟**
Blood withdraws may cause bruising. To avoid such risk from happening, specialists will perform blood withdrawal. Additional risks from obtaining extra tissues during the surgery have not been reported in other similar studies. Although the DEXA involves radiation, it is so low that the Radiographer can safely stay in the room with you. The side effects of sugar drink consumed for the OGTT include headache, dizziness,	قد يسبب سحب الدم رضوض على الساعد. لتجنب هذا الإحتمال, سيقوم مختصون بسحب عينات الدم. لم يتم الإبلاغ عن مخاطر اضافية نتيجة الحصول على أنسجة إضافية خلال عملية جراحية في دراسات أخرى مماثلة. DEXA ينطوي على إشعاع منخفض للغاية بحيث يمكن لفني الأشعة أن يبقى بأمان في الغرفة معك. قد تشمل الأعراض الجانبية للمحلول السكري الذي يتم تناوله في إختبار تحمل الغلوكوز الشعور بالصداع أو الدوار أو الغثيان أو الشعور بالانتفاخ أو انتفاخ البطن أو الإسهال. ويصاب شخص واحد فقط من بين عشرة أشخاص بصداع خفيف ودوار أو غثيان.

English	Arabic
nausea, bloating, flatulence, or diarrhoea. Mild headache, dizziness and/or nausea may occur during the test in only about 1 in 10 people.	

11. Could the research be good for you?	11. هل يمكن لهذا البحث أن يفيدك؟
We cannot promise any benefit to you from you joining this research. However, possible benefits include a comprehensive health check especially geared towards checking for diabetes and its risk factors. The information and encouragement given during the course of this study to participants could be viewed as sound dietary and healthy lifestyle advice.	لا يمكننا أن نعدك بفائدة مباشرة جرّاء انضمامكم لهذا البحث. ومع ذلك، ممكن أن يتضمن انضمامكم الفوائد المحتملة التالية: فحص صحي شامل لاسيما قابلية الإصابة بالسكري ومايترتب عليه من أمراض أخرى كما أن المعلومات التي ستعطى للمشاركين ستفيد كنصائح لأسلوب حياة اكثر صحة.

12. What happens to information about you?	12. ما الذي سيحدث للمعلومات عنك؟
We will make efforts to secure information about you. This includes using a code to identify you in our records instead of using your name. We will not identify you personally in any reports or publications about this research.

We cannot guarantee complete secrecy, but we will limit access to information about you. Only people who have a need to review information will have access. These people might include:
  • members of the research team and other HMC and Anti-Doping Lab staff whose work is related to the research.
  • Representatives of the Qatar Supreme Council of Health and Qatar National Fund, who make sure the study is done properly and that your rights and safety are protected
  • Your doctors and nurses | سنحرص على حماية المعلومات المتعلقة بك. وهذا سيتضمن استخدام رمز للتعرف عليك في سجلاتنا بدلاً من استخدام اسمك. ونحن لن نحدد هويتك الشخصية في أي تقارير أو مطبوعات ناتجة من هذا البحث.

لا يمكننا ضمان السرية التامة, ولكننا سنحدّ من إمكانية الوصول إلى المعلومات المتعلقة بك وعنك. فقط الأشخاص الذين سيكونون بحاجة لمراجعة معلوماتك سيتمكنون من الوصول إليها. هؤلاء الأشخاص ممكن أن يكونوا:
  • فريق البحث وموظفي مؤسسة حمد الطبية, مختبر مكافحة المنشطات-قطر المرتبطة أعمالهم بهذا البحث او بحماية حقوقك وسلامتك.
  • ممثلي المجلس الأعلى للصحة في قطر و الصندوق القطري لرعاية الحث العلمي والتي تتأكد من قيام الدراسة بالشكل الصحيح وتتأكد من حماية حقوقك وسلامتك.
  • أطباؤك وطاقم التمريض

قد نستخدم بيانات هذه الدراسة في مشاريع أخرى في المستقبل ويمكن أن نشارك هذه البيانات مع باحثين آخرين. سوف نلغي كل الروابط بين الهوية الخاصة بك والبيانات عنك قبل أن تخزين البيانات لاستخدامها في المستقبل.

أثناء الدراسة، سيتم الاحتفاظ بالعينات الخاصة بك واستخدامها: في قطر ولكن يمكن أيضا أن ترسل لإجراء التحاليل عليها خارج قطر في جامعة بريستول. نود أن نبقي على أي عينات متبقية في نهاية الدراسة لعشر سنوات لاستخدامها في أبحاث أخرى في المستقبل. |

We plan to use data from this study in other projects in the future. This might include sharing the data with other researchers. Before we store the data for future use, we will destroy all links between your identity and the data about you. During the study, your samples will be kept and used in Qatar but may also be sent outside Qatar to Bristol University for further analysis. We would like to keep any samples left over at the end of the study for 10 years for future research. We will store these leftover samples with a link to your identity. Leftover samples; might be shared with researchers who were not part of this study. Your leftover samples will be used for research into any condition. Samples that we share with other researchers won't include information that identifies you. If you change your mind about the research or about letting us use your samples, we won't be able to get back any samples that we have shared with other researchers. You may join this study even if you do not allow this future use. You can mark your choice at the end of this form. If you do not allow storage of your samples, we will destroy the sample at the end of the study.	سنقوم بتخزين بقايا هذه العينات مع رابط لهويتك. العينات المتبقية قد يتم مشاركتها مع باحثين لم يكونوا جزءاً من هذه الدراسة.ستستخدم عيناتك المتبقية في أية بحوث. عند مشاركة عينات البحث مع باحثين آخرين لن يتضمن ذلك أي معلومات تكشف عن هويتك. إذا قمت بتغيير رأيك حول المشاركة بالبحث أو حول السماح لنا باستخدام العينات الخاصة بك، لن نتمكن من استرجاع أي عينات تمت مشاركتها مع باحثين آخرين. يمكنك الإنضمام لهذه الدراسة حتى لو كنت لا تسمح باستخدامها في المستقبل. يمكنك وضع علامة اختيارك في نهاية هذا النموذج. إذا كنت لا تسمح بتخزين العينات الخاصة بك، وسوف ندمر العينة عند نهاية الدراسة.
13. What if you don't want to join?	**13. ماذا لو كنت لا تريد المشاركة؟**
You can say no, and we will not hold it against you.	يمكنك أن ترفض المشاركة ولن يستخدم قرارك ضدك بأي حال من الأحوال.
14. What if you join but change your mind?	**14. ماذا لو انضممت الآن ولكن غيرت رأيك لاحقاً؟**
You can stop participating at any time and we will not hold it against you. We will tell you about any new information that might affect your health or welfare or might affect your willingness to continue in the research.	يمكنك التوقف عن المشاركة بهذا البحث بأي وقت، ولن يستخدم قرارك ضدك بأي حال من الأحوال. وسنخبرك عن أي معلومات جديدة قد تؤثر على صحتك أو عافيتك، أو تؤثر على استعدادك للإستمرار في هذا البحث.

15. What else should you know?	؟أيضاً تعلمه أن يجب الذي ما .15
This research is being funded by Qatar National Research Fund. If you are injured as a direct result of research procedures, contact the investigator and appropriate care will be made available at HMC. If you seek care outside of HMC, such care will be at your expense. Compensation is not available in case of injury.	ان هذا البحث ممول من قبل الصندوق القطري لرعاية البحث العلمي. إذا أصبت كنتيجة مباشرة من إجراءات البحث، اتصل بالباحث وسوف تتاح لك الرعاية المناسبة في مؤسسة حمد الطبية. إذا كنت تسعى لرعاية صحية خارج مؤسسة حمد الطبية، ستكون هذه الرعاية على نفقتك الخاصة. التعويض غير متوفر في حالة الإصابة.
16. Additional Choices	خيارات إضافية .16
In Section 9, we described some extra **OPTIONAL** procedures These extra procedures are optional, meaning that you can participate in the study even if you refuse the procedures. Please indicate your choice by initialing the appropriate line below: Optional glucose tolerance test - _____I AGREE to participate in o**ptional Glucose tolerance test** - _____I DO NOT AGREE to participate in these optional **g**lucose tolerance test Optional body composition by DEXA - _____I AGREE to participate in these optional **body compositions by DEXA** - _____I DO NOT AGREE to participate in these optional **body compositions by DEXA** Optional follow-up procedures - _____I AGREE to participate in these optional **follow-up** procedures. - _____I DO NOT AGREE to participate in these **follow-up** optional procedures.	في الجزء 9, قمنا بشرح بعض الاجراءات الإضافية **الاختيارية** هذه الإجراءات الإضافية اختيارية، مما يعني أنه يمكنك المشاركة في الدراسة حتى لو كنت ترجى الإشارة إلى ترفض هذه الإجراءات الاضافية. اختيارك بتوقيعك بالسطر المناسب أدناه: **اختبار تحمل الجلوكوز (اختياري):** - _____ نعم, أوافق على الاشتراك باختبار تحمل الجلوكوز الاختياري. - _____ لا, أرفض المشاركة اختبار تحمل الجلوكوز الاختياري. **فحص نسبة الدهون وكثافة العظام (AXED) (اختياري):** - _____ نعم, أوافق على الاشتراك بفحص نسبة الدهون وكثافة العظام (AXED) الاختياري. - _____ لا, أرفض المشاركة بفحص نسبة الدهون وكثافة العظام (AXED) الاختياري. **مواعيد المتابعة (الثالث والرابع والخامس) (اختياري):** - _____ نعم, أوافق على الاشتراك بفحص نسبة الدهون وكثافة العظام (AXED) الاختياري. - _____ لا, أرفض المشاركة نسبة الدهون وكثافة العظام (AXED) الاختياري. في القسم 12، شرحنا أننا نود استخدام العينات الخاصة بك للبحوث في المستقبل. يرجى الإشارة إلى اختيارك بتوقيعك بالسطر المناسب أدناه:

In Section 12, we explained that we would like to use your samples for future research. Please indicate your choice by initialing the appropriate line below:

- _____I **ALLOW** storage and use of my samples for future research.
- _____I **DO NOT ALLOW** storage or use of my samples for future research.

Future Use of Samples

We would like your permission to contact you about participating in future studies. You may still join this study even if you do not permit future contact. You may also change your mind about this choice. Please initial your choice below:
- _____YES, you may contact me
- _____NO, you may NOT contact me

- _____ نعم, أوافق على تخزين واستخدام عيناتي لبحوث في المستقبل.
- _____ لا, أرفض تخزين واستخدام عيناتي لبحوث في المستقبل.

استخدام العينات في المستقبل

نود الحصول على إذنك للاتصال بك حول المشاركة في دراسات مستقبلية. بإمكانك الانضمام لهذه الدراسة حتى لو لم تسمح بأن نتصل بك مستقبلاً. كما ويمكنك أيضا أن تغير رأيك حول هذا الاختيار. الرجاء التوقيع عند اختيارك أدناه:

- _____ نعم, يمكنكم الاتصال بي
- _____ لا, لا تتصلوا بي

Signature Page for Capable Adult	صفحة التوقيع للمشارك البالغ العاقل
Volunteer	**المشارك**
I voluntarily agree to join the research described in this form. _____ Printed Name of Volunteer _____ Signature of Volunteer　　　　Date	**أوافق طوعاً على الانضمام الى البحث المشروح في هذا النموذج** _____ **الاسم الكامل للمشارك بالبحث** **التوقيع**　　　　　　**التاريخ**
Person Obtaining Consent	**الشخص الحاصل على الموافقة**
I document that: 　• *I (or another member of the research team) have fully explained this research to the volunteer.* 　• *I have personally evaluated the volunteer's understanding of the research and obtained their voluntary agreement.* _____ Printed Name of Person Obtaining Consent _____ Signature of Person　　　　Date Obtaining Consent	**أشهد أني:** 　• **أنا (أو أحد أعضاء فريق البحث) قمنا بشرح البحث بشكل وافي للمشارك بالبحث** 　• **قمت شخصياً بتقييم فهم المشارك بالبحث والحصول على موافقته/ها الطوعية.** _____ **الاسم الكامل الشخص الحاصل على الموافقة** **التوقيع**　　　　　　**التاريخ**
Witness (if applicable)	**الشاهد (عند الضرورة)**
I document that the information in this form (and any other written information) was accurately explained to the volunteer, who appears to have understood and freely given Consent to join the research. _____ Printed Name of Witness _____ Signature of Witness　　　　Date	**أشهد أنه تم شرح المعلومات الواردة في هذا النموذج بدقة (وأية معلومات أخرى مكتوبة) للمشارك بالبحث. وإنه يبدو أنه قد فهم البحث وأن موافقته على الإنضمام إلى هذا البحث طوعية.** _____ **الاسم الكامل للشاهد** **التوقيع**　　　　　　**التاريخ**

Appendix 2: Ingenuity Pathways Analysis of the top pathways and genes associated with from differential gene expression in SKM and ME arteries.

Ingenuity Toxicity Lists	-log(p-value)	Ratio	Molecules
Acute Renal Failure Panel (Rat)	2.17	0.145	ACTA2,ADM,ATF3,EIF1AX,FGB,FOS,IGFBP5,TAGLN,VCAM1
NRF2-mediated Oxidative Stress Response	1.6	0.0875	ABCC2,ACTA2,ACTB,ACTG2,CCT7,CYP2A6 (includes others),CYP2D6,DNAJA1,DNAJC5,DNAJC8,ENC1,ERAS,FOS,FTL,JUNB,MAFG,MAP3K5,MAP3K7,MAPK7,PRKCG,RAP1A
Genes associated with Chronic Allograft Nephropathy (Human)	1.58	0.19	COL4A1,FN1,TIMP1,VCAM1
Increases Liver Steatosis	1.42	0.101	CD36,CNOT3,CRBN,CRTC3,DDC,DDIT3,GRB14,ITPRID2,MAF1,MAP3K5,NPC1L1
Recovery from Ischemic Acute Renal Failure (Rat)	1.41	0.214	COL4A1,S100A4,TIMP1
Cholesterol Biosynthesis	1.26	0.188	ACAT1,EBP,MVD
Reversible Glomerulonephritis Biomarker Panel (Rat)	1.23	0.148	GLRA3,GREM1,IGFBP5,LIPA
Cardiac Fibrosis	1.21	0.0809	ATF3,CCN2,CNOT3,DES,FN1,FOXM1,GSK3A,HOPX,LMNA,MAP3K5,MYOCD,PLA2G2A,PRKG1,RERE,RGS5,SGCG,SIRT7,TIMP1,VEGFB
Positive Acute Phase Response Proteins	1.09	0.133	FGB,FGG,MBL2,SERPING1
Persistent Renal Ischemia-Reperfusion Injury (Mouse)	1.09	0.133	AOC1,CTSS,HSPB1,VCAM1
Hepatic Fibrosis	1.06	0.0901	ACTA2,CCR5,COL4A1,ELN,FN1,IGFBP5,IGFBP7,PDGFB,SPARC,TIMP1

Appendix 3: Ingenuity Pathways Analysis of the top pathways and genes associated with from differential gene expression in untreated and 20-HE treated SKM arteries.

Ingenuity Toxicity Lists	-log(p-value)	Ratio	Molecules
Renal Necrosis/Cell Death	5.95	0.108	ABCC10,ABCC3,AGTR1,AMOTL1,API5,AQP3,ATF3,CASP3,CASP4,CD44,CDKN1A,CITED2,COX11,CRYAB,DAXX,DDIT3,DPM3,DYRK3,EMP1,EMP3,EXO5,EZR,FGF2,FOS,GAS7,HIP1,HK1,HK2,HMOX1,HSP90B1,HSPA5,IL18,IRF1,JAK2,LRP6,MYC,NAMPT,NDEL1,NFE2L2,PLA2G4A,PLAT,PMAIP1,PMP22,POLH,PPP1R15A,PTGS2,RELA,RGS16,RNF13,SDHC,SIRT1,SMAD7,STAT2,TAF4B,TARDBP,THBS1,TNFRSF1B,TNFRSF25,TRIM27,TRPM2,VEGFA,YWHAQ
Cardiac Hypertrophy	5.84	0.122	ADCY6,ADGRG1,AGTR1,ATF3,BMX,CACNB2,CAV3,CKM,CKMT2,CREM,CRYAB,DNAJC3,DUSP5,FGF2,FSTL3,H2AFZ,HEXIM1,HMGCR,HSPB8,HTR2B,IL18,LCAT,LMCD1,MYL2,NOX4,NR4A3,PLA2G4A,PLAT,PPP3CC,PRKG1,PTGES,PTGS2,ROCK1,ROCK2,RRAD,SERPINE1,SIRT1,SLC6A4,SMAD7,TCAP,THRA,TIMP1,TNFRSF1B,TNNC1,TNNI3
Liver Proliferation	5.17	0.132	AGTR1,ATF4,CDKN1A,CITED2,CUL3,CXCL3,CXCR4,FGFR2,FOS,HTR2B,IL18,ITIH4,KITLG,MYC,NFE2L2,ODC1,OSMR,PIK3IP1,PML,PROS1,PTGS2,RB1,RELA,SAT1,SIRT1,SMAD7,THBS1,TIMP1,TNFRSF12A,TNFRSF1B,VEGFA,XBP1,YOD1
NRF2-mediated Oxidative Stress Response	5.12	0.133	AKR1A1,ATF4,CUL3,DNAJA1,DNAJA2,DNAJB1,DNAJB11,DNAJB14,DNAJB2,DNAJB4,DNAJB9,DNAJC1,DNAJC13,DNAJC3,EPHX1,FOS,FOSL1,GSTM3,HERPUD1,HMOX1,HSP90AB1,HSP90B1,HSPB8,JUNB,NFE2L2,PIK3C2B,PIK3R2,PIK3R3,RASD1,SQSTM1,STIP1,TXNRD1
Acute Renal Failure Panel (Rat)	5.08	0.226	ADM,ANXA1,ATF3,CD44,CDKN1A,COL3A1,DNAJB9,EIF1AX,FOS,FOSL1,HMOX1,MYC,RRAD,TNFRSF12A
Liver Necrosis/Cell Death	4.71	0.118	ADM,API5,ARF6,ARRB2,CASP3,CD274,CDKN1A,CHUK,CTH,CXCL3,DAXX,DDIT3,DNM1L,FOS,GADD45B,HK2,HMOX1,IRF1,ITIH4,JAK2,MYC,NFE2L2,PDGFB,PROS1,PTGS2,RB1,REL,RELA,SERPINE1,SIRT1,SLC25A5,TIMP1,TMBIM6,TNFRSF1B,TRIM27,UGCG,USP2,XBP1
Cardiac Necrosis/Cell Death	4.52	0.118	ACSL1,ADCY6,ADM,AGTR1,CACNB2,CALCRL,CASP3,CAV3,CDKN1A,CREG1,CREM,CRYAB,CXCR4,DAXX,FGF2,FOSL1,FSTL3,HK1,HK2,HMOX1,HSPB8,HSPE1,HTR2B,IVNS1ABP,MANF,NAMPT,NOX4,PKN1,PLAT,PPP1R15A,RB1,RRAD,SFRP2,SIRT1,TIMP1,VEGFA
RAR Activation	3.9	0.129	ADCY4,ADCY6,AKR1B1,ARID2,BMP2,CDK7,CITED2,CRABP2,FOS,HLTF,JAK2,NRIP1,PIK3R2,PIK3R3,PML,PNRC1,PRKACB,RDH10,REL,RELA,RELB,RPL7A,SMAD7,SNW1,VEGFA
p53 Signaling	3.3	0.152	CDKN1A,GADD45A,GADD45B,GADD45G,PIK3C2B,PIK3R2,PIK3R3,PMAIP1,PML,RB1,SERPINE2,SIRT1,SNAI2,THBS1,TOPBP1

Cell Cycle: G2/M DNA Damage Checkpoint Regulation	3.2	0.192	CDK7,CDKN1A,CKS2,GADD45A,SKP1,WEE1,YWHAE,YWHAG,YWHAH,YWHAQ
Increases Renal Proliferation	3.04	0.124	ABCC5,CDKN1A,ESM1,FGFR2,HAS2,IRF1,KLF5,MED28,PDGFB,PLAUR,PLD2,POLG,PTGES,PTGS2,PTP4A1,RNF144B,SDCBP,SLC36A4,VEGFA,ZBTB5

Appendix 4: Ingenuity Pathways Analysis of the top pathways and genes associated with from differential gene expression in 20-HE treated ME arteries.

Ingenuity Toxicity Lists	-log(p-value)	Ratio	Molecules
Acute Renal Failure Panel (Rat)	8.02	0.226	ACTA2,AKAP12,ANXA1,ATF3,CDKN1A,CXCL12,DNAJB9,FOS,FOSL1,HMOX1,IGFBP5,MYC,TAGLN,TNFRSF12A
Cardiac Hypertrophy	6.22	0.0867	ADRB1,ATF3,BMPR2,CACNB2,CCN2,CIB1,CREM,CXCL12,DUSP5,EPAS1,GLRX3,H2AFZ,HMGB1,LAMA4,MBNL1,MEF2C,MMP2,NOS1,NR4A3,PARP1,PBX1,PDE5A,PRKCB,PTGES,PTGS2,ROCK1,S100A10,SIRT1,TPM1,TRPC6,UTS2R,VEGFB
Cardiac Fibrosis	6.05	0.102	ADRB1,ATF3,CCN2,CIB1,CREM,DES,GNAS,GSK3A,HMOX1,LAMA4,LIMS2,LMNA,MBNL1,NEXN,NLRP3,NOS1,PLN,PRKCB,PTGS2,RGS5,ROCK1,SIRT7,VEGFA,VEGFB
Cardiac Necrosis/Cell Death	5.54	0.0888	ABCB8,ADRB1,BNIP3L,CACNB2,CCN1,CDKN1A,CREM,DES,FOSL1,GNB1,GSK3A,HMOX1,HSPB1,IQGAP1,LRP1,MANF,MMP2,NAMPT,NUB1,PARP1,PRKCB,SIRT1,SIRT7,SST,VEGFA,VEGFB,ZYX
Renal Necrosis/Cell Death	4.83	0.0681	ATF3,BNIP3L,CCN2,CDKN1A,CITED2,DCN,DDIT3,DDX17,EMP1,EMP2,EZR,FOS,GFPT1,GNA13,HIP1,HMOX1,HSPA5,HSPB1,IL24,IRF1,IRS1,MYC,NAMPT,NLRP3,NOS1,PARP1,PARVA,PEA15,PMP22,PRKCB,PTGS2,RGS16,SIRT1,SLK,SRXN1,STMN1,THBS1,TRIB3,VEGFA
Increases Heart Failure	4.12	0.261	ADRB1,CACNB2,FOSL1,PLN,TRPC6,ZFPM2
Hepatic Fibrosis	2.99	0.0991	ACTA2,DCN,ELN,IGFBP5,IGFBP6,LTBP4,LUM,MMP2,SPARC,THBS1,VEGFA
Decreases Transmembrane Potential of Mitochondria and Mitochondrial Membrane	2.9	0.0916	ADRB1,BNIP3L,DDIT3,HSPB1,IFI6,IL24,IRS1,MYC,MYCN,PARP1,SST,TGM2
Hypoxia-Inducible Factor Signaling	2.7	0.114	EIF2S2,EIF2S3,HSP90AB1,PRKCB,UBE2D2,UBE2L6,UBE2N,VEGFA
NRF2-mediated Oxidative Stress Response	2.61	0.0708	ACTA2,ACTB,ACTG2,ATF4,CCT7,CREBBP,DNAJA1,DNAJB1,DNAJB9,FOS,FOSL1,HERPUD1,HMOX1,HSP90AB1,JUNB,PRKCB,RAP1A
Increases Glomerular Injury	2.57	0.088	ABL1,ATF3,CCN2,CDKN1A,GFPT1,IRF1,PTGS2,SDK1,SLK,SPARC,VEGFA